SAPIENZA
UNIVERSITÀ DI ROMA

Department of Physiology and Pharmacology "V. Erspamer"
Ph.D. in Clinical/Experimental Neurosciences and Psychiatry - XXXV Cycle –

ABNORMAL REACTIVITY OF RESTING-STATE EEG ALPHA RHYTHMS DURING EYES OPEN IN PATIENTS WITH ALZHEIMER'S AND LEWY BODY DISEASES

Ph.D. thesis by Dott. Federico Tucci

Tutor: Prof. Claudio Babiloni

Coordinator: Prof. Cristina Limatola

INDEX

Abstract

Previous studies suggest that resting-state electroencephalographic (rsEEG) rhythms recorded in old patients with dementia due to different neurodegenerative diseases have a significant heuristic and clinical potential in identifying peculiar abnormalities of the ascending activating systems and reciprocal thalamocortical circuits in which oscillatory (de)synchronizing signals dynamically underpin cortical arousal in the regulation of quiet vigilance.

In the present PhD program, a new methodological approach based on rsEEG cortical source estimation and individually-based frequency bands was used to test the hypothesis of significant abnormalities in the neurophysiological oscillatory mechanisms underlying the regulation of the quiet vigilance during the transition from an eyes-closed to an eyes-open condition in patients with the most prevalent neurodegenerative dementing disorders such as Alzheimer's disease and Lewy Body and Parkinson's diseases and initial abnormalities in the prodromal stage of ADD, characterized by mild cognitive impairment. Three rsEEG studies were performed for that purpose.

In the **first study**, we tested if the reactivity of posterior rsEEG alpha rhythms from the eye-closed to the eyes-open condition may differ in patients with dementia due to Lewy Bodies (DLB) and Alzheimer's disease (ADD) as a functional probe of the dominant neural synchronization mechanisms regulating the vigilance in posterior visual systems. We used clinical, demographical, and rsEEG datasets in 28 healthy elderly (Healthy) seniors, 42 DLB, and 48 ADD participants. The eLORETA freeware estimated rsEEG cortical sources at individual delta, theta, and alpha frequencies. Results showed a substantial (> -10%) reduction in the posterior alpha activities during the eyes-open condition in 24 Healthy, 26 ADD, and 22 DLB subjects. There were lower reductions in the posterior alpha activities in the ADD and DLB groups than in the Healthy group. The reduction in the occipital region was lower in the DLB than in the ADD group. These results suggest that DLB patients may suffer a greater alteration in the neural synchronization mechanisms regulating vigilance in occipital cortical systems compared to ADD patients.

In the **second study**, we hypothesized that the vigilance dysregulation seen in PDD patients might be reflected by altered reactivity of posterior rsEEG alpha rhythms during the vigilance transition from an eyes-closed to an eyes-open condition. We used clinical, demographical, and rsEEG datasets in 28 healthy elderly (Healthy), 73 PDD, and 35 ADD participants. We have applied the same methodology used for the first study. Results showed substantial (> -10%) reduction (reactivity) in the posterior alpha source activities from the eyes-closed to the eyes-open condition in 88% of the Healthy seniors, 57% of the ADD patients, and only 35% of the PDD patients. In these alpha-reactive participants, there was lower reactivity in the parietal alpha source activities in the

PDD group than in the Healthy and the ADD groups. These results suggest that PDD is characterized by poor reactivity of mechanisms desynchronizing posterior rsEEG alpha rhythms in response to visual inputs. This finding could be an interesting biomarker of impaired vigilance regulation in quiet wakefulness in PDD patients. Indeed, such biomarkers may provide endpoints for pharmacological intervention and brain electromagnetic stimulations to improve the PDD patients' general ability to regulate vigilance and primary visual consciousness in the activities of daily living.

In the **third study**, we tested the exploratory hypothesis that rsEEG alpha rhythms may predict and be sensitive to mild cognitive impairment due to AD (ADMCI) progression at a 6-month follow-up (a relevant feature for intervention clinical trials). Clinical, neuroimaging, and rsEEG datasets in 52 ADMCI and 60 Healthy seniors were used. We applied the same methodology used for the first and the second studies. Results showed a substantial (> -10%) reduction in the posterior alpha source activities during the eyes-open condition in about 90% and 70% of the Healthy and ADMCI participants, respectively. In the younger ADMCI patients (mean age of 64.3±1.1) with "reactive" rsEEG alpha source activities, posterior alpha source activities during the eyes closed condition predicted the global cognitive status at the 6-month follow-up. In all ADMCI participants with "reactive" rsEEG alpha source activities, posterior alpha source activities during the eyes-closed condition reduced in magnitude at that follow-up. These effects could not be explained by neuroimaging and neuropsychological biomarkers of AD. These results suggest that in ADMCI patients, the true ("reactive") posterior rsEEG alpha rhythms, when present, predict (in relation to younger age) and are quite sensitive to the effects of the disease progression on neurophysiological mechanisms underpinning vigilance regulation.

The results of the three studies unveiled the significant extent to which the well-known impairments in the cholinergic and dopaminergic neuromodulatory ascending systems could affect the brain neurophysiological oscillatory mechanisms underpinning the reactivity of rsEEG alpha rhythms during eyes open and, then, the regulation of quiet vigilance in ADD, PDD, and DLB patients, thus enriching the neurophysiological model underlying their known difficulties to remain awake in quiet environmental conditions during daytime.

Introduction

Major neurocognitive disorder, also known as dementia, is a significant cognitive decline from a previous level, with the loss of independence in everyday activities and often emotional, motivational, and behavioral symptoms (American Psychiatric Association, 2013). Patients with dementia are 46 million worldwide. During aging, the most frequent form of dementia is Alzheimer's disease dementia (ADD), accounting for >50% of patients, while dementia due to Parkinson's disease dementia and dementia with Lewy body (PDD and DLB) affect approximately 10%–20% of the cases.

ADD, PDD, and DLB are due to progressive neurodegenerative processes associated with an abnormal accumulation of proteins in the brain (i.e., Aβ1-42 extracellularly and intracellular phosphorylated tau protein or α-synuclein), causing axonal dysfunction, neuronal loss, and brain atrophy (Aarsland et al., 2003). Compared to ADD, PDD and DLB are characterized by prominent intracellular Lewy bodies in subcortical (mostly in PDD) and cortical (primarily in DLB) regions. Moreover, ADD can be detected even in the prodromal stage of mild cognitive impairment (ADMCI) using cerebrospinal fluid and positron emission tomography diagnostic biomarkers of Aβ1-42 and phospho-tau (Dubois et al., 2014; McKhann et al., 2011).

In recent years, the research interest in electroencephalography (EEG) techniques has grown as it is expected to help detect abnormalities in cortical neurophysiological mechanisms associated with cognitive decline and dementia due to different neurodegenerative diseases at a lower cost for mass screening (Lizio et al., 2016). EEG is also widely available and faster to use than other imaging devices (Babiloni et al., 2020a). In this line, a bulk of studies have tested EEG markers to qualify their sensitivity to detect the neurophysiological basis of early manifestations of dementia and even classify the degree of abnormality in the neurophysiological mechanisms underpinning its severity.

Among EEG markers, an interesting heuristic neurophysiological biomarker in neurodegenerative diseases may be the amplitude reduction (“reactivity”) of “background” resting-state EEG (rsEEG) alpha rhythms from the eyes-closed to the eyes-open condition. It seems ideal to reflect the abnormalities in the fine neurophysiological oscillatory regulation of the general brain neural activation (arousal) and related levels of quiet vigilance. To explore that neurophysiological biomarker, previous studies have shown the rsEEG alpha reactivity was lower (1) in the ADD and LBD groups than in the group of matched cognitively unimpaired old (Healthy) persons and (2) in the LBD than the ADD group (Schumacher et al., 2020a). Those results confirmed previous resting-state magnetoencephalographic (rsMEG) evidence showing a lower alpha reactivity in ADD and LBD patients than in Healthy seniors (Franciotti et al., 2006). Furthermore, they extended previous

rsMEG evidence showing that such an alpha reactivity was lower in PDD patients than in Healthy seniors (Bosboom et al., 2006).

In our opinion, a methodological step forward in the study of the rsEEG alpha reactivity in PDD, DLB, ADD, and ADMCI patients may regard the enhancement of the spatial analysis using an analytical procedure to estimate cortical sources of eyes-closed and eyes-open rsEEG alpha rhythms. Moreover, we thought that it might be useful to use individual frequency instead of the standard (fixed) frequency bands in all subjects, therefore considering the remarkable interindividual variability. Finally, a last methodological step forward in the study of the rsEEG alpha reactivity would be represented by a fine neurophysiological definition of rsEEG alpha rhythms. In this regard, we posit that rsEEG alpha rhythms are defined by the following two core features: (1) a clear amplitude maximum in the posterior scalp or cortical regions during the eyes-closed condition and (2) an evident reduction (reactivity) in amplitude in those posterior rsEEG rhythms from the eyes-closed to the eyes-open condition. From a heuristic point of view, these methodological improvements are expected to unveil better how impairments in the cholinergic neuromodulatory ascending systems in ADD patients and a mix of impairments in the dopaminergic and cholinergic neuromodulatory ascending systems in PDD and DLB patients may affect the brain neurophysiological oscillatory mechanisms underpinning the regulation of quiet vigilance in humans. Indeed, it can be hypothesized that previous studies tested the reactivity of the so-called rsEEG alpha rhythms during eyes open in ADD, PDD, and DLB patients in whom the rsEEG alpha rhythms may be practically absent, substituted by unreactive dominant background EEG rhythms at theta frequencies. This bias may have confounded significant abnormalities in the neurophysiological oscillatory mechanisms underlying the regulation of the quiet vigilance during the transition from eyes-cloded to eyes-open condition in ADD, DLB, PDD patients and initial abnormalities in the prodromal stage of ADD, characterized by mild cognitive impairment. In the present PhD thesis, three rsEEG studies were performed for that purpose.

In the **first study**, we used the mentioned methodological advancements to test the hypothesis that the reactivity of posterior rsEEG alpha rhythms from the eye-closed to the eyes-open condition may be lower in DLB than in ADD patients and Healthy persons as a functional probe of the dominant cortical neural synchronization mechanisms regulating the brain arousal and vigilance in posterior visual systems.

In the **second study**, we tested whether the reactivity to the eyes-open condition in the posterior rsEEG alpha source activities may be lower in the PDD than in the ADD and the Healthy groups.

Finally, in the **third study**, we tested the hypothesis that resting-state eyes-closed electroencephalographic (rsEEG) "true" alpha rhythms may predict and be sensitive to the disease progression at a 6-month follow-up in patients with mild cognitive impairment due to AD (ADMCI).

This PhD thesis is structured in two parts. The **first part**, the "Background", introduces the main neurobiological and clinical aspects characterizing ADD, PDD, and DLB patients, as well as the core methods used for the research activity of this PhD thesis. The **second part**, the "Experimental part", reports the three studies with a general discussion of their results and the related neurophysiological and clinical conclusions.

The results of the three studies unveiled the significant extent to which the well-known impairments in the cholinergic and dopaminergic neuromodulatory ascending systems could affect the brain neurophysiological oscillatory mechanisms underpinning the reactivity of rsEEG alpha rhythms during eyes open and, then, the regulation of quiet vigilance in ADD, PDD, and DLB patients, thus enriching the neurophysiological model underlying their known difficulties to remain awake in quiet environmental conditions during daytime.

BACKGROUND

From Mild Cognitive Impairment to Dementia

Mild cognitive impairment (MCI) is a middle stage between normal aging and dementia (Winblad et al., 2004). It produces serious cognitive changes that can be noticed by the person and by family members and friends. This impairment should not affect the individual's ability to carry out everyday activities. MCI is so variable that in some cases could revert to normal cognition or remain stable, while in other cases, it could develop in dementia. Due to the importance of early treatments, is important to find precise techniques to catch the early stage of the disease (Petersen et al., 2001; Winblad et al., 2004; Albert et al., 2011):

1) Amnestic MCI: MCI that primarily affects memory. A person may start to forget important information that he or she would previously have recalled easily, such as appointments, conversations, or recent events;
2) Nonamnestic MCI: MCI that affects thinking skills other than memory, including the ability to make sound decisions, and judge the time or sequence of steps needed to complete a complex task or visual perception.

MCI can develop for multiple reasons, and individuals living with MCI may go on to develop dementia; others will not. For neurodegenerative diseases, MCI can be an early stage of the disease continuum, including Alzheimer's (ADMCI) if the hallmark changes in the brain are present (Bruscoli et al., 2004; Farias et al., 2009). A medical workup for MCI includes the following core elements:
1) Thorough medical history, where the physician documents current symptoms, previous illnesses, and medical conditions, and any family history of significant memory problems or dementia;
2) Assessment of independent function and daily activities, which focuses on any changes from a person's usual level of function;
3) Input from a family member or trusted friend to provide additional perspective on how functionality may have changed;
4) Assessment of mental status using brief tests designed to evaluate memory, planning, judgement, ability to understand visual information, and other key thinking skills.
5) In-office neurological examination to assess the function of nerves and reflexes, movement, coordination, balance, and senses.

6) Evaluation of mood to detect depression; symptoms may include problems with memory or feeling "foggy." Depression is widespread and may be especially common in older adults (Petersen et al., 2001; Winblad et al., 2004).
7) Laboratory tests, including blood tests and imaging of the brain's structure.
8) Neuropsychological testing, which involves a series of written or computerized tests to evaluate specific thinking skills.

Talking about patients with dementia, display increasingly poor judgment and deepening confusion and need more help with daily activities and self-care than patients with MCI (American Psychiatric Association, 2013). An important characteristic of dementia patients is that they lose contact with reality, no longer being able to recognize time and space. Moreover, these characteristics make it difficult for this type of patient to live alone, but also make them a great burden on their families (Petersen et al., 2009).

At a mnemonic level, dementia patients can lose track of personal information, including their residence, phone number, and places of education. Assistance may be needed with self-care activities such as washing, grooming, using the restroom, and dressing appropriately for the situation or the weather. Some people sporadically experience bladder or bowel incontinence. It's common for these patients to harbor erroneous suspicions. For instance, they start to believe that their spouse is having an affair or that their friends, relatives, or professional careers are taking from them. Some people might hear or see things that aren't there. People frequently become anxious or restless, especially later in the day. Some individuals may occasionally display hostile physical conduct (Duong et al., 2017; Bruscoli et al., 2004). Unfortunately, many behavioural and psychiatric symptoms do not respond well to medication, which can be distressing for patients and their caregivers, as well as pose a safety risk.

Alzheimer's, Parkinson's, and Lewy Body diseases (AD, PD, DLB) are the three main neurodegenerative illnesses that can lead to mild cognitive impairment (ADMCI, PDMCI, DLBMCI), and finally dementia (ADD, PDD, DLB) (Petersen et al., 2001; Hughes and Crunelli, 2005).

Dementia due to Lewy body diseases

Patients with dementia are 55 million worldwide (World Health Organization, WHO), and about 10% of them are due to Parkinson’s disease. Parkinson’s disease dementia (PDD) is caused by intraneural inclusions of Lewy bodies (mainly formed by α-synuclein protein) in subcortical and cortical regions, belonging to severe cognitive deficits and disabilities in the activities of daily living even under the effect of levodopa therapy (Aarsland et al., 2003).

These Lewy bodies track progressive neurodegenerative processes resulting in axonal dysfunctions, neuronal loss, and brain atrophy (Bhat et al., 2015). α-synuclein is a human protein encoded by the gene SNCA, which is predominantly expressed in the neocortex, hippocampus, substantia nigra, thalamus, and cerebellum. In the brain, it is localized in presynaptic terminals where it is involved in neurotransmitters released from synaptic vesicles. If the gene is mutated, the protein forms a stably folded tetramer (aggregates).

According to DSM-5 (American Psychiatric Association, 2013; McKeith et al., 2017), the nosological relationships between dementia with Lewy bodies (DLB) and Parkinson's disease dementia (PDD) are still being debated (Aarsland et al., 2009; Friedman et al., 2018; Gomperts et al., 2016; Jellinger et al., 2009; McKeith et al., 2007). Both entities share clinical symptoms such as dementia, cognitive fluctuations, and (visual) hallucinations in the context of overt or latent parkinsonism. PDD and DLB patients also share cognitive impairments such as progressive executive dysfunctions, visual-spatial abnormalities, and memory difficulties, with the latter being more severely affected in PDD patients (Goetz et al., 2008). According to international consensus, DLB is diagnosed when cognitive impairment occurs 2 or 1 year before the onset of parkinsonian motor signs (McKeith et al., 2005), whereas PDD is diagnosed when cognitive impairment develops after a well-established Parkinson's disease (Emre et al., 2007; Goetz et al., 2008).

Almost all people with Parkinson's disease will experience cognitive deterioration over time; however, many will experience modest deficiencies up to 6 years before the onset of motor symptoms (Darweesh et al., 2017). DLB patients, on the other hand, will acquire parkinsonism of increasing severity over time, with a prevalence ranging from 60 to 92% (Ferman et al., 2011). However, 25% of DLB patients will never develop parkinsonian symptoms (Ferman et al., 2011). Despite different temporal sequences of motor and cognitive deficits and clinical differences, both entities exhibit mostly convergent neuropathological lesions also associated with increased cortical amyloid and tau load (Garcia-Esparcia et al., 2017; Hepp et al., 2016; Jellinger et al., 2009; Paleologou et al., 2009; Walker et al., 2015).

Nonetheless, the neurochemical systems most consistently damaged in DLB are dopamine via nigral degeneration and acetylcholine via basal forebrain degeneration (Tiraboschi et al., 2000). Instead, there is evidence in PDD patients of deficits in the dopaminergic nigrostriatal pathway, which is responsible for motor impairment, and in the projecting dopaminergic neurons in the frontostriatal network (Scatton et al., 1983), which is responsible for executive dysfunctions (Middleton & Strick, 2000). Parkinson's disease also affects the noradrenergic network, which controls alertness via projections from the locus coeruleus to the thalamus, amygdala, and cortex (Bertrand et al., 1997) (Figure 1).

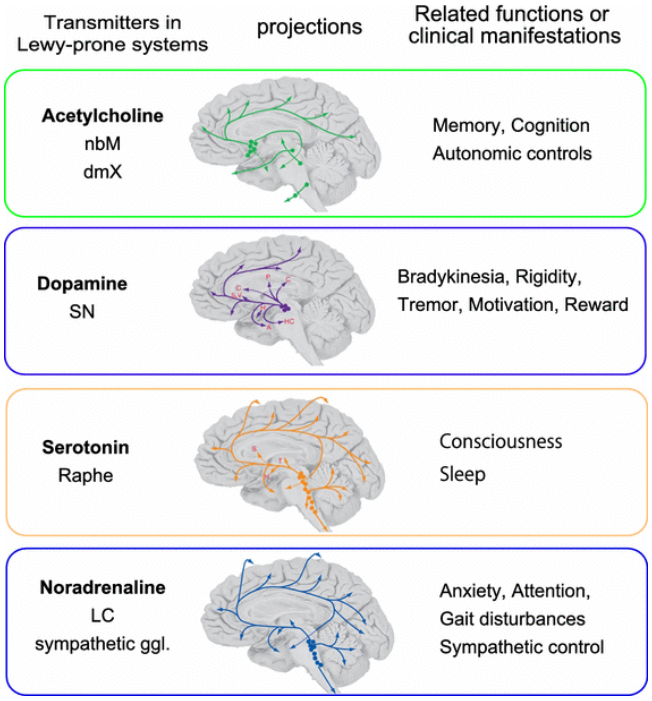

Figure 1. *Lewy-prone systems and neurotransmitters. Although the neurotransmitters are different between associated systems, these Lewy-prone systems are characterized by widespread innervation to the cerebral cortex, basal gangland ia, and hippocampus through hyper branching axons.*

PDD and DLB Neuropathology

PDD has a heterogeneous pathological substrate, which includes (1) Lewy Body/alpha-Synuclein (Syn) pathology in cortical, limbic, and subcortical brainstem structures, (2) AD-related pathologies (amyloid deposition, diffuse and neuritic plaques, and NFTs), and (3) a combination of these pathologies that have been shown to correlate with the severity of cognitive impairment most robustly (Compta et al., 2011; Irwin et al., 2013).

Cognitive impairment is frequently associated with the density of Lewy neurites and neuritic degeneration in the hippocampus and peri amygdaloid cortex, resulting in a disruption of the limbic loop and 'disconnection' from key areas like those described for the hippocampus in Alzheimer's disease (Delbeuck et al., 2003). On this line, earlier clinicopathological research of 242 PD individuals supported the relationship between LBs deposition in the neocortex cognitive decline and bradykinetic start (Selikhova et al., 2009).

As previously said, multiple neurotransmitter deficits resulting from the involvement of subcortical nuclei occur in PDD patients (Halliday et al., 2014; Jellinger et al., 2014). Dementia development is mainly due to:

-the considerable loss of limbic and cortically projecting dopaminergic neurons in the mesocortical limbic system (Halliday et al., 2014);

-the death of neurons in the nucleus basalis of Meynert leading to cortical cholinergic denervation (Colloby et al., 2016; Jellinger et al., 2009);

-the widespread decrease in nicotinic acetylcholine receptors (Hall et al., 2014);

-the LB-induced hippocampal dysfunction (Hall et al., 2014).

Furthermore, PDD patients with hallucinations display cholinergic cell loss in the pedunculopontine, indicating a distinct pattern of cholinergic input structure degradation compared with DLB patients (Hepp et al., 2013).

Figure 2 depicts the neurophysiological model developed by Gratwicke et al., 2015 of the interrelationships between neurotransmitters and their effects on brain cortex functionality in PDD patients.

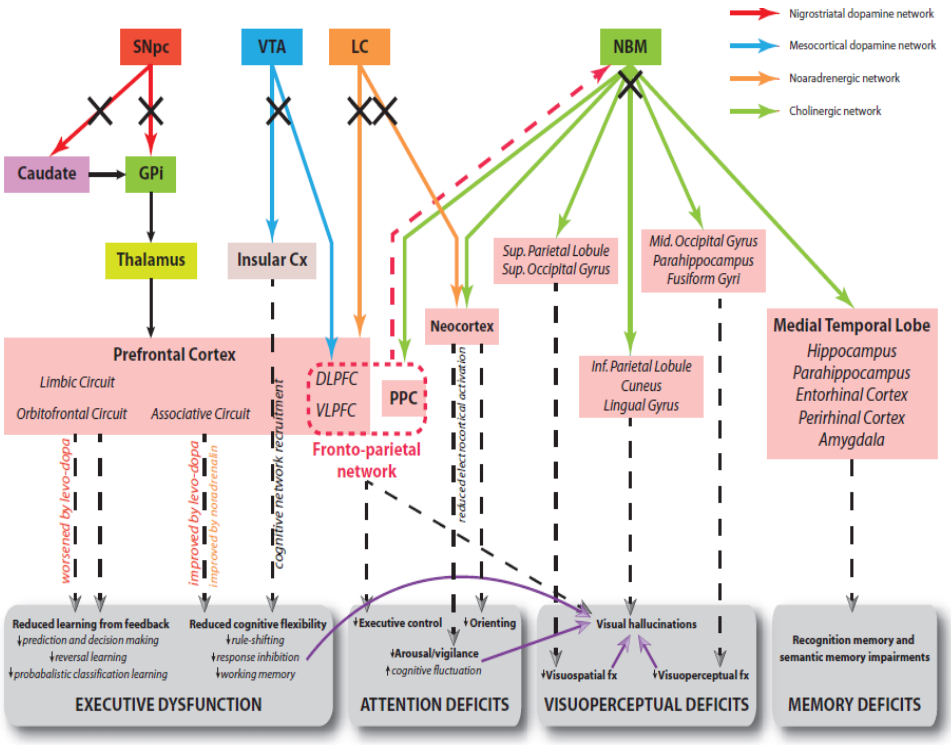

Figure 2. *Hypothetical model of neural circuits malfunctioning in PDD and the corresponding cognitive deficits. Legend: Cx = cortex; DLPFC = dorsolateral prefrontal cortex; GPi = globus pallidus (internus); PPC = posterior parietal cortex; SNpc = substantia nigra pars compacta; VLPFC = ventrolateral prefrontal cortex; VTA = ventral tegmental area (Gratewike et al., 2015).*

Despite many similarities with PDD patients, some studies have demonstrated several morphological differences in DLB patients, including higher amyloid load in the striatum (Halliday et al., 2014; Jellinger et al., 2018) and in the cortex (Ballard et al., 2006; Fujishiro et al., 2010; Jellinger et al., 2018; Ruffmann et al., 2016). Tau pathology in the striatum was also more common in DLB, with the incidence of negative cases being 70% vs 82% in PDD, implying that the morphological distinction between the two illnesses is not limited to amyloid deposition and cortical

Lewy Body pathology (Jellinger et al., 2009). Moreover, it was found a more severe synuclein load in hippocampal subareas CA 2/3 and in the entorhinal cortex (EC) in DLB patients, implying a role for the EC-CA 2 circuitry in the pathophysiology of DLB (Adamowicz et al., 2017). Furthermore, there are differences in the severity and distribution pattern of lesions in SNc: more severe and dominant neuronal loss in the ventrolateral cell groups in PDD (Dickson et al., 2009); more severe damage in the dorsolateral parts in DLB (Aarsland et al., 2005). DLB lacks the distinctive selective degradation of ventral SN neurons seen in Parkinson's disease, which may explain some of the clinical distinctions between the two conditions (Walker et al., 2004).

Finally, DLB patients have significantly higher 5-HT1A receptor-binding density in the cortex than PDD (Francis & Perry, 2007). A recent study has found that reduced levels of the presynaptic protein Rab3A in the DLB inferior parietal lobe were found to be significantly related to the rate of cognitive decline (Bereczki et al., 2016). The significant reduction in synaptic proteins in DLB patients may reflect greater frontal degeneration than in ADD patients, lending credence to the link between cognitive performance and synaptic protein loss in DLB patients (Bereczki et al. 2016).

PDD and DLB patients' clinical features and diagnostic criteria

PDD and DLB patients are both affected by attentional, executive, and memory dysfunctions, mood disturbances, and parkinsonism (defined as bradykinesia in combination with rest tremor, rigidity, or both). Visual symptoms, including visual hallucinations, are common in PDD and DLB. In both, other non-motor features, including autonomic dysfunctions and sleep disorders, may occur according to the severity of dementia, while mood disturbances have a similar frequency (Jellinger et al., 2018).

Even if PDD and DLB have many similar clinical aspects, there are differences in timing and in the profile that allows for the identification of two different clinical syndromes and apply separate diagnostic criteria. In Parkinson's disease, patients primarily suffer from extrapyramidal symptoms that can be followed by slow cognitive impairment, not always progressing into dementia (Jellinger et al., 2018).

According to the guideline described by the Movement Disorder Society (MDS) Task Force (Emre et al., 2007), the diagnosis of dementia associated with Parkinson's disease (PDD) is possible if the patient shows the following summarised in Figure 3 core and associated symptoms.

I. Core features

1. Diagnosis of Parkinson's disease according to Queen Square Brain Bank criteria
2. A dementia syndrome with insidious onset and slow progression, developing within the context of established Parkinson's disease and diagnosed by history, clinical, and mental examination, defined as:
   - Impairment in more than one cognitive domain
   - Representing a decline from premorbid level
   - Deficits severe enough to impair daily life (social, occupational, or personal care), independent of the impairment ascribable to motor or autonomic symptoms

II. Associated clinical features

1. Cognitive features:
   - Attention: Impaired. Impairment in spontaneous and focused attention, poor performance in attentional tasks; performance may fluctuate during the day and from day to day
   - Executive functions: Impaired. Impairment in tasks requiring initiation, planning, concept formation, rule finding, set shifting or set maintenance; impaired mental speed (bradyphrenia)
   - Visuo-spatial functions: Impaired. Impairment in tasks requiring visual-spatial orientation, perception, or construction
   - Memory: Impaired. Impairment in free recall of recent events or in tasks requiring learning new material, memory usually improves with cueing, recognition is usually better than free recall
   - Language: Core functions largely preserved. Word finding difficulties and impaired comprehension of complex sentences may be present
2. Behavioral features:
   - Apathy: decreased spontaneity; loss of motivation, interest, and effortful behavior
   - Changes in personality and mood including depressive features and anxiety
   - Hallucinations: mostly visual, usually complex, formed visions of people, animals or objects
   - Delusions: usually paranoid, such as infidelity, or phantom boarder (unwelcome guests living in the home) delusions
   - Excessive daytime sleepiness

III. Features which do not exclude PD-D, but make the diagnosis uncertain

- Co-existence of any other abnormality which may by itself cause cognitive impairment, but judged not to be the cause of dementia, e.g. presence of relevant vascular disease in imaging
- Time interval between the development of motor and cognitive symptoms not known

IV. Features suggesting other conditions or diseases as cause of mental impairment, which, when present make it impossible to reliably diagnose PD-D

- Cognitive and behavioral symptoms appearing solely in the context of other conditions such as:
  Acute confusion due to
  a. Systemic diseases or abnormalities
  b. Drug intoxication
  Major Depression according to DSM IV
- Features compatible with "Probable Vascular dementia" criteria according to NINDS-AIREN (dementia in the context of cerebrovascular disease as indicated by focal signs in neurological exam such as hemiparesis, sensory deficits, and evidence of relevant cerebrovascular disease by brain imaging AND a relationship between the two as indicated by the presence of one or more of the following: onset of dementia within 3 months after a recognized stroke, abrupt deterioration in cognitive functions, and fluctuating, stepwise progression of cognitive deficits)

Figure 3. *Movement Disorder Society (MDS) Task Force criteria summarized (Emre et al., 2007).*

On the other hand, the core clinical features of DLB have been well described by the DLB Consortium (McKeith et al., 2017) and are summed up in the following:

-**Fluctuations**, occur as spontaneous alterations in cognition, attention, and arousal. They also comprehend incoherent speech, variable attention, or altered consciousness. At least one measure of fluctuation must be documented when considering DLB diagnostic criteria;

-**Recurrent and complex visual hallucinations**, which are present in up to 80% of patients with DLB and so can give support to diagnosis. They are typically well-formed, featuring people, children, or animals, sometimes accompanied by related phenomena including passage hallucinations, sense of presence, and visual illusions;

-**Spontaneous parkinsonian features**, such as bradykinesia and rigidity, are common in DLB, eventually occurring in over 85%, while rest tremor is less frequent (Fritz et al., 2016);

-**REM sleep behavior disorder (RBD)** is a parasomnia characterised by a lack of muscle atonia during REM sleep, thus resulting in the actuation of one's dreams;

Other supportive clinical features that could help for the diagnosis are: severe sensitivity to antipsychotic agents, postural instability, repeated falls, syncope or other transient episodes of unresponsiveness, severe autonomic dysfunction and psychiatric symptoms.
Furthermore, recent scientific advances have discovered indicative biomarkers such as reduced dopamine transporter uptake in basal ganglia demonstrated by SPECT or PET and abnormal (low uptake) 123iodine-MIBG myocardial scintigraphy.

Finally, supportive biomarkers are relative preservation of medial temporal lobe structures on CT/MRI scan; generalized low uptake on SPECT/PET perfusion/metabolism scan with reduced occipital activity, the cingulate island sign on FDG-PET imaging; prominent posterior slow-wave activity on EEG with periodic fluctuations in the pre-alpha/theta range.

For research studies that distinguish between DLB and Parkinson's disease dementia, a 1-year rule is recommended for a diagnosis of DLB, such that dementia should begin no later than one year after the onset of parkinsonism (McKeith et al., 2005).

Risk factors

Different sporadic genetic factors may be involved in the etiopathology of PDD and DLB: mutations in SNCA, the gene of α-synuclein, as well as mutations in GBA (glucocerebrosidase), and MAPT (microtubule-associated protein tau) may be responsible on the onset of the two diseases (McKeith et al., 2017) even if the pathological mechanisms are not yet clarified.

Other risk factors to be considered are:

-**Aging**;

-**APOE-ε4 gene**, provides the blueprint for a protein that transports cholesterol in the bloodstream.

-**Cardiovascular diseases** are risk factors associated with a higher risk of dementia such as smoking (Beydoun et al., 2014), obesity in midlife (Rönnemaa et al., 2001,) and diabetes (Gudala et al., 2013). Midlife hypertension (Rönnemaa et al., 2001) and midlife high cholesterol are also implicated as risk factors for dementia;

-According to the "cognitive reserves" hypothesis, having more **years of education** builds a "cognitive reserve" that enables individuals to better compensate for changes in the brain that could result in symptoms of neurodegenerative diseases (Stern, 2012);

-**Traumatic Brain Injury (TBI)** is associated with twice the risk of developing PDD or DLB, and severe TBI with 4.5 times the risk (Plassman et al., 2000).

PDD and DLB management

There are currently no disease-modifying medications available for LB dementias (Korczyn and Hassin- Baer 2015), although strong evidence supports the use of cholinesterase inhibitors (ChEIs) to treat the cognitive and mental symptoms of these disorders (Galasko, 2017; Rolinski et al., 2012; Wang et al., 2015). This choice is strongly related to a decrease in cholinergic markers in both PDD and DLB (Klein et al., 2010; Shimada et al., 2009). In different meta-analyses, both donepezil and rivastigmine showed favorable effects on both (Boot, 2015; Tsuno, 2016), but only one study identified an effect of memantine in PDD patients (Aarsland et al., 2009). Despite its limited effects, rivastigmine and other ChEIs provided a greater response to cognitive impairment in DLB and PDD than in ADD patients (Connolly & Fox, 2012). Indeed, in both DLB and PDD, ChEIs may reduce apathy, visual hallucinations, and delusions (Sobow, 2007).

It is important to underline that antipsychotics should be avoided due to the possibility of significant reactions in DLB patients (McKeith et al., 2017). Moreover, levodopa is well tolerated in general; however, it caused much less motor response in DLB than in PDD (Boeve et al., 2016) and may be related to an elevated risk of psychosis (Galasko, 2017; Goldman et al., 2008; Molloy et al., 2005).

On a different level, some studies have tried to find strategies for lowering alpha-synuclein levels by inhibiting aggregation or promoting degradation, preventing cell-to-cell transmission of misfolded Syn, and by deep brain stimulation of the cholinergic nucleus basalis of Meynert (Brundin et al., 2017; Zhang et al., 2015).

Alzheimer’s disease introduction and neuropathology

A 2017 report from the Alzheimer's Association stated that almost 50 million patients are suffering from dementia due to AD. Many studies reported that this plague will nearly double every 20 years in the most developed nations, reaching 75 million in 2030 and 131.5 million in 2050.

Alois Alzheimer originally referred to AD as a "peculiar severe disease process of the cerebral cortex". However, it took another 70 years for AD to be acknowledged as a widespread cause of dementia and a significant cause of death. This pathology is initially characterized by an episodic memory disorder, but over time, additional symptoms like language difficulties, disorientation (including a propensity to get lost), mood swings, a lack of motivation, behavioral problems, and eventually a loss of independence in daily living activities appear.

The primary cause of the symptoms in AD is the progressive loss of cholinergic transmission caused by neuronal cell death, which first occurs in the hippocampus and then spreads to the cerebral cortex. It is well known that these parts of the brain are engaged in memory and thinking processing (Selkoe, 1991; Blennow et al., 2006; Mucke, 2009). Two types of protein aggregates are involved in

the neuropathological process that damages the neurons in AD patients: amyloid plaques, also known as senile plaques, and hyper phosphorylated tau-protein tangles, also known as neurofibrillary tangles (Figure 4).

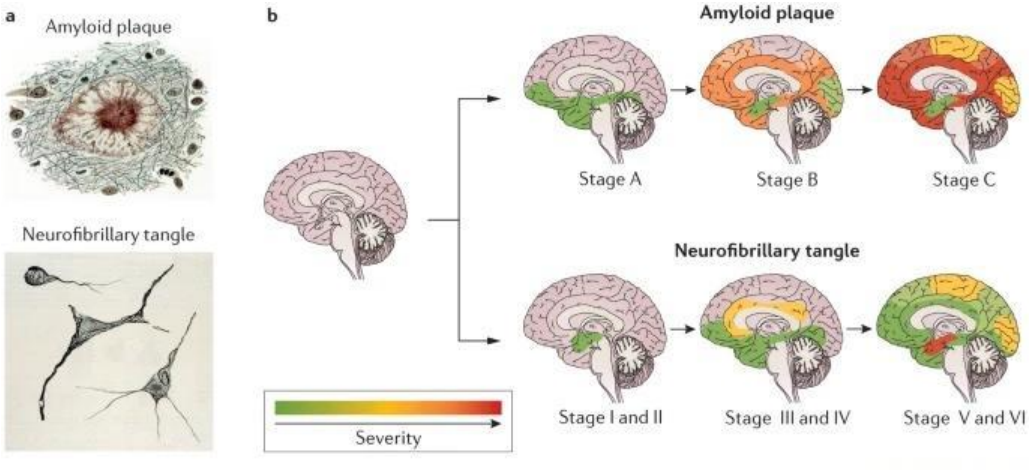

Figure 4. *Schematic representation of amyloid plaques and neurofibrillary tangles spreading in the brain at different stages.*

In particular, extracellular amyloid beta-peptide originates from a transmembrane protein called amyloid precursor protein (APP), which is split into three pieces by the alpha, beta, and gamma secretases (Zhang et al., 2011). Specifically, the APP was normally broken up into tiny fragments by alpha- or beta-secretase, which were subsequently removed from the brain (Zhang et al., 2011). However, a mistake in the sequential cleavage by beta and then gamma-secretase results in the accumulation of 42 amino acid peptides (beta-amyloid 42), which causes neuronal toxicity (Masters et al., 1985). Beta-amyloid 42 accelerates the production of aggregated fibrillary amyloid protein, in contrast to normal APP breakdown. On the other hand, a protein called tau forms neurofibrillary tangles (fibrillary intracytoplasmic aggregates) in neurons. The primary function of tau protein in healthy brains is to maintain axonal microtubules (Braak et al., 2003; Iqbal et al., 2005). The tau protein binds these microtubules together, and they are necessary for intracellular trafficking.

The penetrance of the autosomal dominant disorder Alzheimer's disease is almost 100%. Three genes—AAP on chromosome 21, Presenilin 1 (PSEN1) on chromosome 14, and Presenilin 2 (PSEN2) on chromosome 1—have mutations that lead to the disease's autosomal dominant form. Beta-amyloid peptide synthesis and aggregation may increase as a result of APP mutations. Beta-amyloid aggregation is brought on by PSEN1 and PSEN2 mutations that interfere with gamma-secretase processing. Most cases of early-onset Alzheimer's disease and 5% to 10% of all cases are caused by mutations in these three genes. Apolipoprotein E is yet another genetic risk factor for Alzheimer's disease. It is a lipid metabolism regulator that favors beta-amyloid protein. The APOE gene isoform e4 has been linked to more sporadic and familial variants of Alzheimer's disease that

reveal themselves after the age of 65. Although it is anticipated that 50% of people with one allele and 90% of people with two alleles will eventually develop the condition, the existence of one APOEe4 allele does not guarantee the development of Alzheimer's disease. With each APOE e4 allele, the age at which a disease initially appears gets younger. In conclusion, the APOE e4 allele considerably raises the risk of developing Alzheimer's disease (Nicolas et al., 2018). Both familial and sporadic forms of Alzheimer's disease have been linked to variations in the SORT1 gene, which is necessary for APP to move from the cell surface to the Golgi-endoplasmic reticulum complex.

In addition to the damage to ascending cholinergic projections in Alzheimer's disease, a variety of other neurochemical anomalies have been identified in postmortem human brains (Nicolas et al., 2018). Some of these include decreases in noradrenaline, 5-hydroxytryptamine (5-HT), and 5-HT receptors. Furthermore, it was found that GABA levels are lower in some cerebral cortical regions (Rossor & Iversen, 1986). Additionally, the aetiology of Alzheimer's disease has been linked to both the glutamatergic and cholinergic systems. The glutamatergic hypothesis states that excessive glutamate stimulation of NMDA receptors damages neurons and contributes to cognitive impairment in Alzheimer's patients. The persistent low-level activation of the NMDA receptors required for learning and memory may be brought on by astroglial cells' inability to absorb glutamate in the synaptic cleft (Francis, 2005).

Clinical features and diagnostic criteria

Memory loss and difficulty in executive functions are the primary clinical signs of Alzheimer's disease, both of which are most likely brought on by the death of cholinergic nuclei. The following signs, however, are typical: Alzheimer's Association (2014) lists several symptoms of the disease, including confusion about time or place, difficulty understanding spatial relationships and visual images, new word problems in speaking or writing, losing track of things and being unable to backtrack, decreased or poor judgement, withdrawal from work or social activities, and changes in mood and personality, including apathy and depression. However, the severity of these symptoms is greatly different amongst patients, depending on their premorbid personality, life events, and social and cultural factors. In this competition, the caregiver plays a crucial role in disease management, even if it comes at a great cost in terms of money and quality of life (Megari et al., 2013).

In 1984, the National Institute of Neurological and Communicative Disorders and Stroke-Disease Alzheimer's and Related Disorders Association (NINCDS- ADRDA) issued criteria that recognized Alzheimer's disease as a type of dementia (McKhann et al., 1984). These criteria showed two important critical points: first, the clinical diagnosis of AD could only be given when the disease had advanced to the point of causing significant functional disability and met the dementia threshold

criterion; and second, the clinical diagnosis of AD could only be given when the disease had progressed to the point of causing functional disability and met the AD pathology criterion postmortem. The lack of clinical criteria for the other dementias at the time, as well as a lack of biomarkers, resulted in a low prevalence specificity in distinguishing Alzheimer's disease dementia from other dementias (Varma et al., 1999).

Alzheimer's disease (AD) was changed from a clinicopathological to a clinical biological entity in 2007 by the publication of a new conceptual framework by the International Working Group (IWG) on New Research Criteria for the Diagnosis of AD (Dubois and Albert, 2004). These 2007 IWG criteria proposed that AD could be identified in vivo in the presence of two requisite features and not considering dementia:

1) Evidence of a specific episodic memory profile;
2) Presence of biomarker evidence measured with structural MRI, molecular neuroimaging with PET (F-2-fluoro-2-deoxy-D-glucose PET, FDG PET, or C- labelled Pittsburgh compound B PET, PiB PET); or CSF analysis of amyloid β (Aβ) or tau protein (total tau, T-tau, and phosphorylated tau, P-tau) concentrations.

The most innovative aspect of the 2007 criteria was the first introduction of biomarkers into the core diagnostic framework. New recommendations and diagnostic standards for Alzheimer's disease were released in 2011 by the Alzheimer's Association and the National Institute on Aging (NIA) (Sperling et al., 2011; Albert et al., 2011). These criteria and guidelines update the ADRDA's diagnostic criteria and guidelines issued in 1984 (McKhann et al., 1984) and include three significant changes: (1) They distinguish two stages of Alzheimer's disease: mild cognitive impairment (MCI) caused by Alzheimer's disease and dementia caused by Alzheimer's disease; (2) they propose criteria for a preclinical phase of Alzheimer's disease, which occurs before symptoms such as memory loss develop; and (3) they incorporate biomarker tests.

Finally, the last diagnostic criteria have been proposed by Jack and colleagues in 2018 by the National Institute on Aging—Alzheimer’s Association (NIA-AA) Research Framework. According to that framework, the AD diagnosis can be based on biomarkers derived from in vivo measurements of amyloidosis ('A'), tauopathy ('T'), and neurodegeneration ('N') in the brains of patients with AD, regardless of clinical manifestations of the disease along the continuum from subjective cognitive complaint to mild cognitive impairment (MCI), and then dementia.

While neurodegeneration can be studied using biomarkers from structural magnetic resonance imaging or fluorodeoxyglucose PET mapping, brain amyloidosis and tauopathy can be evaluated using biomarkers from cerebrospinal fluid analysis or positron emission tomography (PET) mapping (Jack et al., 2018). Moreover, brain tauopathy and neurodegeneration biomarkers would provide

information on illness status, whereas brain amyloidosis biomarkers would serve as indicators of disease characteristics (progression).

Despite its advantages, this model had two major objections. The initial complaint centered on the insufficient sensitivity of brain amyloidosis and tauopathy biomarkers in AD diagnosis. It has been hypothesized that a significant proportion of elderly cognitively intact individuals who test positive for the aforementioned brain amyloidosis and tauopathy biomarkers over time do not develop clinical manifestations of the illness (such as MCI and dementia) (Dubois et al., 2021). Due to this, it has been proposed that the presence of positive brain amyloidosis and tauopathy biomarkers may merely represent a risk factor for the onset of AD rather than a definitive diagnosis of AD (Dubois et al., 2021). According to this school of thinking, diagnosing AD should consider not only the existence of brain amyloidosis and tauopathy but also the presence of developing clinical phenotypic characteristics consistent with AD (Dubois et al., 2021).

The second critique centered on the lack of specificity of biomarkers for brain amyloidosis and tauopathy in the diagnosis of AD. According to this theory, aging-related progressive neurodegenerative illnesses including Lewy body disease and Parkinson's disease with dementia can also affect elderly adults with abnormally high levels of the brain biomarkers for amyloidosis and tauopathy (Lemstra et al.,2017). Therefore, in elderly patients with advancing cognitive deficits, the presence of abnormal values in brain amyloidosis and tauopathy biomarkers would not ensure a correct diagnosis of AD.

AD risk factors

The familial form of AD usually appears before age 65, while the sporadic form (not inherited) emerges later in life, after age 65. Less than 1% of instances of Alzheimer's disease are brought on by three gene abnormalities (Bekris et al., 2010). Remarkably, these three genes produce the proteins presenilin 1 and 2 and the amyloid precursor protein (APP) (controlling the action of the enzyme -secretase, as indicated in the preceding paragraph). Because these genes are autosomal dominant, the early onset of AD will result from the presence of almost one copy (allele) of each of these three mutant genes from birth (inherited from a parent). 95% of the time, a mutation in presenilin two results in Alzheimer's disease (Goldman et al., 2011).

There is a hereditary component to both early-onset Alzheimer's and late-onset Alzheimer's. A young age-related risk factor for dementia is trisomy 21. Numerous risk factors have been connected to Alzheimer's disease. Growing older is the leading risk factor for Alzheimer's disease. An increased risk of Alzheimer's disease has been associated with traumatic brain injury, depression, cardiovascular and cerebrovascular disease, older parental age, smoking, a family history of

dementia, raised homocysteine levels, and the presence of the APOE e4 allele. A decreased incidence of Alzheimer's disease has been associated with higher levels of education, estrogen use in women, anti-inflammatory drugs, leisure activities like reading or playing musical instruments, a healthy diet, and frequent aerobic exercise (Nicolas et al., 2018). The likelihood of getting Alzheimer's increases by 10% to 30% if you have a first-degree relative who has the illness. The chance of developing Alzheimer's disease is three times higher in people with two or more siblings than in the general population.

Alzheimer’s disease treatment and management

The cause of Alzheimer's disease is unknown. Only symptomatic treatment is offered (Adlimoghaddam et al., 2018; Leblhuber et al., 2018).

Both partial N-methyl D-aspartate (NMDA) antagonists and cholinesterase inhibitors are used to treat Alzheimer's disease. Acetylcholine is a neurotransmitter that nerve cells use to interact with one another and is crucial for cognition, learning, and memory. Cholinesterase inhibitors operate by increasing the amount of this chemical in the body. FDA-approved treatments for Alzheimer's disease include donepezil, rivastigmine, and galantamine, three drugs in this class.

Throughout all phases of Alzheimer's disease, donepezil is helpful. It is legal to use galantamine and rivastigmine to treat MCI and dementia. Galantamine is available as a once-daily extended-release capsule or a twice-daily pill. Patients with severe liver failure or end-stage renal illness should not use it. Acetylcholinesterase inhibitors that act quickly and are reversible include donepezil and galantamine. Donepezil is commonly preferred over others because it only requires a single daily dose. Rivastigmine inhibits both butyrylcholinesterase and acetylcholinesterase in a reversible manner.

Nausea, vomiting, and diarrhea are typical gastrointestinal adverse effects of cholinesterase inhibitors. The prevalence of sleep problems increases when donepezil is used. Bradycardia, problems with cardiac conduction, and syncope can all result from the elevated vagal tone. These drugs shouldn't be taken by anyone with severe cardiac conduction problems (Winslow et al., 2011).

In addition to that, memantine inhibits NMDA receptors and lessens intracellular calcium accumulation because it is a partial NMDA receptor antagonist. Its use in the management of mild to moderate Alzheimer's disease has received FDA approval. Constipation, headaches, body aches, and dizziness are typical adverse effects. Inhibitors of cholinesterase may be coupled with it. In the medium to late stages of Alzheimer's disease, anxiety, depression, and psychosis are common. It is also helpful in treating these conditions. Tricyclic antidepressants should be avoided due to their anticholinergic action. When all other treatments for acute agitation have failed, antipsychotics are

the last resort. However, the modest risk of stroke and death must be weighed against their modest benefits (Winslow et al., 2011).

To address behavioral difficulties, environmental and behavioral strategies are quite helpful. Simple techniques that can be very helpful in regulating behavioral disorders include maintaining a familiar environment, assessing personal comfort, supplying security objects, redirecting attention, removing door knobs, and avoiding confrontation. By providing exposure to sunlight and daytime activity, mild sleep interruptions can be addressed to lessen caregiver stress.

The anticipated benefits of the treatment are modest. Treatment should be adjusted or stopped if there are no appreciable benefits or unacceptably severe side effects. Finally, regular aerobic exercise has been shown to slow the progression of Alzheimer's disease.

Focus on neuroimaging techniques applied to neurodegenerative diseases

Neuroimaging and fluid biomarkers are a promising area of research for detecting ADD, PDD, and DLB patients (Saeed et al., 2017). Multiple brain imaging procedures such as Positron Emission Tomography (PET), Magnetic Resonance Imaging (MRI), and Computed Tomography (CT) scans can be used to highlight abnormalities in the brain (Lizio et al., 2016).

The high spatial resolution, sensitivity, and specificity of MRI are the reason why this technique is considered the most powerful instrument for identifying structural alterations and cerebral atrophy using volumetric measures of the entire brain (Kochunov et al., 2005). In the field of Alzheimer’s disease pathology, some MRI studies showed that in AD patients, there was greater atrophy of medial temporal lobe structures (hippocampus, amygdala, entorhinal cortex, and parahippocampal gyrus) than in patients with DLB, particularly the hippocampus (Burton et al., 2009). Furthermore, MRI in AD displays ventricular dilatation and a reduced total volume in the brain (Busatto et al., 2008).

In AD, it was found that the atrophy is localized at the medial temporal limbic cortex level, even in the initial phases of the disease. Then it extends to paralimbic cortical regions and to the neocortex (Braak et al., 2003). Several longitudinal MRI studies demonstrated that grey matter atrophy is also seen in ADMCI subjects (Schroeter et al., 2009).

Other promising techniques are the FDG-PET and SPECT, which provide information about regional glucose metabolism and cerebral perfusion, respectively. In AD patients, the common FDG-PET and SPECT patterns are hypometabolism and hypoperfusion of the parietal-temporal cortex (Herholz et al., 2002). PET images allow in vivo analysis of Aβ42 presence in the brain and their spatial distribution. PiB results are closely related to the amyloid plaque burden revealed in the autopsy (Ikonomovic et al., 2008; Small et al., 2000). Hypometabolism in temporoparietal regions

also changes in cerebral structure and may be evident also before the onset of advanced cognitive symptoms in AD.

As said in the previous paragraphs, Dubois and colleagues in 2007 have underlined the importance of cerebrospinal fluid markers (CSF) in the preclinical stages of Alzheimer's disease. In specific, very important is measuring the concentration of Aβ42, total tau (t-tau), and phosphorylated tau (p-tau) in the CSF because it reflects the abnormalities in the brain. Generally, healthy elderly people show a higher level of amyloid protein compared to healthy younger people, but the neurophysiological process allows them to excrete in the CSF the abnormal proteins that are toxic to their health. This process is not working in AD patients, where there happens a high accumulation of amyloid plaques in the brain. On the contrary, high levels of tau protein in the CSF reflect the progression of the disease associated with the presence of tau protein in the cerebral cortex (Seppala et al., 2012). Thus, low levels of Aβ42, together with increased levels of p-tau and t-tau in the CSF, can identify AD with good accuracy (Babiloni et al., 2020b). However, even if low levels of Aβ42 in the CSF appear early in the AD course and seem to predict the conversion from MCI to AD (Buchhave et al., 2012), in some cases, they appear earlier in subjects with normal cognition, during a phase that precedes MCI condition (Fagan et al., 2009). It is not already clear if a decrease in CSF Aβ42 concentration levels precedes the increase in tau levels or vice-versa (Fagan et al., 2009). Interestingly, it was shown that the reduction of Aβ42 levels in CSF precedes cognitive impairment in non-demented subjects by about eight years (Stomrud et al., 2007; Ringman et al., 2012). As mentioned above, Dubois et al. (2014) assert that the information about low Aβ42 and high p-tau and t-tau concentrations in CSF significantly increases the accuracy of AD diagnosis even at a prodromal stage.

Considering the PDD and DLB patients, the DaTScan SPECT or 18-Fluorodopa PET showed a high reduction of dopamine transport binding in caudate and posterior putamen (Gomperts et al., 2016). Voxel-based morphometric MRI studies revealed greater grey matter loss in frontotemporal, occipital, and parietal areas in DLB compared to PDD (Beyer et al.,2007). 11C PIB-PET imaging showed increased Aβ brain deposition in more than 50% of DLB cases, with more modest and less frequent Aβ accumulation in PDD patients (Gomperts et al., 2016). Of interest, PDD patients had a lower dopamine uptake in the striatum compared with DLB patients, which correlated with dopaminergic cell loss in substantia nigra pars compacta and the severity of parkinsonism (Colloby et al., 2012). White matter hyperintensities (WMH) on T2-weighted MRI have been observed in parieto-occipital areas in PDD cases and are associated with low CSF Aβ levels (Compta et al., 2016). More severe WMHs have been observed in the temporal lobe of DLB patients (Sarro et al., 2017).

Promising topographical biomarkers are those derived from the analysis of resting-state eyes-closed electroencephalographic (rsEEG) rhythms (Breslau et al., 1989; Briel et al., 1999; Giaquinto & Nolfe, 1986; Lizio et al., 2016). The recording of rsEEG rhythms is noninvasive and cost-effective. rsEEG markers can probe the mechanisms underlying the brain circuits associated with cognitive functions and provide an index of cortical arousal and vigilance in quiet wakefulness in patients with neurodegenerative diseases (Del Percio et al., 2019; Babiloni et al., 2020a). Despite this marginal importance of rsEEG biomarkers in ADD, ADMCI, PDD, and DLB patients' assessment, previous studies suggest that rsEEG rhythms have a significant heuristic and clinical potential. Indeed, the rsEEG rhythms are extremely interesting as biomarkers of brain systems underpinning the disease-related abnormalities in cortical arousal and vigilance regulation (Babiloni et al., 2020a, 2021a; Rossini et al., 2020).

For example, previous studies showed that as compared to cognitively intact older adults (Healthy), DLB patients were characterized by (1) more variability and greater power in frontal, parietal, and temporal rsEEG delta (<4 Hz) and theta (4–7 Hz) rhythms; (2) slowing in frequency and lower power in posterior rsEEG alpha (7–9 Hz) rhythms; and (3) appearance of additional rhythms between theta and alpha rhythms (5.5–8 Hz), the so-called "pre-alpha" rhythms (Andersson et al., 2008; Bonanni et al., 2008; Jackson et al., 2008; Kai et al., 2005; Walker et al., 2000a,b). In this vein, abnormalities in rsEEG pre-alpha and/or alpha frequencies were evident in posterior areas, but they were even greater in frontal areas (Franciotti et al., 2020). Furthermore, those abnormalities predicted the conversion from mild cognitive impairment (MCI) to DLB (Bonanni et al., 2016). Moreover, there were increased pre-alpha power, decreased beta power, and slower dominant frequency in patients with mild cognitive impairment due to Lewy bodies (LBMCI) as compared to patients with mild cognitive impairment due to Alzheimer's disease (ADMCI) (Schumacher et al., 2020a, 2020b). In LBMCI patients, structural MRIs of the atrophy in the basal cholinergic forebrain were related to abnormalities in rsEEG rhythms, namely, the greater that atrophy, (1) the greater the theta and pre-alpha power, (2) the lower the dominant frequency, and (3) the lower the alpha and beta power density (Schumacher et al., 2021).

Furthermore, in PDD patients, rsEEG rhythms are characterized by a "slowing". Specifically, this "slowing" can be measured as (i) an abnormally high amplitude (power) of topographically widespread rsEEG rhythms at delta (< 4 Hz) and theta (4-7 Hz) frequency bands and (ii) a poor amplitude of the posterior rsEEG rhythms at alpha frequency band (Serizawa et al., 2008; Bonanni et al., 2008; Kamei et al., 2010; Pugnetti et al., 2010; Babiloni et al., 2017). Similar results were observed in PD patients with mild cognitive impairment (PDMCI), namely a prodromal stage of PDD (Babiloni et al., 2017). Furthermore, abnormalities in the individual rsEEG delta and alpha rhythms

were related to global cognitive deficits, motor deficits, and visual hallucinations in PDD and PDMCI patients (Babiloni et al., 2020b). Moreover, a daily dose of levodopa (875 mg) induced a widespread reduction in individual rsEEG delta and alpha source activities in a group of PDD and PDMCI patients under a standard chronic dopaminergic regimen (Babiloni et al., 2019). Another study showed a partial normalization in delta and alpha rsEEG rhythms by dopaminergic therapy (Melgari et al., 2014). From a pathophysiological point of view, the reported "slowing" of the rsEEG rhythms in PDD patients may be associated with the core PD neuropathology.

Finally, as compared to the control seniors with intact cognition (Healthy), AD patients with mild cognitive impairment (ADMCI) and dementia (ADD) were characterized by increased rsEEG rhythms at delta (< 4 Hz) and theta (4-7 Hz) frequencies in widespread cortical regions as well as by decreased rsEEG rhythms at alpha (8-13 Hz) and beta (14-30 Hz) frequencies in central and posterior cortical regions; these effects were typically discussed concerning the death of cortical neurons, axonal pathology, and cholinergic neurotransmission deficits (Babiloni et al., 2020a, 2021a; Rossini et al., 2020). Several studies in ADMCI patients have shown that rsEEG biomarkers can track the disease progression effects on the neurophysiological mechanisms regulating cortical arousal and vigilance at 12 months or longer follow-ups. Specifically, ADMCI patients were characterized by reduced posterior rsEEG alpha rhythms at a follow-up of about 12 months (Babiloni et al., 2013). In another study, a group of ADMCI patients showed increased posterior rsEEG theta-delta rhythms and decreased rsEEG alpha-beta rhythms at a follow-up of 21 months (Jelic et al., 2000). Compared to MCI patients unaffected by AD, the ADMCI patients presented increased posterior rsEEG theta rhythms at a follow-up of 24 months (Jovicich et al., 2019).

The rsEEG biomarkers were also used to track the disease progression in ADD patients. Those patients showed increased posterior rsEEG delta-theta rhythms at a follow-up of 12 months (Soininen et al., 1989). In another study, ADD patients showed increased widespread rsEEG delta rhythms and reduced posterior rsEEG alpha and beta rhythms at a follow-up of about 12 months (Babiloni et al., 2013). In longer longitudinal studies, ADD patients were characterized by increased rsEEG delta-theta rhythms and decreased rsEEG alpha rhythms at a follow-up of 24 months (Sloan & Fenton, 1993), while increased posterior rsEEG theta-delta rhythms and reduced rsEEG alpha-beta rhythms were reported at a follow-up of 30 months (Coben et al., 1985). The above results suggest that rsEEG alpha rhythms may reflect progressive abnormalities in the neurophysiological oscillatory mechanisms regulating cortical arousal and quiet vigilance in ADMCI patients.

In-depth study of electroencephalography (EEG)

Electroencephalography (EEG) is a non-invasive method to record the electrical activity of the brain along the scalp. It has a high temporal resolution (milliseconds), which is sufficient to track brain activity, but a rather low spatial resolution (around a centimetre), which is fundamentally constrained by the distances between the sensors and by the fundamental law of electromagnetic. In 1929, Hans Berger made the discovery that when two tiny metal plates (electrodes) were brought into contact with the skin, there was a difference in their electrical potential. Herbert Jasper later improved the EEG technique by determining the potential difference between an active electrode, which captures neural activity, and a reference electrode. The EEG is primarily the product of the cortex level summation of postsynaptic potentials, which involves the synchronized activity of around 100,000 neurons. Their ions do not line up and produce waves that can be detected if the cells do not have identical spatial orientations. Because they fire in unison, pyramidal neurons in the cortex are thought to produce the highest EEG signal.

Electrons are positioned at precise locations on the scalp to detect and record the electrical impulses within the brain. The oscillations seen in EEG activity exhibit a variety of properties (such as frequency ranges, spatial distributions, etc.) that are connected to distinct states of brain function (e.g., waking and the various sleep stages). The number of times a wave repeats itself in a second is known as a frequency. Our mental performance may deteriorate if any of these frequencies are insufficient, excessive, or challenging to access. The strength of the electrical impulses the brain produces is represented by their amplitude. Microvolts are units used to measure the volume or strength of brain wave activity.

The electroencephalography is typically described in terms of rhythmic activity and transients. The rhythmic activity is divided into frequency bands: gamma greater than 30Hz, beta (13- 30Hz), alpha (8-12 Hz), theta (4-8 Hz), and delta (less than 4 Hz). These designations depend on the rhythmic activity within a certain frequency and are related to a certain distribution over the scalp or a certain biological significance. Usually, the interval of frequencies of interest at the clinical level ranges from 0.1 and 100 Hz and it can be even more restricted in routine clinical settings (e.g., between 0.1 and 70 Hz) (Amzica and Lopes da Silva, 2017). The main frequency bands are shown in Figure 5 and described below:

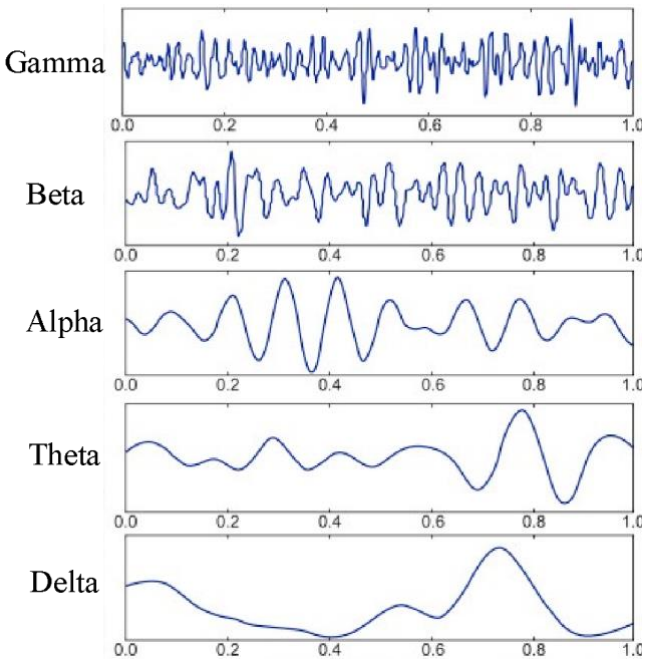

Figure 5. *Normal adult brain waves (they are referred to 1s of duration): delta (< 4 Hz), theta (4-7 Hz), alpha (8-13 Hz), beta (14-30 Hz), and gamma (30-100 Hz).*

Delta is the lowest frequency (range up to 4 Hz). Physiologically, it can be recognized as the rhythm of the third and fourth stage of human sleep and eventually in anesthesia conditions. Delta may also occur in the presence of subcortical lesions and it's usually marked in the frontal areas in adults (e.g. FIRDA - Frontal Intermittent Rhythmic Delta) and in children's posterior areas (e.g. OIRDA - Occipital Intermittent Rhythmic Delta). Slow waves and high amplitudes define the delta band. At the neurophysiological level, delta rhythm can be the result of the exchange between two membrane currents: the transient calcium current (It) undertaking the low-threshold spike (LTS) and a hyperpolarization-activated cation current (Ih) in thalamocortical cells. The depolarization of the membrane near the threshold for a burst of sodium-dependent rapid action potentials is caused by the activation of low threshold calcium current. Then, the portion of Ih that was active just prior to the calcium spike is rendered inactive by depolarization. Repolarization of the membrane due to It inactivation is followed by a hyperpolarizing overshoot due to the reduced depolarizing effect of Ih. The hyperpolarization in turn de-inactivates Ih and stimulates It, which depolarizes the membrane toward the threshold for another calcium spike (Amzica and Lopes da Silva, 2017).

Theta is the frequency that goes from 4 Hz to 7 Hz. Even if theta is present in young children, in older children and adults, it may manifest as drowsiness or arousal; excessive theta for age denotes inappropriate activity. Theta rhythm should not be confused with a slowing down of alpha activity found in metabolic encephalopathy, deep midline abnormalities, or some cases of hydrocephalus; it can be seen as a focal disturbance in specific subcortical lesions (Ingvar et al., 1976; Saunders and

Westmoreland, 1979). It is thought that theta reflects activity in the limbic and hippocampus areas. Anxiety, behavioral activation, and behavioral inhibition are all characterized by theta (Shadli et al., 2021). Theta rhythm mediates and/or encourages sophisticated, adaptive processes like memory and learning when it seems to be operating correctly. There isn't a clear mechanism for how the theta rhythm is produced. The primary theory is on the action of acetylcholine on hippocampal interneurons, which upon activation send theta rhythmic impulses in the direction of the pyramidal cells of the cortex. The main network involved in this connection is the supramammillary nucleus of the hypothalamus to the medial septum with the extension to the brainstem and diencephalon. However, it appears that glutamatergic inputs may potentially contribute to the formation of the theta rhythm (Amzica and Lopes da Silva, 2017).

Alpha is the frequency range from 7 Hz to 13 Hz, generally with a predominant peak at 10 Hz. **It emerges with the closing of the eyes and with relaxation and attenuates with eye-opening or mental exertion**. Alpha rhythm is more evident in the occipital cortex. The posterior basic rhythm is slower than 8 Hz in young children (therefore technically in the theta range.

The brain is constantly in an alpha state, which is characterized by attentiveness (it is a sign of alertness and sleep), but not by active information processing). In addition to the well-known alpha rhythm of the visual cortex, rhythmic activities in the same frequency range can be recorded from the temporal cortex and somatosensory cortex. Experimental studies in vivo and in vitro have tried to explain the mechanism of the generation of the alpha rhythm. Alpha current generators were discovered in all layers using fine microelectrode arrays in monkeys (across the inferior temporal cortex and visual cortex), with the infragranular neurons (layer V) acting as the predominant local generator in the visual cortex. In contrast, in the inferior temporal cortex, alpha current generators were found in supragranular (layers I-III) and infragranular layers (layers V-VI), with the supragranular generator acting as the primary local generator. However, the alpha activity recorded in the cortex should be driven by the activation of thalamic cells (Amzica and Lopes da Silva, 2017). Cats' nucleus geniculate in vitro tests have demonstrated the formation of the alpha rhythm following activation of the metabotropic glutamate receptor (mGLUR1a), which is situated on the postsynaptic level of the corticothalamic fibres (Hughes and Crunelli, 2005).

Beta is the frequency range from 14 Hz to about 30 Hz. It is fast activity, and it reflects desynchronized brain tissue as it is a proper rhythm of the wakefulness. It is seen usually on both sides in symmetrical distribution and is most evident frontally Beta activity is closely linked to motor behaviour and is generally attenuated during active movements. Active, busy, or anxious thinking and active concentration are frequently associated with low amplitude beta with many and variable frequencies. A prominent set of frequencies in rhythmic beta has been linked to several diseases and

pharmacological effects, including benzodiazepines. In regions of cortical injury, it might be lacking or diminished. Patients who are attentive, agitated, or who have their eyes open typically have this rhythm as their primary one. The combination of acetylcholine, serotonin, and noradrenaline on the nucleus reticularis of the thalamus produces beta rhythm, which activates thalamic cells and suppresses the activity of the slow waves on the cortical cells.

Gamma is the frequency range of approximately 30–100 Hz. Gamma rhythms are assumed to be the joining of various populations of neurons into a network to perform a particular motor or cognitive function. It is believed that the 40Hz activity consolidates the necessary areas for simultaneous processing when the brain needs to process information from diverse areas concurrently. A healthy and effective 40Hz activity is linked to a strong memory, but a 40Hz deficit results in learning impairments. Arousal, attentiveness, and electrical stimulation of the mesencephalic reticular formation all contribute to the activation of acetylcholine muscarinic receptors, which in turn produces synchronized gamma frequency oscillations.

EEG data acquisition

The *International Federation of Clinical Neurophysiology* (IFCN) has stated the parameters for recording brain activity in quiet wakefulness. Resting-state electroencephalographic (rsEEG) rhythms are frequently captured from patients' scalps during brief (i.e., minutes) settings with their eyes closed and open during clinical studies. To identify brain dysfunctions in the control of calm wakefulness in psychiatric and neurological illnesses, this research primarily focuses on abnormalities in the frequency and topographical characteristics of rsEEG rhythms. The selectivity and effectiveness of several higher cognitive functions, including attention (i.e., focused, sustained, selective, or reflexive), episodic memory (i.e., encoding and retrieval of autobiographical events), and executive frontal functions, may be impacted by vigilance dysregulations (i.e., working memory and inhibitory control).

First, individuals should be told to get regular sleep the night before the rsEEG rhythm recording a few days before it takes place. Additionally, subjects should be told not to consume any drugs or psychotropic substances (i.e., foods and drinks including nicotine, caffeine, alcohol, and other stimulants in any form in the morning of the experiment). Patients may receive their psychoactive medication (i.e., benzodiazepines, antidepressants, etc.) the day before the EEG recording as usual but not in the morning of that recording (the decision for this act should be agreed upon after proper clinical consultation). It is expected that such a brief drug withdrawal shouldn't be enough to induce discontinuation issues and should enable matching the treatment regimen assumption in all enrolled subjects. Second, the morning following a filling light breakfast is the

optimum period for recording rsEEG rhythms. Thirdly, a quick interview with the subjects should verify the circumstances as well as the typical subjects' level of sleep the night before the recording. If the results are bad, the recording should be put off until later.

The following requirements must be met for the rsEEG rhythm recording experiment in clinical neurophysiology of alertness to be successful: The subject should be positioned on a comfortable half-reclining chair or bed, the room should be quiet and dimly lit, and the wall in front of him or her should be painted with a uniform light color (e.g., white, very pale yellow, or green), leaving only a central fixation target at the height of his or her eyes. There are three common resting-state conditions: the first checks the neurophysiological systems by keeping the eyes closed and in a low alertness state for a few minutes (i.e., 5-15 min). The experimenter (or qualified technologist) shouldn't warn the participant if they start to nod off because it also investigates the shift from alertness to sleep. The subject is instructed to sit still, maintain a relaxed state of mind wandering (i.e., no goal-oriented mental activity), and maintain closed eyelids. The second condition examines the neurophysiological processes that control sequential eye-opening and closure and an increase and decrease in alertness (i.e., 5-10 min). The periods of eyes-open and -closed in response to the experimenter’s suggestions are short (i.e., 1 min), and the alternation of eyes-open and –closed is repeated (i.e., 2-4 times).

Like the first condition, the subject is given instructions. To get enough EEG data pertaining to the right mental set, the experimenter will need to warn the participant if they fall asleep. The experimenter will repeat the instructions if the subject does not comply. The third condition examines the neurophysiological processes that support the steady maintenance of low vigilance for three to five minutes with the eyes closed and moderate vigilance with the eyes open (i.e., 3-5 min). The subject is given instructions that are similar to those in the second condition. The recording of the EEG is obtained by placing electrodes on the scalp with a conductive gel or paste, according to the preferred method (applying single electrodes or a cup). When high-density arrays of electrodes are required, using the cup may be the best option. It is crucial to clean the scalp area before applying the electrodes in order to reduce impedance caused by dead skin cells.

The International 10–20 system is a widely accepted approach for describing and applying where scalp electrodes should be placed during an EEG test or experiment. This technique was created to provide consistent reproducibility so that participants could be compared to one another and to the studies of other subjects across time. This system is based on the relationship between the location of an electrode and the underlying area of the cerebral cortex. The "10" and "20" indicate the actual distances between adjacent electrodes (10% or 20% of the total front–back or right–left distance of the skull.)

Each site has a letter designating the lobe and a number designating the position within the hemisphere. The letters F, T, C, P, and O stand for frontal, temporal, central, parietal, and occipital lobes, respectively. Because there is no center lobe, the letter "C" is merely used for identification. A midline electrode is referred to as a "z" (zero). Electrode placements with even numbers (2,4,6,8) are on the right hemisphere, whereas those with odd numbers (1,3,5,7) are on the left. In addition, the letter codes A, Pg, and Fp identify the earlobes, nasopharyngeal and frontal polar sites respectively. The nasion, which is the clearly depressed area between the eyes, just above the bridge of the nose, and the inion, which is the lowest point of the skull from the back of the head and is typically indicated by a prominent bump, are the two anatomical landmarks used for the crucial positioning of the EEG electrodes (Figure 6). Additionally, the EEG system necessitates the use of a reference electrode, whose voltage is measured, often placed in an electrically neutral location, in order to record the signal of brain activity (this area could have a background electrical activity and could introduce "noise" which is a source of artifact).

The EEG activity, which is visible on the scalp, is the accumulation of ionic currents from several generators. The current is generated by the generator, and it travels through the surrounding tissues and liquids. Because of the distance between the skull and brain and their different resistivities, EEG data collected from any point on the human scalp includes activity generated within a large brain area. This volume conduction provokes the spatial smearing of EEG data and is not possible to have an exact topographic estimation of the electrical source.

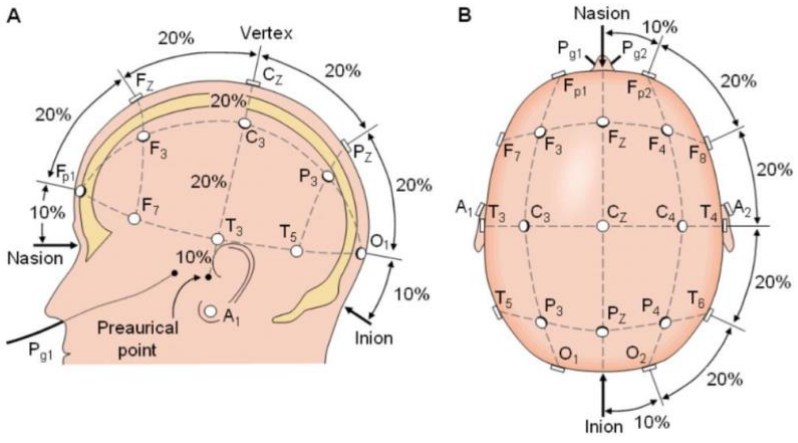

Figure 6. *Diagram of the international 10/20 system seen from the (A) left and (B) above the head. Each electrode is assigned a nomenclature with a letter and a number. The letters indicate the areas of the scalp: F (Frontal), C (Central), T (Temporal), P (Parietal), and O (Occipital); numbers are odd for the left side and even for the right side.*

Inverse solution method

"Inverse solutions approaches" are techniques for localization. A decent method for a real functional tomography enables one to reduce the inaccuracy in the source current estimation. Tomography can never be completely accurate, though. From a more upbeat perspective, it is reasonable to assume that whatever scant information the EEG measurements do contain will be sufficient to enable for at least an "approximate" tomography. The linear inverse problem was solved for this work using the freeware eLoreta (exact low resolution brain electromagnetic tomography) (Pascual-Marqui, 2007). A discrete, three-dimensional (3D), distributed, linear, weighted minimal norm inverse solution is what the eLORETA method achieves. The MNI152 template was used for computations in the current iteration of eLORETA, and the three-dimensional solution space was constrained to cortical grey matter as established by the probabilistic Talairach atlas. On the scalp of the MNI152, the typical electrode positions were taken from (Jurcak et al., 2007; Oostenveld and Praamstra, 2001). At a 5 mm spatial resolution, 6239 voxels make up the intracerebral volume. Therefore, in the neuroanatomic Montreal Neurological Institute (MNI) space, eLORETA images depict the electric activity at each voxel as the precise magnitude of the estimated current density. With Talairach space correction, anatomical designations such as Brodmann regions are also reported using MNI space (Brett et al., 2002).

Influence of Reticular Activating system on EEG rhythms

The first observation of a wake-related structure was that intact brain-stem structures were critical to maintaining arousal, as evidenced by EEG recordings in cats (Moruzzi & Magoun, 1949). The definition of the ascending reticular activation system (ARASs) was given to indicate the arousal systems (Figure 7). It reaches the cortex through (a) a ventral pathway (basal forebrain cholinergic nuclei and histaminergic neurons of posterior hypothalamus); (b) the aminergic nuclei (the noradrenergic neurons of the locus coeruleus, the serotoninergic neurons of the raphe nuclei); (c) and a dorsal pathway, the thalamic relay (Steriade & McCarley, 1990). Most recently, a descending pathway to the spinal cord has been discovered to be important for maintaining muscle tone (it also plays a role in support of vigilance) (Steriade & McCarley, 1990).

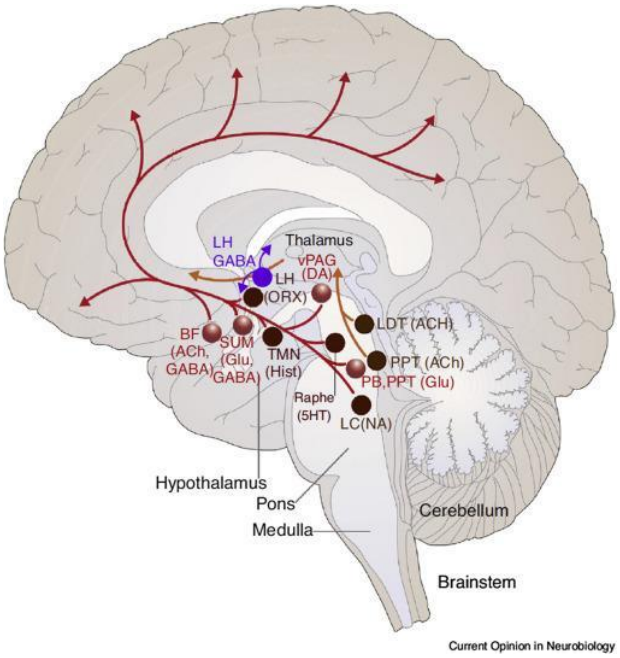

Figure 7. *Neuroanatomy and neurochemistry of wakefulness. In red is the backbone of the arousal system with fast neurotransmitter systems, and in brown are the more modulatory monoaminergic, cholinergic, and peptidergic systems. Abbreviations: 5HT, serotonin; Ach, acetylcholine; DA, dopamine; Glu, glutamate; Hist, histamine; NA, noradrenaline; ORX, orexin (hypocretin).*

The ventral pathway of ARASs

As I shortly said before, it is composed of the basal forebrain and posterior hypothalamus. The first is a set of structures important in the production of acetylcholine, which is then distributed widely throughout the brain. The cholinergic neurons tonically discharge during wakefulness (Buzsaki et al., 1988). They can act directly on the cerebral cortex or thalamic reticular neurons suppressing them and generating the spindles of sleep. The release of **acetylcholine** from the nuclei of the basal forebrain induces cortical desynchronization and fast EEG rhythms, while deactivation of this area induces cortical synchronization with slow waves activity of EEG rhythms (Casamenti et al., 1986). The activity of the basal forebrain is modulated by the neurons of the lower brain reticular structure (i.e., glutamatergic, noradrenergic, histaminergic, and GABAergic).

In particular, **GABAergic ascending neurons** also project to the cortex and play a synergic activity with cholinergic neurons in modulating cortical activation (Freund & Meskenaite, 1992; Jones et al., 2005). On the other hand, the posterior hypothalamus has widespread projection connecting with a lot of brain regions involved in the control of the wakefulness (cortex, thalamus, basal forebrain, anterior hypothalamus, and brain stem cholinergic and noradrenergic nuclei). It contains different neurotransmitters (dopamine, glutamate, GABA, histamine) and neuropeptides.

Some experimental data have shown the importance of another neurotransmitter that is histamine. First discovered as a neuromodulator of an immune response, then it has been recognized as a transmitter inducing drowsiness if blocked (Passani et al., 2007).

The Aminergic system

The location and projections of diffuse ascending reticular monoaminergic system, which includes the dopaminergic (DA), noradrenergic (NA), serotonergic (5-HT), and histaminergic (HA) circuitries, were discovered in the 1960s for their important role in psychiatric disorders. Figure 7 shows the main locations of cholinergic and aminergic nuclei with their projections to the cerebral cortex. Inhibition of catecholamine (dopamine and noradrenaline) synthesis induces waking disturbances; on the contrary, an accumulation of them is responsible for the waking state and behavioral excitation (Fuxe et al., 2007).

The tonic activity of noradrenergic, dopaminergic, and serotoninergic neurons that is observed during the wake decreases during sleep. Noradrenergic neurons are also involved in the activation of wake onset, as revealed by experiments in noradrenergic neurons of the locus coeruleus in mice (Carter et al., 2009). Some brainstem noradrenergic neurons are also involved in paradoxical sleep, and they modulate cortical arousal as well as cognitive aspects of waking, such as perception (Berrige et al., 2012). Dopaminergic neurons play an important role in the control of motor function via mesostriatal pathways as well as motivation and cognitive aspects via mesocortical and mesolimbic pathways that can modulate cortical arousal (Gratewicke et al., 2015). A lesion of dopaminergic cells of periaqueductal grey matter results in increased sleep (Lu et al., 2006). Furthermore, the drug “modafinil" which promotes wake, acts through dopamine D2 receptors in the ventral tegmental area (VTA) (Korotkova et al., 2003).

Finally, serotonin induces inhibition through the action on 5-HT 1 A receptors at the postsynaptic level (Jones et al., 2005), but its synergic activity with acetylcholine may play a role in cortical activation (Dringenberg & Vanderwolf, 1998).

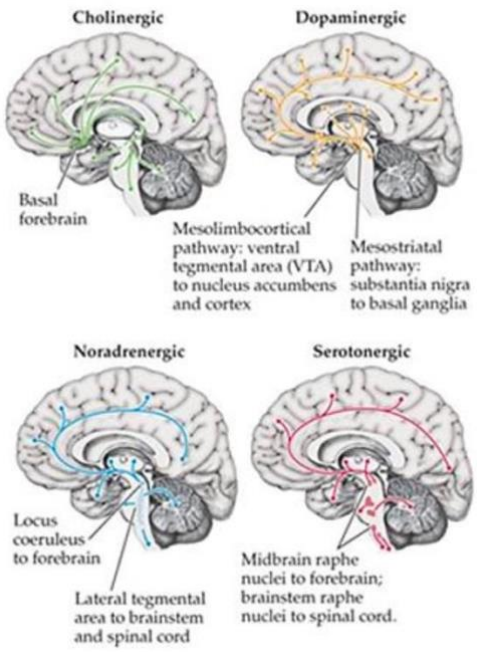

Figure 8. *Single components of ARASs (i.e. cholinergic and aminergic networks) regulating wakefulness (revised from Watson and Breedlove 2016).*

The Dorsal pathway

The critical constituent of the ascending reticular activating system is **the thalamus.** First discovered by Galen in the first century, from the 18th century it is considered the gateway of sensory inputs that receives and sends inputs to the cortex (Bickford et al., 1994) playing an important role in the neuromodulation of the brain. A perithalamic region of reticular nuclei surrounds the thalamus. This region takes the name of the reticular thalamus, and it is rich in GABAergic neurons. It receives inputs from the fifth and sixth layers of the cortex and from the relay thalamus (so defined as they receive excitatory glutamatergic input from peripheral sensory pathways and projects to one or few well-defined cortical areas). The reticular nucleus is important in the control of thalamocortical and corticothalamic connections through the modulation of GABAergic input on the relay thalamus (figure 3). It can be divided into different sections that have connections with the thalamus and cortex and different functions (sight, hearing, touch, movement, or limbic functions).

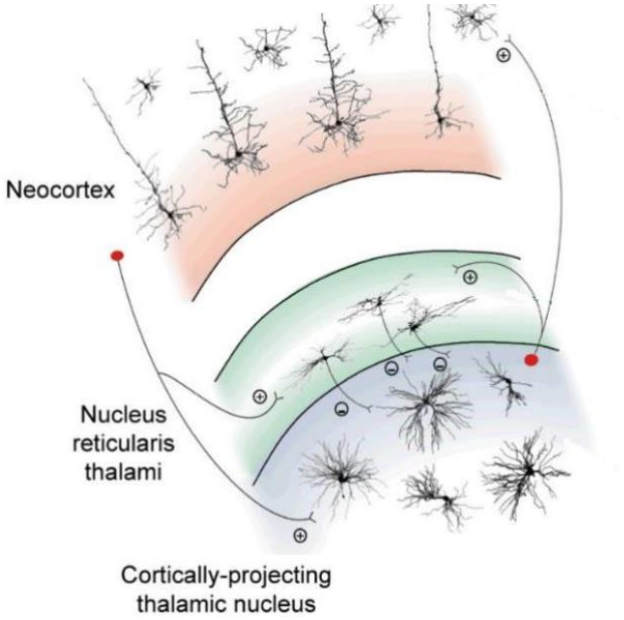

Figure 9. *Schematic diagram of a cortico-thalamo-cortical module with its most relevant cellular components and synaptic connections (thalamic interneurons and neocortical neurons other than those in layer 4 and 5/6 have been omitted for clarity). (+) and (−) indicate excitatory and inhibitory synapses, respectively. (Revised from Crunelli and Hughes 2010).*

Located in the diencephalon, the thalamus is formed by four components (hypothalamus, epithalamus, ventral thalamus, and dorsal-relay thalamus). The most important region is the dorsal thalamus, composed of allothalamic and the isothalamic region. The allothalamic region can be divided in (a) the paraventricular region (receiving afferents from the amygdala); (b) the centre-median-parafascicular complex which appears to be a major element in the basal ganglia system that is involved in motor control (having projections to the striatum); (c) and the intralaminar region that receives inputs from ascending reticular activating system and plays a modulatory role in the regulation of cortical arousal (Edward et al., 2017).

The isothalamic constitutes 90% or more of the dorsal thalamus and contains the major projections to the cortex. Lesions of these areas could affect cognition. The internal and superior laminae divide the isothalamus into several subregions (regio superior, superregio medio- posterior, superregio basalis and regio inferolateral).

Among the above-mentioned subregions: the nucleus medialis receives a large projection from the dorsolateral prefrontal cortex, amygdala, ventral globus pallidus, and nigral projections. It projects to the prefrontal cortex, and it is involved in cognition, the sleep-wake cycle, and executive function (Muzur et al., 2002). The pulvinar-lateral posterior complex, which has a lot of reciprocal connections with the associated parieto-occipito-temporal cortical areas, is involved in attention and it is correlated to visual hallucination; the motor thalamus in the inferolateral region transfers information from the substantia nigra (sub-regio dorsalis), the globus pallidus (subregio oralis) and

the cerebellum (subregio intermedia) to the prefrontal, supplementary, premotor, motor and somatosensory areas of the cerebral cortex. The motor thalamus receives projections from the nucleus perithalamicus in a specific diffuse manner, which can also contribute to the transfer of motor information (Ramanathan et al., 2018).

Electrical experiments on brain slices have suggested that thalamic activity is sufficient to alter the cortical state. Thalamocortical neurons are directly excited by stimulation of the brain stem reticular nuclei. During wakefulness, brief activation of the thalamic reticular nucleus is sufficient to evoke thalamic bursts and cortical spindles (Halassa et al., 2011). They receive cholinergic input from the cholinergic reticular nuclei at the midbrain pontine junction and aminergic input from locus coeruleus and raphe nuclei as shown by some experiments in rats but the monoaminergic neurons seem not be involved in tonic activation processes of thalamocortical systems (Jones and Moore, 1977). On the contrary, the result of the local application of a cholinergic agonist is a loss of hyperpolarizing oscillation, an increase of metabolic activity of the thalamic neurons and an EEG desynchronized (Buzsaki et al., 1988).

EXPERIMENTAL PART: The studies

In seniors, Lewy Body diseases account for almost 10-20% of dementia cases (McKeith et al., 2005). Parkinson's disease (PD) is usually characterized by tremors, bradykinesia, and stiffness. However, cognitive symptoms have recently caught the attention of researchers because of how strongly they emerge over time (humor disturbance, frontal executive dysfunctions, and dementia; Schneider et al., 2017).

On the other hand, Dementia with Lewy bodies (DLB) is clinically defined as increasing dementia, commonly accompanied by parkinsonism and visual hallucinations. DLB patients experience more frequent neuropsychiatric symptoms such as psychosis, sadness, and apathy, as well as disabling cognitive deficits (i.e., dementia) and sleep behavior abnormalities when compared to patients with dementia due to Alzheimer's and Parkinson's diseases (ADD and PDD; Aarsland et al., 2005; Bostrom et al., 2007a, 2007b; Ricci et al., 2009; Rongve et al., 2010a).

Finally, with between 60 and 80 percent of cases, AD is the most frequent cause of dementia (ADD) in elderly adults. At the neuropathological level, AD is characterized by the aggregation of two essential aberrant proteins: extracellular plaques of amyloid protein and neuronal neurofibrillary tangles, which are caused by improper phosphorylation of tau, the microtubule-associated protein. Although all cognitive functions are gradually affected, these changes are predominantly linked to severe memory loss (Alzheimer's Association 2016).

Due to the increasing impact of these disorders among the elderly and the dearth of disease-modifying drugs, costs related to managing these types of patients are projected to increase soon. Consequently, there is much interest in learning more about the neurobiological and neurophysiological aspects of these diseases, with the approval of valuable biomarkers for ADD, PDD, and DLB patients that can verify the functionality of brain circuits underlying cognitive activities, even in the prodromal stage of diseases with mild cognitive impairment, MCI (i.e., ADMCI, PDMCI, LBMCI) (Petersen et al., 2001).

Over the years, different biomarkers have been developed for diagnosing neurodegenerative diseases associated with dementia. Specifically, structural imaging technologies such as computer-assisted tomography (CAT) and magnetic resonance imaging (MRI) were firstly used in clinical research. Then they were followed by the creation of positron emission tomography (PET) and single photon emission computed tomography (SPECT) (Lizio et al., 2016). Finally, thanks to technological developments, functional magnetic resonance imaging (fMRI) made it possible to map oxygen

consumption and regional blood flow in specific brain regions (Lizio et al., 2016). These new procedures have the benefits that they are non-invasive and with a high spatial resolution. However, due to their low temporal resolution, these functional brain imaging approaches are not appropriate for investigating functional brain activations and distinguishing the activation of different relays within a dispersed network.

On the other hand, electroencephalography (EEG) has a low spatial resolution compared to other techniques. However, it has a high temporal resolution, which allows for measuring the temporal synchronization mechanism of cortical pyramidal neurons. The EEG's high temporal resolution is crucial for studying spontaneous and event-related oscillatory activity at different frequencies, which reflect the physiological functioning of a specific brain state (Babiloni et al., 2020a).

Recent works have highlighted that the electroencephalogram measured under resting-state conditions (rsEEG) is a valid candidate for better understanding the neurobiological and neurophysiological aspects of different neurodegenerative diseases (Schumacher et al., 2020a; Babiloni et al., 2020a). Specifically, rsEEG markers can provide an index of cortical arousal and vigilance in a peaceful waking state in patients with neurodegenerative diseases (Del Percio et al., 2019; Babiloni et al., 2020a).

Specifically, vigilance and arousal are regulated by the projections of ascending reticular activating systems (ARASs), primarily composed of neural circuits of sub-systems formed by nuclei and fiber projections (Lin et al., 2011). Anatomically, ARASs are formed by parallel sub-systems running across the brainstem, basal forebrain, and diencephalon using different neurotransmitters such as dopamine, noradrenaline, serotonin, histamine, acetylcholine, and glutamate with different contributions to the regulation of general brain arousal and vigilance states (Moruzzi & Magoun, 1949).

Notably, experimental studies have shown that a high level of vigilance in parallel with high activity of ARASs was associated with desynchronization of the cortical EEG signals at alpha (8-12 Hz) and beta (13-30 Hz) frequency bands and with the synchronization frequencies in the theta (4-7 Hz) and gamma (> 30 Hz) bands. On the contrary, when mental activity is at rest during an eyes-closed condition, in a quiet vigilance, rsEEG signals appear characterized by a synchronized activity at alpha rhythms (Moruzzi & Magoun, 1949; Buzsaki et al., 1988). Moreover, Buzsaki and colleagues demonstrated that cholinergic neurons play a prominent role in the variation of event-related vigilance with consequent changes in ongoing EEG activity (Buzsaki et al., 1988). The malfunctioning of these subcortical cholinergic and dopaminergic neuromodulatory circuits can cause a range of behavioural and cognitive dysfunctions, such as those observed in the most common progressive

neurodegenerative disorders such as ADD and DLB, which are in turn associated with abnormalities in rsEEG rhythms recorded during the eyes-closed condition (Berridge et al., 2003; Gratwicke et al., 2015).

Different studies have shown that ADD and PDD patients exhibited higher power density in widespread rsEEG delta (<4 Hz) and theta (4-7 Hz) rhythms during the eyes-closed condition (Brassen & Adler,2003; Onofrj et al., 2003; Reeves et al., 2002; Rodriguez et al., 2002; Bosboom et al., 2009; Caviness et al., 2016; Kamei et al., 2010; Melgari et al., 2014; Stam et al., 2006). Specifically, DLB patients were characterized by diffuse and fluctuating rsEEG delta and theta power density with some spectral differences from those observed in PDD and ADD (Andersson et al., 2008; Bonanni et al., 2008, 2015, 2016; Kai et al., 2005; McKeith et al., 2017; Onofrj et al., 2003; Walker et al., 2000). These abnormalities can also be found in some prodromal stages. For instance, as compared to the control seniors with intact cognition (Healthy), ADMCI patients were characterized by increased rsEEG rhythms at delta (< 4 Hz) and theta (4-7 Hz) frequencies in widespread cortical regions, in parallel with a decrease in posterior cortical alpha (8-13 Hz) and beta (14-30 Hz) frequencies. In addition, some studies showed that ADMCI patients were characterized by reduced posterior rsEEG alpha rhythms after a 12-month follow-up (Babiloni et al., 2013) and by an increase of posterior rsEEG theta-delta rhythms at a follow-up of 21 months (Jelic et al., 2000).

Another promising neurophysiological biomarker of the quiet vigilance alteration is the measurement of the posterior rsEEG alpha rhythms reduction in amplitude (reactivity) in the transition from the eyes-closed to the eyes-open condition (Babiloni et al., 2022). Indeed, in this passage, most of the inactive cortical neurons oscillating at the alpha frequencies receive sensory signals from thalamocortical projections, which are, in turn, activated by cholinergic projections of the basal forebrain. This activation switches the brain into a state of increased arousal with an oscillatory activity > 30 Hz in the range of high-frequency beta and gamma rhythms (Pfurtscheller and Lopes da Silva, 1999). An altered rsEEG alpha reactivity could be an indicator of neurophysiological damage to the integrity of the thalamocortical and ascending cholinergic and activating systems (McBride et al., 2014; Wan et al., 2019).

Interestingly, recent studies demonstrated that rsEEG alpha reactivity during the eyes open condition is abnormal in ADD, PDD, and DLB patients (Schumacher et al., 2020a). Specifically, the rsEEG alpha reactivity was lower in the ADD and DLB groups than in the Healthy group, and in the DLB, the reactivity was less than in the ADD group (Schumacher et al., 2020a). Further evidence reported that the rsEEG alpha reactivity was significantly lower in ADMCI patients and patients with Mild Cognitive Impairment due to Lewy Bodies (LBMCI) than in Healthy seniors, with no significant difference between the two MCI groups (Schumacher et al., 2021).

Although the above results on the rsEEG alpha reactivity are insightful, some considerations suggest that they present some methodological limits. Usually, the topographical and spectral analysis of rsEEG rhythms is performed at the scalp level so that it may be affected by reference electrode and head volume conduction effects (Nunez, 1996). The usage of eLORETA freeware for the estimation of the cortical sources of rsEEG rhythms (eLORETA; Pascual-Marqui, 2007) may be an essential tool for the spatial analysis of the rsEEG alpha reactivity (Babiloni et al., 2022).

Furthermore, many studies on rsEEG rhythms applied the standard (fixed) frequency bands in all participants despite their remarkable interindividual variability. Indeed, the choice of fixed EEG bands did not consider the "slowing" of the EEG rhythms in ADD, DLB, and PDD patients (Bonanni et al., 2016; Cozac et al., 2016; Moretti et al., 2004). Thus, another step forward in studying the rsEEG alpha reactivity during the eyes-open condition might regard the usage of individual bands in frequency analysis calculated by evaluating some frequency landmarks such as the transition frequency (TF) and the individual alpha frequency peak (IAF; Klimesch, 1996, 1998, 1999).

Finally, the last considerations could be related to a good rsEEG alpha neurophysiological definition. As said before, in normal conditions, the rsEEG alpha rhythm is highest in amplitude when a subject is awake and relaxed with eyes closed and is attenuated when the subject opens the eyes or when occupied with a mental effort. However, the rsEEG alpha rhythm could also be substituted during the resting-state condition if the subject goes to sleep and is in drowsiness (Bonanni et al., 2016; Cozac et al., 2016; Moretti et al., 2004). Therefore, a fine analysis of rsEEG alpha rhythms should be based on two criteria to define them: (i) the presence of a sharp power density peak of the rsEEG alpha rhythms in the posterior regions of the scalp during the eyes-closed condition; (ii) an evident reduction (reactivity) of that amplitude in the passage from the eyes-closed to the eyes-open condition (Bonanni et al., 2008, 2015; Franciotti et al., 2020; Schumacher et al., 2020b).

All the above methodological improvements were used in the present PhD thesis. We expected that those improvements would help us to better understand how the damages in the cholinergic neuromodulatory ascending systems in ADMCI and ADD patients and the impairments of both dopaminergic and cholinergic neuromodulatory ascending systems in PDD and DLB patients could affect the brain neurophysiological oscillatory mechanisms underpinning the regulation of quiet vigilance in humans. Specifically, here we tested the hypothesis of significant abnormalities in the neurophysiological oscillatory mechanisms underlying the regulation of quiet vigilance during the transition from an eyes-closed to an eyes-open condition in ADD, DLB, and PDD patients and initial abnormalities in the prodromal stages of ADMCI. Three rsEEG studies were performed for that purpose.

This aim was pursued by three retrospective and exploratory rsEEG studies developed in the international clinical and EEG databases of the High-resolution EEG Laboratory at the Department of Physiology and Pharmacology “V. Erspamer " at the Sapienza University of Rome. These studies were developed in cooperation with the Partners of the PDWAVES Consortium(www.pdwaves.eu).

First study

REACTIVITY OF POSTERIOR CORTICAL ELECTROENCEPHALOGRAPHIC ALPHA RHYTHMS DURING EYES OPENING IN COGNITIVELY INTACT OLDER ADULTS AND PATIENTS WITH DEMENTIA DUE TO ALZHEIMER'S AND LEWY BODY DISEASES

Methods and Participants

In the present retrospective and observational study, clinical and rsEEG data were derived from an international archive formed by the following Clinical Units of The PDWAVES Consortium (www.pdwaves.eu) and European DLB Consortium: Sapienza University of Rome (Italy), IRCCS SDN of Naples (Italy), IRCCS Oasi of Troina (Italy), Hospital San Raffaele of Cassino (Italy), IRCCS Hospital San Raffaele Pisana of Rome (Italy), University "G. D'Annunzio" of Chieti and Pescara (Italy), Istanbul University (Turkey), Izmir University (Turkey), and Newcastle University (UK). Specifically, those data referred to age-, gender-, and education-matched DLB (N = 42), ADD (N = 48), and Healthy (N = 28) participants having rsEEG recordings with consistent eyes-closed and eyes-open conditions. Of note, each clinical unit of the present study provided at least Healthy participants and patients with dementia of one pathological group (i.e., ADD or DLB). A larger contribution of patients came from the Istanbul University, Izmir University, and Newcastle University clinical units.

The diagnosis of ADD was based on the criteria of the Diagnostic and Statistical Manual of Mental Disorders, fourth edition (DSM-IV-TR; American Psychiatric Association) and the National Institute of Neurological Disorders and Stroke–Alzheimer Disease and Related Disorders (NINCDS–ADRDA; McKhann et al., 2011). Exclusion criteria for the ADD patients were other significant neurological, systemic, or psychiatric illness, mixed dementing diseases, enrolment in a clinical trial with experimental drugs, the use of antidepressant drugs with anticholinergic side effects, high dose of neuroleptics or chronic sedatives or hypnotics, antiparkinsonian medication and the use of narcotic analgesics (Babiloni et al., 2020b).

The diagnosis of the probable DLB was carried out according to the mentioned consensus guidelines (McKeith et al., 2017). Among the datasets used in this study, 13 out of 42 DLB patients received a DaTSCAN to confirm the diagnosis of DLB. The clinical features of the DLB patients were detected as follows: (1) the Neuropsychiatric Inventory (NPI) item-2 tested the occurrence frequency and the severity of hallucinations (Cummings JL et al., 1994); (2) the severity of the

frontal dysfunction was investigated by Frontal Assessment Battery (FAB) (Dubois et al., 2000); (3) the presence and severity of the cognitive fluctuations by Clinician Assessment of Fluctuations (Walker et al., 2000a; 200b); (4) extrapyramidal signs were evaluated by Unified Parkinson Disease Rating Scale-III (UPDRS-III) (Fahn et al., 1987); and (5) minimal International Classification of Sleep Disorders criteria (1992) were used to determinate the presence and/or absence of rapid eye movement (REM) sleep behavior disorder (RBD).

Twenty-eight Healthy seniors, selected from the Clinical Units in equal percentages of the patients, were also studied as age-matched controls (17 males, mean age 74.2 years ± 1.5 standard error of the mean, SE; range of 57-87 years). Exclusion criteria for Healthy seniors were (1) the presence of neurological or psychiatric diseases (previous or present), (2) the presence of a condition of depression (detected with a GDS score higher than 5), (3) the use of chronic psychoactive drugs, and (4) significant chronic systemic illnesses (e.g., diabetes mellitus).

All participants received the Mini-Mental State Examination (MMSE) to measure the status of global cognition. Table 2 summarises the relevant demographic and clinical (i.e., MMSE score) information about the Healthy, ADD, and DLB groups, together with the results of the statistical analyses computed to evaluate the presence or absence of statistically significant differences among them as age (ANOVA), gender (Freeman-Halton test), education (ANOVA), and MMSE score (Kruskal-Wallis test). As expected, a statistically significant difference was found between the Healthy and the other two groups for the MMSE score ($p = 0.0001$), showing a higher score in the Healthy than the ADD and DLB groups (post-hoc test = $p < 0.05$). On the contrary, no statistically significant differences were found in the age, gender, and education among the groups ($p > 0.05$).

	HEALTHY	**ADD**	**DLB**	**Statistical Analysis**
N	28	48	42	
Age (mean years ± SE)	74.2 ± 1.5	74.6 ± 1.0	74.8 ± 1.5	n.s. (ANOVA
Age (min ÷ max)	57 ÷ 87	56 ÷ 87	53 ÷ 89	-
Gender (M/F; % of M)	17/11; 60.7%	32/16; 66.7%	31/10; 76.2%	n.s. (Freeman-Halton)
Education (mean years ± SE)	9.8 ± 0.8	9.9 ± 0.4	9.1 ± 0.6	n.s. (ANOVA)
MMSE (mean score ± SE)	28.4 ± 0.3	20.1 ± 0.6	21.2 ± 0.8	H (2, 118) = 59.6, p < 0.00001 (Kruskal-Wallis test) Healthy > ADD, DLB

Table 1. *Mean values (± standard error of the mean, SE) of the demographic and clinical data as well as the results of their statistical comparisons ($p < 0.05$) in the groups of cognitively normal older adults (Healthy, N = 28) and patients with dementia due to Alzheimer's disease (ADD, N = 48) and Lewy Body Disease (DLB, N= 42). Legend: M/F = males/females; n.s. = not significant ($p > 0.05$); MMSE = Mini Mental State Evaluation.*

The local institutional Ethical Committees approved the study. All experiments were performed with the informed and overt consent of each participant or caregiver, in line with the Code of Ethics of the World Medical Association (Declaration of Helsinki) and the standards established by the local Institutional Review Board.

Cognitive assessments of participants

The performance in various cognitive domains including language, visuospatial function, executive function/attention, and memory was assessed by a battery of neuropsychological tests. Specifically, it included: (i) language was tested by Verbal fluency test for letters (Novelli et al., 1986) and Verbal fluency test category (fruits, animals, or car trades; Novelli et al., 1986); (ii) visuospatial functions were assessed by Line Orientation test (Benton et al., 1978) and Face Recognition test (Benton et al., 1983); (iii) executive functions and attention were evaluated by the Trail making test part A and B (Reitan, 1958), Stroop test (Stroop, 1935), and Confusion Assessment Method (executive function part; Inouye et al., 1990); and (iv) memory was tested by Digit Span Forward and Backward (Wechsler et al., 1987), Oktem Verbal Memory test (Oktem et al., 1992), and Confusion Assessment Method (memory part; Inouye et al., 1990). Finally, to evaluate global cognitive status, Mini-Mental State Exam (MMSE) was performed (Folstein et al., 1975). Of note, for each cognitive domain, the clinical units provided one or more of the above-mentioned neuropsychological tests.

The rsEEG recordings

Electrophysiological data were recorded by professional digital EEG systems licensed for clinical applications. The following digital EEG systems were used: BrainAmp 32-Channel DC System (Brain Product GmbH, Germany), Waveguard caps (ANT Neuro, The Netherlands), EB Neuro-BE LIGHT (EB Neuro, Italy), Galileo NT Line - EB Neuro (EB Neuro, Italy), and EB Neuro-Sirius BB (EB Neuro, Italy).

All rsEEG recordings were performed in the late morning. The rsEEG recordings were performed in all participants using at least 30 scalp exploring electrodes placed according to the 10–10 system. These electrodes were denoted as “selected electrodes” and their location is illustrated in Figure 1. The ground electrode was attached to the right clavicle or on the forehead, while linked earlobes (A1 and A2) or Fz served as the active reference for all the electrodes during recording. Electrode impedance was kept below 5 kΩ; continuous EEG data were recorded at a sampling frequency of 500-1024 Hz and related antialiasing bandpass between 0.01 Hz and 60-100 Hz.

Horizontal electrooculography (EOG) potentials (0.3-70 Hz bandpass) were also recorded to control eye movements and blinking.

The participants were seated in a comfortable armchair during the rsEEG recording and instructed to remain awake, psychophysically relaxed (no movement), and with the mind freely wandering (no mental planning or particular cognitive operations). Based on the instructions given by an experiment, each rsEEG recording lasted 3-5 minutes in the condition of eyes closed, followed by 3-5 minutes in the condition of eyes open. Participants were supervised by the experimenter during the rsEEG recording to monitor adherence to the protocol. The experimenter may kindly invite participants to adhere to the protocol if needed. All deviations by the protocol and verbal interventions were annotated and used during the phase of rsEEG data analysis.

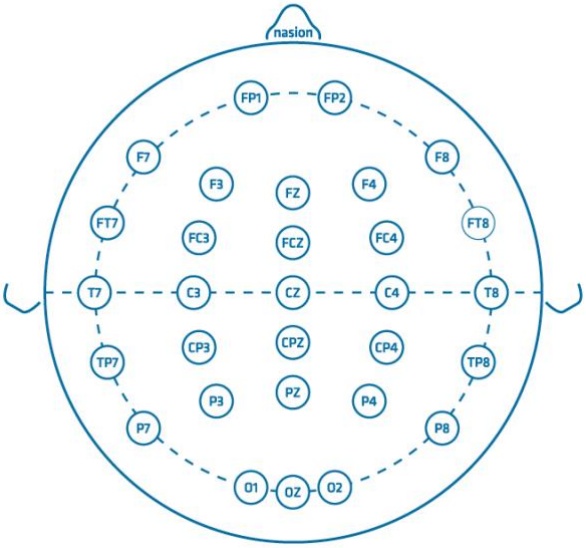

Figure 1. *Electroencephalographic (EEG) electrode montage. The electrode montage included 30 scalp monopolar sensors placed following the 10–10 System (i.e., Fp1, Fp2, F7, F3, Fz, F4, F8, FT7, FC3, FCz, FC4, FT8, T7, C3, Cz, C4, T8, TP7, CP3, CPz, CP4, TP8, P7, P3, Pz, P4, P8, O1, Oz and O2).*

Preliminary rsEEG data analysis

The rsEEG data were centrally analyzed by experts blind about the participants' diagnosis by the Sapienza University of Rome unit. The recorded rsEEG data were exported as European data format (.edf) or EEGLAB set (.set) files and then processed offline using the EEGLAB toolbox (Delorme A and Makeig S, 2004; version eeglab14_1_2b) running in the MATLAB software (Mathworks, Natic, MA, USA; version: R2014b). The rsEEG data were divided into epochs lasting 2 s (i.e., 5 minutes = 150 rsEEG epochs of 2 s for each experimental condition) and analyzed offline. Afterwards, they received a 3-step procedure aimed at detecting and removing (1) recording channels (electrodes) showing prolonged artifactual rsEEG activity due to bad electric contacts or other

reasons; (2) rsEEG epochs with artifacts at recording channels characterized by general good signals; (3) intrinsic components of the rsEEG epochs with artifacts.

The first step was based on a visual analysis of the recorded rsEEG activity by two independent experimenters among four experts (i.e., C.D.P, R.L., G.N., S.L., F.T., and I. L.) for a first identification of the selected electrodes affected by irremediable artifacts. Indeed, there were no more than 3 selected electrodes removed for each participant. For the clinical units with a digital EEG system using > 30 exploring electrodes, the removed electrodes were substituted with the nearest electrodes not included among the 30 selected electrodes. The added electrodes were then used together with the artifact-free selected electrodes to compute the interpolation of artifact-free rsEEG data at all scalp sites of the removed electrodes (EEGLAB toolbox, Delorme A and Makeig S, 2004; version eeglab14_1_2b), thus ensuring that all participants had artefact-free EEG data at the locations of the 30 selected electrodes.

The second step was based on a visual analysis of the recorded rsEEG activity by two independent experimenters (i.e., C.D.P, R.L., G.N., S.L., F.T., and I.L.) for a first selection of artifactual rsEEG epochs. The rsEEG epochs contaminated by muscular, ocular, head movements, or non-physiological artifacts were removed. Of note, the rsEEG epochs with the ocular artifact were less than 5% in the Healthy group and 8% in the ADD and DLB groups. The rsEEG epochs with the muscular artifact were less than 2% in the Healthy group and 3% in the ADD and DLB groups.

The third step was implemented by an independent component analysis (ICA) from the EEGLAB toolbox, applied to remove the ICA components representing the residual artifacts due to (1) blinking and eye movements, (2) involuntary head movements, (3) neck and shoulder muscle tensions, and (4) electrocardiographic activity (Crespo-Garcia, 2008; Jung 2000). For each rsEEG dataset, less than 5 ICA components were removed from the original ICA solutions based on 30 ICA components. In the third step, the rsEEG datasets were reconstructed with the remaining (artifact-free) ICA components, and the putative artifact-free rsEEG epochs were visually double-checked again by two independent experimenters (i.e., C.D.P, R.L., G.N., S.L., F.T., and I. L.) to confirm or make the final decision about the inclusion or the exclusion of each of those rsEEG epochs.

The resulting artifact-free EEG data for the common 30 selected electrodes have used an input for 2 additional methodological steps. The first additional step served to harmonize rsEEG data recorded by the clinical units using different reference electrodes and sampling frequency rates. The rsEEG data were frequency-band passed at 0.1-45 Hz and down sampled, when appropriate, to make the sampling rate of all artifact-free rsEEG datasets in the Healthy, ADD, and DLB participants equal to 256 Hz. Furthermore, all those rsEEG epochs were re-referenced to the common average reference.

The second additional step was used to minimize the habituation effects in rsEEG data recorded during the eyes-open condition. Only the first minute of those rsEEG data (when the rsEEG alpha reactivity is supposed to be well represented) was considered in the further analyses.

As a result of the above procedures, the artifact-free epochs showed a similar proportion (> 75%) of the total amount of rsEEG activity recorded in all groups of participants (i.e., Healthy, ADD, DLB). For the eyes-closed condition (5 minutes = 150 rsEEG epochs each lasting 2 s), the mean of artefact-free rsEEG epochs was 125 (± 3 standard error, SE, 83%; 125 rsEEG epochs X 2 seconds = 250 s) in the Healthy group, 120 (± 2 SE, 80%; 120 rsEEG epochs X 2 s = 240 s) in the ADD group, and 124 (± 3 SE, 83%; 124 rsEEG epochs X 2 ss = 248 s) in the DLB group. For the eyes-open condition (1 minute = 30 rsEEG epochs of 2 seconds), the mean of the artefact-free rsEEG epochs was 29 (± 1 SE, 96%; 29 rsEEG epochs X 2 s = 58 s) in the Healthy group, 28 (± 1 SE, 95%; 28 rsEEG epochs X 2 s = 56 s) in the ADD group, and 28 (± 1 SE, 95%; 28 rsEEG epochs X 2 s = 56 s) in the DLB group. A statistical procedure (ANOVA) showed no statistically significant difference ($p > 0.05$) in the amount of the artifact-free rsEEG epochs between the three groups of participants ($p > 0.5$) for both conditions (eyes-closed and eyes-open).

Spectral analysis of the rsEEG epochs

A standard digital FFT-based analysis (Welch technique, Hanning windowing function, no phase shift) computed the power density of artifact-free rsEEG epochs at all 30 scalp electrodes (0.5 Hz of frequency resolution). From those spectral solutions, the rsEEG frequency bands of interest were individually identified based on the following frequency landmarks, namely the transition frequency (TF) and background frequency (BGF) observed in the eyes-closed condition. In the eyes-closed rsEEG power density spectrum, the TF was defined as the minimum of the rsEEG power density between 3 and 8 Hz, while the BGF peak was defined as the maximum power density peak between 6 and 14 Hz. The TF and BGF were computed for each participant involved in the study. Based on the TF and BGF, we estimated the individual delta, theta, and BGF bands as follows: delta from TF -4 Hz to TF -2 Hz, theta from TF -2 Hz to TF, low BGF (BGF 1 and BGF 2) from TF to BGF peak, and high-frequency BGF (or BGF 3) from BGF to BGF + 2 Hz. Specifically, the individual BGF 1 and BGF 2 bands were computed as follows: BGF 1 from TF to the frequency midpoint of the TF-BGF range and BGF 2 from that midpoint to BGF peak. The other bands were defined based on the standard fixed frequency ranges used in the reference rsEEG studies of our Consortium (Babiloni et al., 2017, 2018a,b,c, 2019, 2020b; Pascarelli et al., 2020): beta 1 from 14 to 20 Hz, beta 2 from 20 to 30 Hz, and gamma from 30 to 40 Hz (see Figure 2).

As mentioned in the Introduction, the BGFs were denoted as "alpha rhythms" if there was a reduction in magnitude (reactivity) of rsEEG rhythms at the BGFs from the eyes-closed to the eyes-open condition, as shown by rsEEG spectral measures.

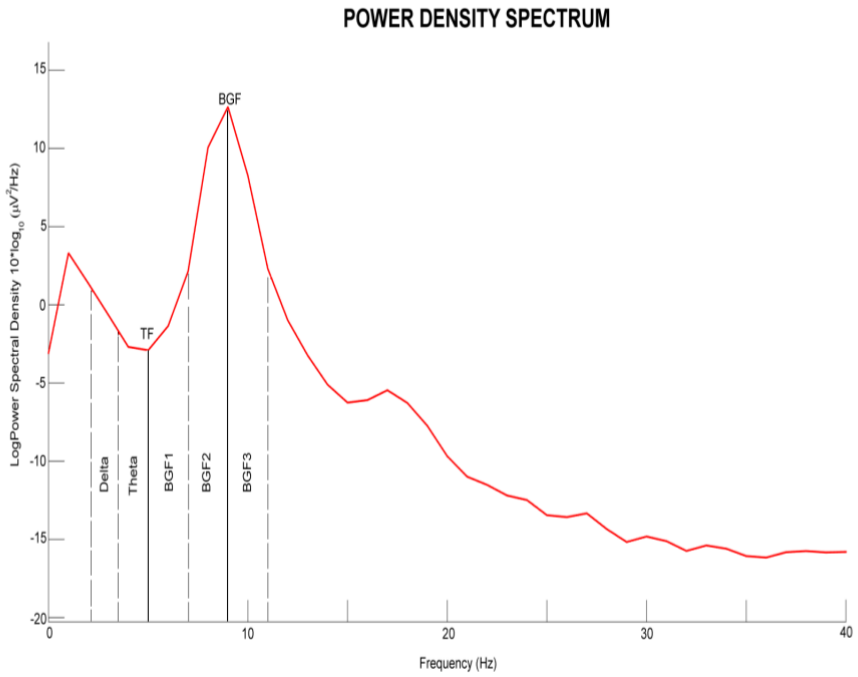

Figure 2. *Example of global scalp normalized eyes-closed resting-state electroencephalographic (rsEEG) power density spectrum. For each frequency bin (0.5-45 Hz), such a spectrum was calculated by averaging the normalized scalp rsEEG power density values across all 30 electrodes of the 10-10 montage system. The rsEEG frequency bands of interest were individually identified based on the following frequency landmarks, namely the transition frequency (TF) and background frequency (BGF) observed in the eyes-closed condition. In the eyes-closed rsEEG power density spectrum, the TF was defined as the minimum of the rsEEG power density between 3 and 8 Hz, while the BGF peak was defined as the maximum power density peak between 6 and 14 Hz. The TF and BGF were computed for each participant involved in the study. Based on the TF and BGF, we estimated the individual delta, theta, and BGF bands as follows: delta from TF -4 Hz to TF -2 Hz, theta from TF -2 Hz to TF, low BGF (BGF 1 and BGF 2) from TF to BGF peak, and high-frequency BGF (or BGF 3) from BGF to BGF + 2 Hz. Specifically, the individual BGF 1 and BGF 2 bands were computed as follows: BGF 1 from TF to the frequency midpoint of the TF-BGF range and BGF 2 from that midpoint to BGF peak. The other bands were defined based on the standard fixed frequency ranges: beta 1 from 14 to 20 Hz, beta 2 from 20 to 30 Hz, and gamma from 30 to 40 Hz. The BGFs were denoted as "alpha rhythms" if there was a reduction in magnitude (reactivity) of rsEEG rhythms at the BGFs from the eyes-closed to the eyes-open condition, as shown by rsEEG spectral measures.*

Cortical sources of rsEEG epochs as computed by eLORETA

The procedures for the rsEEG cortical source estimations were described in a previous reference article of our Consortium (Babiloni et al., 2019). We used the official freeware tool called exact LORETA (eLORETA) for the linear estimation of the cortical source activity generating scalp-recorded rsEEG rhythms (Pascual-Marqui, 2007). The present implementation of eLORETA uses a head volume conductor model composed of the scalp, skull, and brain. In the scalp compartment, exploring electrodes can be virtually positioned to give EEG data as an input to the source estimation (Pascual-Marqui, 2007). The brain model is based on a realistic cerebral shape taken from a template typically used in the neuroimaging studies, namely that of the Montreal Neurological Institute (MNI152 template). The eLORETA freeware solves the so-called EEG inverse problem estimating

“neural” current density values at any cortical voxel of the mentioned head volume conductor model. The solutions are computed rsEEG frequency bin-by-frequency bin.

The input for this estimation is the EEG spectral power density computed at scalp electrodes. The output is the electrical brain source space formed by 6,239 voxels with 5 mm resolution, restricted to the cortical grey matter of the head volume conductor model. An equivalent current dipole is in each voxel. For each voxel, the eLORETA package provides the Talairach coordinates, the lobe, and the Brodmann area (BA). The eLORETA solutions of rsEEG closed-eyes and open-eyes data were normalized by the following procedure. We averaged eLORETA solutions across two conditions (eyes-closed and eyes-open), all frequency bins from 0.5 to 45 Hz, and 6,239 voxels of the brain model volume, to obtain the eLORETA “mean” solution. Afterwards, we computed the ratio between any original eLORETA solutions at a given condition/frequency bin/voxel and the eLORETA “mean” solution. As a result, any original eLORETA solution at a given condition/frequency bin/voxel changed to a normalized eLORETA solution. In line with the general low spatial resolution of the current EEG methodological approach (i.e., 30 scalp electrodes), we performed a regional analysis of the eLORETA solutions. For this purpose, we collapsed the eLORETA solutions within frontal, central, parietal, occipital, temporal, and limbic macro-regions (ROIs) considered separately. Table 2 reports the list of the BAs used for the ROIs considered in the present study. Of note, the main advantage of the regional analysis of eLORETA solutions was that we could disentangle the rsEEG source activity in contiguous cortical areas. For example, the rsEEG source activity in the occipital ROI was disentangled from that estimated in the parietal and temporal ROIs, etc. This was made possible by the fact that eLORETA solves the linear inverse problem by considering (at least in part) the effects of the head as a volume conductor. In contrast, the solutions of rsEEG power density computed at a parietal scalp electrode reflect the contribution of source activities not only of the underlying parietal cortex but also of surrounding occipital and temporal cortices. For the present eLORETA cortical source estimation, a frequency resolution of 0.5 Hz was used, namely, the maximum frequency resolution allowed using 2-s artefact-free EEG epochs.

BRODMANN AREAS INTO THE REGIONS OF INTEREST (ROIs)	
Frontal	8, 9, 10, 11, 44, 45, 46, 47
Central	1, 2, 3, 4, 6
Parietal	5, 7, 30, 39, 40, 43
Occipital	17, 18, 19
Temporal	20, 21, 22, 37, 38, 41, 42
Limbic	31, 32, 33, 34, 35, 36

Table 2*. Regions of interest (ROIs) used for the estimation of the cortical sources of the resting-state electroencephalographic (rsEEG) rhythms in the present study. Any ROI is defined by some Brodmann areas of the cerebral source space in the freeware used in this study, namely the exact low-resolution brain electromagnetic source tomography (eLORETA).*

The computation of the rsEEG alpha reactivity

For the analysis of the rsEEG alpha reactivity from the eyes-closed to the eyes-open condition, we considered the eLORETA source solutions estimated in the central, parietal, and occipital ROIs. Based on the reference rsEEG studies of our Consortium (Babiloni et al., 2017, 2018a,b,c, 2019, 2020b; Pascarelli et al., 2020), the rsEEG alpha reactivity was measured at alpha 2 frequency band, which showed the maximum source activities in the Healthy participants during the eyes-closed condition.

The "reactivity" dependent variable for the statistical analyses was obtained by averaging the eLORETA alpha 2 source solutions in the central, parietal, and occipital ROIs. To avoid habituation effects in the eyes-open condition, that reactivity was computed based on the eLORETA solutions estimated during the first minute of the rsEEG recordings in that condition (when the rsEEG alpha reactivity is maximum). As no significant habituation effect was described in the eyes-closed condition, eLORETA solutions were estimated during all five minutes of the rsEEG recordings in that condition. The rsEEG alpha reactivity from the eyes-closed to the eyes-open condition was computed by the following formula similar to the one used by Wan et al. (2019):

$$\text{Reactivity (\%)} = \frac{eyes\ open - eyes\ closed}{eyes\ closed} * 100$$

According to this definition, the percent negative values (i.e., weaker BGF source activities during the eyes-open than the eyes-closed condition) indexed a reduction (reactivity) in the source BGF activities from the eyes-closed to the eyes-open condition (Babiloni et al., 2010; Del Percio et al., 2011). On the contrary, the percent positive values (i.e., greater BGF source activities during the eyes-open than the eyes-closed condition) indexed an increase in the source BGF activities from the eyes-closed to the eyes-open condition.

Figure 3 plots the individual values of the reactivity (%) of the central-parietal-occipital rsEEG (eLORETA) background frequency 2 (BGF 2) source activity from the eyes-open (1 minute) to the eyes-closed (5 minutes) condition for all Healthy (N = 28), ADD (N = 48) and DLB (N = 42) participants.

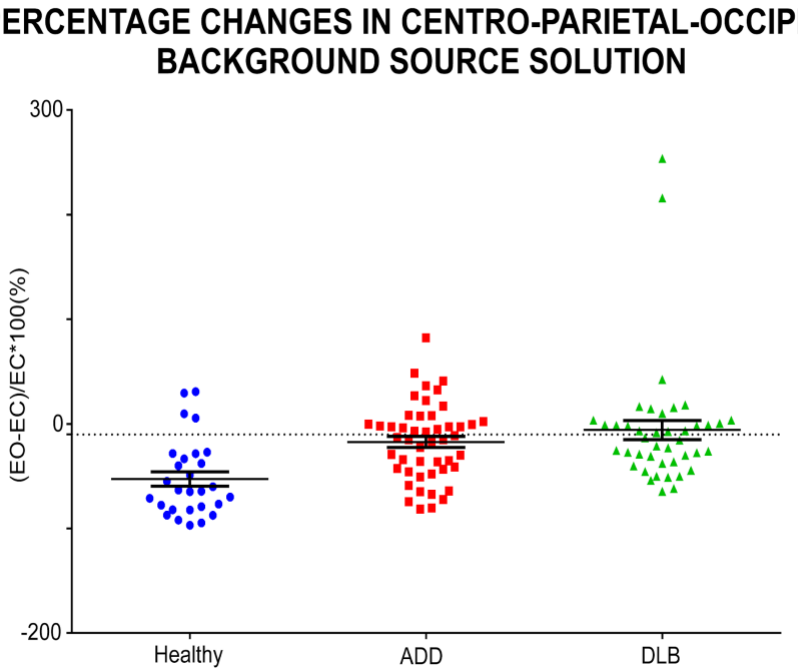

Figure 3. *Individual values of the reactivity (%) of the central-parietal-occipital rsEEG (eLORETA) BGF 2 source activity from the eyes-open (1 minute) to the eyes-closed (5 minutes) condition for all Healthy (N = 28), ADD (N = 48), and DLB (N = 42) participants. The percent negative values indexed a reduction (reactivity) in the rsEEG alpha 2 source activities from the eyes-closed (EC) to the eyes-open (EO) condition. In contrast, the percent positive values indexed an increase in the rsEEG alpha 2 source activities from the eyes-closed to the eyes-open condition.*

Figure 4 illustrates the percentage of BGF (alpha)-reactive Healthy, ADD, and DLB subjects as a function of the reactivity threshold of the central-parietal-occipital rsEEG (eLORETA) BGF 2 source activity. The percentage of BGF-reactive Healthy subjects does not change when the reactivity threshold changes between 0% and -25%; that percentage remains 85.7% (22 background-reactive Healthy participants). On the contrary, the percentage of BGF-reactive ADD and DLB patients decreases when the reactivity threshold changes between 0% and -25%; that reduction is similar in the ADD and DLB groups. Specifically, the percentage of the BGF-reactive ADD patients decreases from 75% (36 background-reactive ADD subjects) to 41.7% (20 BGF-reactive ADD patients).

Similarly, the percentage of BGF-reactive DLB patients decreases from 73.8% (31 BGF-reactive DLB patients) to 42.9% (18 BGF-reactive DLB patients).

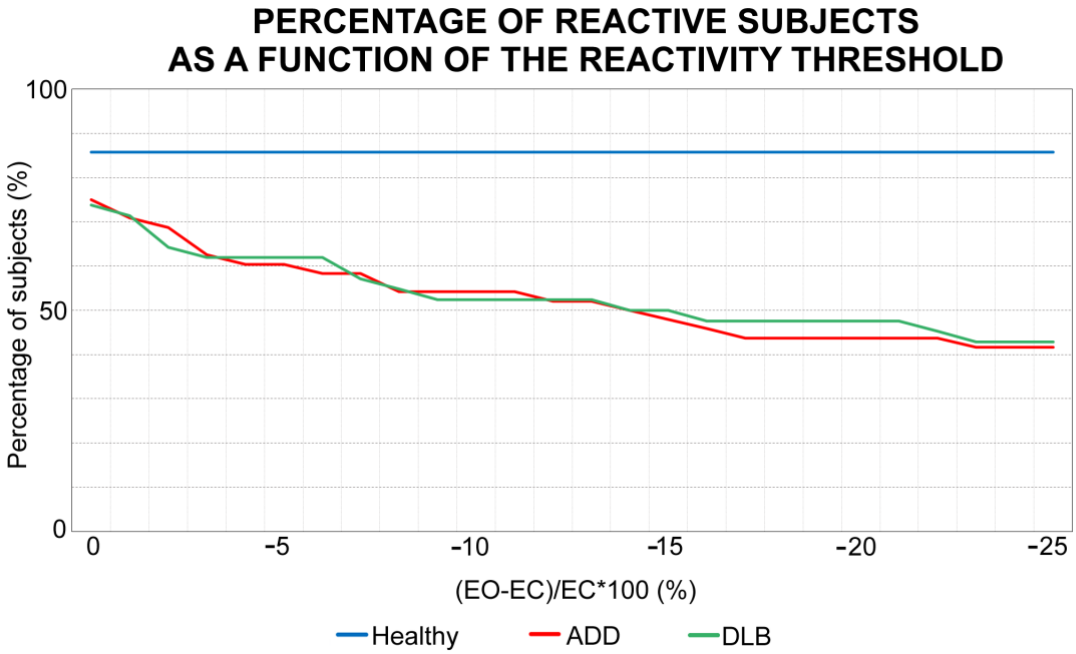

Figure 4. *Percentage of BGF-reactive Healthy, ADD, and DLB participants as a function of the reactivity threshold of the central-parietal-occipital rsEEG (eLORETA) BGF 2 source reactivity*.

In the present study, we used an arbitrary threshold of BGF (alpha) source reactivity set at -10 %. Based on this threshold value, we identified 4 Healthy, 22 ADD, and 20 DLB participants showing the lack of a significant BGF-reactivity as defined above (They showed either increased BGF source activities from the eyes-closed to the eyes-open condition or decreased alpha source activities from -10% to 0%). Therefore, the BGF 2 source reactivity was seen in 24 out of 28 Healthy seniors, 26 out of 48 ADD patients, and 22 out of 42 DLB patients. They were denoted as "alpha-reactive" participants in the following analyses.

Table 3 summarises the most relevant demographic (i.e., age, gender, and education) and clinical (i.e., MMSE score) features of the subgroups of the alpha-reactive Healthy, alpha-reactive ADD, alpha-reactive DLB, alpha-nonreactive ADD, and alpha-nonreactive DLB participants. Furthermore, Table 3 reports the results of the presence or the absence of statistically significant differences ($p < 0.05$) among the five groups for the age (ANOVA), gender (Freeman-Halton test), education (analysis of variance, ANOVA), and MMSE score (Kruskal-Wallis test). As expected, a statistically significant difference was found for the MMSE score ($H(2, 118) = 40.4$, $p < 0.0001$), showing a higher score in the alpha-reactive Healthy group than the demented groups (post-hoc test = $p < 0.0001$). On the contrary, no statistically significant differences were found for the age, gender, and education among all demented groups ($p > 0.05$).

	HEALTHY	ADD	DLB	Statistical Analysis
N	24	26	22	
Age (mean years ± SE)	73.8 ± 1.7	74.3 ± 1.2	74.2 ± 1.5	n.s. (ANOVA)
Gender (M/F)	13/11	17/9	17/5	n.s. (Freeman-Halton)
Education (mean years ± SE)	9.7 ± 1.0	9.7 ± 0.6	8.6 ± 0.8	n.s. (ANOVA)
MMSE (mean score ± SE)	28.3 ± 0.4	20.3 ± 0.6	21.9 ± 1.1	H (2, 72) = 39.4, p < 0.00001 (Kruskal-Wallis test) Healthy > ADD, DLB

Table 3. *Mean values (±SE) of the demographic and clinical data as well as the results of their statistical comparisons ($p < 0.05$) in the subgroups of the alpha-reactive Healthy (N = 24), alpha-reactive ADD (N = 26), alpha-reactive DLB (N = 22), alpha-nonreactive ADD (N = 22), and alpha-nonreactive DLB (N = 20) participants. Legend: M/F = males/females; n.s. = not significant ($p > 0.05$); MMSE = Mini Mental State Evaluation.*

Statistical analysis of cognitive measures in Healthy, ADD, and DLB groups

For each subject, the compositive cognitive scores of the language, visuospatial function, executive function/attention, and memory were calculated. Specifically, the following procedure was performed: (i) for each ADD and DLB participant, the individual scores of the neuropsychological tests (Verbal fluency test for letters, Verbal fluency test for categories, Line Orientation test, Face Recognition test, Trail making test B-A, Stroop test, Confusion Assessment Method-executive function part, Digit Span Forward, Digit Span Backward, Oktem Verbal Memory test, and Confusion Assessment Method-memory part) were z-transformed based on the mean and standard deviation of the Healthy group; (ii) for each Healthy participant, the individual scores of the neuropsychological tests were z-transformed based on the mean and standard deviation of the Healthy group not considering the subject on which the z-transformation is being calculated; (iii) for each participant, the sign of the z-transformed measures was adjusted such that the test scores expressing a good performance were always positive; (iv) for each participant, the compositive cognitive score of the language were evaluated averaging the z-transformed measures of the Verbal fluency test for letters, Verbal fluency test for categories; the compositive cognitive score of the visuospatial functions was evaluated averaging the z-transformed measures of the Line Orientation test and Face Recognition test; the compositive cognitive score of executive function and attention was evaluated averaging the z-transformed measures of the Trail making test B-A, Stroop test, and Confusion Assessment Method-executive function part; the compositive cognitive score of memory was evaluated averaging the z-transformed measures of the Digit Span Forward, Digit Span Backward, Oktem Verbal Memory test, and Confusion Assessment Method-memory part.

Furthermore, for each subject, the global composite cognitive score was calculated by averaging the composite cognitive score scores of the language, visuospatial function, executive

function/attention, and memory. Finally, five Kruskal-Wallis ANOVAs ($p < 0.05$) were performed to evaluate the presence or absence of statistically significant differences among the Healthy, ADD, and DLB groups for the global, language, visuospatial function, executive function/attention, and memory composite cognitive scores. Those statistical analyses of the cognitive measures in Healthy, ADD, and DLB groups were performed by the STATISTICA software, version 10.0 (StatSoft Inc., www.statsoft.com).

Statistical analysis of background reactivity in Healthy, ADD, and DLB groups

Two statistical sessions were performed to evaluate the clinical relevance of the background reactivity in Healthy, ADD, and DLB participants.

As a first statistical analysis at the individual level, the Spearman test ($p < 0.05$) evaluated the correlation between the global composite cognitive score, as an index of the global cognition, and the reactivity (%) of the central-parietal-occipital rsEEG (eLORETA) BGF 2 source activity from the eyes-open to the eyes-closed condition, as an index of background reactivity. That correlation analysis was performed considering all Healthy, ADD, and DLB individuals as a whole group for 2 reasons. On the one hand, the hypothesis was that background reactivity may be correlated with the global cognitive status in seniors in general, namely including cases with both normal and impaired cognitive functions. On the other hand, the correlation study would have had a low statistical sensitivity if performed only in the separate groups, owing to the very limited scatter of global composite cognitive scores within a given group. This statistical analysis was performed by the STATISTICA software, version 10.0 (StatSoft Inc., www.statsoft.com).

As a second statistical analysis at the individual level, the reactivity (%) of the central-parietal-occipital rsEEG (eLORETA) BGF 2 source activity from the eyes-open to the eyes-closed condition, as an index of background reactivity, was used as a discriminant variable for the classification of the Healthy, ADD and DLB participants. These classifications were performed by GraphPad Prism software (GraphPad Software, Inc, California, USA) using its implementation of ROC curves (DeLong et al., 1988). The following indexes measured the results of the binary classifications: (1) Sensitivity: It measures the rate of the cases that were correctly classified as cases (i.e., "true positive rate" in the signal detection theory); (2) Specificity: It measures the rate of the controls who were correctly classified as controls (i.e., "true negative rate" in the signal detection theory); (3) Accuracy: It is the mean between the sensitivity and specificity weighted for the number of cases and controls; and (4) AUROC curve: The AUROC curve was used as a major reference index of the global classification accuracy.

Statistical analysis of rsEEG source activities in alpha-reactive Healthy, ADD, and DLB groups

The statistical analyses of the rsEEG source activities in alpha-reactive Healthy, ADD, and DLB groups were performed by the STATISTICA software, version 10.0 (StatSoft Inc., www.statsoft.com).

The ANOVA was used to analyze the differences among means of rsEEG eLORETA source activities ***within*** and ***between*** the alpha-reactive Healthy, ADD, and DLB groups. The Mauchly's test of sphericity was used to assess whether the assumption of sphericity was met, while the Greenhouse-Geisser correction was applied when the data violated that assumption (Abdi, 2010). The Duncan test was used for post-hoc comparisons ($p < 0.05$). Furthermore, the size effect was also computed by Cohen's d.

As the use of an ANOVA implies that the dependent variable must be normally distributed, the Kolmogorov-Smirnov test ($p < 0.05$) was used to determine if the regional normalized eLORETA rsEEG current density distributions (i.e., the eLORETA source activities) of a given ANOVA model approximated to Gaussian distributions (null hypothesis of non-Gaussian distributions tested at $p < 0.05$). This was not the case in some cases, so all regional eLORETA source activities were used as inputs to the log 10 transformation to make them Gaussian. The Kolmogorov-Smirnov test confirmed that all eLORETA regional solutions were Gaussian after that transformation ($p > 0.05$).

Three statistical sessions were performed. The first statistical session tested the hypothesis that the eyes-closed rsEEG source activities (i.e., regional normalized eLORETA solutions) may differ ***between*** the alpha-reactive Healthy, ADD, and DLB groups. To this aim, an ANOVA was computed using eyes-closed rsEEG source activities as a dependent variable ($p < 0.05$). The ANOVA factors were Group (alpha-reactive Healthy, alpha-reactive ADD, and alpha-reactive DLB), Band (delta, theta, alpha 1, alpha 2, alpha 3, beta 1, beta 2, and gamma), and ROI (frontal, central, parietal, occipital, temporal, and limbic). The clinical unit was used as a covariate. The confirmation of this control hypothesis may require: (1) a statistically significant ANOVA interaction including the factor Group ($p < 0.05$) and (2) a post-hoc Duncan test indicating statistically significant ($p < 0.01$) differences in the reactivity of the rsEEG source activities among the Healthy, ADD, and DLB groups.

The second statistical session tested the hypothesis that the rsEEG alpha source activities may be reduced from the eyes-closed to the eyes-open condition ***within*** each alpha-reactive group of interest (i.e., alpha-reactive Healthy, alpha-reactive ADD group, alpha-reactive DLB). To address this aim, four ANOVAs were computed using the rsEEG source activities (i.e., regional normalized eLORETA solutions) as a dependent variable ($p < 0.05$). The four ANOVAs used the following

factors: Condition (eyes-open and eyes-closed), Band (delta, theta, alpha 1, alpha 2, alpha 3, beta 1, beta 2, and gamma), and ROI (central, parietal, and occipital). The clinical unit was used as a covariate. The confirmation of the first working hypothesis required: (1) a statistically significant ANOVA effect including the factor Condition ($p < 0.05$) and (2) a post-hoc Duncan test indicating statistically significant ($p < 0.01$) reductions (reactivity) of the rsEEG alpha source activities from the eyes-closed to the eyes-open condition (i.e., eyes-closed ≠ eyes-open) ***within*** the groups.

The third statistical session tested the hypothesis that the percent reactivity of the central, parietal, and occipital alpha 2 and 3 sources (showing the maximum activation in the eyes-closed condition) from the eyes-closed to the eyes-open condition may differ ***between*** the alpha-reactive Healthy, ADD, and DLB groups (The percent reactivity was defined as reported in the previous section). To this aim, an ANOVA was computed using that reactivity (i.e., the reactivity of the regional normalized eLORETA solutions) as a dependent variable ($p < 0.05$). The ANOVA factors were Group (alpha-reactive Healthy, alpha-reactive ADD, and alpha-reactive DLB), Band (alpha 2 and alpha 3), and ROI (central, parietal, and occipital). The clinical unit was used as a covariate. The confirmation of the second working hypothesis required: (1) a statistically significant ANOVA interaction including the factors Group and Band ($p < 0.05$) and (2) a post-hoc Duncan test indicating statistically significant differences in the reactivity of the rsEEG alpha source activities ***between*** the alpha-reactive groups, with greater values in the Healthy than the ADD and DLB groups ($p < 0.01$).

Results

Cognitive measures in Healthy, ADD, and DLB groups

Figure 5 reports the individual values of the cognitive composite scores of the language, visuospatial functions, attention/executive functions, and memory in all Healthy (N = 28), ADD (N = 48), and DLB (N = 42) participants. As expected, the Kruskal-Wallis ANOVAs ($p < 0.05$) showed statistically significant differences among the three groups for the cognitive composite scores of the language ($H (2, 118) = 23.4$, $p< 0.00001$; Healthy > ADD and DLB, post-hoc test = $p < 0.0001$), visuospatial functions ($H (2, 118) = 11.1$, $p< 0.001$; Healthy > ADD and DLB, post-hoc test = $p < 0.00001$), attention/executive functions ($H (2, 118) = 37.9$, $p< 0.00001$; Healthy > ADD > DLB, post-hoc test = $p < 0.01$), and memory ($H (2, 118) = 59.3$, $p< 0.00001$; Healthy > DLB > ADD, post-hoc test = $p < 0.01$).

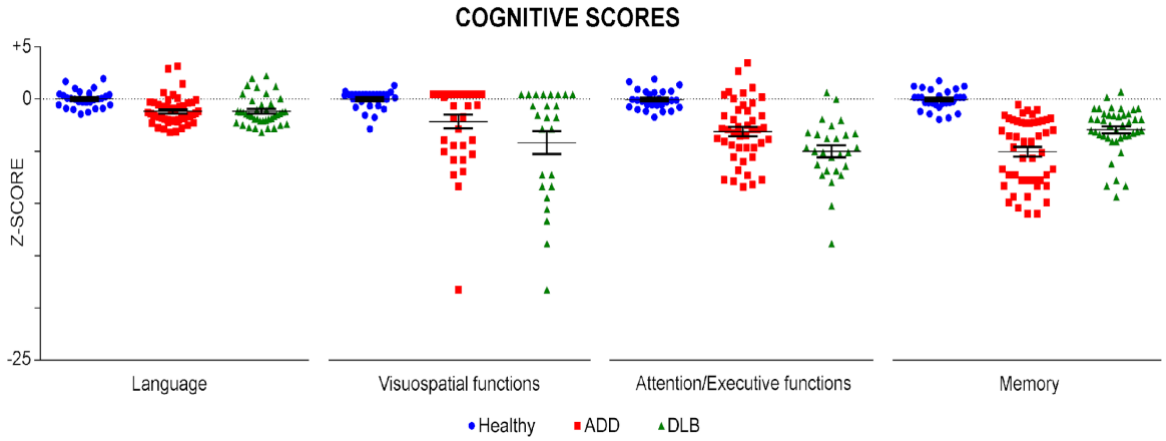

Figure 5. *Individual values of the cognitive composite scores in various cognitive domains in all Healthy (N = 28), ADD (N = 48) and DLB (N = 42) participants. The following four cognitive domains were considered: language, visuospatial functions, attention/executive functions, and memory.*

Figure 6 reports the individual values of the global cognitive composite score in all Healthy (N = 28), ADD (N = 48), and DLB (N = 42) participants. As expected, the Kruskal-Wallis ANOVA ($p < 0.05$) unveiled a statistically significant difference among the three groups ($H (2, 118) = 52.1$, $p< 0.00001$; Healthy > ADD and DLB), showing a higher score in the Healthy than the ADD and DLB groups (post-hoc test = $p < 0.00001$).

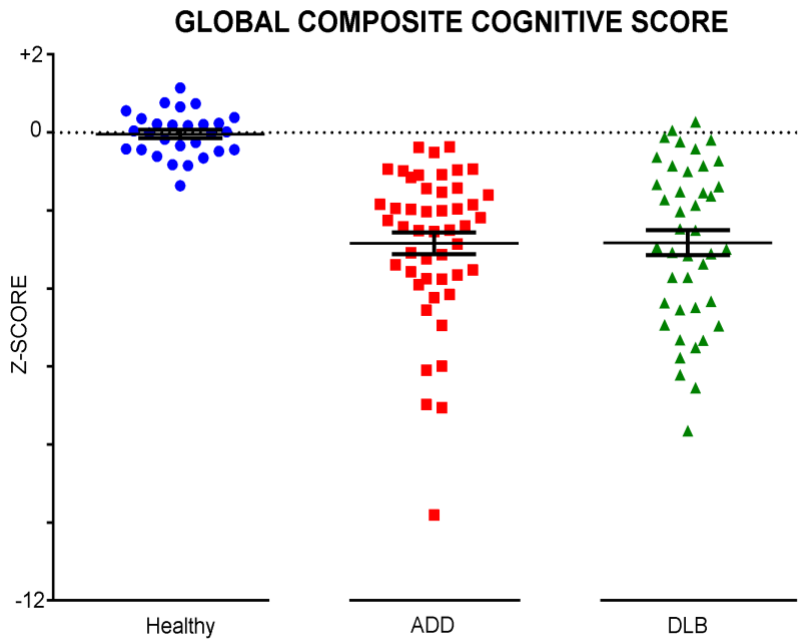

Figure 6. *Individual values of the global cognitive composite score in all Healthy (N = 28), ADD (N = 48) and DLB (N = 42) participants.*

Correlation of background reactivity and global composite cognitive score in Healthy, ADD, and DLB groups

Figure 7 illustrates the scatterplot showing the statistically significant negative correlation between the global composite cognitive score and the reactivity (%) of the central-parietal-occipital rsEEG (eLORETA) BGF 2 source activity from the eyes-open to the eyes-closed condition ($r = -0.275$; $p < 0.005$). The higher the reactivity (%) of the central-parietal-occipital rsEEG (eLORETA) background 2 frequency (BGF 2) source activity, the lower the global composite cognitive (performance) measure.

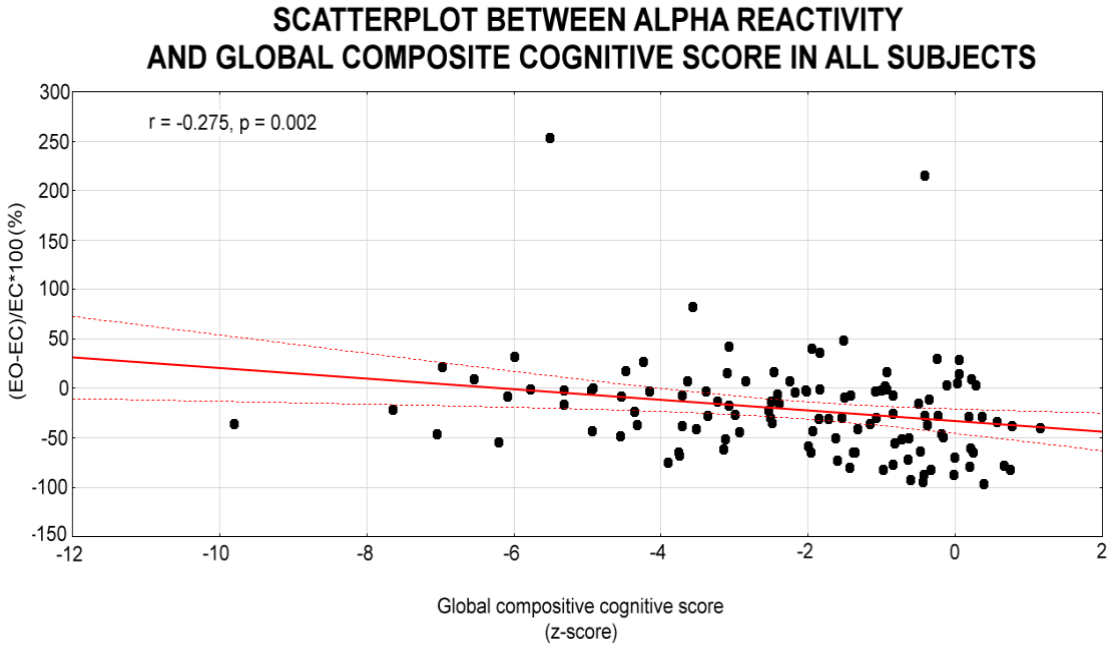

Figure 7. *Scatterplot showing the (negative) correlation between the reactivity (%) of the central-parietal-occipital rsEEG (eLORETA) BGF 2 source activity from the eyes-open (1 minute) to the eyes-closed (5 minutes) condition and the global composite cognitive score in all (N = 118) participants of the present study. In the scatterplots, the R coefficient of Spearman test and the relative p values are reported.*

Classification among Healthy, ADD, and DLB individuals based on the background reactivity

The results of the classification analysis, using the reactivity (%) of the central-parietal-occipital rsEEG (eLORETA) BGF 2 source activity from the eyes-open to the eyes-closed condition as discriminant variable, showed: (1) a moderate classification accuracy for the contrast between Healthy vs. ADD individuals (AUROC = 0.757, sensitivity = 81.3%, specificity = 64.3%, accuracy = 70.5%; see Figure 8 top); (2) a good classification accuracy for the contrast between Healthy vs. DLB individuals (AUROC = 0.803, sensitivity = 95.2%, specificity = 60.7%, accuracy = 74.5%; see Figure 8 bottom); and (3) a low classification accuracy for the contrast between ADD vs. DLB individuals (AUROC < 0.70).

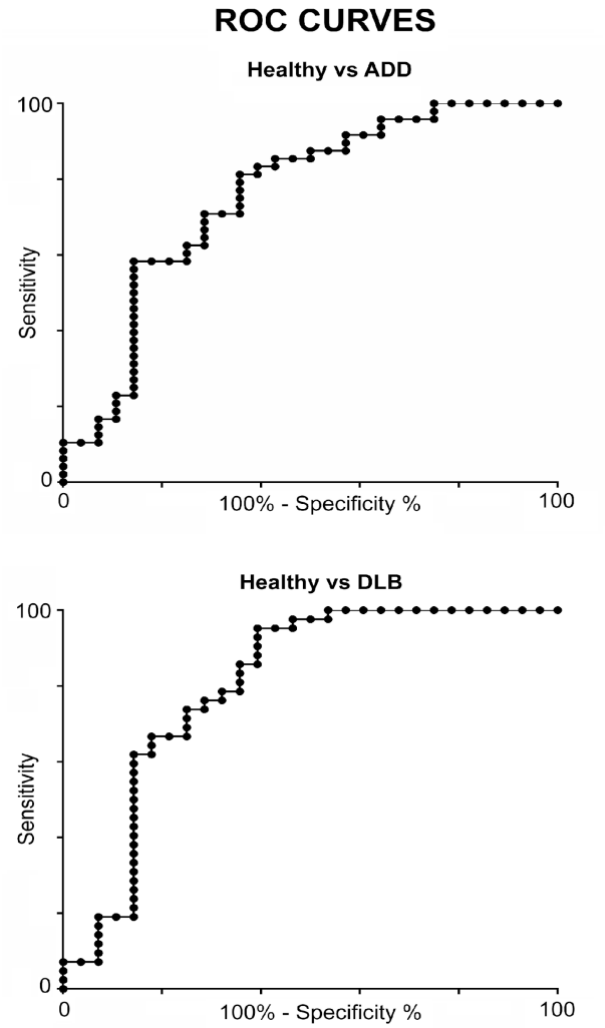

Figure 8. *Receiver operating characteristic (ROC) curves illustrating the classification of the patients with dementia (ADD, N = 48; DLB, N = 42) and Healthy (N = 28) individuals based on the reactivity (%) of the central-parietal-occipital rsEEG (eLORETA) BGF 2 source activity from the eyes-open (1 minute) to the eyes-closed (5 minutes) condition. The area under the ROC (AUROC) curve was 0.76 in the classification of the Healthy and ADD individuals and 0.80 in the classification of the Healthy and DLB individuals. These results indicate a moderate/good classification performance.*

Individual frequencies of rsEEG source activities in alpha-reactive Healthy, ADD, and DLB groups

The mean TF was 5.7 Hz (± 0.2 SE) in the alpha-reactive Healthy group, 5.2 Hz (± 0.2 SE) in the ADD group, and 4.8 Hz (± 0.1 SE) in the DLB group. Furthermore, the mean BGF was 8.9 Hz (± 0.2 SE) in the alpha-reactive Healthy group, 8.1 Hz (± 0.2 SE) in the alpha-reactive ADD group, and 7.4 Hz (± 0.2 SE) in the alpha-reactive DLB group. The ANOVAs of these data showed the following statistically significant effects: (1) the mean TF was greater ($F(2,68) = 5.3$; $p < 0.005$) in the alpha-reactive Healthy than the alpha-reactive DLB group ($p < 0.005$), while (2) the mean BGF was greater ($F(2,68) = 8.1$, $p < 0.001$) in the Healthy group than the alpha-reactive ADD ($p < 0.01$) and alpha-reactive DLB ($p < 0.0005$) groups.

Distribution of rsEEG source activities in alpha-reactive Healthy, ADD, and DLB groups

The results of the first statistical session about the eyes-closed rsEEG source activities in alpha-reactive participants are illustrated in Figure 9. This Figure shows the mean values (± SE, log 10 transformed) of the regional rsEEG (eLORETA) source activities during the eyes-closed condition in the alpha-reactive Healthy (N = 24), ADD (N = 26) and DLB (N = 22) groups. The distribution of those source activities differed across the groups, the ROIs, and the frequency bands. In the alpha-reactive Healthy group (as a physiological reference), the temporal, parietal, and occipital (eLORETA) alpha 2 and 3 source activities showed dominant values among all ROIs and frequency bands. Delta, theta, and alpha 1 source activities were characterized by relatively low values in all ROIs, while the beta and gamma source activities were generally very low. As compared to the alpha-reactive Healthy group, the alpha-reactive ADD and DLB groups exhibited a substantial decrease in occipital rsEEG alpha 2 and alpha 3 source activities. That decrease was also observed in the central and parietal regions in the alpha-reactive ADD group. Furthermore, the alpha-reactive ADD and DLB groups exhibited an increase in widespread delta, theta, and alpha 1 source activity in the alpha-reactive ADD group. Based on these input data, the ANOVA results showed a statistical interaction effect ($F(70, 2380) = 2.6$, $p < 0.00001$) among the factors Group (alpha-reactive Healthy, alpha-reactive ADD, and alpha-reactive DLB), Band (delta, theta, alpha 1, alpha 2, alpha 3, beta 1, beta 2, and gamma), and ROI (central, parietal, and occipital). The Duncan planned post-hoc ($p < 0.01$) testing produced the following core results: (1) the discriminant pattern alpha-reactive DLB > alpha-reactive ADD > alpha-reactive Healthy was fitted by the parietal and occipital delta source activities ($p < 0.01$-0.000001, Cohen's $d = 0.49$-1.73) as well as the parietal alpha 1 source activities ($p < 0.005$-0.000001, Cohen's $d = 0.64$-1.29); (2) the discriminant pattern alpha-reactive DLB and ADD > alpha-reactive Healthy was fitted by i) the frontal, central, temporal, and limbic delta source activities ($p < 0.0005$-0.000001, Cohen's $d = 0.84$-1.45); ii) the frontal, central, parietal, occipital, temporal, and limbic theta source activities ($p < 0.005$-0.000001, Cohen's $d = 0.87$-1.46); and iii) the frontal, central, occipital, temporal, and limbic alpha 1 source activities ($p < 0.005$-0.000001, Cohen's $d = 0.59$-1.49); (3) the discriminant pattern alpha-reactive DLB and ADD < alpha-reactive Healthy was fitted by the occipital alpha 2 source activities ($p < 0.0005$-0.00001, Cohen's $d = 0.44$-0.55) as well as the parietal and occipital alpha 3 source activities ($p < 0.01$-0.000001, Cohen's $d = 0.35$-0.81); (4) the discriminant pattern alpha-reactive ADD < alpha-reactive Healthy and DLB was fitted by the central alpha 3 source activities ($p < 0.005$-0.0005, Cohen's $d = 0.51$-0.60); (5) the discriminant pattern alpha-reactive ADD < alpha-reactive Healthy was fitted by the parietal alpha 2 source activities ($p < 0.001$, Cohen's $d = 0.41$); and (6) the discriminant pattern alpha-reactive DLB < alpha-reactive Healthy was fitted by the occipital and temporal beta 1 source activities ($p < 0.005$-0.0005,

Cohen's d = 1.01-1.28). Of note, these findings were not due to outliers from those individual regional normalized eLORETA current densities (log 10 transformed), as shown by Grubbs' test with an arbitrary threshold of $p > 0.001$.

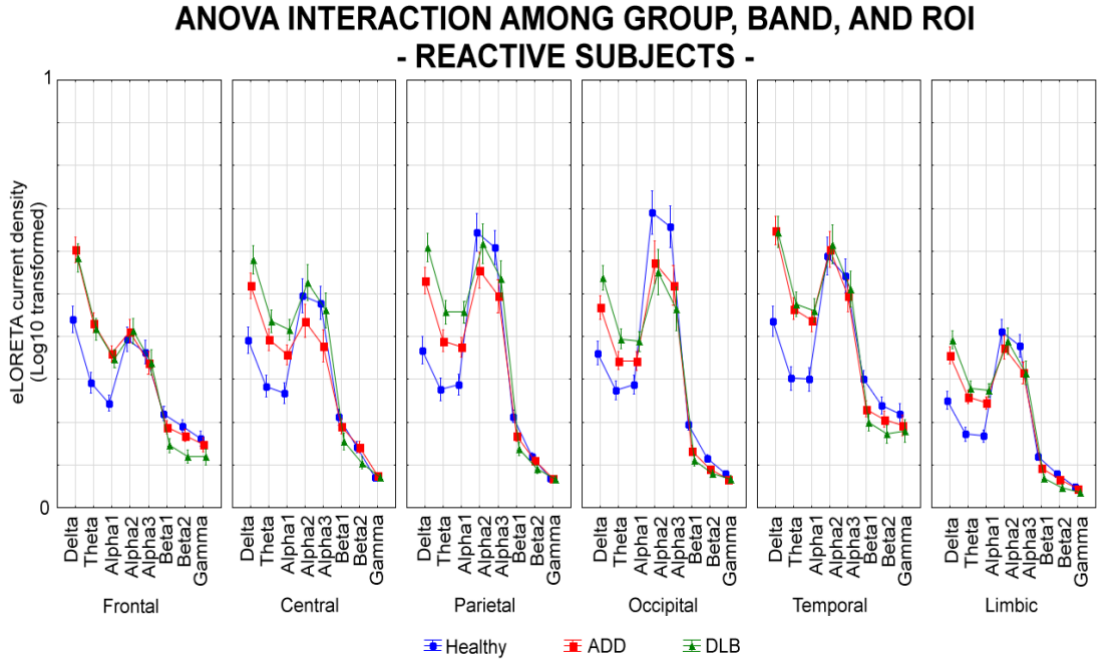

Figure 9. *Mean values (± SE, log 10 transformed) of the rsEEG (eLORETA) source activities during the eyes-closed (5 minutes) condition in the alpha-reactive Healthy (N = 24), ADD (N = 26) and DLB (N = 22) participants. The ANOVA design showed a statistical interaction effect (F (70, 2380) = 2.6, p < 0.00001) among the factors Group (alpha-reactive Healthy, ADD, and DLB), Band (delta, theta, alpha 1, alpha 2, alpha 3, beta 1, beta 2, and gamma), and ROI (central, parietal, and occipital).*

The results of the second statistical session about the eyes-closed and eyes-open rsEEG source activities in alpha-reactive groups are illustrated in Figures 10, 11, and 12. Figure 10 shows the mean values (± SE, log 10 transformed) of rsEEG (eLORETA) source activities during the eyes-open (1 minute) and eyes-closed (5 minutes) conditions in the alpha-reactive Healthy group (N = 24). The ANOVA design showed a statistical interaction effect (F (14, 308) = 8.9; p < 0.00001) among the factors Condition (eyes-open, eyes-closed), Band (delta, theta, alpha 1, alpha 2, alpha 3, beta 1, beta 2, and gamma), and ROI (central, parietal, and occipital). The Duncan planned post-hoc (p < 0.01) testing showed that the discriminant pattern eyes-closed > eyes-open was fitted by the following eLORETA solutions: (1) the occipital delta source activities (p < 0.001, Cohen's d = 0.28); (2) the central (p < 0.01, Cohen's d = 0.30), parietal (p < 0.001, Cohen's d = 0.34), and occipital (p < 0.000005, Cohen's d = 0.59) theta source activities; (3) the central (p < 0.0005, Cohen's d = 0.48), parietal (p < 0.000005, Cohen's d = 0.76), and occipital (p < 0.000001, Cohen's d = 1.05) alpha 1 source activities; (4) the central (p < 0.000005, Cohen's d = 1.10), parietal (p < 0.000005, Cohen's d = 1.82), and occipital (p < 0.000001, Cohen's d = 1.93) alpha 2 source activities; and (5) the central (p < 0.000005, Cohen's d = 0.96), parietal (p < 0.000001, Cohen's d = 1.66), and occipital (p <

0.000001, Cohen's d = 1.76) alpha 2 source activities. Furthermore, the discriminant pattern eyes-closed < eyes-open was fitted by the occipital beta 2 source activity ($p < 0.0005$, Cohen's d = 0.70) as well as the parietal ($p < 0.00001$, Cohen's d = 1.31) and occipital gamma ($p < 0.00001$, Cohen's d = 0.92) source activities. Of note, these findings were not due to outliers from those individual regional normalized eLORETA current densities (log 10 transformed), as shown by Grubbs' test with an arbitrary threshold of $p > 0.001$.

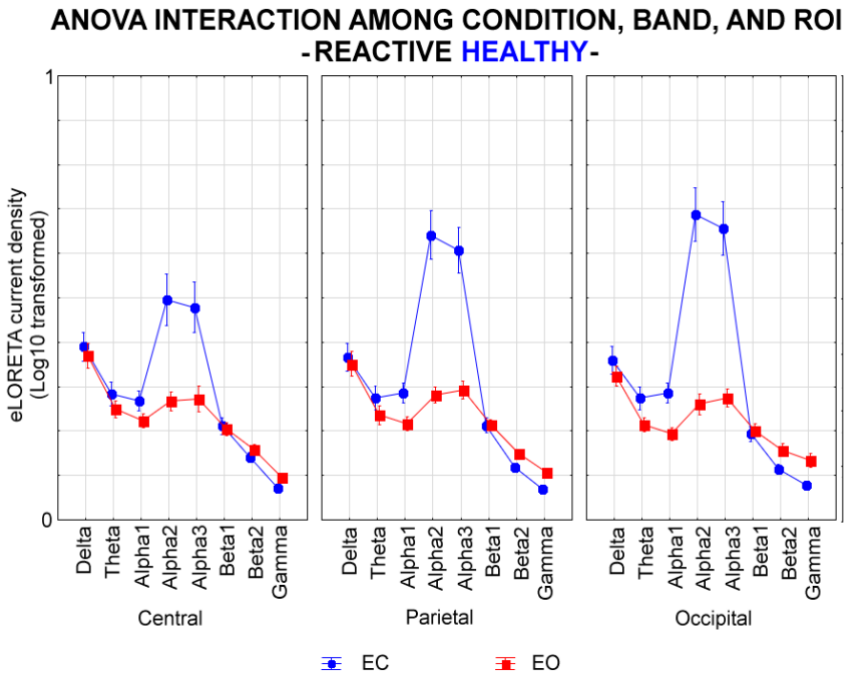

Figure 10. *Mean values (± SE, log 10 transformed) of the rsEEG (eLORETA) source activities during the eyes-open (1 minute) and eyes-closed (5 minutes) conditions in the alpha-reactive Healthy (N = 24) group. The ANOVA design showed a statistical interaction effect (F (14, 308) = 8.9; p < 0.00001) among the factors Condition (eyes-open, EO and eyes-closed, EC), Band (delta, theta, alpha 1, alpha 2, alpha 3, beta 1, beta 2, and gamma), and ROI (central, parietal, and occipital).*

Figure 11 plots the mean values (± SE, log 10 transformed) of rsEEG (eLORETA) source activities during the eyes-open (1 minute) and eyes-closed (5 minutes) conditions in the alpha-reactive ADD group (N = 26). The ANOVA design showed a statistical interaction effect (F (14, 336) = 2.2; $p < 0.01$) among the factors Condition (eyes-open, eyes-closed), Band (delta, theta, alpha 1, alpha 2, alpha 3, beta 1, beta 2, and gamma), and ROI (central, parietal, and occipital). The Duncan planned post-hoc ($p < 0.01$) testing showed that the discriminant pattern eyes-closed > eyes-open was fitted by the following eLORETA solutions: (1) the central ($p < 0.01$, Cohen's d = 0.18) and parietal ($p < 0.005$, Cohen's d = 0.19) theta source activities; (2) the central ($p < 0.00001$, Cohen's d = 0.37), parietal ($p < 0.000005$, Cohen's d = 0.54), and occipital ($p < 0.000005$, Cohen's d = 0.64) alpha 1 source activities; (3) the central ($p < 0.000005$, Cohen's d = 0.82), parietal ($p < 0.000005$, Cohen's d = 1.12), and occipital ($p < 0.000005$, Cohen's d = 1.11) alpha 2 source activities; and (4) the central

($p < 0.000005$, Cohen's $d = 0.60$), parietal ($p < 0.000005$, Cohen's $d = 0.99$), and occipital ($p < 0.000001$, Cohen's $d = 1.03$) alpha 3 source activities. In contrast, the discriminant pattern eyes-closed < eyes-open was fitted by the occipital beta 2 source activity ($p < 0.005$, Cohen's $d = 0.66$) as well as the central ($p < 0.0005$, Cohen's $d = 1.01$), parietal ($p < 0.005$, Cohen's $d = 0.90$) and occipital gamma ($p < 0.001$, Cohen's $d = 0.77$) source activities. Of note, these findings were not due to outliers from those individual regional normalized eLORETA current densities (log 10 transformed), as shown by Grubbs' test with an arbitrary threshold of $p > 0.001$.

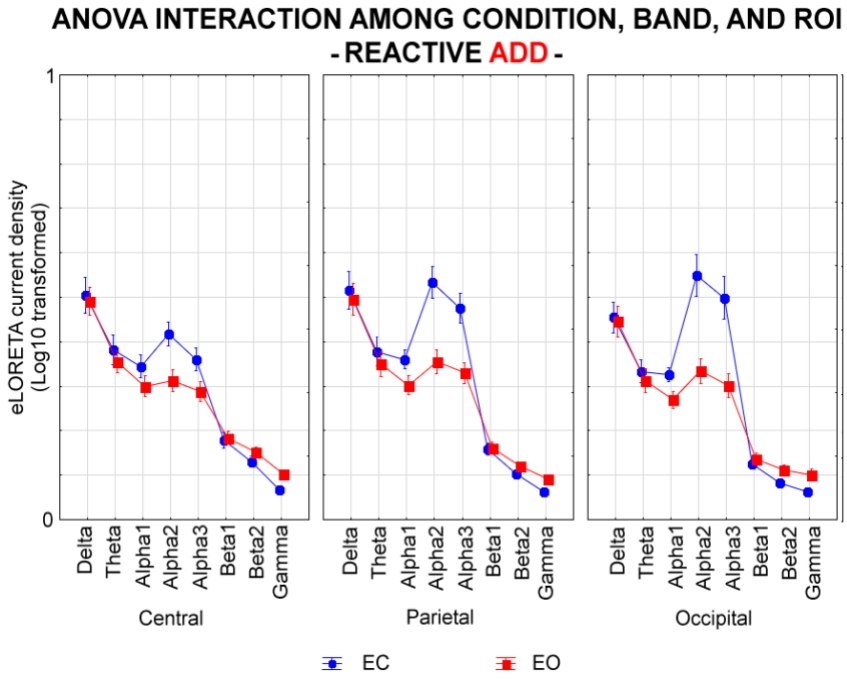

Figure 11. *Mean values (± SE, log 10 transformed) of the rsEEG (eLORETA) source activities during the eyes-open (1 minute) and eyes-closed (5 minutes) conditions in the alpha-reactive ADD (N = 26) group. The ANOVA design showed a statistical interaction effect (F (14, 336) = 2.2; p < 0.01) among the factors Condition (eyes-open, EO and eyes-closed, EC), Band (delta, theta, alpha 1, alpha 2, alpha 3, beta 1, beta 2, and gamma), and ROI (central, parietal, and occipital).*

Figure 12 illustrates the mean values (± SE, log 10 transformed) of rsEEG (eLORETA) source activities during the eyes-open (1 minute) and eyes-closed (5 minutes) conditions in the alpha-reactive DLB group (N = 22). The ANOVA design showed a statistical interaction effect ($F (7, 140) = 3.8$; $p < 0.001$) between the factors Condition (eyes-open, eyes-closed) and Band (delta, theta, alpha 1, alpha 2, alpha 3, beta 1, beta 2, and gamma). The Duncan planned post-hoc ($p < 0.01$) testing showed that the discriminant pattern eyes-closed > eyes-open was fitted by the delta ($p < 0.00001$, Cohen's $d = 0.57$), theta ($p < 0.000005$, Cohen's $d = 0.54$), alpha 1 ($p < 0.000005$, Cohen's $d = 0.60$), alpha 2 ($p < 0.000005$, Cohen's $d = 0.74$), and alpha 3 ($p < 0.000005$, Cohen's $d = 0.64$) source activities. Of note, these findings were not due to outliers from those individual regional normalized eLORETA

current densities (log 10 transformed), as shown by Grubbs' test with an arbitrary threshold of p > 0.001.

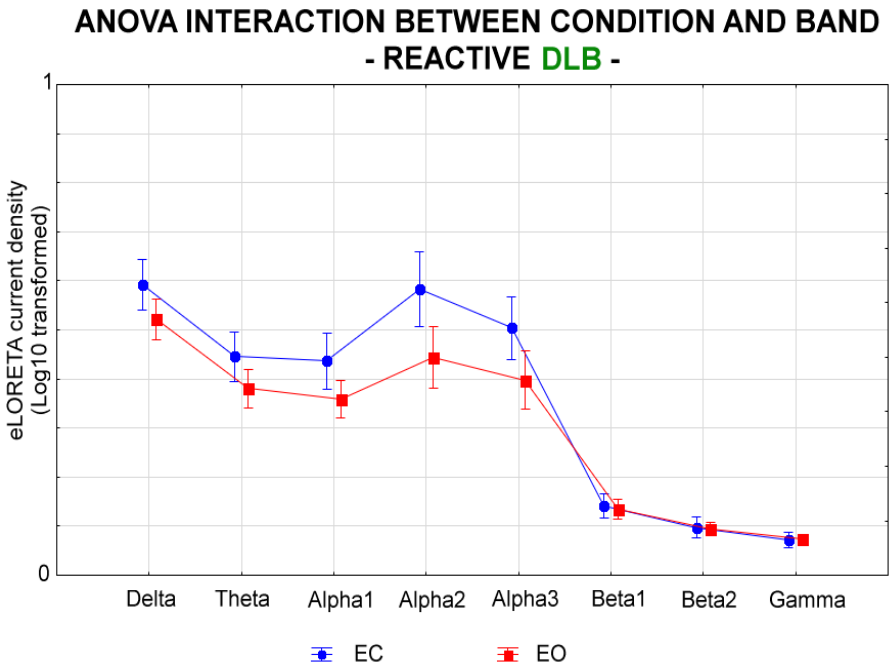

Figure 12. *Mean values (± SE, log 10 transformed) of the rsEEG (eLORETA) source activities during the eyes-open (1 minute) and eyes-closed (5 minutes) conditions in the alpha-reactive DLB (N = 22) group. The ANOVA design showed a statistical interaction effect (F (7, 140) = 3.8; p < 0.001) among the factors Condition (eyes-open, EO and eyes-closed, EC) and Band (delta, theta, alpha 1, alpha 2, alpha 3, beta 1, beta 2, and gamma), regardless the factor ROI.*

In the third statistical session about the rsEEG alpha 2 and 3 source reactivity to eyes-opening in the alpha-reactive Healthy (N = 24), ADD (N = 26), and DLB (N = 22) participants, the ANOVA showed a statistical interaction effect (F (4, 136) = 8.5; p < 0.00001) between the factors Group (alpha-reactive Healthy, alpha-reactive ADD, and alpha-reactive DLB) and ROI (central, parietal, and occipital). Figure 13 depicts the variables of this statistical interaction effect. Namely, it illustrates the mean values (± SE) of the reactivity of the rsEEG (eLORETA) alpha source activities from the eyes-open (1 minute) to the eyes-closed (5 minutes) condition in the alpha-reactive Healthy, ADD, and DLB groups. In Figure 13, the source activities are averaged across alpha 2 and alpha 3 bands to account for the statistical interaction between the factors Group (alpha-reactive Healthy, alpha-reactive ADD, and alpha-reactive DLB) and ROI. Duncan planned post-hoc (p < 0.01) testing showed a discriminant pattern alpha-reactive Healthy > alpha-reactive ADD > alpha-reactive DLB fitted by the occipital (alpha-reactive Healthy vs. alpha-reactive ADD: p < 0.01, Cohen's d = 0.97; alpha-reactive Healthy vs. alpha-reactive DLB: p < 0.000001, Cohen's d = 1.83; alpha-reactive ADD vs. alpha-reactive DLB: p < 0.001, Cohen's d = 0.69) alpha source activities. Furthermore, there was a discriminant pattern alpha-reactive Healthy > alpha-reactive ADD and DLB fitted by the parietal

alpha source activities (alpha-reactive Healthy vs. alpha-reactive ADD: $p < 0.01$, Cohen's $d = 0.91$; alpha-reactive Healthy vs. alpha-reactive DLB: $p < 0.005$, Cohen's $d = 1.17$).

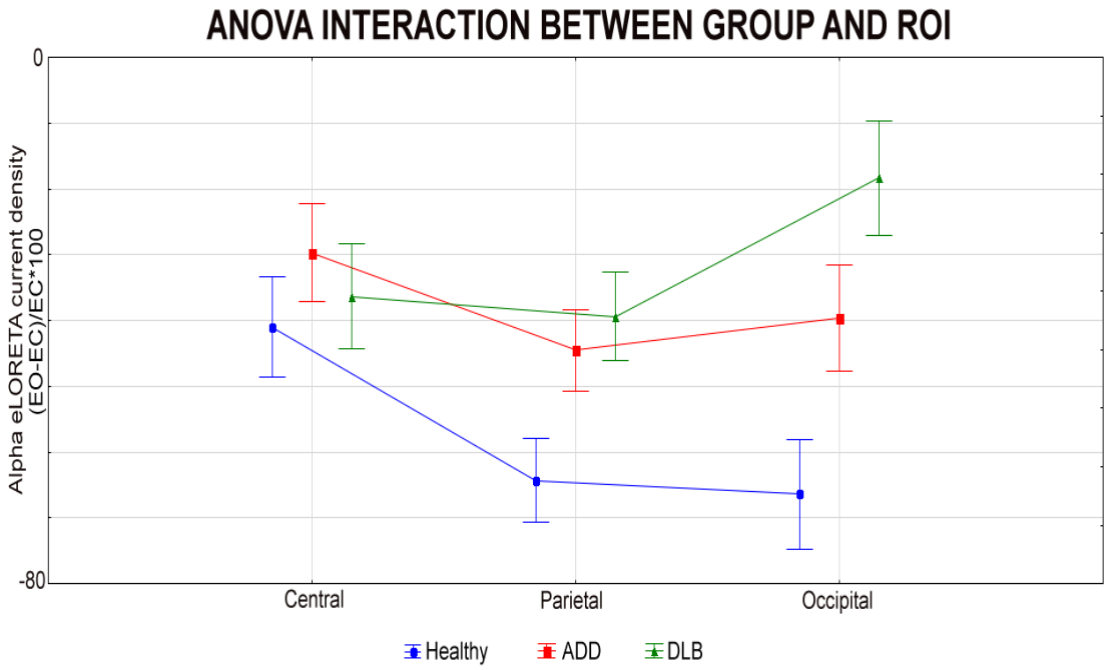

Figure 13. *Mean values (± SE) of the reactivity of the rsEEG (eLORETA) source activities from the eyes-open (1 minute) to the eyes-closed (5 minutes) condition in the alpha-reactive Healthy (N = 24), ADD (N = 26) and DLB (N = 22) participants. The reactivity values are relative to two frequency bands (alpha 2 and alpha 3) and three ROIs (central, parietal, and occipital). The ANOVA design showed a statistical interaction effect (F (4, 136) = 8.5; p < 0.00001) among the factors Group and ROI.*

Of note, these findings were not due to outliers from those individual regional normalized eLORETA current densities (log 10 transformed), as shown by Grubbs' test with an arbitrary threshold of $p > 0.001$.

Control analyses

A first control statistical analysis was performed to evaluate whether the correlation between the global composite cognitive score, as an index of the global cognition and the reactivity (%) of the central-parietal-occipital rsEEG (eLORETA) BGF 2 source reactivity from the eyes-open to the eyes-closed condition was also observed in the subgroup of alpha-reactive subjects. To address this aim, the Spearman test ($p < 0.05$) between the above-mentioned variables was executed. A statistically significant negative correlation was found ($r = -0.33$; $p < 0.005$). The higher the reactivity (%) of the central-parietal-occipital rsEEG (eLORETA) BGF 2 source activity, the lower the global composite cognitive (performance) measure.

A second control statistical analysis was performed to evaluate whether the difference of the rsEEG alpha 2 and 3 source reactivity to eyes-opening in the alpha-reactive Healthy, ADD, and DLB

groups may be due to the selected arbitrary threshold of the reactivity at -10%. To this aim, we selected two additional arbitrary thresholds for that reactivity at -15% and -20%, respectively. Based on the threshold value at -15%, we identified 24 alpha-reactive Healthy, 23 alpha-reactive ADD, and 21 alpha-reactive DLB participants. Based on the threshold value at -15%, we identified 24 alpha-reactive Healthy, 21 alpha-reactive ADD, and 20 alpha-reactive DLB participants. Afterwards, for each threshold, an ANOVA was computed using the rsEEG BGF (alpha) reactivity as a dependent variable ($p < 0.05$). The ANOVA factors were Group (alpha-reactive Healthy, alpha-reactive ADD, and alpha-reactive DLB), Band (alpha 2 and alpha 3), and ROI (central, parietal, and occipital). Results showed the results with both control thresholds were like those based on the main threshold (i.e., – 10%; see Figure 14). There was a lower reduction in the parietal and occipital rsEEG alpha source reactivity in the ADD and DLB groups than the Healthy group. Furthermore, that reduction in the occipital rsEEG alpha source reactivity was lower in the DLB than in the ADD group. Overall, these results suggest that the difference of the rsEEG alpha source reactivity in the alpha-reactive Healthy, ADD, and DLB groups may not be due to the selected arbitrary thresholds for that reactivity.

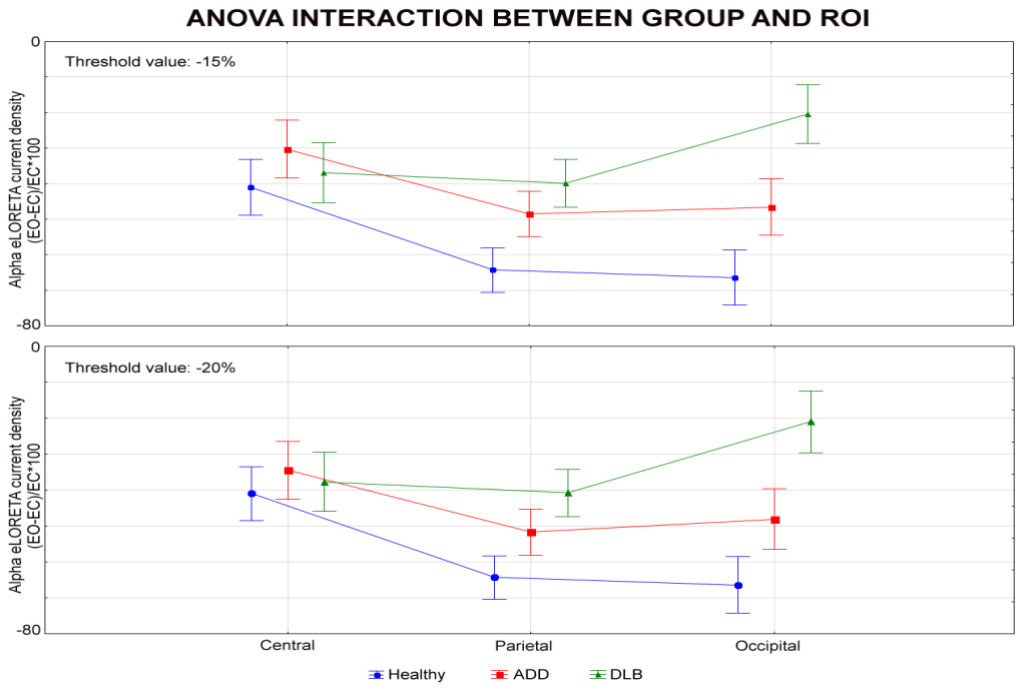

Figure 14. (Top): *Mean values (± SE) of the reactivity of the rsEEG (eLORETA) source activities from the eyes-open (1 minute) to the eyes-closed (5 minutes) condition in subgroups of the alpha-reactive Healthy (N = 24), ADD (N = 23) and DLB (N = 21) participants using a threshold of the rsEEG BGF (alpha) reactivity at -15%. The ANOVA design showed a statistical interaction effect (F (4, 128) = 8.7; p < 0.00001) among the factors Group and ROI (central, parietal, and occipital). (Bottom): Mean values (± SE) of the rsEEG (eLORETA) source reactivity from the eyes-open (1 minute) to the eyes-closed (5 minutes) condition in subgroups of the alpha-reactive Healthy (N = 24), ADD (N = 21), and DLB (N = 20) participants using a threshold of the reactivity at -20%. The ANOVA design showed a statistical interaction effect (F (4, 122) = 8.1; p < 0.00005) among the factors Group and ROI (central, parietal, and occipital).*

A third control statistical analysis was performed to evaluate that the rsEEG alpha source activities are not reduced from the eyes-closed to the eyes-open condition within each alpha-nonreactive group of interest (i.e., alpha-nonreactive ADD and alpha-nonreactive DLB). To address this aim, two ANOVAs were computed using the rsEEG source activities (i.e., regional normalized eLORETA solutions) as a dependent variable ($p < 0.05$). The ANOVAs used the following factors: Condition (eyes-open and eyes-closed), Band (delta, theta, alpha 1, alpha 2, alpha 3, beta 1, beta 2, and gamma), and ROI (central, parietal, and occipital). The clinical unit was used as a covariate. The ANOVAs did not show statistically significant differences including factor Condition ($p < 0.05$).
Finally, a fourth control statistical analysis (Mann-Whitney U tests, $p < 0.05$) was performed to evaluate the presence or absence of statistically significant differences among the Healthy, ADD, and DLB groups for the global, language, visuospatial function, executive function/attention, and memory composite cognitive scores. No statistically significant result was found ($p > 0.4$).

Methodological remarks

In this exploratory study, the interpretation of the results should consider some significant methodological limitations.

Firstly, we analyzed the rsEEG activity from 30 scalp exploring electrodes (10–10 system). This rsEEG spatial sampling is good, but optimal rsEEG source estimates may benefit from > 48-64 scalp electrodes (Liu et al., 2018; Marino et al., 2016; Michel and Koening, 2018). Furthermore, the rsEEG source estimation was performed using the standard eLORETA template brain model (i.e., MNI152 developed by Montreal Neurologic Institute) rather than brain models derived from individual MRI scans. To mitigate these limitations, we averaged eLORETA solutions within cortical lobes. Notably, the eLORETA toolbox is generally suitable to model distributed cortical source activities (Halder et al., 2019) as those generating posterior rsEEG alpha rhythms (Babiloni et al., 2020a).

Secondly, the exploratory nature of this study was reflected using a statistical post-hoc test threshold at $p < 0.01$, which might produce potential false positive discoveries with multiple comparisons. Therefore, the present results just represent preliminary evidence. Future studies will have to cross-validate the present results when related to statistical effects around $p < 0.01$.

Thirdly, each clinical unit provided clinical and rsEEG data from a different number of Healthy, ADD, and DLB participants, and some clinical units collected data from Healthy and only one group of patients.

Fourthly, the rsEEG data were recorded from clinical units using different hardware systems and various rsEEG recording parameters (i.e., frequency sampling, antialiasing passband, electrode arrays, and reference electrode) in the clinical units. To mitigate these potential sources of variability, we performed some procedures for the harmonization of the recorded data across the clinical units including a common antialiasing bandpass filtering and down-sampling to 256 Hz, a re-referencing of all rsEEG data to the common average reference, and a normalization of the eLORETA rsEEG sources to remove the effects of the local amplifier gain and electrode resistance.

Finally, the diagnosis of ADD was based only on the criteria of the Diagnostic and Statistical Manual of Mental Disorders, fourth edition (DSM-IV-TR; American Psychiatric Association) and the National Institute of Neurological Disorders and Stroke–Alzheimer Disease and Related Disorders (NINCDS–ADRDA; McKhann et al., 2011). We did not have available biological or imaging demonstrations of either amyloidosis or tauopathy.

A lack of information concerning biomarkers and neuroimaging is also present in the DLB group. Only 13 out of 42 DLB patients received a DaTSCAN to confirm the diagnosis of DLB.

Second study

POOR REACTIVITY OF POSTERIOR ELECTROENCEPHALOGRAPHIC ALPHA RHYTHMS DURING THE EYES OPEN CONDITION IN PATIENTS WITH DEMENTIA DUE TO PARKINSON'S DISEASE

Methods and Participants

The clinical and rsEEG datasets for the present investigation were taken from the Eurasian archive of The PDWAVES Consortium (www.pdwaves.eu) and European DLB Consortium whose clinical units are listed in the following: Sapienza University of Rome (Italy), University of Genoa (Italy), University of Padua (Italy), University "G. D'Annunzio" of Chieti and Pescara (Italy), IRCCS Synlab SDN of Naples (Italy), IRCCS Oasi of Troina (Italy), IRCCS Hospital San Raffaele Roma (Italy), Hospital San Raffaele of Cassino (Italy), Istanbul University (Turkey), Izmir University (Turkey), and Newcastle University (UK). Specifically, those data referred to age-, sex-, and education-matched PDD (N = 73), ADD (N = 35), and Healthy (N = 25) participants having rsEEG recordings with eyes-closed and eyes-open conditions. Each clinical unit contributed with at least Healthy participants and patients with dementia of one pathological group (i.e., ADD or PDD). Istanbul University, Izmir University, and Newcastle University were the main clinical contributors. The diagnosis of ADD was based on the criteria of the Diagnostic and Statistical Manual of Mental Disorders, fourth edition (DSM-IV-TR; American Psychiatric Association) and the National Institute of Neurological Disorders and Stroke–Alzheimer Disease and Related Disorders (NINCDS–ADRDA; McKhann et al., 2011). Exclusion criteria for the ADD patients were other significant neurological, systemic, or psychiatric illness, mixed dementing diseases, enrolment in a clinical trial with experimental drugs, the use of antidepressant drugs with anticholinergic side effects, high dose of neuroleptics or chronic sedatives or hypnotics, antiparkinsonian medication and the use of narcotic analgesics (Babiloni et al., 2017). All ADD patients were under standard long-term chronic cholinergic treatment and all exams were performed under the ON state.

The diagnosis of PD was based on a standard clinical assessment of tremor, rigidity, and bradykinesia (Gelb et al., 1999). As measures of severity of a motor disability, the Hoehn and Yahr stage (Hoehn and Yahr, 1967) and the Unified Parkinson Disease Rating Scale-III (UPDRS III; Fahn and Elton, 1987) for extrapyramidal symptoms were used. Furthermore, the diagnosis of PDD was given to the patients with a history of dementia, preceded by a typical levodopa-responsive

parkinsonian motor syndrome for at least 12 months and not related to other pathologic conditions than PD. The PDD was diagnosed according to the criteria of the Diagnostic and Statistical Manual of Mental Disorders, fourth edition (DSM-IV-TR; American Psychiatric Association). The following inclusion criteria were fulfilled: (i) diagnosis of PD as specified previously; (ii) a gradual neurocognitive decline in the context of established PD reported by either the patient or a reliable informant or observed by clinicians; (iii) an abnormally low score in at least one of the neuropsychological tests mentioned in the following section, as defined by performances beyond 1.5 times the SD from the mean value for age- and education-matched controls or equivalent scores for abnormality according to the manuals of the tests used; and (iv) moderate to severe impairment in instrumental activities of the daily living and dependency. All PDD patients were under standard long-term chronic dopaminergic treatment and all exams were performed under the ON state.

Comparable numbers of Healthy serving as normal age-, sex, and education-matched controls were selected from the clinical units of the co-workers of the study. Exclusion criteria for healthy seniors were (i) neurological or psychiatric diseases (previous or present), (ii) a depressive episode (detected with a GDS (15 items version) score higher than 5), (iii) the use of chronic psychoactive drugs, and (iv) significant chronic systemic illnesses (e.g., diabetes mellitus).

All participants underwent global cognitive screening using the Mini-Mental State Examination (MMSE). Table 1 summarizes the relevant demographic and clinical (i.e., MMSE score) information about the Healthy, ADD, and PDD groups, together with the results of the statistical analyses computed to evaluate the presence or absence of statistically significant differences between these groups regarding age (ANOVA), sex (Freeman-Halton test), education (ANOVA), and MMSE score (Kruskal-Wallis test). As expected, statistically significant differences were found between the Healthy and the other two groups for the MMSE score ($H = 56.6$, $p < 0.00001$), showing a higher score in the Healthy than the ADD and PDD groups (post-hoc test = $p < 0.00001$). On the contrary, no statistically significant differences in age, sex, and education were found between the groups ($p > 0.05$).

The local institutional ethical committees approved the study. All experiments were performed with the informed and overt consent of each participant or caregiver, in line with the Code of Ethics of the World Medical Association (Declaration of Helsinki) and the standards established by the local institutional review boards.

It should be remarked that all datasets of the alpha source reactivity to eyes opening used in the present 73 PDD patients were unpublished. In contrast, about 50% of datasets of the alpha source reactivity to eyes opening relative to the present 25 Healthy and 35 ADD control persons were re-used from the first study of the thesis. We could not re-use more clinical and rsEEG datasets as the

present PDD patients were on average older, comprising a higher proportion of male persons and persons with lower educational levels compared to the healthy control group and ADD seniors. Similarly, the present PDD patients were on average older, comprised more male subjects, the educational level was lower, and global motor and cognitive performances were lower when compared to the DLB patients enrolled for the first study of this thesis. Selecting healthy control subjects, ADD, DLB, and PDD groups matched for all the above demographic and/or clinical variables would have strongly reduced the number of persons in each group, making the results unreliable from a statistical point of view.

	Healthy	**ADD**	**PDD**	**Statistical Analysis**
N	25	35	73	
Age (mean years ± SE)	72.4 ± 1.6	73.0 ± 1.1	72.7 ± 0.7	ANOVA: n.s.
Sex (M/F; % of M)	18/7; 72%	27/8; 77%	61/12; 83%	Freeman-Halton: n.s.
Education (mean years ± SE)	9.9 ± 0.8	9.7 ± 0.5	9.4 ± 0.5	ANOVA: p = n.s.
MMSE (mean score ± SE)	27.7 ± 0.3	19.3 ± 0.8	18.9 ± 0.5	Kruskal-Wallis test: H = 56.6, p = 0.00001; Healthy > ADD, PDD

Table 1. *Mean values (± standard error of the mean, SE) of the demographic and clinical data as well as the results of their statistical comparisons ($p < 0.05$) in the groups of cognitively normal older adults (Healthy, N = 25) and patients with dementia due to Alzheimer's disease (ADD, N = 30) and Parkinson's disease (PDD, N= 73). Legend: M/F = males/females; n.s. = not significant ($p > 0.05$); MMSE = Mini Mental State Evaluation.*

Cognitive assessment

The performance in various cognitive domains, including language, visuospatial function, executive function/attention, and memory, was assessed using a battery of neuropsychological tests. Specifically, it included: (i) language was tested by Verbal fluency test for letters (Novelli et al., 1986) and Verbal fluency test category (fruits, animals, or car trades; Novelli et al., 1986); (ii) visuospatial functions were assessed by Line Orientation test (Benton et al., 1978) and Face Recognition test (Benton et al., 1983); (iii) evaluation of executive functions and attention were evaluated by the Trail Making Test Part A and B (Reitan, 1958), Stroop test (Stroop, 1935), and Confusion Assessment Method (executive function part; Inouye et al., 1990); and (iv) memory was tested by Digit Span Forward and Backward (Wechsler et al., 1987), Oktem Verbal Memory test (Oktem et al., 1992), and Confusion Assessment Method (memory part; Inouye et al., 1990). Finally, to evaluate global cognitive status, Mini-Mental State Exam (MMSE) was performed (Folstein et al.,

1975). Of note, for each cognitive domain, the clinical units provided one or more of the above-mentioned neuropsychological tests.

The rsEEG recordings

Electrophysiological data were recorded by professional digital EEG systems licensed for clinical applications. The following digital EEG systems were used: BrainAmp 32-Channel DC System (Brain Product GmbH, Germany), Waveguard caps (ANT Neuro, The Netherlands), EB Neuro-BE LIGHT (EB Neuro, Italy), Galileo NT Line - EB Neuro (EB Neuro, Italy), and EB Neuro-Sirius BB (EB Neuro, Italy).

All rsEEG recordings were performed in the late morning. The rsEEG recordings were performed in all participants using at least 30 scalp exploring electrodes placed according to the 10–10 system. These electrodes were denoted as "selected electrodes" and their location is illustrated in Figure 1. The ground electrode was attached to the right clavicle or on the forehead, while linked earlobes (A1 and A2) or Fz served as the active reference for all the electrodes during recording. Electrode impedance was kept below 5 kΩ; continuous EEG data were recorded at a sampling frequency of 500-1024 Hz and related antialiasing bandpass between 0.01 Hz and 60-100 Hz. Horizontal electrooculographic (EOG) potentials (0.3-70 Hz bandpass) were also recorded to control eye movements and blinking.

The participants were seated in a comfortable armchair during the rsEEG recording and instructed to remain awake, psychophysically relaxed (no movement), and with the mind freely wandering (no mental planning or cognitive operations). Based on the instructions given by an experiment, each rsEEG recording lasted 3-5 minutes in the condition of eyes closed, followed by 3-5 minutes in the condition of eyes open. Participants were supervised by the experimenter during the rsEEG recording to monitor adherence to the protocol. The experimenter may kindly invite participants to adhere to the protocol if needed. All deviations by the protocol and verbal interventions were annotated and used during the phase of rsEEG data analysis.

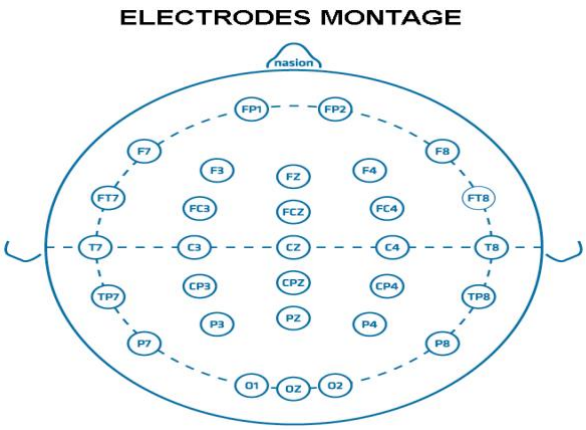

Figure 1. *Electroencephalographic (EEG) electrode montage. The electrode montage included 30 scalp monopolar sensors placed following the 10–10 System (i.e., Fp1, Fp2, F7, F3, Fz, F4, F8, FT7, FC3, FCz, FC4, FT8, T7, C3, Cz, C4, T8, TP7, CP3, CPz, CP4, TP8, P7, P3, Pz, P4, P8, O1, Oz and O2).*

Preliminary rsEEG data analysis

The rsEEG data were centrally analyzed by experts blinded to the participants' diagnosis by the Sapienza University of Rome unit. The recorded rsEEG data were exported as European data format (.edf) or EEGLAB set (.set) files and then processed offline using the EEGLAB toolbox (Delorme A and Makeig S, 2004; version eeglab14_1_2b) running in the MATLAB software (Mathworks, Natic, MA, USA; version: R2014b). The rsEEG data were divided into epochs lasting 2 s (i.e., 5 minutes = 150 rsEEG epochs of 2 s for each experimental condition) and analyzed offline. Afterwards, they received a 3-step procedure aimed at detecting and removing (i) recording channels (electrodes) showing prolonged artifactual rsEEG activity due to bad electric contacts or other reasons; (ii) rsEEG epochs with artifacts at recording channels characterized by general good signals; and iii) intrinsic components of the rsEEG epochs with artifacts.

The first step was based on a visual analysis of the recorded rsEEG activity by two independent experimenters among four experts (i.e., C.D.P, R.L., G.N., and F.T.) for a first identification of the selected electrodes affected by irremediable artifacts. Indeed, there were no more than 3 selected electrodes removed for each participant. For the clinical units with a digital EEG system using > 30 exploring electrodes, the removed electrodes were substituted with the nearest electrodes not included among the 30 selected electrodes. The added electrodes were then used together with the artifact-free selected electrodes to compute the interpolation of artifact-free rsEEG data at all scalp sites of the removed electrodes (EEGLAB toolbox, Delorme A and Makeig S, 2004; version eeglab14_1_2b), thus ensuring that all participants had artefact-free EEG data at the locations of the 30 selected electrodes.

The second step was based on a visual analysis of the recorded rsEEG activity by two among the mentioned independent experimenters (i.e., C.D.P, G.N., and F.T.) for a first selection of

artifactual rsEEG epochs. The rsEEG epochs contaminated by muscular, ocular, head movements, or non-physiological artifacts were removed.

The third step was implemented by an independent component analysis (ICA) from the EEGLAB toolbox, applied to remove the ICA components representing the residual artifacts due to (i) blinking and eye movements, (ii) involuntary head movements, (iii) neck and shoulder muscle tensions, and (iv) electrocardiographic activity (Crespo-Garcia, 2008; Jung, 2000). For each rsEEG dataset, less than 5 ICA components were removed from the original ICA solutions based on 30 ICA components. In the third step, the rsEEG datasets were reconstructed with the remaining (artifact-free) ICA components, and the putative artifact-free rsEEG epochs were visually double-checked again by two among the mentioned independent experimenters (i.e., C.D.P, G.N., and F.T.) to confirm or make the final decision about the inclusion or the exclusion of each of those rsEEG epochs.

The resulting artifact-free EEG data for the common 30 electrodes were used as an input for two additional methodological steps. The first additional step served to harmonize rsEEG data recorded by the clinical units using different reference electrodes and sampling frequency rates. The rsEEG data were frequency-band passed at 0.1-45 Hz and down-sampled, when appropriate, to make the sampling rate of all artifact-free rsEEG datasets in the Healthy, ADD, and PDD participants equal to 256 Hz. Furthermore, all those rsEEG epochs were re-referenced to the common average reference. The second additional step was used to minimize the habituation effects in rsEEG data recorded during the eyes-open condition. Only the first minute of those rsEEG data (when the rsEEG alpha reactivity is supposed to be well-represented) was considered in the further analyses.
As a result of the above procedures, the artifact-free epochs showed a similar proportion (> 75%) of the total amount of rsEEG activity recorded in all groups of participants (i.e., Healthy, ADD, PDD).

Spectral analysis of the rsEEG epochs

A standard digital FFT-based analysis (Welch technique, Hanning windowing function, no phase shift) computed the power density of artifact-free rsEEG epochs at all 30 scalp electrodes (0.5 Hz of frequency resolution). From those spectral solutions, the rsEEG frequency bands of interest were individually identified based on the following frequency landmarks, namely the transition frequency (TF) and background frequency (BGF) observed in the eyes-closed condition. In the eyes-closed rsEEG power density spectrum, the TF was defined as the minimum of the rsEEG power density between 3 and 8 Hz, while the BGF peak was defined as the maximum power density peak between 6 and 14 Hz. The TF and BGF were computed for each participant involved in the study. Based on the TF and BGF, we estimated the individual delta, theta, and BGF bands as follows: delta from TF -4 Hz to TF -2 Hz, theta from TF -2 Hz to TF, low BGF (BGF 1 and BGF 2) from TF to

BGF peak, and high-frequency BGF (or BGF 3) from BGF to BGF + 2 Hz. Specifically, the individual BGF 1 and BGF 2 bands were computed as follows: BGF 1 from TF to the frequency midpoint of the TF-BGF range and BGF 2 from that midpoint to BGF peak. The other bands were defined based on the standard fixed frequency ranges used in the reference rsEEG studies of our Consortium (Babiloni et al., 2017, 2019, 2020b): beta 1 from 14 to 20 Hz, beta 2 from 20 to 30 Hz, and gamma from 30 to 40 Hz.

As mentioned in the Introduction, the BGFs were denoted as "alpha rhythms" if there was a reduction in magnitude (reactivity) of rsEEG rhythms at the BGFs from the eyes-closed to the eyes-open condition, as shown by rsEEG spectral measures.

Cortical sources of rsEEG epochs as computed by eLORETA

The procedures for the rsEEG cortical source estimations were described in previous reference articles of our Consortium (Babiloni et al., 2017, 2019, 2020b). We used the official freeware tool called exact LORETA (eLORETA) for the linear estimation of the cortical source activity generating scalp-recorded rsEEG rhythms (Pascual-Marqui, 2007). The present implementation of eLORETA uses a head volume conductor model composed of the scalp, skull, and brain. In the scalp compartment, exploring electrodes can be virtually positioned to give EEG data as an input to the source estimation (Pascual-Marqui, 2007). The brain model is based on a realistic cerebral shape taken from a template typically used in the neuroimaging studies, namely that of the Montreal Neurological Institute (MNI152 template). The eLORETA freeware solves the so-called EEG inverse problem estimating "neural" current density values at any cortical voxel of the mentioned head volume conductor model. The solutions are computed rsEEG frequency bin-by-frequency bin.
The input for this estimation is the EEG spectral power density computed at scalp electrodes. The output is the electrical brain source space formed by 6,239 voxels with 5 mm resolution, restricted to the cortical grey matter of the head volume conductor model. An equivalent current dipole is in each voxel. For each voxel, the eLORETA package provides the Talairach coordinates, the lobe, and the Brodmann area (BA).

The eLORETA solutions of rsEEG closed-eyes and open-eyes data were normalized by the following procedure. We averaged eLORETA solutions across two conditions (eyes-closed and eyes-open), all frequency bins from 0.5 to 45 Hz, and 6,239 voxels of the brain model volume, to obtain the eLORETA "mean" solution. Afterwards, we computed the ratio between any original eLORETA solutions at a given condition/frequency bin/voxel and the eLORETA "mean" solution. As a result, any original eLORETA solution at a given condition/frequency bin/voxel changed to a normalized eLORETA solution.

In line with the general low spatial resolution of the current EEG methodological approach (i.e., 30 scalp electrodes), we performed a regional analysis of the eLORETA solutions. For this purpose, we collapsed the eLORETA solutions within frontal, central, parietal, occipital, temporal, and limbic macro-regions (ROIs) considered separately. Table 2 reports the list of the BAs used for the ROIs considered in the present study. Of note, the main advantage of the regional analysis of eLORETA solutions was that we could disentangle the rsEEG source activity in contiguous cortical areas. For example, the rsEEG source activity in the occipital ROI was disentangled from that estimated in the parietal and temporal ROIs, etc. This was made possible by the fact that eLORETA solves the linear inverse problem by considering (at least in part) the effects of the head as a volume conductor. In contrast, the solutions of rsEEG power density computed at a parietal scalp electrode reflect the contribution of source activities not only of the underlying parietal cortex but also of surrounding occipital and temporal cortices.

For the present eLORETA cortical source estimation, a frequency resolution of 0.5 Hz was used, namely, the maximum frequency resolution allowed by the use of 2-s artefact-free EEG epochs.

BRODMANN AREAS INTO THE REGIONS OF INTEREST (ROIs)	
Frontal	8, 9, 10, 11, 44, 45, 46, 47
Central	1, 2, 3, 4, 6
Parietal	5, 7, 30, 39, 40, 43
Occipital	17, 18, 19
Temporal	20, 21, 22, 37, 38, 41, 42
Limbic	31, 32, 33, 34, 35, 36

Table 2*. Regions of interest (ROIs) used for the estimation of the cortical sources of the resting-state electroencephalographic (rsEEG) rhythms in the present study. Any ROI is defined by some Brodmann areas of the cerebral source space in the freeware used in this study, namely the exact low-resolution brain electromagnetic source tomography (eLORETA).*

The computation of the rsEEG background frequency (BGF) reactivity

To analyze the rsEEG background frequency (BGF) reactivity from the eyes-closed to the eyes-open condition, we considered the eLORETA source solutions estimated in the central, parietal, and occipital ROIs. Based on the reference rsEEG studies of our Consortium (Babiloni et al., 2017, 2019, 2020b), the rsEEG BGF reactivity was measured at the BGF 2 frequency band, which showed the maximum source activities in the Healthy participants during the eyes-closed condition.

The "reactivity" dependent variable for the statistical analyses was obtained by averaging the eLORETA BGF 2 source solutions in the central, parietal, and occipital ROIs. To avoid habituation effects in the eyes-open condition, that reactivity was computed based on the eLORETA solutions estimated during the first minute of the rsEEG recordings in that condition (when the rsEEG BGF reactivity is maximum). As no significant habituation effect was described in the eyes-closed condition, eLORETA solutions were estimated during all five minutes of the rsEEG recordings in that condition.

The rsEEG BGF reactivity from the eyes-closed to the eyes-open condition was computed by the following formula:

$$\text{Reactivity (\%)} = \frac{eyes\ open - eyes\ closed}{eyes\ closed} * 100$$

According to this definition, the percent negative values (i.e., weaker BGF source activities during the eyes-open than the eyes-closed condition) indexed a reduction (reactivity) in the source BGF activities from the eyes-closed to the eyes-open condition (Babiloni et al., 2010; Del Percio et al., 2011). On the contrary, the percent positive values (i.e., greater BGF source activities during the eyes-open than the eyes-closed condition) indexed an increase in the source BGF activities from the eyes-closed to the eyes-open condition.

Figure 2 plots the individual values of the reactivity (%) of the central-parietal-occipital rsEEG (eLORETA) BGF 2 source activity from the eyes-open (1 minute) to the eyes-closed (5 minutes) condition for all Healthy (N = 25), ADD (N = 35) and PDD (N = 73) participants.

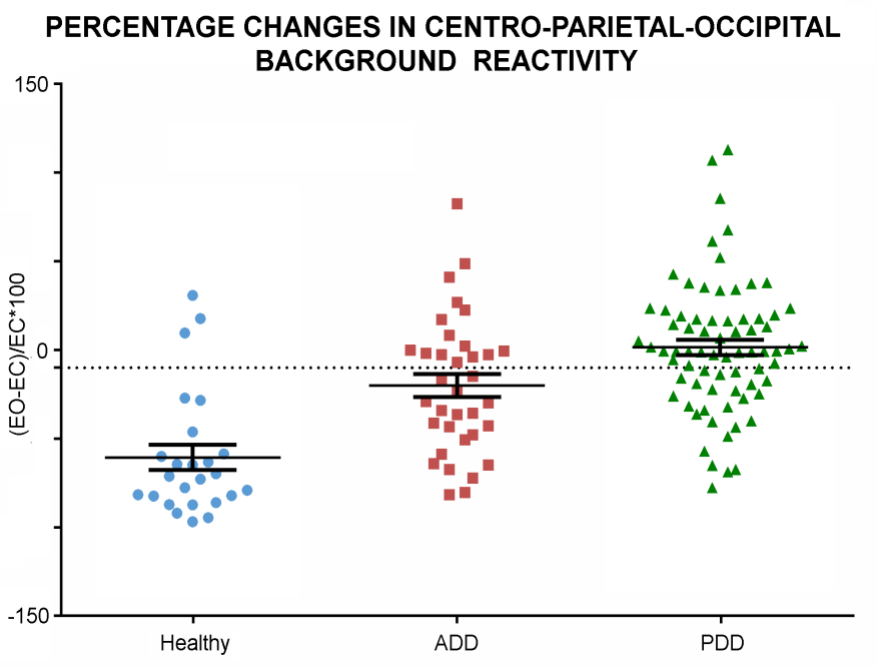

Figure 2. *Individual values of the reactivity (%) of the central-parietal-occipital rsEEG (eLORETA) background frequency 2 (BGF 2) source activity from the eyes-open (1 minute) to the eyes-closed (5 minutes) condition for all cognitively normal older adults (Healthy, N = 25) and patients with dementia due to Alzheimer's disease (ADD, N = 35) and Parkinson's disease (PDD, N= 73). The percent negative values indexed a reduction (reactivity) in the BGF 2 source activities from the eyes-closed (EC) to the eyes-open (EO) condition. In contrast, the percent positive values indexed an increase in the BGF 2 source activities from the eyes-closed to the eyes-open condition.*

Figure 3 illustrates the percentage of BGF (alpha)-reactive Healthy, ADD, and PDD subjects as a function of the reactivity threshold of the central-parietal-occipital rsEEG (eLORETA) BGF 2 source activity. The percentage of BGF-reactive Healthy subjects does not change when the reactivity threshold changes between 0% and -25%; that percentage remains 88.0% (22 BGF-reactive Healthy participants). On the contrary, the percentage of BGF-reactive ADD and PDD patients decreases when the reactivity threshold changes between 0% and -25%. Of note, the percentage of BGF-reactive subjects was lower in (i) the PDD and ADD groups than the Healthy group and (ii) the PDD group than the ADD group. Specifically, the percentage of the BGF-reactive ADD patients decreased from 77.1% (27 BGF-reactive ADD patients) to 48.6% (17 BGF-reactive ADD patients). The percentage of BGF-reactive PDD patients decreases from 53.4% (39 BGF-reactive PDD patients) to 20.5% (15 BGF-reactive PDD patients).

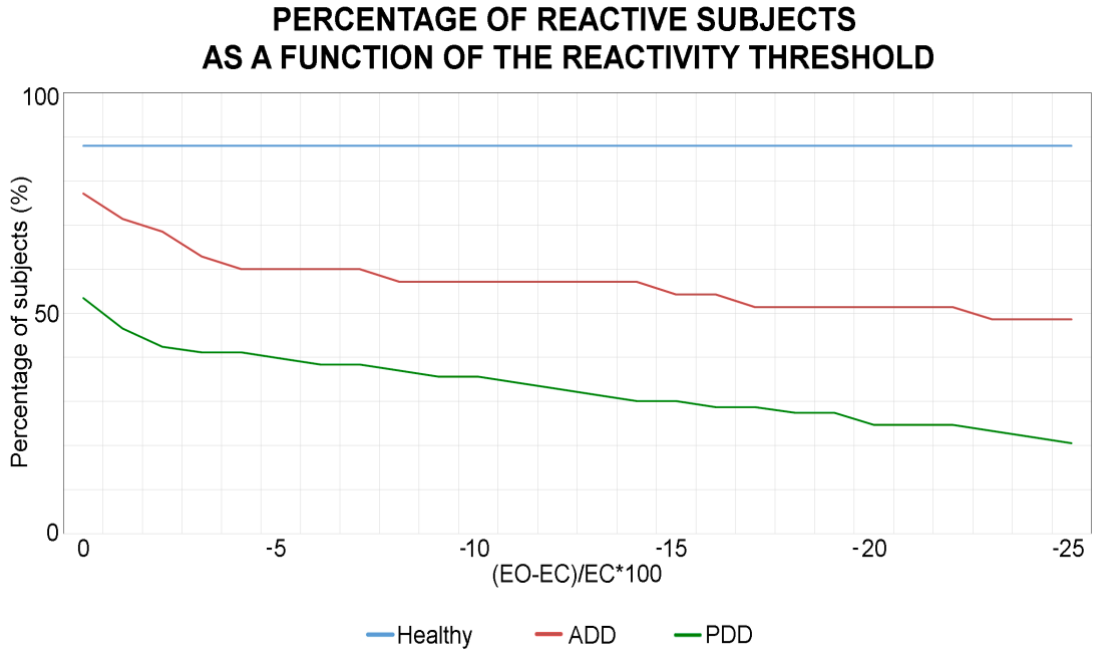

Figure 3. *Percentage of background frequency (BGF)-reactive Healthy, ADD, and PDD participants as a function of the reactivity threshold of the central-parietal-occipital rsEEG (eLORETA) BGF 2 source reactivity.*

In the present study, we used an arbitrary threshold of BGF (alpha) source reactivity set at -10 %. Based on this threshold value, we identified 3 Healthy, 15 ADD, and 47 PDD participants showing the lack of a significant BGF-reactivity as defined above (they showed either increased BGF

source activities from the eyes-closed to the eyes-open condition or decreased alpha source activities from -10% to 0%). Therefore, the BGF 2 source reactivity was seen in 22 out of 25 Healthy seniors, 20 out of 35 ADD patients, and 26 out of 73 PDD patients. They were denoted as "alpha-reactive" participants in the following analyses. Fisher tests ($p < 0.05$) showed a statistically significant reduction of the percentage of "alpha-reactive" participants in (i) the PDD ($p < 0.00001$) and ADD ($p < 0.01$) groups than the Healthy group and (ii) the PDD group than the ADD group ($p < 0.05$). Table 3 summarizes the most relevant demographic (i.e., age, sex, and education) and clinical (i.e., MMSE score) features of the subgroups of the alpha-reactive Healthy, alpha-reactive ADD, alpha-reactive PDD, alpha-nonreactive ADD, and alpha-nonreactive PDD participants.

Furthermore, Table 3 reports the results of the presence or the absence of statistically significant differences ($p < 0.05$) among the five groups for the age (ANOVA), sex (Freeman-Halton test), education (analysis of variance, ANOVA), and MMSE score (Kruskal-Wallis test). As expected, a statistically significant difference was found for the MMSE score ($H = 56.6$, $p < 0.00001$), showing a higher score in the alpha-reactive Healthy group than in the demented groups (post-hoc test = $p < 0.0001$). On the contrary, no statistically significant differences were found in the age, sex, and education among all demented groups ($p > 0.05$).

	Alpha-reactive Healthy	**Alpha-reactive ADD**	**Alpha-reactive PDD**	**Alpha-nonreactive ADD**	**Alpha-nonreactive PDD**	**Statistical Analysis**
N	22	20	26	15	47	-
Age (mean score ± SE)	72.8 ± 1.7	73.6 ± 1.4	72.9 ± 1.3	72.3 ± 1.9	72.6 ± 0.9	ANOVA: n.s.
Sex (M/F; % of M)	15/7; 68%	16/4;80%	22/4; 85%	11/4; 73%	39/8; 83%	Freeman-Halton: n.s.
Education (mean years ± SE)	10.1 ± 0.9	9.6 ± 0.7	9.6 ± 0.8	9.7 ± 0.8	9.3 ± 0.6	ANOVA: p = n.s.
MMSE (mean score ± SE)	27.8 ± 0.4	19.4 ± 0.9	19.0 ± 1.0	19.3 ± 1.2	18.8 ± 0.6	Kruskal- Wallis test: H = 50.6, p = 0.00001

Table 3. *Mean values (±SE) of the demographic and clinical data as well as the results of their statistical comparisons ($p < 0.05$) in the subgroups of the alpha-reactive Healthy (N = 22), alpha-reactive ADD (N = 20), alpha-reactive PDD (N = 26), alpha-nonreactive ADD (N = 15), and alpha-nonreactive PDD (N = 47) participants. Legend: M/F = males/females; n.s. = not significant ($p > 0.05$); MMSE = Mini Mental State Evaluation.*

Statistical analysis of cognitive measures in Healthy, ADD, and PDD groups

For each subject, the compositive cognitive scores of the language, visuospatial function, executive function/attention, and memory were calculated. Specifically, the following procedure was performed: (i) for each ADD and PDD participant, the individual scores of the neuropsychological

tests (Verbal fluency test for letters, Verbal fluency test for categories, Line Orientation test, Face Recognition test, Trail making test B-A, Stroop test, Confusion Assessment Method-executive function part, Digit Span Forward, Digit Span Backward, Oktem Verbal Memory test, and Confusion Assessment Method-memory part) were z-transformed based on the mean and standard deviation of the Healthy group; (ii) for each Healthy participant, the individual scores of the neuropsychological tests were z-transformed based on the mean and standard deviation of the Healthy group not considering the subject on which the z-transformation is being calculated; (iii) for each participant, the sign of the z-transformed measures was adjusted such that the test scores expressing a good performance were always positive; (iv) for each participant, the compositive cognitive score of the language were evaluated averaging the z-transformed measures of the Verbal fluency test for letters, Verbal fluency test for categories; the compositive cognitive score of the visuospatial functions was evaluated averaging the z-transformed measures of the Line Orientation test and Face Recognition test; the compositive cognitive score of executive function and attention was evaluated averaging the z-transformed measures of the Trail making test B-A, Stroop test, and Confusion Assessment Method-executive function part; the compositive cognitive score of memory was evaluated averaging the z-transformed measures of the Digit Span Forward, Digit Span Backward, Oktem Verbal Memory test, and Confusion Assessment Method-memory part.

Furthermore, for each subject, the global composite cognitive score was calculated by averaging the composite cognitive score scores of the language, visuospatial function, executive function/attention, and memory.

Finally, five Kruskal-Wallis ANOVAs ($p < 0.05$) were performed to evaluate the presence or absence of statistically significant differences among the Healthy, ADD, and PDD groups for the global, language, visuospatial function, executive function/attention, and memory composite cognitive scores. Those statistical analyses of the cognitive measures in Healthy, ADD, and PDD groups were performed by the STATISTICA software, version 10.0 (StatSoft Inc., www.statsoft.com).

Statistical analysis of background reactivity in Healthy, ADD, and PDD groups

Two statistical sessions were performed to evaluate the clinical relevance of the background reactivity in Healthy, ADD, and PDD participants.

As a first statistical analysis at the individual level, the Spearman test ($p < 0.05$) evaluated the correlation between the global composite cognitive score, as an index of the global cognition, and the reactivity (%) of the central-parietal-occipital rsEEG (eLORETA) BGF 2 source activity from the eyes-open to the eyes-closed condition, as an index of background reactivity. That correlation analysis

was performed considering all Healthy, ADD, and PDD individuals as a whole group for 2 reasons. On the one hand, the hypothesis was that background reactivity may be correlated with the global cognitive status in seniors in general, namely including cases with both normal and impaired cognitive functions. On the other hand, the correlation study would have had a low statistical sensitivity if performed only in the separate groups, owing to the very limited scatter of global composite cognitive scores within a given group. This statistical analysis was performed by the STATISTICA software, version 10.0 (StatSoft Inc., www.statsoft.com).

As a second statistical analysis at the individual level, the reactivity (%) of the central-parietal-occipital rsEEG (eLORETA) BGF 2 source activity from the eyes-open to the eyes-closed condition, as an index of background reactivity, was used as a discriminant variable for the classification of the Healthy, ADD and PDD participants. These classifications were performed by GraphPad Prism software (GraphPad Software, Inc, California, USA) using its implementation of ROC curves (DeLong et al., 1988). The following indexes measured the results of the binary classifications: (i) Sensitivity: It measures the rate of the cases that were correctly classified as cases (i.e., "true positive rate" in the signal detection theory); (ii) Specificity: It measures the rate of the controls who were correctly classified as controls (i.e., "true negative rate" in the signal detection theory); (iii) Accuracy: It is the mean between the sensitivity and specificity weighted for the number of cases and controls; and (iv) AUROC curve: The AUROC curve was used as a major reference index of the global classification accuracy.

Statistical analysis of rsEEG source activities in alpha-reactive Healthy, ADD, and PDD groups

The statistical analyses of the rsEEG source activities in alpha-reactive Healthy, ADD, and PDD groups were performed by the STATISTICA software, version 10.0 (StatSoft Inc., www.statsoft.com). The ANOVA was used to analyze the differences among means of rsEEG eLORETA source activities within and between the alpha-reactive Healthy, ADD, and PDD groups. The Mauchly's test of sphericity was used to assess whether the assumption of sphericity was met, while the Greenhouse-Geisser correction was applied when the data violated that assumption (Abdi, 2010). The Duncan test was used for post-hoc comparisons ($p < 0.01$).

As the use of an ANOVA implies that the dependent variable must be normally distributed, the Kolmogorov-Smirnov test ($p < 0.05$) was used to determine if the regional normalized eLORETA rsEEG current density distributions (i.e., the eLORETA source activities) of a given ANOVA model approximated to Gaussian distributions (null hypothesis of non-Gaussian distributions tested at $p < 0.05$). This was not the case in some cases, so all regional eLORETA source activities were used as

inputs to the log 10 transformation to make them Gaussian. The Kolmogorov-Smirnov test confirmed that all eLORETA regional solutions were Gaussian after that transformation ($p > 0.05$).

Three statistical sessions were performed. The first statistical session tested the hypothesis that the eyes-closed rsEEG source activities (i.e., regional normalized eLORETA solutions) may differ between the alpha-reactive Healthy, ADD, and PDD groups. For this aim, an ANOVA was computed using eyes-closed rsEEG source activities as a dependent variable ($p < 0.05$). The ANOVA factors were group (alpha-reactive Healthy, alpha-reactive ADD, and alpha-reactive PDD), frequency band (Band) (delta, theta, alpha 1, alpha 2, alpha 3, beta 1, beta 2, and gamma), and region of interest (ROI) (frontal, central, parietal, occipital, temporal, and limbic). The clinical unit was used as a covariate. The confirmation of this control hypothesis may require: (i) a statistically significant ANOVA interaction including the factor Group ($p < 0.05$) and (ii) a post-hoc Duncan test indicating statistically significant ($p < 0.01$) differences in the reactivity of the rsEEG source activities among the Healthy, ADD, and PDD groups.

The second statistical session tested the hypothesis that the rsEEG alpha source activities may be reduced from the eyes-closed to the eyes-open condition within each alpha-reactive group of interest (i.e., alpha-reactive Healthy, alpha-reactive ADD group, alpha-reactive PDD). To address this aim, three ANOVAs were computed using the rsEEG source activities (i.e., regional normalized eLORETA solutions) as a dependent variable ($p < 0.05$). The three ANOVAs used the following factors: Condition (eyes-open and eyes-closed), Band (delta, theta, alpha 1, alpha 2, alpha 3, beta 1, beta 2, and gamma), and ROI (central, parietal, and occipital). The clinical unit was used as a covariate. The confirmation of the first working hypothesis required: (i) a statistically significant ANOVA effect including the factor Condition ($p < 0.05$) and (ii) a post-hoc Duncan test indicating statistically significant ($p < 0.01$) reductions (reactivity) of the rsEEG alpha source activities from the eyes-closed to the eyes-open condition (i.e., eyes-closed $\neq$ eyes-open) within the groups.

The third statistical session tested the hypothesis that the percent reactivity of the central, parietal, and occipital alpha 2 and 3 sources (showing the maximum activation in the eyes-closed condition) from the eyes-closed to the eyes-open condition may differ between the alpha-reactive Healthy, ADD, and PDD groups (The percent reactivity was defined as reported in the previous section). To this aim, an ANOVA was computed using that reactivity (i.e., the reactivity of the regional normalized eLORETA solutions) as a dependent variable ($p < 0.05$). The ANOVA factors were Group (alpha-reactive Healthy, alpha-reactive ADD, and alpha-reactive PDD), Band (alpha 2 and alpha 3), and ROI (central, parietal, and occipital). The clinical unit was used as a covariate. The confirmation of the second working hypothesis required: (i) a statistically significant ANOVA interaction including the factors Group and Band ($p < 0.05$) and (ii) a post-hoc Duncan test indicating

statistically significant differences in the reactivity of the rsEEG alpha source activities between the alpha-reactive groups, with greater values in the Healthy than the ADD and PDD groups ($p < 0.01$).

Results

Cognitive measures in Healthy, ADD, and PDD groups

Figure 4 reports the individual values of the cognitive composite scores of the language, visuospatial functions, attention/executive functions, and memory in all Healthy (N = 25), ADD (N = 35), and PDD (N = 73) participants. As expected, the Kruskal-Wallis ANOVAs ($p < 0.05$) showed statistically significant differences among the three groups for the cognitive composite scores of the language ($H = 43.9$, $p < 0.00001$; Healthy > ADD and PDD, post-hoc test = $p < 0.005$), attention/executive functions ($H = 40.2$, $p < 0.00001$; Healthy > ADD and PDD, post-hoc test = $p < 0.0005$), and memory ($H = 52.4$, $p < 0.00001$; Healthy > ADD and PDD, post-hoc test = $p < 0.000001$).

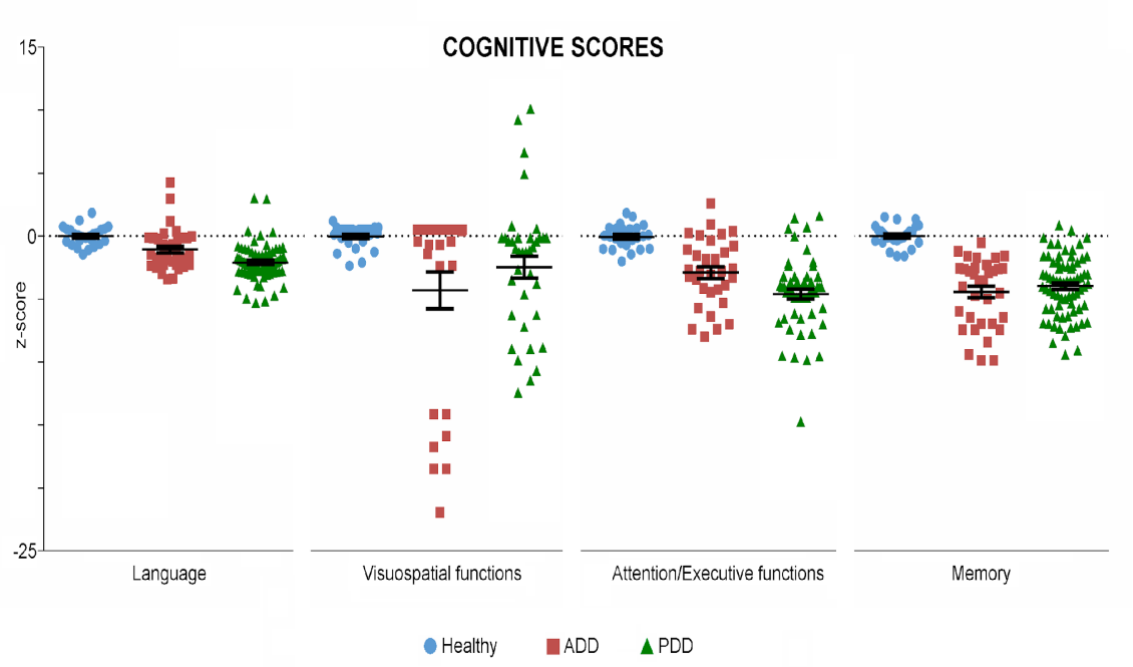

Figure 4. *Individual values of the cognitive composite scores in various cognitive domains in all Healthy (N = 25), ADD (N = 35), and PDD (N= 73) participants. The following four cognitive domains were considered: language, visuospatial functions, attention/executive functions, and memory.*

Figure 5 reports the individual values of the global cognitive composite score in all Healthy (N = 25), ADD (N = 35), and PDD (N = 73) participants. As expected, the Kruskal-Wallis ANOVA ($p < 0.05$) unveiled a statistically significant difference among the three groups ($H = 58.1$, $p < 0.00001$; Healthy > ADD and PDD, post-hoc test = $p < 0.000001$).

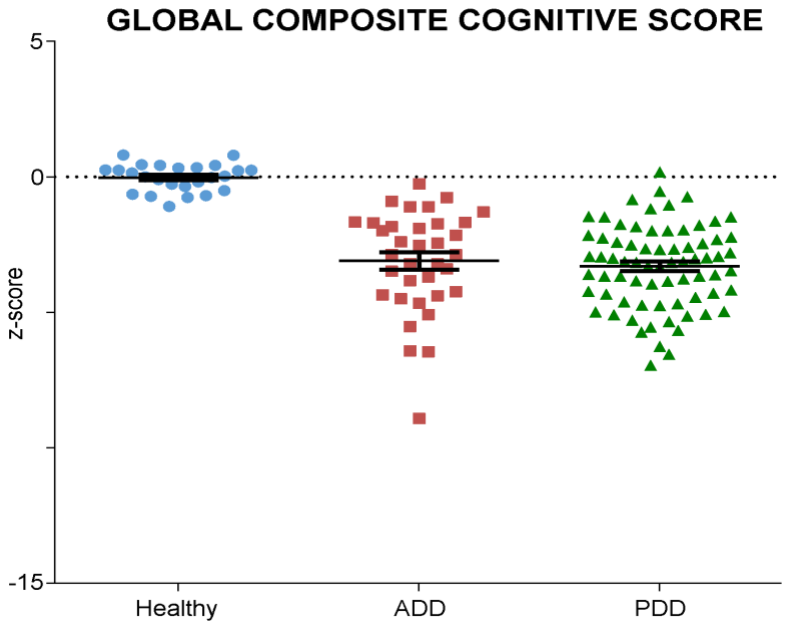

Figure 5. *Individual values of the global cognitive composite score in all Healthy (N = 25), ADD (N = 35) and PDD (N= 73) participants*

Correlation of background reactivity and global composite cognitive score in Healthy, ADD, and PDD groups

Figure 6 illustrates the scatterplot showing the statistically significant negative correlation between the global composite cognitive score and the reactivity (%) of the central-parietal-occipital rsEEG (eLORETA) BGF 2 source activity from the eyes-open to the eyes-closed condition ($r = -0.34$; $p < 0.0001$). The higher the reactivity (%) of the central-parietal-occipital rsEEG (eLORETA) background 2 frequency (BGF 2) source activity, the lower the global composite cognitive (performance) measure.

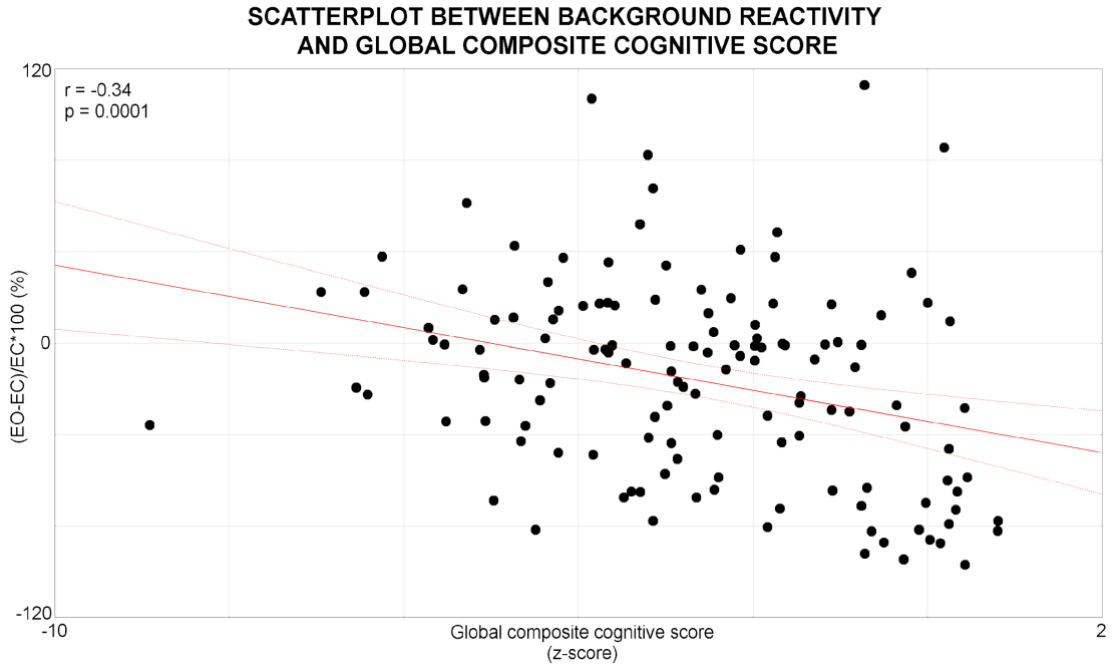

Figure 6. *Scatterplot showing the (negative) linear correlation between the reactivity (%) of the central-parietal-occipital rsEEG (eLORETA) BGF 2 source activity from the eyes-open (1 minute) to the eyes-closed (5 minutes) condition and the global composite cognitive score in all (N = 133) participants of the present study. In the scatterplots, the R coefficient of Spearman test and the relative p values are reported.*

Classification among Healthy, ADD, and PDD individuals based on the background reactivity

The results of the classification analysis, using the reactivity (%) of the central-parietal-occipital rsEEG (eLORETA) BGF 2 source activity from the eyes-open to the eyes-closed condition as discriminant variable, showed: (i) a good classification accuracy for the contrast between Healthy vs. ADD individuals (AUROC = 0.80, sensitivity = 80.0%, specificity = 76.0%, accuracy = 77.7%; see Figure 7 top); (ii) a good classification accuracy for the contrast between Healthy vs. PDD individuals (AUROC = 0.88, sensitivity = 91.8%, specificity = 80.0%, accuracy = 83.0%; see Figure 7 bottom); and (iii) 3) a low classification accuracy for the contrast between ADD versus PDD individuals (AUROC < 0.70).

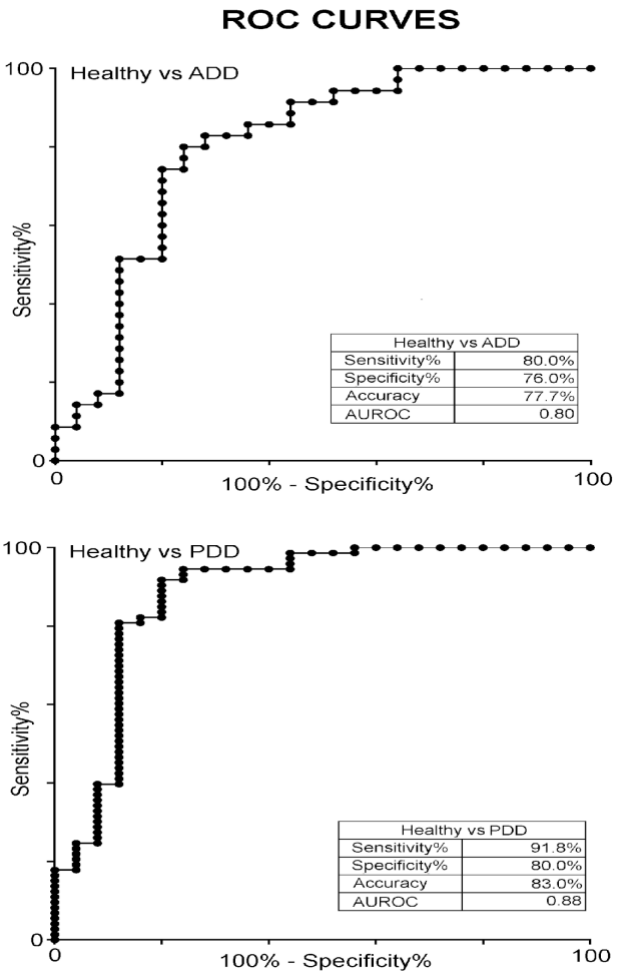

***Figure** 7. Receiver operating characteristic (ROC) curves illustrating the classification of all Healthy (N = 25), ADD (N = 35), and PDD (N= 73) individuals based on the reactivity (%) of the central-parietal-occipital rsEEG (eLORETA) BGF 2 source activity from the eyes-open (1 minute) to the eyes-closed (5 minutes) condition. The area under the ROC (AUROC) curve was 0.80 in the classification of the Healthy and ADD individuals, 0.89 in the classification of the Healthy and PDD individuals, and 0.70 in the classification of the ADD and PDD individuals. These results indicate a moderate/good classification performance.*

Individual frequencies of rsEEG source activities in alpha-reactive Healthy, ADD, and PDD groups

The mean TF was 5.9 Hz (± 0.2 SE) in the alpha-reactive Healthy group (N = 22), 5.0 Hz (± 0.2 SE) in the alpha-reactive ADD group (N = 20), and 4.8 Hz (± 0.2 SE) in the alpha-reactive PDD group (N = 26). Furthermore, the mean BGF was 9.0 Hz (± 0.2 SE) in the alpha-reactive Healthy group, 8.0 Hz (± 0.3 SE) in the alpha-reactive ADD group, and 7.1 Hz (± 0.2 SE) in the alpha-reactive PDD group. The ANOVAs of these data showed the following statistically significant effects: (i) the mean TF was greater ($F = 7.1$; $p < 0.001$) in the alpha-reactive Healthy than the alpha-reactive ADD (post-hoc test = $p < 0.005$) and PDD ($p < 0.001$) groups; (ii) the mean BGF was greater ($F = 15.2$; $p < 0.0001$) in the alpha-reactive Healthy group than the alpha-reactive ADD ($p < 0.005$) and PDD (p

< 0.00005) groups as well as in the alpha-reactive ADD group than the alpha-reactive PDD group ($p < 0.01$).

Distribution of rsEEG source activities in alpha-reactive Healthy, ADD, and PDD groups

There was substantial (> -10%) reactivity to eyes opening in the posterior alpha source activities in 88% of the Healthy seniors, 57% of the ADD patients, and only 35% of the PDD patients. The results of the first statistical session about the eyes-closed rsEEG source activities in alpha-reactive participants are illustrated in Figure 8. This Figure shows the mean values (± SE, log 10 transformed) of the regional rsEEG (eLORETA) source activities during the eyes-closed condition in the alpha-reactive Healthy (N = 22), ADD (N = 20) and PDD (N = 26) groups. The distribution of those source activities differed across the groups, the ROIs, and the frequency bands. In the alpha-reactive Healthy group (as a physiological reference), the temporal, parietal, and occipital (eLORETA) alpha 2 and 3 source activities showed dominant values among all ROIs and frequency bands. Delta, theta, and alpha 1 source activities were characterized by relatively low values in all ROIs, while the beta and gamma source activities were generally very low. As compared to the alpha-reactive Healthy group, the alpha-reactive ADD and alpha-reactive PDD groups exhibited a substantial decrease in occipital rsEEG alpha 2 and alpha 3 source activities. That decrease was also observed in the central and parietal regions in the alpha-reactive ADD group. Furthermore, the alpha-reactive ADD and PDD groups exhibited an increase in widespread delta, theta, and alpha 1 source activity. Based on these input data, the ANOVA results showed a statistical interaction effect ($F = 2.4$, $p < 0.00001$) among the factors Group (alpha-reactive Healthy, alpha-reactive ADD, and alpha-reactive PDD), Band (delta, theta, alpha 1, alpha 2, alpha 3, beta 1, beta 2, and gamma), and ROI (frontal, central, parietal, occipital, temporal, and limbic). The Duncan planned post-hoc ($p < 0.01$) testing produced the following core results: (i) the discriminant pattern alpha-reactive PDD and ADD > alpha-reactive Healthy was fitted by 1) the frontal, central, parietal, occipital, temporal, and limbic delta source activities ($p < 0.001$-0.000001); 2) the frontal, central, parietal, occipital, temporal, and limbic theta source activities ($p < 0.005$-0.000001); and 3) the frontal, central, parietal, and temporal alpha 1 source activities ($p < 0.005$-0.000001); (ii) the discriminant pattern alpha-reactive PDD and ADD < alpha-reactive Healthy was fitted by 1) the occipital alpha 2 source activities ($p < 0.00001$-0.000001) and 2) the occipital alpha 3 source activities ($p < 0.00005$-0.000001); (iii) the discriminant pattern alpha-reactive PDD > alpha-reactive Healthy was fitted by the occipital and limbic alpha 1 ($p < 0.0005$-0.0001); (iv) the discriminant pattern alpha-reactive ADD < alpha-reactive Healthy was fitted by the central and parietal alpha 3 source activities ($p < 0.001$-0.0001); and (v) the discriminant

pattern alpha-reactive PDD > alpha-reactive ADD was fitted by 1) the central alpha 2 source activities ($p < 0.0005$) and 2) the frontal and central alpha 3 source activities ($p < 0.001$-0.0005).

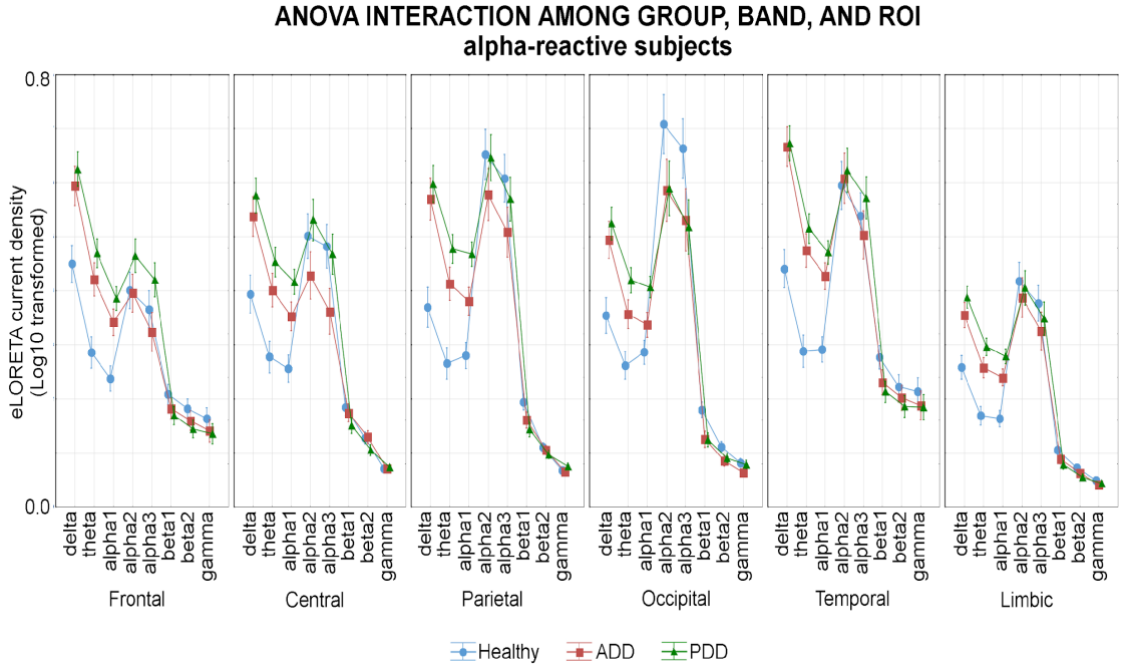

Figure 8. *Mean values (± SE, log 10 transformed) of the rsEEG (eLORETA) source activities during the eyes-closed (5 minutes) condition in the in the subgroups of the alpha-reactive Healthy (N = 22), alpha-reactive ADD (N = 20), and alpha-reactive PDD (N = 26) participants. The ANOVA design showed a statistical interaction effect (F = 2.4, p < 0.00001) among the factors Group (alpha-reactive Healthy, alpha-reactive ADD, and alpha-reactive PDD), Band (delta, theta, alpha1, alpha2, alpha3, beta1, beta2, and gamma), and ROI (frontal, central, parietal, occipital, temporal, and limbic).*

The results of the second statistical session about the eyes-closed and eyes-open rsEEG source activities in alpha-reactive groups are illustrated in Figures 9, 10, and 11. Figure 9 shows the mean values (± SE, log 10 transformed) of rsEEG (eLORETA) source activities during the eyes-open (1 minute) and eyes-closed (5 minutes) conditions in the alpha-reactive Healthy group (N = 22). The ANOVA design showed a statistical interaction effect (F = 3.6; $p < 0.00005$) among the factors Condition (eyes-open, eyes-closed), Band (delta, theta, alpha 1, alpha 2, alpha 3, beta 1, beta 2, and gamma), and ROI (central, parietal, and occipital). The Duncan planned post-hoc ($p < 0.01$) testing showed that the discriminant pattern eyes-closed > eyes-open was fitted by the following eLORETA solutions: (i) the occipital delta source activities ($p < 0.00005$); (ii) the central, parietal, and occipital theta source activities ($p < 0.005$-0.000005); (iii) the central, parietal, and occipital alpha 1 source activities ($p < 0.001$-0.000005); (iv) the central, parietal, and occipital alpha 2 source activities ($p < 0.000005$-0.000001); and (v) the central, parietal, and occipital alpha 3 source activities ($p < 0.000005$-0.000001). Furthermore, the discriminant pattern eyes-closed < eyes-open was fitted by the occipital gamma source activity ($p < 0.001$).

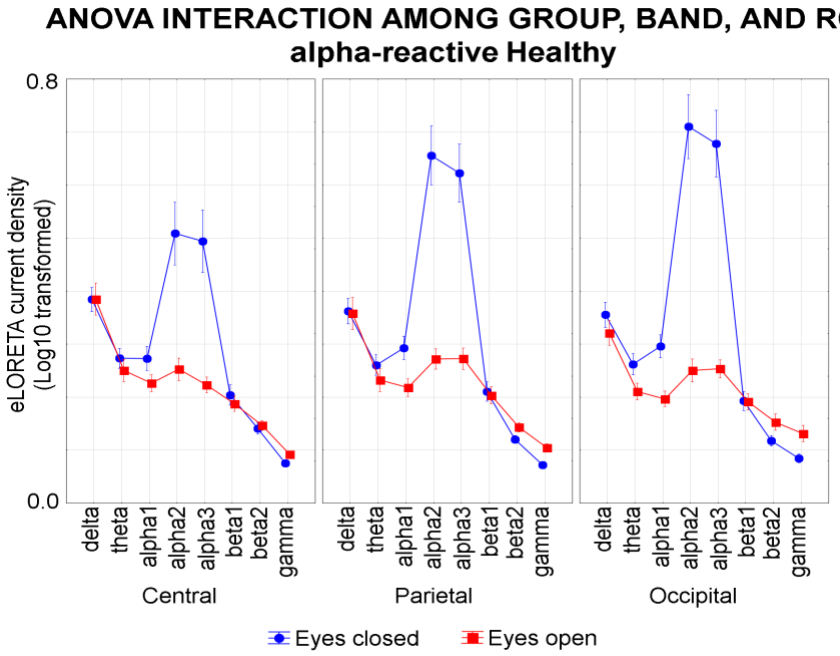

Figure 9. *Mean values (± SE, log 10 transformed) of the rsEEG (eLORETA) source activities during the eyes-open (1 minute) and eyes-closed (5 minutes) conditions in the alpha-reactive Healthy (N = 22) subgroup. The ANOVA design showed a statistical interaction effect (F = 3.6; p < 0.00005) among the factors Condition (open-eyes, EO and eyes-closed, EC), Band (delta, theta, alpha 1, alpha 2, alpha 3, beta 1, beta 2, and gamma), and ROI (central, parietal, and occipital).*

Figure 10 plots the mean values (± SE, log 10 transformed) of rsEEG (eLORETA) source activities during the eyes-open (1 minute) and eyes-closed (5 minutes) conditions in the alpha-reactive ADD group (N = 20). The ANOVA design showed a statistical interaction effect (F = 2.2; p < 0.01) among the factors Condition (eyes-open, eyes-closed), Band (delta, theta, alpha 1, alpha 2, alpha 3, beta 1, beta 2, and gamma), and ROI (central, parietal, and occipital). The Duncan planned post-hoc (p < 0.01) testing showed that the discriminant pattern eyes-closed > eyes-open was fitted by the following eLORETA solutions: (i) the central and parietal theta source activities (p < 0.005-0.001); (ii) the central, parietal, and occipital alpha 1 source activities (p < 0.00001-0.000005); (iii) the central, parietal, and occipital alpha 2 source activities (p < 0.000005-0.000001); and (iv) the central, parietal, and occipital alpha 3 source activities (p < 0.000005-0.000001). Furthermore, the discriminant pattern eyes-closed < eyes-open was fitted by the occipital gamma source activity (p < 0.01).

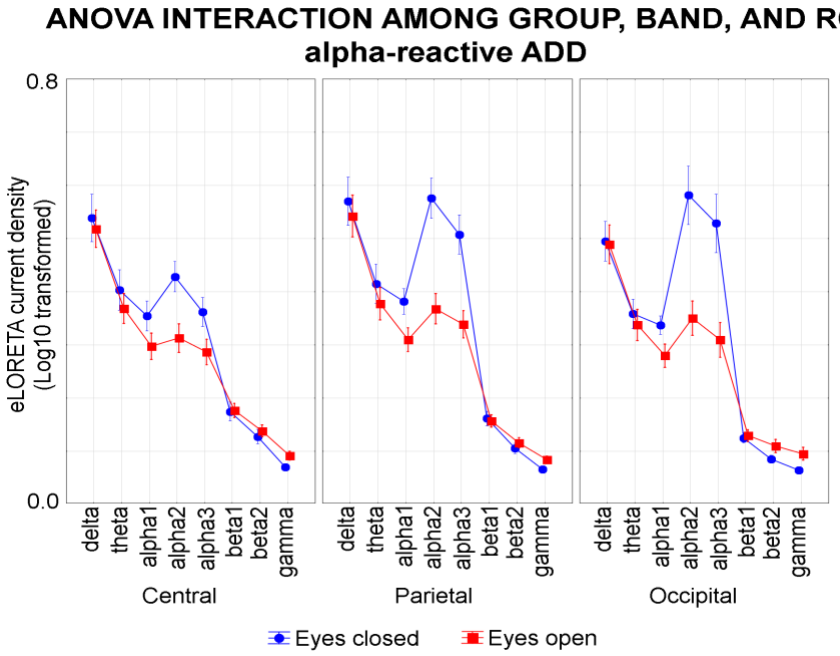

Figure 10. *Mean values (± SE, log 10 transformed) of the rsEEG (eLORETA) source activities during the eyes-open (1 minute) and eyes-closed (5 minutes) conditions in the alpha-reactive ADD (N = 20) subgroup. The ANOVA design showed a statistical interaction effect (F = 2.1; p < 0.01) among the factors Condition (open-eyes, EO and eyes-closed, EC), Band (delta, theta, alpha 1, alpha 2, alpha 3, beta 1, beta 2, and gamma), and ROI (central, parietal, and occipital).*

Figure 11 illustrates the mean values (± SE, log 10 transformed) of rsEEG (eLORETA) source activities during the eyes-open (1 minute) and eyes-closed (5 minutes) conditions in the alpha-reactive PDD group (N = 26). The ANOVA design showed a statistical interaction effect (F = 9.3; p < 0.00001) between the factors Condition (eyes-open, eyes-closed) and Band (delta, theta, alpha 1, alpha 2, alpha 3, beta 1, beta 2, and gamma). The Duncan planned post-hoc (p < 0.01) testing showed that the discriminant pattern eyes-closed > eyes-open was fitted by the delta, theta, alpha 1, alpha 2, and alpha 3 source activities (p < 0.001-0.000005).

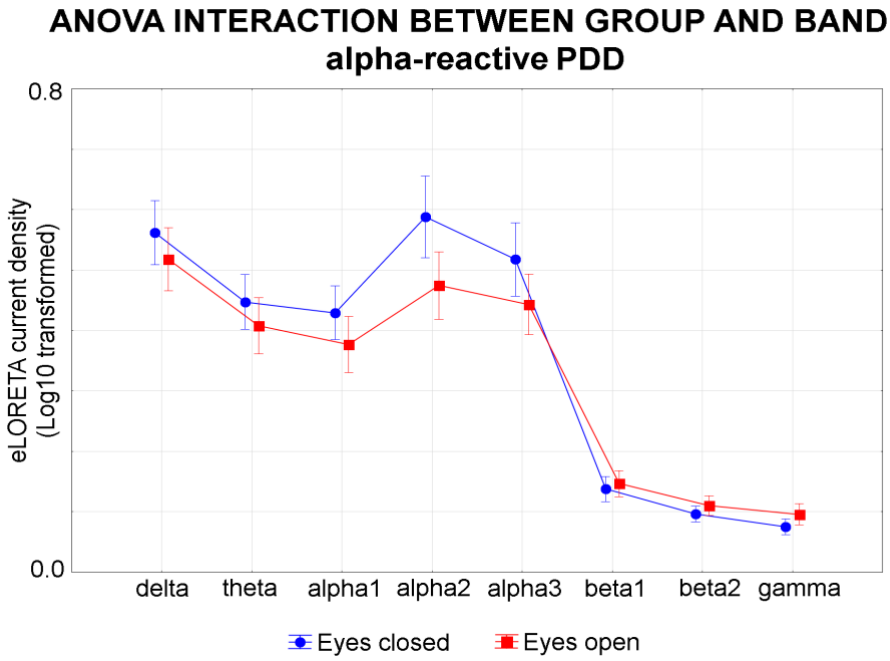

Figure 11. *Mean values (± SE, log 10 transformed) of the rsEEG (eLORETA) source activities during the eyes-open (1 minute) and eyes-closed (5 minutes) conditions in the alpha-reactive PDD (N = 26) subgroup. The ANOVA design showed a statistical interaction effect (F = 9.3; p < 0.00001) among the factors Condition (eyes-open, EO and eyes-closed, EC) and Band (delta, theta, alpha 1, alpha 2, alpha 3, beta 1, beta 2, and gamma), regardless the factor ROI.*

In the third statistical session about the rsEEG alpha 2 and 3 source reactivity to eyes-opening in the alpha-reactive Healthy (N = 22), ADD (N = 20), and PDD (N = 26) participants, the ANOVA showed a statistical interaction effect (F = 3.2; p < 0.01) between the factors Group (alpha-reactive Healthy, alpha-reactive ADD, and alpha-reactive PDD) and ROI (central, parietal, and occipital). Figure 12 depicts the variables of this statistical interaction effect. Namely, it illustrates the mean values (± SE) of the reactivity of the rsEEG (eLORETA) alpha source activities from the eyes-open (1 minute) to the eyes-closed (5 minutes) condition in the alpha-reactive Healthy, ADD, and PDD groups.

In Figure 12, the source activities are averaged across alpha 2 and alpha 3 bands to account for the statistical interaction between the factors Group and ROI. Duncan planned post-hoc (p < 0.01) testing showed a discriminant pattern alpha-reactive Healthy > alpha-reactive ADD > alpha-reactive PDD fitted by the parietal alpha source activities (p < 0.005-0.00005). Furthermore, there was a discriminant pattern alpha-reactive Healthy > alpha-reactive ADD and PDD fitted by the occipital alpha source activities (p < 0.005-0.00001). Finally, there was a discriminant pattern alpha-reactive Healthy > alpha-reactive PDD fitted by the central alpha source activities (p < 0.005).

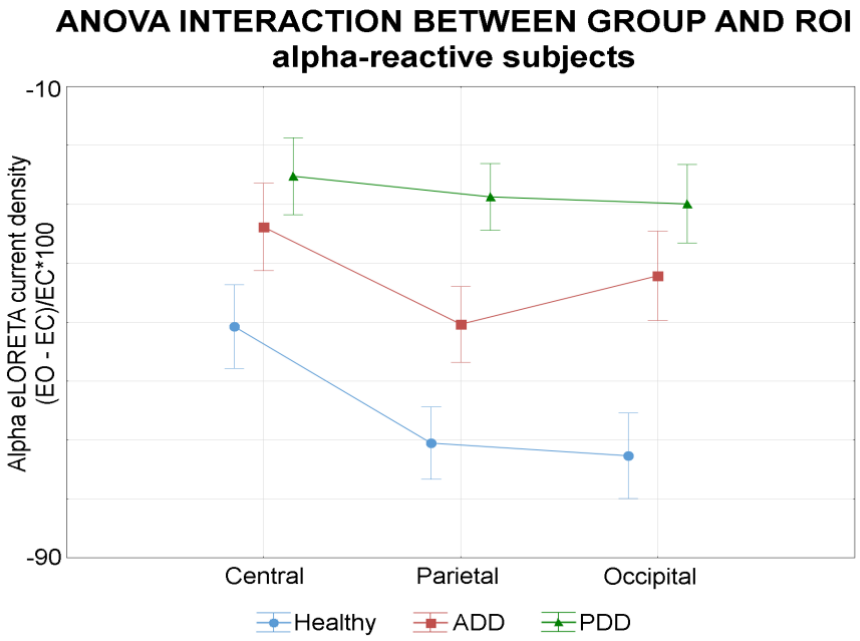

Figure 12. *Mean values (± SE) of the reactivity of the rsEEG (eLORETA) source activities from the eyes-open (1 minute) to the eyes-closed (5 minutes) condition in the alpha-reactive Healthy (N = 22), ADD (N = 20) and PDD (N = 26) participants. The reactivity values are relative to two frequency bands (alpha 2 and alpha 3) and three ROIs (central, parietal, and occipital). The ANOVA design showed a statistical interaction effect (F = 3.2; p < 0.01) among the factors Group and ROI.*

Of note, the above-mentioned findings were not due to outliers from those individual regional normalized eLORETA current densities (log 10 transformed), as shown by Grubbs' test with an arbitrary threshold of $p > 0.001$.

Control analyses

A first control statistical analysis was performed to evaluate whether the correlation between the global composite cognitive score, as an index of the global cognition and the reactivity (%) of the central-parietal-occipital rsEEG (eLORETA) BGF 2 source reactivity from the eyes-open to the eyes-closed condition was also observed in the subgroup of alpha-reactive subjects. To address this aim, the Spearman test ($p < 0.05$) between the above-mentioned variables was executed. A statistically significant negative correlation was found ($r = -0.47$; $p < 0.00005$). The higher the reactivity (%) of the central-parietal-occipital rsEEG (eLORETA) BGF 2 source activity, the lower the global composite cognitive (performance) measure.

A second control statistical analysis was performed to evaluate whether the difference of the rsEEG alpha 2 and 3 source reactivity to eyes-opening in the alpha-reactive Healthy, ADD, and PDD groups may be due to the selected arbitrary threshold of the reactivity at -10%. To this aim, we selected an additional arbitrary threshold for that reactivity at -15%. Based on the threshold value at

-15%, we identified 22 alpha-reactive Healthy, 19 alpha-reactive ADD, and 22 alpha-reactive PDD participants. An ANOVA was computed using the rsEEG BGF (alpha) reactivity as a dependent variable ($p < 0.05$). The ANOVA factors were Group (alpha-reactive Healthy, alpha-reactive ADD, and alpha-reactive PDD), Band (alpha 2 and alpha 3), and ROI (central, parietal, and occipital). Results showed that the results with the control threshold were like those based on the main threshold (i.e., – 10%; see Figure 13). There was a lower reduction in the parietal and occipital rsEEG alpha source reactivity in the alpha-reactive ADD and PDD groups than in the alpha-reactive Healthy group. Furthermore, the reduction in the parietal rsEEG alpha source reactivity was lower in the alpha-reactive PDD than in the alpha-reactive ADD group. Overall, these results suggest that the difference of the rsEEG alpha source reactivity in the alpha-reactive Healthy, ADD, and PDD groups may not be due to the selected arbitrary thresholds for that reactivity.

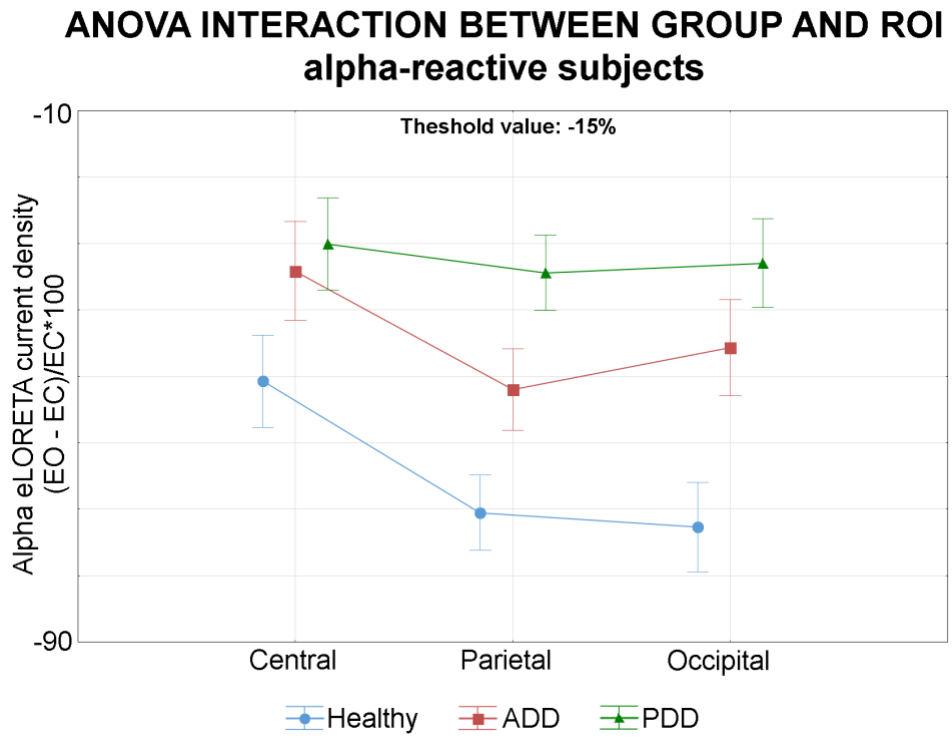

Figure 13. *Mean values (± SE) of the reactivity of the rsEEG (eLORETA) source activities from the eyes-open (1 minute) to the eyes-closed (5 minutes) condition in subgroups of the alpha-reactive Healthy (N = 22), ADD (N = 19) and PDD (N = 22) participants using a threshold of the rsEEG BGF (alpha) reactivity at -15%. The ANOVA design showed a statistical interaction effect ($F = 3.1$; $p < 0.01$) among the factors Group and ROI (central, parietal, and occipital).*

A third control statistical analysis was performed to evaluate that the rsEEG alpha source activities are not reduced from the eyes-closed to the eyes-open condition within each alpha-nonreactive group of interest (i.e., alpha-nonreactive ADD and alpha-nonreactive PDD). To address this aim, two ANOVAs were computed using the rsEEG source activities (i.e., regional normalized eLORETA solutions) as a dependent variable ($p < 0.05$). The ANOVAs used the following factors:

Condition (eyes-open and eyes-closed), Band (delta, theta, alpha 1, alpha 2, alpha 3, beta 1, beta 2, and gamma), and ROI (central, parietal, and occipital). The clinical unit was used as a covariate. The ANOVAs did not show statistically significant differences including factor Condition ($p < 0.05$).

Finally, a fourth control statistical analysis (Mann-Whitney U tests, $p < 0.05$) was performed to evaluate the presence or absence of statistically significant differences between alpha-reactive PDD (ADD) and alpha-nonreactive PDD (ADD) groups for the global, language, visuospatial function, executive function/attention, and memory composite cognitive scores. No statistically significant result was found ($p > 0.05$).

Methodological remarks

In this retrospective and exploratory study, clinical and rsEEG datasets were derived from clinical units that did not follow a preliminary phase of harmonization of the standard operating procedures for the data collection. Furthermore, we could find only a relatively small number of PDD datasets showing rsEEG alpha reactivity from the archive of the present Consortium (www.pdwaves.eu), so we had to use a liberal statistical post-hoc test threshold of $p < 0.01$. Therefore, a future multicentric study should cross-validate the present findings with a larger group of PDD and PDMCI patients, a perfectly balanced number of cases and controls in each clinical unit, and a more conservative statistical threshold to mitigate the risk of false-positive discoveries with multiple comparisons.

Again, one limitation of this study is that the diagnosis of ADD was based only on the criteria of the Diagnostic and Statistical Manual of Mental Disorders, fourth edition (DSM-IV-TR; American Psychiatric Association) and the National Institute of Neurological Disorders and Stroke–Alzheimer Disease and Related Disorders (NINCDS–ADRDA; McKhann et al., 2011).

Moreover, the diagnosis of PDD was based on the criteria of the Diagnostic and Statistical Manual of Mental Disorders, fourth edition (DSM-IV-TR; American Psychiatric Association). No PDD patients underwent neuroimaging investigation.

Third study

RESTING-STATE ELECTROENCEPHALOGRAPHIC RHYTHMS DETERIORATE IN PATIENTS WITH ALZHEIMER'S DISEASE MILD COGNITIVE IMPAIRMENT AT A 6-MONTH FOLLOW-UP

Materials and Methods

Participants

To test the study hypothesis, we used the data from the PDWAVES Consortium archive (www.pdwaves.eu). Specifically, we used clinical, neuropsychological, genetic, cerebrospinal fluid (CSF), magnetic resonance imaging (MRI), and rsEEG data collected in 52 ADMCI patients and 60 Healthy participants matched for age, sex, and education. They were previously recruited from the following clinical units: the Sapienza University of Rome (Italy), the University of Genoa (Italy), the Medipol University of Istanbul (Turkey), the Izmir University (Turkey), the Institute for Research and Evidence-based Care (IRCCS) "Fatebenefratelli" of Brescia (Italy), the IRCCS SDN of Naples (Italy), the IRCCS Oasi Maria SS of Troina (Italy), and the IRCCS San Raffaele Pisana of Rome (Italy). All participants received (1) the rsEEG recording in the conditions of eyes closed and open, (2) the clinical and neuropsychological testing, and (3) structural MRIs at the baseline (T0) and a follow-up of 6 months (T6).

According to the NIA-AA guidelines, the diagnosis of AD was typically based on the "positivity" to the Aβ1-42/phospho-tau ratio in the CSF; in some cases, it was based on biomarkers of (1) brain hypometabolism, derived from18F-fluorodeoxyglucose positron emission tomography (FDG-PET), and (2) atrophy of the hippocampus, parietal, temporal, and posterior cingulate regions as revealed by volumetric MRIs (Albert et al., 2011; Jack et al., 2018). That "positivity" was judged by the physicians in charge of releasing the clinical diagnosis to the patients, according to the local diagnostic routine of the participating clinical Units.

The clinical inclusion criteria for the selection of the ADMCI patients were as follows: (1) age of 55-90 years; (2) reported memory complaints confirmed by a relative; (3) Mini-Mental State Evaluation (MMSE) score of 24 or higher; (4) Clinical Dementia Rating (CDR) score of 0.5 (Morris et al., 1993); (5) logical memory test (Wechsler, 1987) score of 1.5 standard deviations (SD) lower than the mean adjusted as age; (2) the cognitive deficits had not to interfere significantly with the functional independence in the activities of daily living; (6) Geriatric Depression Scale (15-item GDS; Brown et al., 2005) score of 5 or lower; (7) modified Hachinski ischemia (Rosen et al., 1980) score

of 4 or lower; (8) education of 5 years or higher; and (8) amnesic syndrome within single or multi-domain MCI status.

The clinical exclusion criteria for the selection of the ADMCI patients were as follows: (1) other significant neurological, systemic, or psychiatric illness; (2) mixed dementing disease; (3) actual participation in a clinical trial using disease-modifying drugs; (4) systematic use of antidepressant drugs with anticholinergic side effects; (5) chronic use of neuroleptics, narcotics, analgesics, sedatives or hypnotics (i.e., benzodiazepines); (6) anti-parkinsonian medications (cholinesterase inhibitors and Memantine allowed); (7) diagnosis of epilepsy or report of seizures or epileptiform EEG signatures in the past; and (8) major depression disorders described in the Diagnostic and Statistical Manual of Mental Disorders (DSM-5).

In all ADMCI patients, *APOE4* genotyping, and AD-relevant CSF biomarkers were assessed in the framework of a neurobiological definition of AD in line with the NIA-AA Research Framework (Jack et al., 2018). The CSF samples were pre-processed, frozen, and stored in line with the Alzheimer's Association Quality Control Programme for CSF biomarkers (Mattson et al., 2011). Dedicated single-parameter colorimetric enzyme-linked immunosorbent assay ELISA kits (Innogenetics, Ghent, Belgium) were used to measure amyloid beta 1-42 (i.e., Aβ42). Levels of the protein tau (i.e., total tau, t-tau) and a phosphorylated form of tau at residue 181 (i.e., p-tau) were also measured. From one frozen aliquot of CSF, the assays were run parallel according to the manufacturer's instructions. Each sample was assessed in duplicate. A standard sigmoidal curve was plotted to allow the quantitative expression (pg mL^{-1}) of measured light absorbance. All ADMCI patients in the present study were "positive" to the CSF Aβ42/p-tau biomarker with a threshold defined in a previous investigation of our Workgroup (Marizzoni et al., 2019). In that investigation, the cut-off of "positivity" to that CSF Aβ42/p-tau biomarker was 15.2 for *APOE4* carriers and 8.9 for *APOE4* non-carriers. In the present study, all ADMCI patients with *APOE4* status had the CSF Aβ42/p-tau lower than 15.2, whereas the ADMCI patients without *APOE4* status had the CSF Aβ42/p-tau lower than 8.9.

Furthermore, in all ADMCI patients, relevant MRI markers were measured at baseline and 6-month follow-up. All MRI scans were performed using 3.0 Tesla machines. The MRI protocol consisted of several acquisitions, including two anatomical T1, anatomical T2, fluid-attenuated inversion recovery (FLAIR), and diffusion tensor imaging scans. Only anatomical T1 scans were available for all units and were analyzed in the present study. In the centralized MRI analysis, all data were visually inspected for quality assurance before extracting the MRI biomarkers. Specifically, we checked that there were no gross partial brain coverage errors and no major visible artifacts, including motion, wrap-around, radio frequency interference, and signal intensity or contrast inhomogeneities.

The two anatomical T1 scans were averaged, and the anatomical scans obtained were analyzed using FreeSurfer version 5.1.0 to automatically generate: (1) MRI-based volumes of the hippocampus and lateral ventricle (normalized concerning total intracranial volume, TIV) for the left and right hemispheres and (2) MRI-based cortical thicknesses of the parahippocampal gyrus, fusiform gyrus, entorhinal cortex, praecuneus, and cuneus for the left and right hemispheres.

In all ADMCI patients, global cognitive status, and performances in various cognitive domains (e.g., episodic memory, language, executive function, attention, and visuospatial function) were assessed at the baseline and the 6-month follow-up. Specifically, (1) the global cognitive status was tested by the MMSE and the Alzheimer's Disease Assessment Scale–Cognitive Subscale (ADAS-Cog; Folstein et al., 1975; Rosen et al., 1984); (2) the episodic memory was assessed by the immediate and delayed recall of Rey Auditory Verbal Learning Test (Rey et al., 1968); (3) the language function was evaluated by 1-min Verbal fluency test for letters (Novelli et al., 1986) and 1-min Verbal fluency test for category (fruits, animals or car trades; Novelli et al., 1986); (4) the executive functions and the attention were tested by the Trail making test (TMT) parts A and B (Reitan, 1958); and (5) the visuospatial functions were assessed by the Clock drawing test (Freedman et al., 1994).

In all ADMCI patients, the use of selective serotonin reuptake inhibitors (SSRIs), noradrenaline reuptake inhibitors (SNRIs), acetylcholinesterase inhibitors (AChEIs), and inhibitors of N-methyl-D-aspartate receptors (iNMDARs) were allowed. The ADMCI patients using those drugs could take their medications immediately after the rsEEG experiments, which were planned in the late morning. Therefore, the ADMCI patients delayed the intake of their medications only for a few hours during their routine.

All Healthy seniors underwent a cognitive screening (including MMSE and GDS) and physical and neurological examinations to exclude subjective memory complaints (SMCs), cognitive deficits, and mood disorders. They had an MMSE score equal to or greater than 27, a CDR scores equal to 0, and a GDS score lower than the threshold of 5 (no depression) or were evaluated as having no depression after an interview with a physician or a clinical psychologist at the time of the enrolment. The Healthy seniors with previous or present neurological or psychiatric disease were excluded. Furthermore, the Healthy seniors affected by any chronic systemic illnesses (e.g., diabetes mellitus) were excluded, as were the Healthy seniors taking chronically psychoactive drugs. Unfortunately, the Healthy datasets were not available at the 6-month follow-up.

Table 1 summarizes the most relevant demographic (i.e., age, sex, and education attainment) and clinical (i.e., MMSE score) features observed in the Healthy (N = 60) and ADMCI (N = 52) groups. Furthermore, Table 1 reports the results of the presence or absence of statistically significant differences ($p < 0.05$) between the two groups for age (T-test), sex (Fisher test), educational

attainment (T-test), and MMSE score (Mann Whitney U test). As expected, a statistically significant difference was found in the MMSE score ($p < 0.00001$), showing a higher score in the Healthy than the ADMCI group. On the contrary, no statistically significant differences were found in the age, sex, and educational attainment between the groups ($p > 0.05$).

DEMOGRAPHIC AND CLINICAL DATA IN HEALTHY AND ADMCI			
	Healthy	**ADMCI**	**Statistical analysis**
N	60	52	-
Age (years, mean ± SE)	69.1 ± 0.9	69.6 ±0 .9	T-test = n.s.
Sex (M/F)	28/32	20/32	Fisher test = n.s.
Education (years, mean ± SE)	11.0 ± 0.6	11.3 ± 0.6	T-test = n.s.
MMSE (scores, mean ± SE)	28.6 ± 0.2	26.5 ± 0.3	Mann-Whitney U test: $p < 0.00001$

Table 1. *Mean values (± standard error of the mean, SE) of the demographic and clinical data as well as the results of their statistical comparisons ($p < 0.05$) in the groups of cognitively normal older adults (Healthy, N = 60) and patients with mild cognitive impairment due to Alzheimer's disease (ADMCI, N = 52). Legend: M/F = males/females; n.s. = not significant ($p > 0.05$); MMSE = Mini-Mental State Evaluation.*

Table 2 reports the most relevant clinical (i.e., GDS, CDR, and Hachinski Ischemic Score), genetic (i.e., *APOE* genotyping), and CSF (i.e., Aβ42, t-tau, p-tau, and Aβ42/ p-tau) features in the ADMCI group (N = 52). Table 2 also reports the number and the percentages of ADMCI patients assuming the following drug classes: selective serotonin reuptake inhibitors (SSRIs), noradrenaline reuptake inhibitors (SNRIs), acetylcholinesterase inhibitors (AChEIs), and inhibitors of N-methyl-D-aspartate receptors (iNMDARs).

CLINICAL, GENETIC (APOE), CEREBROSPINAL FLUID MARKERS, AND DRUGS IN THE ADMCI GROUP	
Clinical markers	
Geriatric depression scale (GDS)	2.6 ± 0.2
Clinical dementia rating (CDR)	0.5 ± 0.0
Hachinski ischemic score (HIS)	0.8 ±0.1
Genetic marker	
APOE4 (%)	81%
Cerebrospinal fluid markers	
Aβ42 (pg/ml)	502 ± 20
p-tau (pg/ml)	84 ± 5
t-tau (pg/ml)	592 ± 44
Aβ42/p-tau	7.0 ± 0.4
Drugs	
Selective serotonin reuptake inhibitors (SSRIs; N, %)	25% (N=13)
Selective serotonin and noradrenaline reuptake inhibitors (SNRIs, N, %)	7.7% (N=4)
Acetylcholinesterase inhibitors (AChEIs; N, %)	15.4% (N=8)
Antagonists of N-methyl-D-aspartate receptors (aNMDARs, N, %)	0% (N=0)

Table 2. *Mean values (±SE) of the clinical (i.e., Geriatric Depression Scale, Clinical Dementia Rating, and Hachinski Ischemic Score), genetic (i.e., Apolipoprotein E genotyping, APOE), and cerebrospinal fluid (i.e., beta-amyloid 1-42, Aβ 42; protein tau, t-tau; a phosphorylated form of the protein tau, p-tau; and Aβ 42/ p-tau ratio) data in the ADMCI patients (N =52). In line with the inclusion criteria, all ADMCI patients had a CDR score of 0.5, a GDS score of ≤ 5, anaan HIS score of ≤ 4. The number and percentages of ADMCI patients assuming the selective serotonin reuptake inhibitors (SSRIs), selective serotonin and noradrenaline reuptake inhibitors (SNRIs), acetylcholinesterase inhibitors (AChEIs), and antagonists of N-methyl-D-aspartate receptors (aNMDARs) are also reported*

The local institutional Ethical Committees approved the study. All experiments were performed with the informed and overt consent of each participant or caregiver, in line with the Code of Ethics of the World Medical Association (Declaration of Helsinki) and the standards established by the local Institutional Review Board.

The rsEEG recordings

The electrophysiological data were recorded by professional digital EEG systems licensed for clinical applications. The following digital EEG systems were used: BrainAmp 32-Channel DC System (Brain Product GmbH, Germany), Waveguard caps (ANT Neuro, The Netherlands), EB Neuro-BE LIGHT (EB Neuro, Italy), Galileo NT Line - EB Neuro (EB Neuro, Italy), and EB Neuro-Sirius BB (EB Neuro, Italy).

As mentioned above, the rsEEG recordings were performed at the baseline and the 6-month follow-up in the ADMCI patients and just at the baseline in the Healthy seniors.

All rsEEG recordings were performed in the late morning. The rsEEG recordings were performed in all participants using at least 19 scalp exploring electrodes, placed according to the 10–20 system. These electrodes were denoted as "selected electrodes" and their location is illustrated in Figure 1.

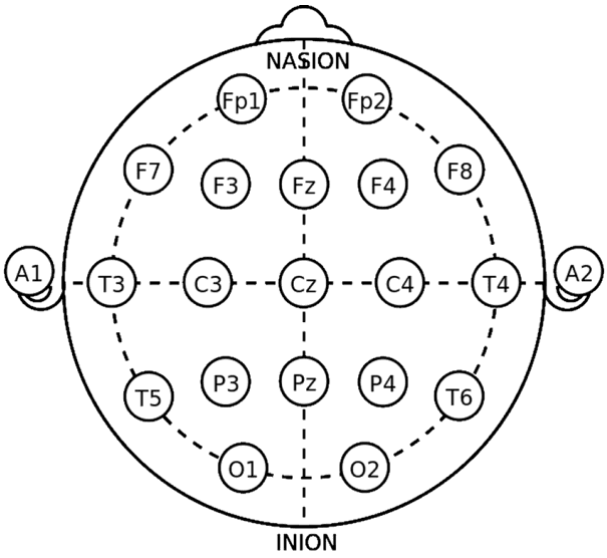

Figure 1. *Electroencephalographic (EEG) electrode montage. The selected electrode montage included 19 scalp monopolar sensors placed following the 10–20 System (i.e., Fp1, Fp2, F7, F3, Fz, F4, F8, T7, C3, Cz, C4, T8, P7, P3, Pz, P4, P8, O1, and O2).*

The ground electrode was attached to the right clavicle or on the forehead, while linked earlobes (A1 and A2) or Fpz served as the active reference for all the electrodes during recording. Electrode impedance was maintained below 5 kΩ; continuous EEG data were recorded at a sampling frequency of 128-1,024 Hz and related antialiasing bandpass between 0.01 Hz and 60-100 Hz. Horizontal electrooculographic (EOG) potentials (0.3-70 Hz bandpass) were also recorded to control eye movements and blinking.

The participants were seated in a comfortable armchair during the rsEEG recording and instructed to remain awake, psychophysically relaxed (no movement), and with the mind freely wandering (no mental planning or cognitive operations). Based on the instructions given by an

experiment, each rsEEG recording lasted 3-5 minutes in the condition of eyes closed, followed by 3-5 minutes in the condition of eyes open. Participants were supervised by the experimenter during the rsEEG recording to monitor adherence to the protocol. The experimenter could kindly invite participants to adhere to the protocol if needed. All deviations by the protocol and verbal interventions were annotated and used during the phase of rsEEG data analysis.

Preliminary rsEEG data analysis

The rsEEG data were centrally analyzed by experts blinded to the participants' diagnosis by the Sapienza University of Rome unit. The recorded rsEEG data were exported as a European data format (.edf) file and then processed offline using the EEGLAB toolbox (Delorme A and Makeig S, 2004; version eeglab14_1_2b) running in the MATLAB software (Mathworks, Natic, MA, USA; version: R2014b). The rsEEG data were divided into epochs lasting 2 s (i.e., 5 minutes = 150 rsEEG epochs of 2 s for each experimental condition) and analyzed offline.

Afterwards, the EEG datasets were analyzed by a 3-step procedure aimed at detecting and removing (1) recording channels (electrodes) showing prolonged artefactual rsEEG activity due to bad electric contacts or other reasons, (2) rsEEG epochs with artifacts at recording channels characterized by general good signals, and (3) intrinsic components of the rsEEG epochs with artifacts.

The first step was based on a visual analysis of the recorded rsEEG activity by two independent experimenters among six experts (i.e., C.D.P, G.N., S.L., F.T., and D.J.) for a first identification of the selected electrodes affected by irremediable artifacts. Indeed, no more than 3 selected electrodes were removed for each participant. For the clinical units with a digital EEG system using > 19 exploring electrodes, the removed electrodes were substituted with the nearest electrodes not included among the 19 selected electrodes. The added electrodes were then used together with the artifact-free selected electrodes to compute the interpolation of artifact-free rsEEG data at all scalp sites of the removed electrodes (EEGLAB toolbox, Delorme A and Makeig S, 2004; version eeglab14_1_2b), thus ensuring that all participants had artefact-free EEG data at the locations of the 19 selected electrodes.

The second step was based on a visual analysis of the recorded rsEEG activity by two of the mentioned independent experimenters (i.e., C.D.P, G.N., S.L., F.T., and D.J.) for the first selection of artefactual rsEEG epochs. The rsEEG epochs contaminated by muscular, ocular, head movements, or non-physiological artifacts were removed.

The third step was implemented by an independent component analysis (ICA) from the EEGLAB toolbox, applied to remove the ICA components representing the residual artifacts due to

(1) blinking and eye movements, (2) involuntary head movements, (3) neck and shoulder muscle tensions, and (4) electrocardiographic activity (Crespo-Garcia, 2008; Jung, 2000). For each rsEEG dataset, less than 5 ICA components were removed from the original ICA solutions based on 19 ICA components. In the third step, the rsEEG datasets were reconstructed with the remaining (artifact-free) ICA components, and the putative artifact-free rsEEG epochs were visually double-checked again by two of the mentioned independent experimenters (i.e., C.D.P, G.N., S.L., F.T., and D.J.) to confirm or make the final decision about the inclusion or the exclusion of each of those rsEEG epochs. The resulting artifact-free EEG data for the common 19 electrodes were used as an input for two additional methodological steps. The first additional step served to harmonize rsEEG data recorded by the clinical units using different reference electrodes and sampling frequency rates. The rsEEG data were frequency-band passed at 0.5-45 Hz and down-sampled, when appropriate, to make the sampling rate of all artifact-free rsEEG datasets in the Healthy and ADMCI participants equal to 128 Hz. Furthermore, all those rsEEG epochs were re-referenced to the common average reference.
The second additional step was used to minimize the habituation effects in the rsEEG data recorded during the eyes-open condition. Only the first minute of those rsEEG data (when the rsEEG alpha reactivity is supposed to be well-represented) was considered in the further analyses.
As a result of the above procedures, the artifact-free epochs showed a similar proportion (> 75%) of the total amount of rsEEG activity recorded in the two groups of participants (i.e., Healthy and ADMCI) and in all rsEEG recordings (baseline and 6-month follow-up for the ADMCI participants).

Spectral analysis of the rsEEG epochs

A standard digital FFT-based analysis (Welch technique, Hanning windowing function, no phase shift) computed the power density of artifact-free rsEEG epochs at all 19 scalp electrodes (0.5 Hz of frequency resolution). From those spectral solutions, the rsEEG frequency bands of interest were individually identified based on the following frequency landmarks: the transition frequency (TF) and the background frequency (BGF) observed in the eyes-closed condition. In the eyes-closed rsEEG power density spectrum, the TF was defined as the minimum of the rsEEG power density between 3 and 8 Hz, while the BGF peak was defined as the maximum power density peak between 6 and 14 Hz. The TF and BGF were computed for each participant involved in the study. Based on the TF and BGF, we estimated the individual delta, theta, and BGF bands as follows: delta from TF -4 Hz to TF -2 Hz, theta from TF -2 Hz to TF, low BGF (BGF 1 and BGF 2) from TF to BGF peak, and high-frequency BGF (or BGF 3) from BGF to BGF + 2 Hz. Specifically, the individual BGF 1 and BGF 2 bands were computed as follows: BGF 1 from TF to the frequency midpoint of the TF-BGF range and BGF 2 from that midpoint to the BGF peak. The other bands were defined based on

the standard fixed frequency ranges used in the reference rsEEG studies of our Consortium (Babiloni et al., 2017, 2019, 2020b): beta 1 from 14 to 20 Hz, beta 2 from 20 to 30 Hz, and gamma from 30 to 40 Hz. The BGFs were denoted as "alpha rhythms" if there was a reduction in magnitude (reactivity) of the rsEEG rhythms at the BGFs from the eyes-closed to the eyes-open condition, as shown by the rsEEG spectral measures.

Cortical sources of rsEEG epochs as computed by eLORETA

The procedures for the rsEEG cortical source estimations were described in previous reference articles of our Consortium (Babiloni et al. 2019, 2020b). We used the official freeware tool called exact LORETA (eLORETA) for the linear estimation of the cortical source activity generating scalp-recorded rsEEG rhythms (Pascual-Marqui, 2007). The present implementation of the eLORETA freeware uses a head volume conductor model composed of the scalp, skull, and brain. In the scalp compartment, the exploring electrodes can be virtually positioned to give EEG data as an input to the source estimation (Pascual-Marqui, 2007). The brain model is based on a realistic cerebral shape taken from a template typically used in neuroimaging studies, namely that of the Montreal Neurological Institute (MNI152 template). The eLORETA freeware solves the so-called EEG inverse problem from scalp-recorded EEG activity estimating the associated "neural" current density values at any cortical voxel of the mentioned head volume conductor model. The cortical source solutions are computed at each voxel of the brain model and at each frequency bin.

For the estimation of EEG cortical source activities (i.e., the eLORETA solutions), the input is the EEG spectral power density computed at the 19 scalp electrodes. This estimation is performed in the electrical brain source space formed by 6,239 voxels with 5 mm resolution, restricted to the cortical grey matter of the head volume conductor model. Into each voxel, an equivalent current dipole is located to represent the mean ionic currents generated by the local populations of cortical pyramidal neurons. The eLORETA package provides the Talairach coordinates, the lobe, and the Brodmann area (BA) for each voxel of the brain model.

The eLORETA solutions from the rsEEG data were normalized by the following procedure. We averaged the eLORETA solutions across (1) the two experimental conditions (i.e., resting-state eyes-closed and eyes-open conditions), (2) all frequency bins from 0.5 to 45 Hz, and (3) 6,239 voxels of the brain model volume to obtain the eLORETA "mean" solution. Afterward, we computed the ratio between any original eLORETA solution at a given condition/frequency-bin/voxel and the eLORETA "mean" solution. As a result, any original eLORETA solution at a given condition/frequency-bin/voxel changed to a normalized eLORETA solution.

In line with the general low spatial resolution of the current EEG methodological approach (i.e., 19 scalp electrodes), we performed a regional analysis of the eLORETA solutions. For this purpose, we collapsed the eLORETA solutions within frontal, central, parietal, occipital, temporal, and limbic macro-regions (ROIs) considered separately. Table 3 reports the list of the BAs used for the ROIs considered in the present study. Of note, the main advantage of the regional analysis of eLORETA solutions was that we could disentangle the rsEEG source activity in contiguous cortical areas. For example, the rsEEG source activity in the occipital ROI was disentangled from that estimated in the parietal and temporal ROIs, etc. This was made possible by the fact that eLORETA solves the linear inverse problem by considering (at least in part) the effects of the head as a volume conductor. In contrast, the solutions of the rsEEG power density computed at a parietal scalp electrode reflect the contribution of source activities not only of the underlying parietal cortex but also of surrounding occipital and temporal cortices. For the present eLORETA cortical source estimation, a frequency resolution of 0.5 Hz was used, namely, the maximum frequency resolution allowed using 2-s artefact-free EEG epochs.

BRODMANN AREAS INTO THE REGIONS OF INTEREST (ROIs)	
Frontal	8, 9, 10, 11, 44, 45, 46, 47
Central	1, 2, 3, 4, 6
Parietal	5, 7, 30, 39, 40, 43
Occipital	17, 18, 19
Temporal	20, 21, 22, 37, 38, 41, 42
Limbic	31, 32, 33, 34, 35, 36

Table 3. *Regions of interest (ROIs) were used for the estimation of the cortical sources of the resting-state electroencephalographic (rsEEG) rhythms in the present study. Any ROI is defined by some Brodmann areas of the cerebral source space in the freeware used in this study, namely the exact low-resolution brain electromagnetic source tomography (eLORETA).*

The computation of the rsEEG background frequency (BGF) reactivity

To analyze the rsEEG BGF reactivity from the eyes-closed to the eyes-open condition, we considered the eLORETA source solutions estimated in the central, parietal, and occipital ROIs. Based on the reference rsEEG studies of our Consortium (Babiloni et al., 2020b), the rsEEG BGF

reactivity was measured at the BGF 2 frequency band, which showed the maximum source activities in the Healthy participants during the eyes-closed condition.

The "reactivity" dependent variable for the statistical analyses was obtained by averaging the eLORETA BGF 2 source solutions in the central, parietal, and occipital ROIs. To avoid habituation effects in the eyes-open condition, that reactivity was computed based on the eLORETA solutions estimated during the first minute of the rsEEG recordings in that condition (when the rsEEG BGF reactivity is maximum). As no significant habituation effect was described in the eyes-closed condition, eLORETA solutions were estimated during all five minutes of the rsEEG recordings in that condition.

The rsEEG BGF reactivity from the eyes-closed to the eyes-open condition was computed by the following formula:

$$\text{Reactivity (\%)} = \frac{\text{eyes open} - \text{eyes closed}}{\text{eyes closed}} * 100$$

According to this definition, the percent negative values (i.e., weaker BGF source activities during the eyes-open than the eyes-closed condition) indexed a reduction (reactivity) in the source BGF activities from the eyes-closed to the eyes-open condition (Babiloni et al., 2010; Del Percio et al., 2019). On the contrary, the percent positive values (i.e., greater BGF source activities during the eyes-open than the eyes-closed condition) indexed an increase in the source BGF activities from the eyes-closed to the eyes-open condition.

Figure 2 plots the individual values of the reactivity (%) of the central-parietal-occipital rsEEG (eLORETA) BGF 2 source activity from the eyes-open (1 minute) to the eyes-closed (5 minutes) condition for all Healthy (N = 60) and ADMCI (N =52) participants. For the ADMCI participants, those individual values are plotted for the rsEEG recordings at baseline and 6-month follow-up.

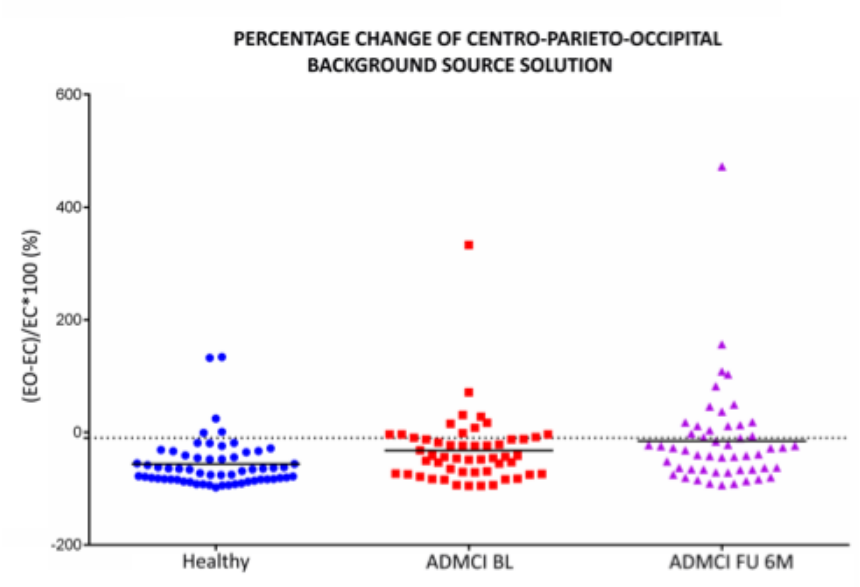

Figure 2. *Individual values of the reactivity (%) of the central-parietal-occipital rsEEG (eLORETA) background frequency 2 (BGF 2) source activity from the eyes-open (1 minute) to the eyes-closed (5 minutes) condition for all Healthy (N = 60) and ADMCI (N = 52) participants. For the ADMCI participants, those individual values were plotted for the rsEEG recordings at baseline (ADMCI Baseline) and 6-month follow-up (ADMCI Follow-up). The percent negative values indexed a reduction (reactivity) in the BGF 2 source activities from the eyes-closed (EC) to the eyes-open (EO) condition. In contrast, the percent positive values indexed an increase in the BGF 2 source activities from the eyes-closed to the eyes-open condition. The dashed line indicates the value of -10% of the reduction (reactivity) in the central-parietal-occipital BGF 2 source activities from the eyes-closed (EC) to the eyes-open (EO) condition.*

Figure 3 illustrates the percentage of Healthy and ADMCI participants showing BGF (alpha)-reactivity over a given percentage threshold of the central-parietal-occipital rsEEG (eLORETA) BGF 2 source activity. For the ADMCI patients, that percentage is reported for the rsEEG recordings at the baseline and the 6-month follow-up. The percentage of BGF-reactive Healthy participants slightly changes when the reactivity threshold of the central-parietal-occipital rsEEG (eLORETA) BGF 2 source activity changes between 0% and -25%; that percentage decreases from 93.3% (55 BGF-reactive Healthy participants) to 85% (51 BGF-reactive Healthy participants). On the contrary, the percentage of BGF-reactive ADMCI patients at the baseline and the 6-month follow-up strongly decreases when the reactivity threshold of the central-parietal-occipital rsEEG (eLORETA) BGF 2 source activity changes between 0% and -25%. Specifically, the percentage of the BGF-reactive ADMCI patients at the baseline decreases from 86.5% (45 BGF-reactive ADMCI patients) to 57.7% (30 BGF-reactive ADMCI patients). The percentage of the BGF-reactive ADMCI patients at the 6-month follow-up decreases from 73.3% (38 BGF-reactive ADMCI patients) to 55.8% (29 BGF-reactive ADMCI patients).

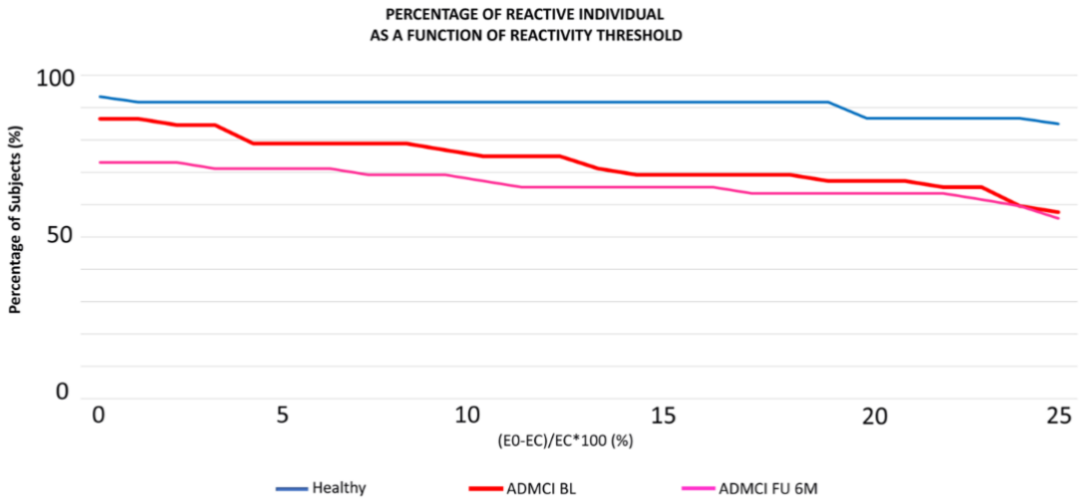

Figure 3. *Percentage of background frequency (BGF)-reactive Healthy and ADMCI participants as a function of the reactivity threshold of the central-parietal-occipital rsEEG (eLORETA) BGF 2 source activity. For the ADMCI patients, that percentage is illustrated for the rsEEG recordings performed at the baseline (ADMCI Baseline) and the 6-month follow-up (ADMCI Follow-up)*

In the present study, we applied an arbitrary threshold for the BGF (alpha) source reactivity of -10% (Babiloni et al., 2022). Based on this threshold, we identified 5 Healthy participants and 13 ADMCI patients who did not exhibit significant BGF reactivity at the baseline, such reactivity being defined above (Specifically, they showed either increased BGF source activity from the eyes-closed to eyes-open condition or decreased alpha source activity from -10% to 0%). Thus, the BGF-2 source reactivity was detected in 55 out of 60 Healthy seniors and in 39 out of 52 ADMCI patients at the baseline. In the following analyses, we will refer to them as "alpha-reactive" participants. Moreover, the BGF-2 source reactivity was detected in 32 out of 39 "alpha-reactive" ADMCI patients at the 6-month follow-up. In the following analyses, we will refer to them as "6-month follow-up alpha-reactive" participants.

Table 4 summarizes the most relevant demographic (i.e., age, sex, and education attainment) and clinical (i.e., MMSE score) features observed in the subgroups of the alpha-reactive Healthy seniors (N = 55) and alpha-reactive ADMCI patients (N = 39). Furthermore, Table 4 reports the results of the presence or absence of statistically significant differences ($p < 0.05$) between the two subgroups for age (T-test), sex (Fisher test), educational attainment (T-test), and MMSE score (Mann Whitney U test). As expected, a statistically significant difference was found for the MMSE score ($p < 0.00001$), showing a higher score in the alpha-reactive Healthy than the alpha-reactive ADMCI subgroup. On the contrary, no statistically significant differences were found in age, sex, and educational attainment between the subgroups ($p > 0.05$).

Demographic and clinical data in alpha-reactive Healthy and alpha-reactive ADMCI			
	Healthy	**ADMCI**	**Statistical analysis**
N	55	39	-
Age	68.8±0.9	70.0±1.1	T-test =n.s.
Sex (M/F)	23/32	17/22	Fisher test =n.s.
Education	11.1±0.6	11.6±0.8	T-test =n.s.
MMSE	28.5±0.2	26.6±0.3	Mann-Whitney U test: $p < 0.00001$

Table 4. *Mean values (± standard error of the mean, SE) of the demographic and clinical data as well as the results of their statistical comparisons ($p < 0.05$) in the subgroups of the alpha-reactive Healthy seniors ($N = 55$) and alpha-reactive ADMCI patients ($N = 39$). Legend: M/F = males/females; n.s. = not significant ($p > 0.05$); MMSE = Mini Mental State Evaluation.*

Table 5 reports the most relevant clinical (i.e., GDS, CDR, and Hachinski Ischemic Score), genetic (i.e., *APOE* genotyping), and CSF (i.e., Aβ42, t-tau, p-tau, and Aβ42/ p-tau) features in the subgroups of alpha-reactive ADMCI participants (N = 39). Table 5 also reports the number and the percentages of the ADMCI patients assuming the following drug classes: selective serotonin reuptake inhibitors (SSRIs), noradrenaline reuptake inhibitors (SNRIs), acetylcholinesterase inhibitors (AChEIs), and inhibitors of N-methyl-D-aspartate receptors (iNMDARs).

Clinical, genetic (APOE), cerebrospinal fluid markers, and drugs in alpha-reactive ADMCI group	
Clinical markers	
Geriatric depression scale (GDS)	2.7 ± 0.3
Clinical dementia rating (CDR)	0.5 ± 0.0
Hachinski ischemic score (HIS)	0.9 ± 0.1
Genetic marker	
APOE4 (%)	77%
Cerebrospinal fluid markers	
Aβ42 (pg/ml)	497 ± 25
p-tau (pg/ml)	85 ± 6
t-tau (pg/ml)	601 ± 54
Aβ42/p-tau	6.8 ± 0.5
Drugs	
Selective serotonin reuptake inhibitors (SSRIs; N, %)	17.9% (N=7)
Selective serotonin and noradrenaline reuptake inhibitors (SNRIs, N, %)	7.7% (N=3)
Acetylcholinesterase inhibitors (AChEIs; N, %)	15.3% (N=6)
Antagonists of N-methyl-D-aspartate receptors (aNMDARs, N, %)	0% (N=0)

Table 5. *Mean values (±SE) of the clinical (i.e., Geriatric Depression Scale, Clinical Dementia Rating, and Hachinski Ischemic Score), genetic (i.e., Apolipoprotein E genotyping, APOE), and cerebrospinal fluid (i.e., beta-amyloid 1-42, Aβ 42; protein tau, t-tau; a phosphorylated form of the protein tau, p-tau; and Aβ 42/ p-tau ratio) data in the alpha-reactive ADMCI patients (N =39). The number and percentages of ADMCI patients assuming the selective serotonin reuptake inhibitors (SSRIs), selective serotonin and noradrenaline reuptake inhibitors (SNRIs), acetylcholinesterase inhibitors (AChEIs), and antagonists of N-methyl-D-aspartate receptors (aNMDARs) are also reported*

Table 6 reports the most relevant demographic (age, sex, educational attainment) clinical (i.e., GDS, CDR, and Hachinski Ischemic Score), genetic (i.e., *APOE* genotyping), and CSF (i.e., Aβ42, t-tau, p-tau, and Aβ42/ p-tau) features in the subgroups of 6-month follow-up alpha-reactive ADMCI patients (N = 32). Table 6 also reports the number and the percentages of the ADMCI patients assuming the above-mentioned drug classes.

Demographic, clinical, genetic (APOE), cerebrospinal fluid markers and drugs in 6-months follow-up alpha-reactive ADMCI group(N=32)	
Demographic markers	
Age	69.8 ±1.3
Sex (M/F)	13/19
Education	11.5 ±0.8
Clinical markers	
Geriatric depression scale (GDS)	2.7 ±0.3
Clinical dementia rating (CDR)	0.5 ±0.0
Hachinski ischemic score (HIS)	0.9 ±0.1
Genetic marker	
APOE4 (%)	75%
Cerebrospinal fluid markers	
Aβ42 (pg/ml)	490 ± 30
p-tau (pg/ml)	87 ± 7
t-tau (pg/ml)	614 ± 61
Aβ42/p-tau	6.6 ± 0.6
Drugs	
Selective serotonin reuptake inhibitors (SSRIs; N, %)	18.8% (N=6)
Selective serotonin and noradrenaline reuptake inhibitors (SNRIs, N, %)	3.13% (N=1)
Acetylcholinesterase inhibitors (AChEIs; N, %)	18.8% (N=6)
Antagonists of N-methyl-D-aspartate receptors (aNMDARs, N, %)	0.0% (N=0)

Table 6. *Mean values (±SE) of the demographic (age, sex, educational attainment), clinical (i.e., Geriatric Depression Scale, Clinical Dementia Rating, and Hachinski Ischemic Score), genetic (i.e., Apolipoprotein E genotyping, APOE), and cerebrospinal fluid (i.e., beta-amyloid 1-42, Aβ 42; protein tau, t-tau; a phosphorylated form of the protein tau, p-tau; and Aβ 42/ p-tau ratio) data in the 6-month follow-up alpha-reactive ADMCI patients (N =32). The number and percentages of ADMCI patients assuming the selective serotonin reuptake inhibitors (SSRIs), selective serotonin and noradrenaline reuptake inhibitors (SNRIs), acetylcholinesterase inhibitors (AChEIs), and antagonists of N-methyl-D-aspartate receptors (aNMDARs) are also reported*

Statistical analysis of the rsEEG source activity

Three statistical sessions were performed by the commercial tool STATISTICA 10 (StatSoft Inc., www.statsoft.com) to test the control hypothesis and the two working hypotheses. In all the statistical sessions, an ANOVA was computed using the eyes-closed rsEEG source activities (i.e., regional normalized eLORETA solutions) as a dependent variable ($p < 0.05$). Mauchly's test evaluated the sphericity assumption, and degrees of freedom were corrected by the Greenhouse-Geisser procedure when appropriate ($p < 0.05$). Duncan test was used for post hoc comparisons using a statistical threshold of $p < 0.05$ Bonferroni corrected for the planned contrasts.

It is well-known that the use of ANOVA models implies that dependent variables approximate Gaussian distributions, so we tested this feature in the regional normalized eLORETA current densities of interest by the Kolmogorov-Smirnov test. The hypothesis of Gaussian distributions was tested at $p > 0.05$ (i.e., $p > 0.05$= Gaussian, $p \leq 0.05$ = non-Gaussian). As the distributions of the regional normalized eLORETA current densities were not Gaussian in several cases, all eLORETA variables underwent the log10 (x+1) transformation (log10 transformed) and re-tested ($p > 0.05$ = Gaussian). Such a transformation is a popular method to transform skewed data distribution with all positive values (as regional normalized eLORETA current densities are) to Gaussian distributions, thus augmenting the reliability of the ANOVA results. Indeed, the outcome of the procedure approximated the distributions of all regional normalized eLORETA current densities to Gaussian distributions ($p > 0.05$ = Gaussian), allowing the use of the ANOVA model.

The results of the following statistical analyses were controlled by the iterative (leave-one-out) Grubbs' test detecting for the presence of one or more outliers in the distribution of the eLORETA source solutions. The null hypothesis of the non-outlier status was tested at the arbitrary threshold of $p < 0.01$ to remove only individual values with a high probability to be outliers.

The first ANOVA tested the control hypothesis that the eyes-closed rsEEG source activities (i.e., regional normalized eLORETA solutions) were abnormal in the ADMCI group (N = 52) as compared to the Healthy group (N = 60). The ANOVA factors were Group (Healthy and ADMCI), Band (delta, theta, BGF1, BGF2, BGF3, beta 1, beta 2, and gamma), and ROI (frontal, central, parietal, occipital, temporal, and limbic). The confirmation of the control hypothesis may require: (1) a statistically significant ANOVA effect including the factor Group ($p < 0.05$) and (2) a post-hoc Duncan test indicating statistically significant ($p < 0.05$ Bonferroni corrected) differences in the eyes-closed rsEEG source activities between the Healthy and ADMCI groups (i.e., Healthy ≠ ADMCI, $p < 0.05$ Bonferroni corrected).

The second ANOVA evaluated the first working hypothesis that the eyes-closed rsEEG source activities (i.e., regional normalized eLORETA solutions) were abnormal in the alpha-reactive ADMCI group (N = 39) as compared to the alpha-reactive Healthy group (N = 55). The ANOVA

factors were Group (alpha-reactive Healthy and alpha-reactive ADMCI), Band (delta, theta, alpha 1, alpha 2, alpha 3, beta 1, beta 2, and gamma), and ROI (frontal, central, parietal, occipital, temporal, and limbic). The confirmation of the control hypothesis may require: (1) a statistically significant ANOVA effect including the factor Group ($p < 0.05$) and (2) a post-hoc Duncan test indicating statistically significant ($p < 0.05$ Bonferroni corrected) differences in the eyes-closed rsEEG source activities between the alpha-reactive Healthy group and the alpha-reactive ADMCI BL group (i.e., alpha-reactive Healthy ≠ alpha-reactive ADMCI, $p < 0.05$ Bonferroni corrected).

The third ANOVA evaluated the second working hypothesis that the eyes-closed rsEEG source activities (i.e., regional normalized eLORETA solutions) deteriorated across time (6 months) in the 6-month follow-up alpha-reactive ADMCI group (N = 32). The ANOVA factors were Time (Baseline and Follow-up), Band (delta, theta, alpha 1, alpha 2, alpha 3, beta 1, beta 2, and gamma), and ROI (frontal, central, parietal, occipital, temporal, and limbic). The confirmation of this second working hypothesis may require: (1) a statistically significant ANOVA effect including the factor Time ($p < 0.05$) and (2) a post-hoc Duncan test indicating statistically significant ($p < 0.05$ Bonferroni corrected) differences in the rsEEG source activities between the baseline and 6-month follow-up in the 6-month follow-up alpha-reactive ADMCI participants (i.e., Baseline ≠ Follow-up, $p < 0.05$ Bonferroni corrected)

Association between baseline alpha eyes-closed rsEEG source activities and cognitive decline

We performed an exploratory statistical analysis to evaluate the ability of the baseline alpha eyes-closed rsEEG source activities to predict the cognitive decline at the 6-month follow-up. For this purpose, we computed several linear regression models (R software; https://www.R-project.org/) having the 6-month follow-up ADASCog score as a target variable and the following predictors: (1) the baseline rsEEG eyes-closed alpha source activities showing differences between the Nold and ADMCI groups with alpha reactivity and (2) the age, education or gender, in relation to the well-known effects of these variables on rsEEG alpha rhythms (Babiloni et al., 2021a). We also included the baseline ADASCog score as a covariate in each model, as well as the above-mentioned cognitive reserve factors and the total cortical thickness as revealed by structural MRI measures. A statistically significant association ($p < 0.05$) between the baseline rsEEG eyes-closed alpha source activities and the 6-month follow-up ADASCog score may confirm the prediction of the cognitive decline at the 6-month follow-up based on the baseline rsEEG source activities in the alpha-reactive ADMCI patients.

Results

Individual frequencies and distributions of rsEEG source activities in the Healthy and ADMCI groups

The mean TF was 5.7 Hz (± 0.1 SE) in the Healthy group (N = 60) and 5.2 Hz (± 0.2 SE) in the ADMCI group (N = 52). Furthermore, the mean BGF was 9.1 Hz (± 0.1 SE) in the Healthy group and 8.9 Hz (± 0.2 SE) in the ADMCI group. The T-tests of these data showed that the mean TF was greater in the Healthy than the ADMCI group ($p < 0.005$). No statistically significant difference was found for the mean BGF ($p > 0.05$).

The results of the first statistical session about the eyes-closed rsEEG source activities in all participants are illustrated in Figure 4. This Figure shows the mean values (± SE, log 10 transformed) of the regional rsEEG (eLORETA) source activities during the eyes-closed condition in the Healthy (N = 60) and ADMCI (N = 52) groups. The distribution of those source activities differed across the groups, the ROIs, and the bands. In the Healthy group, as a physiological reference, the temporal, parietal, and occipital (eLORETA) BGF2 and BGF3 source activities showed dominant values among all ROIs. Delta, theta, and BGF1 source activities were characterized by relatively low values in all ROIs, while the beta and gamma source activities were generally very low. As compared to the Healthy group, the ADMCI group exhibited a substantial decrease in posterior rsEEG BGF2 and BGF3 source activities. Furthermore, the ADMCI group exhibited an increase in widespread delta and theta source activities.

Based on these input data, the ANOVA results showed a statistical interaction effect ($F = 4.0$, $p < 0.00001$) among the factors Group (Healthy and ADMCI), Band (delta, theta, BGF1, BGF2, and BGF3, beta 1, beta 2, and gamma), and ROI (frontal, central, parietal, occipital, temporal, and limbic). The Duncan planned post-hoc ($p < 0.05$ Bonferroni correction for 8 Bands X 6 ROIs, $p < 0.05/48 = 0.001$) testing produced the following core results: (1) the discriminant pattern Healthy < ADMCI was fitted by the frontal, central, parietal, occipital, and temporal delta source activities ($p < 0.00005 - 0.000005$) as well as the frontal, parietal, occipital, and temporal theta source activities ($p < 0.0001 - 0.000005$); and (2) the discriminant pattern Healthy > ADMCI was fitted by the central, parietal occipital, temporal, and limbic BGF2 source activities ($p < 0.0005 - 0.000005$) as well as the central, parietal, occipital, temporal, and limbic BGF3 source activities ($p < 0.00005 - 0.000001$). Of note, these findings were not due to outliers from those individual regional normalized eLORETA current densities (log 10 transformed), as shown by Grubbs' test with an arbitrary threshold of $p > 0.001$.

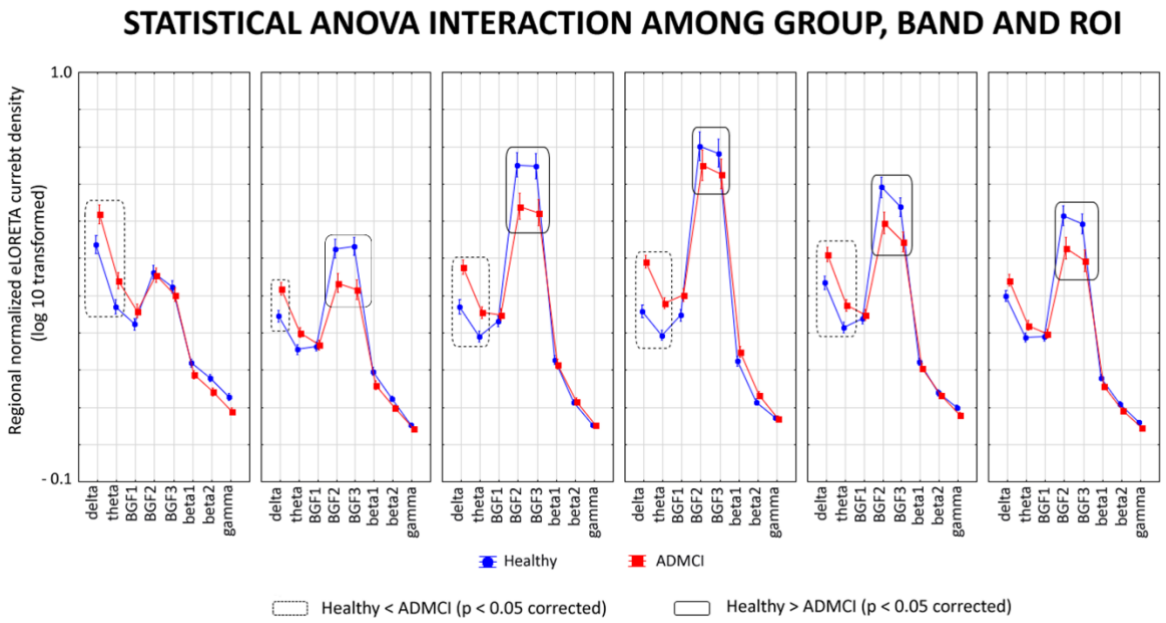

Figure 4. *Regional normalized eLORETA solutions (mean across subjects, log 10 transformed) of cortical sources of eyes-closed rsEEG rhythms relative to a statistical ANOVA interaction among the factors Group (Healthy, N = 60; ADMCI, N = 52), Band (delta, theta, BGF1, BGF2, and BGF3, beta1, beta2, and gamma), and ROI (central, frontal, parietal, occipital, temporal, and limbic). This ANOVA design used the eyes-closed regional normalized eLORETA solutions as a dependent variable. The rectangles indicate the cortical regions and frequency bands in which the eLORETA solutions statistically presented a significant eLORETA pattern of Healthy ≠ ADMCI (p < 0.05 Bonferroni corrected). Legend: background frequency 1, 2, and 3 (BGF1, BGF2, and BGF3).*

Individual frequencies and distributions of rsEEG source activities in the alpha-reactive Healthy and alpha-reactive ADMCI groups

The mean TF was 5.7 Hz (± 0.1 SE) in the alpha-reactive Healthy group (N = 55) and 5.2 Hz (± 0.2 SE) in the alpha-reactive ADMCI group (N = 39). Furthermore, the mean BGF was 9.1 Hz (± 0.1 SE) in the alpha-reactive Healthy group and 9.0 Hz (± 0.2 SE) in the alpha-reactive ADMCI group. The T-tests of these data showed that the mean TF was greater in the Healthy than the ADMCI groups ($p < 0.01$). No statistically significant difference was found for the mean BGF ($p > 0.05$).

The results of the second statistical session about the eyes-closed rsEEG source activities in the alpha-reactive participants are illustrated in Figure 5. This Figure shows the mean values (± SE, log 10 transformed) of the regional rsEEG (eLORETA) source activities during the eyes-closed condition in the alpha-reactive Healthy group (N = 55) and in the alpha-reactive ADMCI group (N = 39). The distribution of those source activities differed across the Groups, the ROIs, and the Bands. As compared to the alpha-reactive Healthy group, the alpha-reactive ADMCI group exhibited a substantial decrease in central, parietal, temporal, and limbic rsEEG alpha 2 and alpha 3 source activities. Furthermore, the ADMCI group exhibited an increase in widespread delta and theta source activities. Based on these input data, the ANOVA results showed a statistical interaction effect ($F = 2.7$, $p < 0.00001$) among the following factors: Group (Healthy and ADMCI), Band (delta, theta,

alpha 1, alpha 2, alpha 3, beta 1, beta 2, and gamma), and ROI (frontal, central, parietal, occipital, temporal, and limbic). The Duncan planned post-hoc ($p < 0.05$ Bonferroni correction for 8 Bands X 6 ROIs, $p < 0.05/48 = 0.001$) testing produced the following core results: (1) the discriminant pattern Healthy < ADMCI was fitted by the frontal, central, parietal, occipital, and temporal delta source activities ($p < 0.001$-0.000001) as well as the frontal, parietal, occipital, and temporal theta source activities ($p < 0.0001$ - 0.000001); and (2) the discriminant pattern Healthy > ADMCI was fitted by the central, parietal, temporal, and limbic alpha 2 source activities ($p < 0.0005$ - 0.00001) as well as the central, parietal temporal, and limbic alpha 3 source activities ($p < 0.00001$ - 0.000005). Of note, these findings were not due to outliers from those individual regional normalized eLORETA current densities (log 10 transformed), as shown by Grubbs' test with an arbitrary threshold of $p > 0.001$.

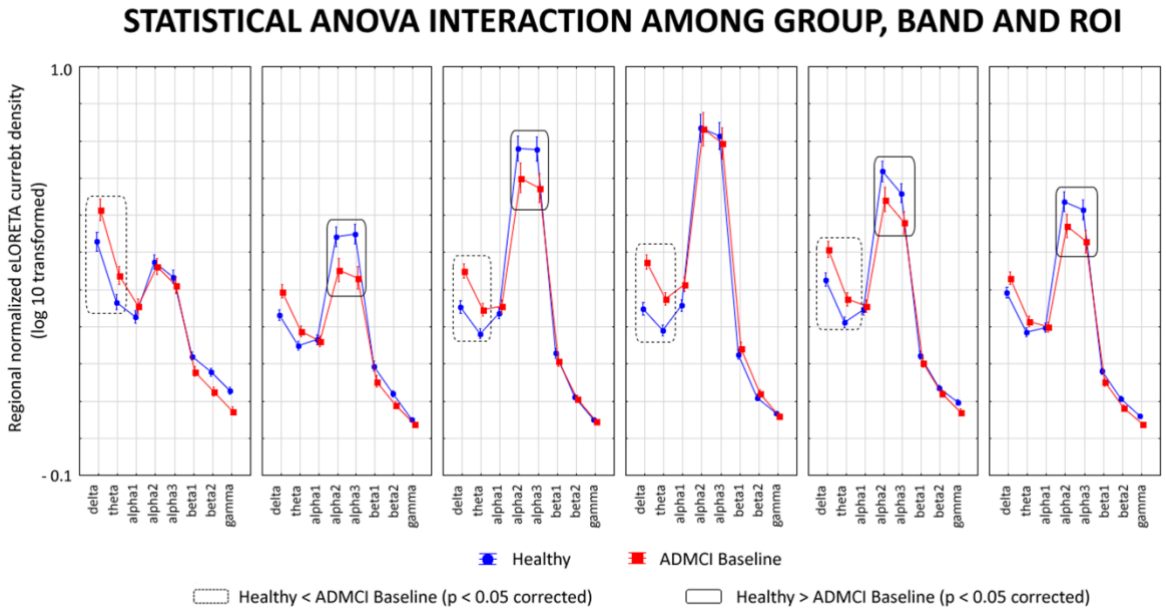

Figure 5. *Regional normalized eLORETA solutions (mean across subjects, log 10 transformed) of cortical sources of eyes-closed rsEEG rhythms relative to a statistical ANOVA interaction among the factors Group (alpha-reactive Healthy, N = 55; alpha-reactive ADMCI, N = 39), Band (delta, theta, alpha1, alpha2, alpha3, beta1, beta2, and gamma), and ROI (central, frontal, parietal, occipital, temporal, and limbic). This ANOVA design used the eyes-closed regional normalized eLORETA solutions as a dependent variable. The rectangles indicate the cortical regions and frequency bands in which the eLORETA solutions statistically presented a significant eLORETA pattern alpha-reactive Healthy ≠ alpha-reactive ADMCI ($p < 0.05$ Bonferroni corrected).*

Individual frequencies and distributions of rsEEG source activities in the 6-month follow-up alpha-reactive ADMCI group

In the 6-month follow-up alpha-reactive ADMCI group (N = 32), the mean TF was 5.1 Hz (± 0.1 SE) at the baseline and 5.3 Hz (± 0.2 SE) at the 6-month follow-up. Furthermore, the mean BGF was 9.1 Hz (± 0.1 SE) at the baseline and 8.7 Hz (± 0.2 SE) at the 6-month follow-up. No statistically significant difference was found for the mean TF and the mean BGF (T-test, $p > 0.05$).

The results of the third statistical session about the eyes-closed rsEEG source activities in the 6-month follow-up alpha-reactive ADMCI (N = 32) are illustrated in Figure 6. This Figure shows the mean values (± SE, log 10 transformed) of the regional rsEEG (eLORETA) source activities during the eyes-closed condition at the baseline and the 6-month follow-up in the alpha-reactive ADMCI group (N = 32). The distribution of those source activities differed across the Time, the ROIs, and the Bands. The 6-month follow-up alpha-reactive ADMCI group exhibited a substantial decrease in posterior rsEEG alpha 2 and alpha 3 source activities as well as temporal beta 1 and beta 2 source activities after 6 months. Furthermore, the 6-month follow-up alpha-reactive ADMCI group exhibited an increase in frontal central, and parietal delta and theta source activities after 6 months. Based on these input data, the ANOVA results showed a statistical interaction effect ($F = 1.6$, $p < 0.01$) among the factors Time (Baseline and Follow-up), Band (delta, theta, alpha 1, alpha 2, alpha 3, beta 1, beta 2, and gamma), and ROI (frontal, central, parietal, occipital, temporal, and limbic). The Duncan planned post-hoc ($p < 0.05$ Bonferroni correction for 8 Bands X 6 ROIs, $p < 0.05/48 = 0.001$) testing produced the following core results: (1) the discriminant pattern Baseline < Follow-up was fitted by the frontal, central, and parietal delta source activities ($p < 0.0001$ - 0.000005) as well as the central and parietal theta source activities ($p < 0.0005$ - 0.0001); and (2) the discriminant Baseline > Follow-up was fitted by: (i) the central, parietal, occipital, temporal, and limbic alpha 2 source activities ($p < 0.00005$ - 0.00001); (ii) the central, occipital, parietal temporal, and limbic alpha 3 source activities ($p < 0.0001$ - 0.00001); (iii) the temporal beta 1 source activity ($p < 0.00001$); and (iv) temporal beta 2 source activity ($p < 0.0001$). Of note, these findings were not due to outliers from those individual regional normalized eLORETA current densities (log 10 transformed), as shown by Grubbs' test with an arbitrary threshold of $p > 0.001$.

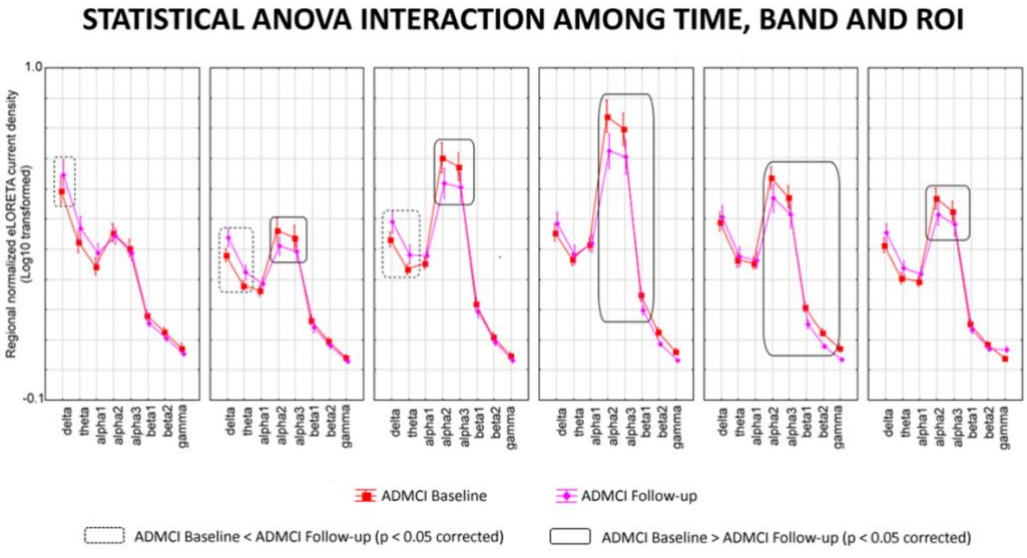

Figure 6. *Regional normalized eLORETA solutions (mean across subjects, log 10 transformed) of cortical sources of eyes-closed rsEEG rhythms in the 6-month follow-up alpha-reactive ADMCI group (N = 32) relative to a statistical*

ANOVA interaction among the factors Time (Baseline and Follow-up), Band (delta, theta, alpha1, alpha2, alpha3, beta1, beta2, and gamma), and ROI (central, frontal, parietal, occipital, temporal, and limbic). This ANOVA design used the eyes-closed regional normalized eLORETA solutions as a dependent variable. The rectangles indicate the cortical regions and frequency bands in which the eLORETA solutions statistically presented a significant eLORETA pattern alpha-reactive Baseline ≠ Follow-up ($p < 0.05$ Bonferroni corrected).

Association between baseline alpha eyes-closed rsEEG source activities and cognitive decline

In the regression analyses, we considered the following baseline rsEEG eyes-closed alpha source activities showing differences between the Nold and ADMCI groups with alpha reactivity (the ADMCI group included all ADMCI patients showing the rsEEG alpha reactivity at the baseline recording regardless the presence of that reactivity at the 6-month follow-up): baseline central, parietal, temporal, and limbic alpha2 and alpha3 sources. To reduce the number of tests, we calculated a global baseline alpha2 and global baseline alpha3 source activity by averaging all the above-mentioned baseline alpha2 and alpha3 regional source activities, respectively.

For the linear regression analysis, we considered the age of the ADMCI patients, in line with previous evidence from the present Workgroup (Babiloni et al., 2021b). Specifically, the ADMCI patients were divided into the Age- and Age+ subgroups based on the mean age value in the ADMCI group (Age- = 18 ADMCI patients; Age+ = 21 ADMCI patients), in line with previous evidence of the present Workgroup (Babiloni et al., 2021b). Specifically, the mean age of the Age-subgroup was 64.3 (± 1.1 SE) years old while that of the Age+ subgroup was 75.3 (± 0.7 SE) years old. The results of the linear regression analysis are reported in Figure 7. We observed a statistically significant association ($p < 0.05$) between the global baseline alpha2 source activity and age as predictors and the 6-month follow-up ADASCog score as a target variable. In the model, the baseline ADASCog score was considered as a covariate (upper left diagram). This result was confirmed also including the education (upper right diagram), gender (lower left diagram), and total MRI-based cortical thickness (lower left diagram) as covariates (one covariate per model). More specifically, Figure 7 illustrates the estimated marginal means of the 6-month follow-up ADASCog score, as well as the p-value of the global baseline alpha2 source activity and age interaction, and the regression coefficient for the Age- and Age+ ADMCI subgroups (b) in the four different models. A different trend between the younger (Age-) and older (Age+) ADMCI subgroups was observed, with only the younger ADMCI subgroup (Age-) showing a greater global cognitive decline at the 6-month follow-up (higher ADASCog score) in relation to higher individual values of the global alpha2 source activity at the baseline recording.

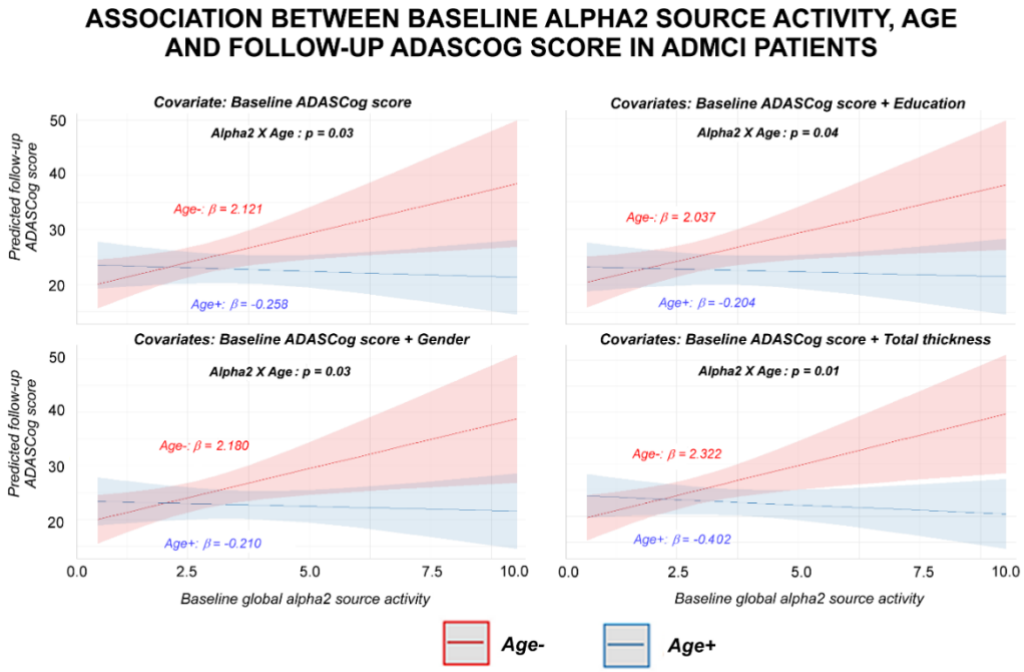

Figure 7. *Estimated marginal means of the 6-month follow-up ADASCog score as predicted by the linear regression models including the following predictor variables: (1) the global baseline alpha2 source activity (average of baseline central, parietal, temporal, and limbic alpha2 source activities) and (2) Age (Age- and Age+ subgroups defined according to the mean value of age within the ADMCI patients; the mean age of the Age-subgroup was 64.3±1.1years-old while that of the Age+ subgroup was 75.3±0.7 years-old). A statistically significant association was observed between the 6-month follow-up ADASCog score and the global baseline alpha2 source activity and age as predictors ($p < 0.05$). This effect was confirmed using the following covariates in four different models: (1) the baseline ADASCog score (upper left diagram), (2) the baseline ADASCog score and education (upper right diagram), (3) the baseline ADASCog score and gender (lower left diagram), and (4) the baseline ADASCog score and total cortical thickness (lower left diagram). P-values of the global baseline alpha2 and age interaction, as well as the regression coefficient (b) for Age- and Age+ subgroups are reported in each subplot. The shadow areas correspond to the 95% confidence interval.*

No statistically significant association ($p > 0.05$) was observed between the global baseline alpha2 source activity and the education or gender as predictors and the 6-month follow-up ADASCog score as a target variable (without the age as a factor). Furthermore, no statistically significant association ($p > 0.05$) was observed between the global baseline alpha3 source activity and age, education, or gender as predictors and the 6-month follow-up ADASCog score as a target variable.

Control analyses

A first control analysis ($p < 0.05$ corrected) was performed to evaluate whether the neuropsychological scores may worsen across time (6 months) in the 6-month follow-up alpha-reactive ADMCI group (N = 32). For each 6-month follow-up alpha-reactive ADMCI patient, the procedure was as follows: (1) the neuropsychological tests included: the ADAS-Cog, Immediate recall of Rey Auditory Verbal Learning Test, Delayed recall of Rey Auditory Verbal Learning Test,

Verbal fluency test for letters, Verbal fluency test for the category, TMT B-A, and Clock drawing test; (2) the neuropsychological scores were log 10 transformed to make them Gaussian before the subsequent parametric statistical analysis; (3) t-tests were computed to evaluate the presence or absence of statistically significant differences between the baseline and the 6-month follow-up for the above-mentioned neuropsychological scores. To consider the inflating effects of multiple univariate tests, the statistical threshold was set at $p < 0.007$ (i.e., 7 neuropsychological scores, $p < 0.05/7 = 0.007$) to obtain the Bonferroni correction at $p < 0.05$. No statistically significant difference was found ($p > 0.05$; see Table 7).

Neuropsychological scores in the 6-month follow-up alpha-reactive ADMCI group				
		Baseline	**Follow-up**	
	Cut-off of abnormality	**Mean ± SE *(%subjects with abnormal score)***	**Mean ± SE *(%subjects with abnormal score)***	**T-test**
ADAS-Cog	*≥ 17*	21.2 ± 1.4 (75.9%)	23.3 ± 1.6 (75.9%)	n.s.
RAVLT imm. recall	*< 28.53*	30.0 ± 2.0 (53.1%)	28.9 ± 2.0 (50.0%)	n.s.
RAVLT delayed recall	*< 4.69*	5.1 ± 1.5 (68.8%)	2.9 ± 0.6 (71.9%)	n.s.
Letter fluency	*< 17*	33.4 ± 1.8 (3.1%)	33.0 ± 2.1 (9.4%)	n.s.
Letter category	*< 25*	31.6 ± 2.3 (31.3%)	30.6 ± 2.9 (34.4%)	n.s.
TMT B-A	*≥ 187*	119.4 ± 12.4 (20.7%)	138.1 ± 14.0 (24.1%)	n.s.
Clock drawing	*> 3*	4.0 ± 0.2 (75.0%)	4.1 ± 0.2 (78.1%)	n.s.

***Table** 7. Mean values (± SE) of the neuropsychological scores (i.e., ADAS-Cog, Rey Auditory Verbal Learning Test immediate recall, Rey Auditory Verbal Learning Test delayed recall, Verbal fluency for letters, Verbal fluency for category, Trail Making Test Part B-A, and Clock drawing) as well as the results of their statistical comparisons (T-test on log-10 transformed data; $p < 0.05$ corrected) in the 6-month follow-up alpha-reactive ADMCI patients at baseline and 6-months follow-up. The cut-off scores of the neuropsychological tests are also reported. Legend: ADAS-Cog = Alzheimer's Disease Assessment Scale-Cognitive Subscale; RAVLT = Rey Auditory Verbal Learning Test; TMT B-A = Trail Making Test Part B-A.*

A second control analysis ($p < 0.05$ corrected) was performed to evaluate whether the standard MRI markers reflecting brain neurodegeneration may worsen at the 6-month follow-up in the 6-month follow-up alpha-reactive ADMCI group (N = 32). For each 6-month follow-up alpha-reactive

ADMCI patient, the procedure was as follows: (1) the MRI markers included: (i) the volumes of the hippocampus and lateral ventricle for the left and right hemispheres (these markers were normalized with respect to the total intracranial volume); and (ii) the cortical thicknesses of the parahippocampal gyrus, fusiform gyrus, entorhinal cortex, precuneus, and cuneus for the left and right hemispheres; (2) the MRI markers were log 10 transformed to make them Gaussian before the subsequent parametric statistical analysis; (3) t-tests were computed to evaluate the presence or absence of statistically significant differences between baseline and 6-month follow-up for the above-mentioned MRI markers. To consider the inflating effects of multiple univariate tests, the statistical threshold was set at $p < 0.00357$ (i.e., 14 MRI markers, $p < 0.05/16 = 0.00357$) to obtain the Bonferroni correction at $p < 0.05$. Statistically significant differences ($p < 0.05$ corrected) showed significant lower values of the following MRI-based variables at the 6-month follow-up than the baseline: (1) the volumes of the left hippocampus, left lateral ventricle, and right lateral ventricle and (2) the cortical thickness of the left entorhinal cortex and right entorhinal cortex (see Table 8).

MRI markers in 6-month follow-up alpha-reactive ADMCI group			
	Baseline	**Follow-up**	**T-test**
Normalized volumes			
Left hippocampus	0.0022 ± 0.0001	0.0021 ± 0.0001	$p < 0.001$
Right hippocampus	0.0023 ± 0.0001	0.0022 ± 0.0001	n.s.
Left lateral ventricle	0.0106 ± 0.0007	0.0110 ± 0.0007	$p < 0.00001$
Right lateral ventricle	0.0104 ± 0.0008	0.0108 ± 0.0008	$p < 0.0001$
Cortical thickness			
Left parahippocampal gyrus	2.43 ± 0.06	2.43 ± 0.07	n.s.
Right parahippocampal gyrus	2.44 ± 0.06	2.43 ± 0.06	n.s.
Left fusiform gyrus	2.48 ± 0.04	2.45 ± 0.04	n.s.
Right fusiform gyrus	2.51 ± 0.04	2.48 ± 0.04	n.s.
Left entorhinal cortex	3.08 ± 0.08	3.00 ± 0.09	$p < 0.003$
Right entorhinal cortex	3.25 ± 0.10	3.15 ± 0.10	$p < 0.001$
Left praecuneus	2.09 ± 0.03	2.07 ± 0.04	n.s.
Right precuneus	2.11 ± 0.03	2.08 ± 0.04	n.s.
Left cuneus	1.71 ± 0.03	1.70 ± 0.03	n.s.
Right cuneus	1.69 ± 0.03	1.67 ± 0.03	n.s.

Table 8. *Mean values (± SE) of the magnetic resonance imaging (MRI) markers (i.e., volumes of the hippocampus and lateral ventricle for the left and right hemispheres; cortical thicknesses of the parahippocampal gyrus, fusiform gyrus, entorhinal cortex, precuneus, and cuneus for the left and right hemispheres) as well as the results of their statistical comparisons (T-test on log-10 transformed data; $p < 0.05$ corrected) in the alpha-reactive ADMCI patients between the baseline and the 6-month follow-up. The volumes were normalized with reference to the total intracranial volume.*

EXPERIMENTAL PART: Discussion

rsEEG alpha reactivity to eyes opening in the DLB, PDD, ADD, and ADMCI patients

The **first study** findings reported a substantial (> -10%; for example, from -10% to -100%) reactivity of the posterior rsEEG alpha source activities during the eyes-open condition in 93% of Healthy seniors, 77% of ADD patients, and 64% of DLB patients. It is, therefore, possible to observe less reactivity of the posterior rsEEG alpha source activities in the ADD and DLB groups than in the Healthy group and that there was less reactivity in the occipital rsEEG alpha source activities in the DLB than in the ADD group.

In the **second study**, a surprising result was the very low percentage (35%) of PDD patients showing a substantial (> -10%) reactivity of the posterior rsEEG alpha source activities during the eyes-open condition when compared to matched Healthy (88%) and ADD (57%) participants. Considering only the alpha-reactive participants, the posterior rsEEG alpha source activities manifested lower reactivity in the PDD group than in the ADD and in Healthy groups.

Finally, in the **third study**, we demonstrated a substantial (> -10%) reduction in the posterior rsEEG alpha source activities during the eyes-open condition in about 90% and 70% of Healthy and ADMCI participants, respectively. Therefore, the presence of true posterior rsEEG alpha rhythms is quite common in ADMCI patients, and the present study confirms that those rhythms can represent a pathophysiological biomarker of the neurophysiological mechanisms underpinning quiet vigilance in AD patients.

These core results extend previous findings showing less rsEEG alpha reactivity during the eyes-open condition (1) in ADD and DLB-PDD (i.e., 24 DLB + 17 PDD) groups as compared to a Healthy group and (2) in the DLB-PDD than the ADD group (Schumacher et al., 2020a). The present results also extend previous findings showing (1) less rsMEG alpha reactivity in ADD and DLB groups as compared to a Healthy group and (2) no significant difference in that reactivity between the two pathological groups (Franciotti et al., 2006). Moreover, the present results extend previous findings showing less rsMEG alpha reactivity in a PDD than in a Healthy group (Bosboom et al., 2006).

Notably, in those previous studies, the experimental procedure did not distinguish between participants who showed or not the reactivity of the rsEEG/MEG alpha rhythms during the eyes-open

condition (Franciotti et al., 2006; Schumacher et al., 2020b). Therefore, the effects reported in those previous studies may be partially due to some DLB and PDD patients showing an increase in background rsEEG theta or pre-alpha rhythms during the eyes-open condition. Indeed, here we reported the case of several ADD, DLB, and PDD patients not showing a reduction (reactivity) of rsEEG alpha source activities during the eyes-open condition.

Finally, the present results complement previous findings showing (1) less rsEEG alpha reactivity during the eyes-open condition in ADMCI and LBMCI groups when compared to a Healthy group and (2) no significant difference in that reactivity between the two MCI groups (Schumacher et al., 2021).

Further research is needed to clarify if the present methodology (i.e., selection of all participants showing the mentioned reactivity of rsEEG alpha rhythms) could show differences in reactivity between ADMCI, LBMCI, and PDMCI groups or whether those differences may be only related to late disease stages characterized by dementia.

Clinical relevance of rsEEG alpha reactivity to eyes opening in the DLB, PDD, and ADD patients

A clinically interesting result shown in this PhD thesis is a negative correlation between the global composite cognitive score (as a marker of global cognitive status) and the reactivity (%) of the central-parietal-occipital rsEEG (eLORETA) BGF 2 source activity from the eyes-open to the eyes-closed condition (as a marker of reactivity of posterior rsEEG background rhythms) across all Healthy, ADD, DLB, and PDD participants as a whole population.

The current results suggest that such reactivity of rsEEG rhythms is clinically relevant in ADD, DLB, and PDD patients and extend previous findings reporting a correlation between the MMSE score as an index of global cognitive status and biomarkers of alpha source activity and functional connectivity in the eyes-closed condition across all Healthy, PDD (PDMCI), DLB/DLBMCI, and ADD (ADMCI) participants as a whole population (Babiloni et al., 2017, 2018a, 2018b).

Overall, the present findings hint that the vigilance regulation in quiet wakefulness, as probed by the rsEEG alpha reactivity to the eyes opening, may explain a certain part of the global cognitive performances in old individuals in the range of those with intact cognition to dementia.

Another clinically interesting result was the moderate/good accuracy in the classification between demented (ADD and DLB) vs Healthy individuals based on the mentioned reactivity of background posterior rsEEG (alpha) rhythms (i.e., 0.75-0.80 of the AUROC curve). Furthermore, we

found a good accuracy (i.e., 0.88 of the AUROC curve) in the classification of PDD vs Healthy individuals using the rsEEG alpha reactivity.

The current results extend previous findings reporting a classification accuracy of 0.95-0.45 between ADD vs Healthy, DLB vs Healthy, and PPD (PDMCI) vs Healthy based on posterior rsEEG alpha source activity and functional source connectivity estimated in the resting-state and eyes-closed condition (Knyazeva et al., 2010; Lehmann et al., 2007; Lizio et al., 2016; Missonnier et al., 2006; Babiloni et al., 2017, 2018b, 2018c).

Keeping in mind those data, the present results of the correlation rsEEG-MMSE score, and those of the AUROC curves, indicate that the present measures of reactivity of the posterior rsEEG rhythms at alpha/BGF have clinical relevance in relation to the global cognitive status and the diagnosis at the individual level. This outcome is clearly significant for future studies testing hypotheses on clinical applications of the present rsEEG biomarkers.

A speculative pathophysiological model underpinning the poor alpha reactivity in DLB, PDD, and ADD patients

At the present early stage of the research, we do not know what pathoneurophysiological mechanisms may be responsible for the poor reactivity in the posterior rsEEG alpha source activities during the eyes-open condition in ADD, DLB, and PDD patients. It can be speculated that the AD-related amyloid and tau neuropathology, the alpha-synucleinopathy, and/or the cortical neurodegeneration typically observed in those diseases might interact with the brain neural networks involved in the generation of posterior rsEEG alpha rhythms.

In healthy adults, EEG alpha rhythms are dominant in the posterior cortical regions during the resting-state eyes-closed condition, as a marker of cortical inhibition. These rhythms are reduced (reactivity) in amplitude during the eyes-open condition and during tasks involving the active sensorimotor or cognitive information processing, showing optimal features as a marker of event-related cortical activation (Pfurtscheller and Lopes da Silva, 1999). Therefore, the general interpretation of the present data is that the higher the rsEEG alpha reactivity in the transition from the resting state eyes-closed to eyes-open condition, the higher the ability of the participants' brains to modulate the quiet vigilance level during wakefulness.

In this line of neurophysiological interpretation, the amplitude of cortical rsEEG alpha rhythms may be modulated by signals (de) synchronizing the activity of cortical neural populations oscillating at alpha frequencies to produce an inhibitory (excitatory) mode in the eyes-closed (eyes-

open) condition (Pfurtscheller and Lopes da Silva, 1999). Among others, these signals may be transmitted through the cortico-basal ganglia-thalamocortical and reciprocal thalamic-cortical neural circuits (Pfurtscheller and Lopes da Silva, 1999; Hughes & Crunelli, 2005; Bočková et al., 2011; Weiss et al., 2015; Sanders & Jaeger, 2016).

More specifically, the cortico-basal ganglia-thalamocortical neural circuit may involve (i) glutamatergic cortico-striatal, subthalamic, and thalamocortical neurons; (ii) GABAergic interneurons; and (iii) dopaminergic modulatory nigrostriatal neurons. Differently, the reciprocal thalamic-cortical neural circuit may involve (i) glutamatergic thalamocortical high-threshold neurons; (ii) glutamatergic thalamocortical relay-mode neurons; (iii) GABAergic neurons of the reticular thalamic nucleus; and (iv) glutamatergic corticothalamic neurons (Hughes & Crunelli, 2005; Lörincz et al., 2008; Crunelli et al., 2015, 2018).

The cortico-basal ganglia-thalamocortical and the reciprocal thalamic-cortical neural circuits may be mainly modulated by subcortical ascending activating neural systems. Those systems are characterized by (i) noradrenergic ascending projections from locus coeruleus in the pons for alerting, (ii) dopaminergic ascending projections from midbrain nuclei for the support and reinforcement of motor actions, and (iii) cholinergic ascending projections from basal forebrain for the implementation of focused attention (Hughes & Crunelli, 2005; Lörincz et al., 2008; Crunelli et al., 2015, 2018; Li et al., 2018; Vorobyov et al., 2019; Broncel et al., 2020; Moënne-Loccoz et al., 2020; Noei Set al., 2022).

The inputs from the mentioned neuromodulatory projections may induce: (i) the enhancement (synchronization) in alpha rhythms, inhibiting the local information processing in cortical regions irrelevant to the ongoing event, and (ii) the block (desynchronization) of alpha rhythms associated with the enhancement (synchronization) in theta rhythms phase-coupled with the enhancement in beta and gamma rhythms, promoting the event-related local information processing, e.g., the elaboration of visual stimuli and visuomotor transformations (Pfurtscheller and Lopes da Silva; 1999; Hughes & Crunelli, 2005; Crunelli et al., 2015; Babiloni et al., 2020a).

Keeping in mind the above neurophysiological framework, the AD-, PD- and DLB-related neuropathology and neurodegeneration might induce (i) variable delays in the signal neurotransmission within ascending activating systems and thalamus-cortical loops, resulting in an abnormal timing of the synchronization and desynchronization of occipital neural activities at alpha frequencies and (ii) prolonged and less effective temporal summations of postsynaptic potentials in

parietal and occipital neural populations, resulting in an abnormal amplitude of rsEEG alpha source activities (Pfurtscheller and Lopes da Silva; 1999; Babiloni et al., 2020a,b,c, 2021a). The dysregulation of such signal neurotransmission might produce a "brain disconnection syndrome" underpinning abnormalities in the regulation of vigilance from eyes-closed to eyes-open conditions.

But how can we explain the present evidence of less reactivity of the posterior rsEEG alpha source activities in the DLB and in PDD patients than in the ADD group?

A spontaneous explanation derives from the recent evidence that a significant percentage (> 40%) of DLB patients presented AD-related amyloid neuropathology (Ferreira et al., 2020), and even PDD patients showed mixed AD-related amyloid neuropathology and Lewy bodies (Knox et al., 2020). Furthermore, there is an indication that cholinergic therapy may induce beneficial effects on cognitive processes in DLB and PDD patients, thus suggesting combined abnormalities in the cholinergic and dopaminergic system, which are part of the mentioned subcortical and cortical circuits generating rsEEG alpha rhythms (Barrett et al., 2020).

The role of the cholinergic system in rsEEG alpha reactivity has been highlighted by a previous study in healthy persons; in that study, functional rsMRI connectivity between the basal cholinergic forebrain and occipital cortex increased from the eyes-closed to the eyes-open condition proportionally to the reduction in amplitude (i.e., desynchronization) of local rsEEG alpha rhythms (Wan et al., 2019). In aged persons, lesions in the white matter connectivity between the basal cholinergic forebrain and occipital cortex were related to a reduction in alpha reactivity to eye-opening (Wan et al., 2019). In other studies, structural MRI evidence showed that an impairment of the pedunculopontine cholinergic nucleus was related to visual hallucinations in PD patients (Janzen et al., 2012), while functional MRI evidence unveiled that cholinesterase inhibition modulated visual and attentional brain responses in Healthy and ADD seniors (Bentley et al., 2008). In the same line, Schumacher et al. (2020a) showed that alpha reactivity was reduced more in DLB and PDD patients compared to AD and healthy controls and that this effect was related to structural MRI measures of volume loss within the Nucleus Basalis of Meynert (NBM), particularly in the PDD.

In this line of reasoning, recent studies in animal models showed that brain arousal related to the elaboration of biologically relevant environmental stimuli, the control of behavior, and the evaluation of its consequences might be modulated by signals released from (i) the cholinergic basal forebrain tract to the cerebral cortex and (ii) the tract connecting the cholinergic pedunculopontine nucleus to pons reticular formation and midbrain dopaminergic nuclei (i.e., substantia nigra and

ventral tegmental area), which target basal ganglia and cerebral cortex (Azzopardi et al., 2018; Aitta-Aho et al., 2018). Future studies in a larger DLB population will have to investigate the potential relationship between the poor reactivity of the rsEEG alpha source activities, visual hallucinations, and abnormalities in hypnagogic activity. Moreover, in a future study, it would be interesting to collect enough data and compare the rsEEG data between the DLB and PDD groups.

In the above neurophysiological model, one should consider the dramatic loss of the alpha reactivity to the eyes-open condition in the PDD patients (e.g., only about 35% of the PDD patients showed a substantial alpha reactivity to the eyes-open condition). A tentative explanation may be the obvious stronger impairment of the ascending dopaminergic neuromodulation systems in the PDD than in the ADD patients. In previous studies concerning the human data on dopaminergic neuromodulation, positron emission tomography (PET) in healthy individuals showed that the pharmacological enhancement of dopaminergic transmission increased regional cerebral blood flow mainly in the anterior cingulate areas (Kapur et al., 1994), which is a node of the salience network probing biologically relevant novelty in the environment. Furthermore, such a pharmacological enhancement also induced (i) a widespread modulation in cortical delta and alpha sources in PD patients during the resting-state condition (Babiloni et al., 2019) and (ii) improved (transcranial magnetic stimulation) evoked functional connectivity from the primary motor cortex (Leodori et al., 2022) and the supplementary motor area (Turco et al., 2018) contralateral to the affected limb in PD patients set in the resting-state condition. Indeed, dopamine depletion in PDD patients may depress the resting-state cortical functional connectivity, reducing the normal temporal dynamics of that connectivity within and between cortical neural networks (Fiorenzato et al., 2019; Formaggio et al., 2021; Maidan et al., 2021). This effect of dopamine depletion may prevent the normal transitions of rsEEG alpha rhythms from different levels of vigilance in wakefulness.

The predictive value of the posterior alpha source activities during the eyes-open condition

In the ADMCI participants with reactive rsEEG alpha source activities at the baseline recordings, the posterior rsEEG alpha source activities during the eyes-open condition were lower than those observed in the Healthy participants, thus suggesting an abnormal neurophysiological regulation of the quiet vigilance. Furthermore, the younger ADMCI patients (mean age of 64.3±1.1) with rsEEG alpha source reactivity and greater posterior rsEEG alpha source activities during the eyes-open condition showed more cognitive decline at the 6-month follow-up, possibly due to (1) the

more aggressive nature of AD (Babiloni et al., 2021b) and less resilient (compensatory) brain factors (Babiloni et al., 2020c).

The above results observed at 6-month follow-ups extend those of the previous rsEEG studies aimed at predicting the global cognitive status in AD patients at follow-ups equal to or greater than 12 months. In those previous studies, it was reported that (i) high rsEEG delta-theta and low background frequency power density at scalp electrodes did predict the cognitive status in patients with subjective cognitive complaints and MCI due to AD at ≥ 12-month follow-ups (Gouw et al., 2017); (ii) a combination of posterior rsEEG theta and background frequency power density values at scalp electrodes did predict the cognitive status in ADMCI patients at 12-month follow-ups (Jelic et al., 2000); (iii) anterior localization of rsEEG background frequency source activities did predict the cognitive status in ADMCI patients at about 24-month follow-ups (Huang et al., 2000); (iv) low posterior rsEEG background frequency power density at scalp electrodes did predict the cognitive status in ADMCI and ADD patients at 12-month follow-ups (Luckhaus et al., 2008); (v) high ratio between rsEEG high- and low-background frequency power density values at posterior scalp electrodes did predict the cognitive status in ADMCI and ADD patients at 36-month follow-ups (Moretti, 2015); (vi) high temporal rsEEG delta source activities did predict the cognitive status in ADMCI patients at 14-month follow-ups (Rossini et al., 2006); (vii) high posterior rsEEG theta power density and slowing of the background frequency at scalp electrodes did predict the cognitive status from the subjective cognitive complaints to ADD condition at > 80-month follow-ups (Prichep et al., 1994; 2006; 2014); and (viii) high posterior rsEEG theta power density at scalp electrodes and cognitive status did predict the global cognitive status from the cognitively unimpaired to the ADD condition at 20-month follow-ups (Nobili et al., 1999; Van der Hiele et al., 2007).

Noteworthy, the above previous rsEEG studies were performed in AD patients (i) not distinguishing rsEEG rhythms at alpha and non-alpha background dominant frequency based on the present neurophysiological criteria; (ii) not considering that AD may be especially aggressive in younger ADMCI patients (Babiloni et al., 2021b); and (iii) targeting relatively long follow-ups equal to or greater than 12 months. In this line, the current results provide the novel insight that in the younger ADMCI patients with reactive rsEEG alpha rhythms (mean age of 64.3±1.1), a good prediction of the global cognitive status at 6-month follow-ups can be performed grounding on posterior rsEEG “true” alpha source activities during the eyes-closed condition.

Another novel finding of the present study unveiled the effects of the ADMCI progression for six months on the true rsEEG alpha rhythms during the eyes-closed condition as a reflection of the neurophysiological systems underpinning the regulation of quiet vigilance. To investigate this aspect, we selected the ADMCI participants with reactive posterior rsEEG alpha source activities at both baseline and 6-month follow-ups (61.5% of all ADMCI participants).

The results showed that in those ADMCI participants, there was a substantial reduction in posterior rsEEG alpha source activities during the eyes-closed condition from baseline to the 6-month follow-up, associated with higher delta source activities in widespread regions. Therefore, in ADMCI patients, the true rsEEG alpha rhythms during the eyes-closed condition, when present, are sensitive to the disease progression at a 6-month follow-up. This is a feature of interest to test the effects of (non) pharmacological interventions aimed at improving the neurophysiological mechanisms underpinning the regulation of the quiet vigilance (level of consciousness) in ADMCI patients. Notably, standard neuroimaging and neuropsychological measures did not show similar substantial worsening in the present ADMCI patients at the 6-month follow-ups, thus suggesting that the derangement of the neurophysiological mechanisms underpinning the regulation of quiet vigilance may be faster than the AD-related neurodegenerative processes and the rate of deterioration of the global cognitive dysfunctions in ADMCI patients.

The current results extend those of the previous rsEEG studies aimed at investigating the effects of AD progression on rsEEG rhythms. In those previous studies, it was reported that (i) posterior rsEEG theta-delta power density at scalp electrodes increased and rsEEG beta power density decreased in ADMCI patients at 21-month follow-ups (Jelic et al., 2000); (ii) limbic rsEEG theta source activities increased in ADMCI (MCI not due to AD) patients at 24-month follow-up in relation to reduced functional connectivity within cortical default mode network as revealed by resting-state fMRI (Jovicich et al., 2019); (iii) widespread rsEEG delta source activities increased and posterior rsEEG alpha and beta source activities decreased in ADD patients at about 12-month follow-ups (Babiloni et al., 2013); (iv) posterior rsEEG alpha source activities decreased in ADMCI patients at about 12-month follow-ups (Babiloni et al., 2014); v) posterior rsEEG delta-theta power density at scalp electrodes increased and posterior rsEEG alpha-beta power density decreased in ADD patients at 30-month follow-ups (Coben et al., 1985); (vi) posterior rsEEG delta-theta power density at scalp electrodes increased in ADD patients at 12-month follow-ups (Soininen et al., 1989); and (vii)

posterior rsEEG delta-theta power density at scalp electrodes increased and posterior rsEEG alpha-beta power density decreased in ADD patients at 24-month follow-ups (Sloan et al., 1993).

Again, the above previous rsEEG studies were performed in AD patients (i) not distinguishing rsEEG rhythms at alpha and non-alpha background dominant frequency based on the present neurophysiological criteria and (ii) targeting relatively long follow-ups equal to or greater than 12 months. In this line, the current results provide the novel insight that in the ADMCI patients with reactive rsEEG alpha rhythms, widespread rsEEG delta rhythms during the eyes-closed condition increased, and posterior rsEEG alpha rhythms decreased at 6-month follow-ups, as candidate pathophysiological biomarkers for (non)pharmacological interventions treating disturbances in the regulation of quiet vigilance in those patients.

CONCLUSIONS

In the present PhD thesis, we decided to extend the research on a promising and heuristic neurophysiological biomarker which is the amplitude reduction ("reactivity") of "background" rsEEG alpha rhythms from the eyes-closed to the eyes-open condition. In the eyes-open condition, a large amount of cortical visual neurons and those arousing the cerebral cortex abandon the idling 10-Hz "background" synchronization of cortical inhibition to form neural subpopulations oscillating at frequencies > 30 Hz in the range of high-frequency beta and gamma rhythms (Pfurtscheller and Lopes da Silva, 1999). Therefore, this "background" rsEEG alpha reactivity may reflect increased brain arousal, enhanced vigilance, and active visual information processing in parietal, temporal, and occipital cortical areas (Babiloni et al., 2020a). Of note, the "background" rsEEG alpha reactivity is not only related to visual information processing but is also positively related to attention and cognitive performances (Stipacek et al., 2003; Hanslmayr et al., 2005) and may serve as a possible marker for the assessment of aD patients (McBride et al., 2014). Moreover, it has been shown that cholinergic basal forebrain projections to the thalamus and cortical neurons may affect "background" rsEEG alpha reactivity, suggesting that impaired rsEEG alpha reactivity during the eyes open may serve as a marker of the integrity of the cholinergic system (Wan et al., 2019).

In the methodological approach of the present PhD thesis, we proposed the study of the rsEEG alpha reactivity in ADD, DLB, and PDD patients by rsEEG source estimations. In precedence, the topographical analysis of rsEEG rhythms in those patients has been mostly performed at scalp electrodes and may be affected by reference electrode and head volume conduction effects, which blur spatial analysis of the distribution of rsEEG potentials.

Another methodological step forward of the present methodological approach was the use of individual frequency alpha bands for investigating the rsEEG alpha reactivity during the eyes open. In most of the previous studies, the frequency analysis of rsEEG rhythms was performed using standard (fixed) frequency bands in all subjects despite their remarkable interindividual variability. Several previous studies of our Workgroup successfully used the above-mentioned two methodological approaches in ADD, DLB, and PDD patients to investigate the rsEEG rhythms at the eyes-closed condition (Babiloni et al., 2017, 2018b,c, Pascarelli et al., 2020). The main results can be summarised as follows. Compared to Healthy subjects, DLB patients showed lower activation in individual occipital, parietal, and temporal cortical sources of rsEEG alpha rhythms, associated with an increase in topographically widespread delta source activities (Babiloni et al., 2017). Such abnormalities in the individual delta and alpha source activities were intermediate in magnitude in

relation to those observed in ADD and PDD patients, where PDD and ADD patients showed maximum abnormalities in the individual delta and alpha source activities, respectively (Babiloni et al., 2017). Similar results were observed even in LBMCI patients (Babiloni et al., 2018). Furthermore, the DLB and LBMCI patients showed abnormalities in the individual rsEEG delta and alpha source activities associated with global cognitive deficits and visual hallucinations (Pascarelli et al., 2020).

Finally, a third methodological step forward in the study of the rsEEG alpha reactivity would be represented by a fine neurophysiological definition of rsEEG alpha rhythms. In this regard, we posit that rsEEG alpha rhythms are defined by the following two core features: (i) a clear amplitude maximum in the posterior scalp or cortical regions during the eyes-closed condition and (ii) an evident reduction (reactivity) in amplitude in those posterior rsEEG rhythms from the eyes-closed to the eyes-open condition. The lack of these features, especially in DLB and PDD patients, may denote the substitution of physiological rsEEG alpha rhythms with pathological ample theta rhythms as a possible sign of thalamocortical dysrhythmia (Bonanni et al., 2008, 2015; Schumacher et al., 2020b; Franciotti et al., 2020).

Considering this, in the **first study**, we tested if the reactivity of posterior rsEEG alpha rhythms from the eye-closed to the eyes-open condition may differ in DLB, PDD, and ADD patients as a functional probe of the dominant cortical neural synchronization mechanisms regulating the vigilance in posterior visual systems.

Results showed a substantial (> -10%) reduction in the posterior alpha source activities from the eyes-closed to the eyes-open condition in 86% of the Healthy seniors, 54% of the ADD patients, and 52% of the DLB patients. In these participants, there was less reactivity of the posterior rsEEG alpha source activities in the ADD and DLB groups than in the Healthy group. Furthermore, there was less reactivity of the occipital rsEEG alpha source activities in the DLB than in the ADD group. These results suggest that in relation to ADD patients, DLB patients may suffer from a greater alteration in the neural synchronization mechanisms regulating the vigilance in posterior visual cortical systems. Future longitudinal studies should test its relation to the progression of cognitive fluctuations and visual hallucinations in DLB patients.

In the **second study**, we hypothesized that the dysregulation of vigilance might be reflected by a poor reactivity of posterior rsEEG alpha rhythms during the vigilance transition from the eyes-closed to the eyes-open condition. Results showed substantial (> -10%) reduction (reactivity) in the posterior alpha source activities from the eyes-closed to the eyes-open condition in 88% of the Healthy seniors, 57% of the ADD patients, and only 35% of the PDD patients. In the alpha-reactive participants, there was lower reactivity in the parietal rsEEG alpha source activities in the PDD group than in the Healthy and the ADD groups. These results suggest that the present PDD patients were

characterized by poor reactivity in the posterior cortical mechanisms desynchronizing rsEEG alpha rhythms in relation to the eyes-open condition and the related visual inputs as an interesting biomarker of the vigilance dysregulation in quiet wakefulness. This kind of vigilance dysregulation may particularly impact the level of consciousness in PDD patients (e.g., visual primary consciousness) and the quality of social interactions. To mitigate these symptoms, the present rsEEG biomarkers may provide endpoint targets for interventions with drugs for vigilance or brain electromagnetic simulations and may be used in the early stages of the discovery pathways testing those interventions. Effective pharmacological intervention and (invasive or non-invasive) brain electromagnetic simulations are expected to determine recovery of the rsEEG alpha reactivity to the eyes-open condition in many PDD patients and improve their general ability to regulate vigilance and primary visual consciousness in their activities of daily living.

In the **third study**, we tested the exploratory hypothesis that rsEEG alpha rhythms may predict and be sensitive to AD progression at a 6-month follow-up in ADMCI patients. Results showed a substantial (> -10%) reduction in the posterior alpha source activities during the eyes-open condition in about 90% and 70% of the Healthy and ADMCI participants, respectively. In the younger ADMCI participants (mean age of 64.3±1.1) with reactive rsEEG alpha source activities, posterior alpha source activities during the eyes-closed condition predicted the global cognitive status at the 6-month follow-up. In all younger ADMCI participants with reactive rsEEG alpha source activities, posterior alpha source activities during the eyes-closed condition reduced in magnitude at that follow-up. These effects could not be explained by neuroimaging and neuropsychological biomarkers of AD.
These results suggest that in ADMCI patients, the true (reactive) posterior rsEEG alpha rhythms, when present, predict (in relation to younger age) and are quite sensitive to the effects of the disease progression on neurophysiological mechanisms underpinning vigilance regulation.

The results of the three studies unveiled the significant extent to which the well-known impairments in the cholinergic and dopaminergic neuromodulatory ascending systems could affect the brain neurophysiological oscillatory mechanisms underpinning the reactivity of rsEEG alpha rhythms during eyes open and, then, the regulation of quiet vigilance in ADD, PDD, and DLB patients, thus enriching the neurophysiological model underlying their known difficulties to remain awake in quiet environmental conditions during daytime.

Future research could shed light on whether there are specific differences between patients with DLB and those with PDD matched for demographic and clinical variables. Moreover, it could be interesting to stratify the PDD, PDMCI, DLB, and LBMCI patients based on (i) the treatment with dopaminergic and/or cholinergic drugs and (ii) the presence of visual hallucinations, abnormalities in hypnagogic activity, and/or cognitive fluctuations, in order to much better investigate the potential

relationship between these symptoms, the dopaminergic neuromodulation, the pharmacological treatment, and the poor reactivity to the eyes-open condition of the rsEEG alpha source activities.

Finally, the results of this PhD thesis motivate further investments and research aimed at testing the beneficial heuristic and clinical effects of the inclusion of rsEEG measures in the actual biomarkers panel for the assessment of ADD, DLB, and PDD patients. Those rsEEG measures may be considered pathophysiological "P" biomarkers in that panel (typically based on CSF and neuroimaging biomarkers) to probe the neurophysiological mechanisms generating rsEEG rhythms and reflecting the ascending activating subcortical and thalamus-cortical systems underpinning the regulation of cortical arousal and quiet vigilance, the treatment of the vigilance disturbances in ADD, DLB, and PDD patients being an important omitted chapter of the present fight to this dramatic disease.

BIBLIOGRAPHY

Aarsland D, Brønnick K, Larsen JP, Tysnes OB, Alves G; Norwegian ParkWest Study Group. Cognitive impairment in incident, untreated Parkinson disease: the Norwegian ParkWest study. Neurology. 2009 Mar 31;72(13):1121-6. doi: 10.1212/01.wnl.0000338632.00552.cb. Epub 2008 Nov 19. PMID: 19020293.

Aarsland D, Litvan I, Salmon D, Galasko D, Wentzel-Larsen T, Larsen JP. Performance on the dementia rating scale in Parkinson's disease with dementia and dementia with Lewy bodies: comparison with progressive supranuclear palsy and Alzheimer's disease. J Neurol Neurosurg Psychiatry. 2003 Sep;74: 1215-20.

Aarsland D, Perry R, Larsen JP, McKeith IG, O'Brien JT, Perry EK, Burn D, Ruffmann CG. Neuroleptic sensitivity in Parkinson's disease and parkinsonian dementias. J Clin Psychiatry. 2005 May;66(5):633-7.

Abdi, H., 2010. Greenhouse geisser correction. In: Salkind, N.J., Dougherty, D.M., Frey, B. (Eds.), Encyclopedia of Research Design. Sage, Thousand Oaks CA, pp. 544–548.

Adamowicz DH, Roy S, Salmon DP, Galasko DR, Hansen LA, Masliah E, Gage FH. Hippocampal α-Synuclein in Dementia with Lewy Bodies Contributes to Memory Impairment and Is Consistent with Spread of Pathology. J Neurosci. 2017 Feb 15;37(7):1675-1684. doi: 10.1523/JNEUROSCI.3047-16.2016. Epub 2016 Dec 30. PMID: 28039370; PMCID: PMC5320602.

Adler G, Brassen S, Jajcevic A. EEG coherence in Alzheimer's dementia. J Neural Transm. 2003 Sept;110(9):1051-8

Adlimoghaddam A, Neuendorff M, Roy B, Albensi BC. A review of clinical treatment considerations of donepezil in severe Alzheimer's disease. CNS Neurosci Ther. 2018 Oct;24(10):876-888. doi: 10.1111/cns.13035. Epub 2018 Jul 29. PMID: 30058285; PMCID: PMC6489741.

Aitta-Aho, T, Hay, YA, Phillips, BU, Saksida, LM, Bussey, TJ, Paulsen, O, Apergis-Schoute, J., 2018. Basal forebrain and brainstem cholinergic neurons differentially impact amygdala circuits and learning-related behavior. Curr Biol 28 (16), 2557–2569.

Albert MS, DeKosky ST, Dickson D, Dubois B, Feldman HH, Fox NC, Gamst A, Holtzman DM, Jagust WJ, Petersen RC, Snyder PJ, Carrillo MC, Thies B, Phelps CH. The diagnosis of mild cognitive impairment due to Alzheimer's disease: recommendations from the National Institute on Aging-Alzheimer's Association workgroups on diagnostic guidelines for Alzheimer's disease. Alzheimer’s Dement. 2011 May;7(3):270-9. doi: 10.1016/j.jalz.2011.03.008. Epub 2011 Apr 21. PMID: 21514249; PMCID: PMC3312027.

Alzheimer's Association. 2016 Alzheimer's disease facts and figures. Alzheimers Dement. 2016 Apr;12(4):459-509. doi: 10.1016/j.jalz.2016.03.001. PMID: 27570871.

American Psychiatric Association, DSM-5 Task Force. (2013). (5th ed.). American Psychiatric Publishing, Inc. https://doi.org/10.1176/appi.books.9780890425596

Amzica F, Lopes da Silva FH. Niedermeyer's Electroencephalography: Basic Principles, Clinical Applications, and Related Fields (7 ed.). Oxford University Press. 2017

Andersson, M, Hansson, O, Minthon, L, Rosén, I, Londos, E., 2008. Electroencephalogram variability in dementia with lewy bodies, Alzheimer’s disease and controls. Dement Geriatr Cogn Disord 26 (3), 284–290.

Azzopardi, E, Louttit, AG, DeOliveira, C, Laviolette, SR, Schmid, S., 2018. The role of cholinergic midbrain neurons in startle and prepulse inhibition. J Neurosci 38 (41), 8798–8808.

Babiloni C, Lorenzo I, Lizio R, Lopez S, Tucci F, Ferri R, Soricelli A, Nobili F, Arnaldi D, Famà F, Buttinelli C, Giubilei F, Cipollini V, Onofrj M, Stocchi F, Vacca L, Fuhr P, Gschwandtner U, Ransmayr G, Aarsland D, Parnetti L, Marizzoni M, D'Antonio F, De Lena C, Güntekin B, Yıldırım E, Hanoğlu L, Yener G, Gündüz DH, Taylor JP, Schumacher J, McKeith I, Frisoni GB, De Pandis MF, Bonanni L, Percio CD, Noce G. Reactivity of posterior cortical electroencephalographic alpha rhythms during eyes opening in cognitively intact older adults and patients with dementia due to Alzheimer's and Lewy body diseases. Neurobiol Aging. 2022 Jul;115:88-108. DOI: 10.1016/j.neurobiolaging.2022.04.001. Epub 2022 Apr 9. PMID: 35512497.

Babiloni C, Arakaki X, Azami H, Bennys K, Blinowska K, Bonanni L, Bujan A, Carrillo MC, Cichocki A, de Frutos-Lucas J, Del Percio C, Dubois B, Edelmayer R, Egan G, Epelbaum S, Escudero J, Evans A, Farina F, Fargo K, Fernández A, Ferri R, Frisoni G, Hampel H, Harrington MG, Jelic V, Jeong J, Jiang Y, Kaminski M, Kavcic V, Kilborn K, Kumar S, Lam A, Lim L, Lizio R, Lopez D, Lopez S, Lucey B, Maestú F, McGeown WJ, McKeith I, Moretti DV, Nobili F, Noce G, Olichney J, Onofrj M, Osorio R, Parra-Rodriguez M, Rajji T, Ritter P, Soricelli A, Stocchi F, Tarnanas I, Taylor JP, Teipel S, Tucci F, Valdes-Sosa M, Valdes-Sosa P, Weiergräber M, Yener G, Guntekin B. Measures of resting state EEG rhythms for clinical trials in Alzheimer's disease: Recommendations of an expert panel. Alzheimer's Dement. 2021a Sep;17(9):1528-1553. doi: 10.1002/alz.12311. Epub 2021a Apr 15. PMID: 33860614; PMCID: PMC8647863.

Babiloni C, Ferri R, Noce G, Lizio R, Lopez S, Lorenzo I, Tucci F, Soricelli A, Nobili F, Arnaldi D, Famà F, Orzi F, Buttinelli C, Giubilei F, Cipollini V, Marizzoni M, Güntekin B, Aktürk T, Hanoğlu L, Yener G, Özbek Y, Stocchi F, Vacca L, Frisoni GB, Del Percio C. Resting State Alpha Electroencephalographic Rhythms Are Differently Related to Aging in Cognitively Unimpaired Seniors and Patients with Alzheimer's Disease and Amnesic Mild Cognitive Impairment. J Alzheimers Dis. 2021b;82(3):1085-1114. doi: 10.3233/JAD-201271. PMID: 34151788.

Babiloni C, Barry RJ, Başar E, Blinowska KJ, Cichocki A, Drinkenburg WHIM, Klimesch W, Knight RT, Lopes da Silva F, Nunez P, Oostenveld R, Jeong J, Pascual-Marqui R, Valdes-Sosa P, Hallett M. International Federation of Clinical Neurophysiology (IFCN) - EEG research workgroup: Recommendations on frequency and topographic analysis of resting state EEG rhythms. Part 1: Applications in clinical research studies. Clin Neurophysiol. 2020a Jan;131(1):285-307. DOI: 10.1016/j.clinph.2019.06.234. Epub 2019 Sep 19. PMID: 31501011.

Babiloni C, Lopez S, Del Percio C, Noce G, Pascarelli MT, Lizio R, Teipel SJ, González-Escamilla G, Bakardjian H, George N, Cavedo E, Lista S, Chiesa PA, Vergallo A, Lemercier P, Spinelli G, Grothe MJ, Potier MC, Stocchi F, Ferri R, Habert MO, Fraga FJ, Dubois B, Hampel H; INSIGHT-preAD Study Group. Resting-state posterior alpha rhythms are abnormal in subjective memory complaint seniors with preclinical Alzheimer's neuropathology and high education level: the INSIGHT-preAD study. Neurobiol Aging. 2020b Jun;90:43-59. DOI: 10.1016/j.neurobiolaging.2020.01.012. Epub 2020 Feb 1. PMID: 32111391.

Babiloni C, Pascarelli MT, Lizio R, Noce G, Lopez S, Rizzo M, Ferri R, Soricelli A, Nobili F, Arnaldi D, Famà F, Orzi F, Buttinelli C, Giubilei F, Salvetti M, Cipollini V, Bonanni L, Franciotti R, Onofrj M, Stirpe P, Fuhr P, Gschwandtner U, Ransmayr G, Aarsland D, Parnetti L, Farotti L, Marizzoni M, D'Antonio F, De Lena C, Güntekin B, Hanoğlu L, Yener G, Emek-Savaş DD, Triggiani AI, Taylor JP, McKeith I, Stocchi F, Vacca L, Hampel H, Frisoni GB, De Pandis MF, Del Percio C. Abnormal cortical neural synchronization mechanisms in quiet wakefulness are related to motor deficits, cognitive symptoms, and visual hallucinations in Parkinson's disease patients: an electroencephalographic study. Neurobiol Aging. 2020c;91: 88-111.

Babiloni, C, Blinowska, K, Bonanni, L, Cichocki, A, De Haan, W, Del Percio, C, Dubois, B, Escudero, J, Fernández, A, Frisoni, G, Guntekin, B, Hajos, M, Hampel, H, Ifeachor, E, Kilborn, K, Kumar, S, Johnsen, K, Johannsson, M, Jeong, J, LeBeau, F, Lizio, R, Lopes da Silva, F, Maestú, F, McGeown, WJ, McKeith, I, Moretti, DV, Nobili, F, Olichney, J, Onofrj, M, Palop, JJ, Rowan, M, Stocchi, F, Struzik, ZM, Tanila, H, Teipel, S, Taylor, JP, Weiergräber, M, Yener, G, Young– Pearse, T, Drinkenburg, WH, Randall, F, 2020d. What electrophysiology tells us about Alzheimer's disease: a window into the synchronization and connectivity of brain neurons. Neurobiol Aging 85, 58–73.

Babiloni C, Del Percio C, Lizio R, Noce G, Lopez S, Soricelli A, Ferri R, Pascarelli MT, Catania V, Nobili F, Arnaldi D, Famà F, Orzi F, Buttinelli C, Giubilei F, Bonanni L, Franciotti R, Onofrj M, Stirpe P, Fuhr P, Gschwandtner U, Ransmayr G, Fraioli L, Parnetti L, Farotti L, Pievani M, D'Antonio F, De Lena C, Güntekin B, Hanoğlu L, Yener G, Emek-Savaş DD, Triggiani AI, Taylor JP, McKeith I, Stocchi F, Vacca L, Frisoni GB, De Pandis MF. Levodopa may affect cortical excitability in Parkinson's disease patients with cognitive deficits as revealed by reduced activity of cortical sources of resting state electroencephalographic rhythms. Neurobiol Aging. 2019 Jan;73:9-20. DOI: 10.1016/j.neurobiolaging.2018.08.010. Epub 2018 Aug 30. PMID: 30312790.

Babiloni C, Del Percio C, Lizio R, Noce G, Lopez S, Soricelli A, Ferri R, Nobili F, Arnaldi D, Famà F, Aarsland D, Orzi F, Buttinelli C, Giubilei F, Onofrj M, Stocchi F, Stirpe P, Fuhr P, Gschwandtner U, Ransmayr G, Garn H, Fraioli L, Pievani M, Frisoni GB, D'Antonio F, De Lena C, Güntekin B, Hanoğlu L, Başar E, Yener G, Emek-Savaş DD, Triggiani AI, Franciotti R, Taylor JP, Vacca L, De Pandis MF, Bonanni L. Abnormalities of resting-state functional cortical connectivity in patients with dementia due to Alzheimer's and Lewy body diseases: an EEG study. Neurobiol Aging. 2018a; 65: 18-40.

Babiloni, C, Del Percio, C, Lizio, R, Noce, G, Lopez, S, Soricelli, A, Ferri, R, Pascarelli, MT, Catania, V, Nobili, F, Arnaldi, D, Famà, F, Orzi, F, Buttinelli, C, Giubilei, F, Bonanni, L, Franciotti, R, Onofrj, M, Stirpe, P, Fuhr, P, Gschwandtner, U, Ransmayr, G, Garn, H, Fraioli, L, Pievani, M, D'Antonio, F, De Lena, C, Güntekin, B, Hanoglu, ˘ L, Bas¸ ar, E, Yener, G, Emek-Savas¸ , DD, Triggiani, AI, Taylor, JP, De Pandis, MF, Vacca, L, Frisoni, GB, Stocchi, F, 2018b. Functional cortical source connectivity of resting state electroencephalographic alpha rhythms shows similar

abnormalities in patients with mild cognitive impairment due to Alzheimer's and Parkinson's diseases. Clin Neurophysiol 129 (4), 766–782.

Babiloni, C, Del Percio, C, Lizio, R, Noce, G, Lopez, S, Soricelli, A, Ferri, R, Nobili, F, Arnaldi, D, Famà, F, Aarsland, D, Orzi, F, Buttinelli, C, Giubilei, F, Onofrj, M, Stocchi, F, Stirpe, P, Fuhr, P, Gschwandtner, U, Ransmayr, G, Garn, H, Fraioli, L, Pievani, M, Frisoni, GB, D'Antonio, F, De Lena, C, Güntekin, B, Hanoglu, ˘ L, Bas¸ ar, E, Yener, G, Emek-Savas¸ , DD, Triggiani, AI, Franciotti, R, Taylor, JP, Vacca, L, De Pandis, MF, Bonanni, L, 2018c. Abnormalities of resting-state functional cortical connectivity in patients with dementia due to Alzheimer's and Lewy body diseases: an EEG study. Neurobiol Aging 65, 18–40.

Babiloni, C, Del Percio, C, Lizio, R, Noce, G, Cordone, S, Lopez, S, Soricelli, A, Ferri, R, Pascarelli, MT, Nobili, F, Arnaldi, D, Famà, F, Aarsland, D, Orzi, F, Buttinelli, C, Giubilei, F, Onofrj, M, Stocchi, F, Stirpe, P, Fuhr, P, Gschwandtner, U, Ransmayr, G, Caravias, G, Garn, H, Sorpresi, F, Pievani, M, D'Antonio, F, De Lena, C, Güntekin, B, Hanoglu, ˘ L, Bas¸ ar, E, Yener, G, Emek-Savas¸ , DD, Triggiani, AI, Franciotti, R, Frisoni, GB, Bonanni, L, De Pandis, MF, 2017. Abnormalities of cortical neural synchronization mechanisms in subjects with mild cognitive impairment due to Alzheimer's and Parkinson's diseases: an EEG study. J Alzheimers Dis 59 (1), 339–358

Babiloni C, Lizio R, Marzano N, Capotosto P, Soricelli A, Triggiani AI, Cordone S, Gesualdo L, Del Percio C. Brain neural synchronization and functional coupling in Alzheimer's disease as revealed by resting state EEG rhythms. Int J Psychophysiol. 2016; 103: 88-102.

Babiloni C, Del Percio C, Lizio R, Marzano N, Infarinato F, Soricelli A, Salvatore E, Ferri R, Bonforte C, Tedeschi G, Montella P, Baglieri A, Rodriguez G, Famà F, Nobili F, Vernieri F, Ursini F, Mundi C, Frisoni GB, Rossini PM. Cortical sources of resting state electroencephalographic alpha rhythms deteriorate across time in subjects with amnesic mild cognitive impairment. Neurobiol Aging. 2014 Jan;35(1):130-42. DOI: 10.1016/j.neurobiolaging.2013.06.019. Epub 2013 Jul 30. PMID: 23906617.

Babiloni C, Lizio R, Del Percio C, Marzano N, Soricelli A, Salvatore E, Ferri R, Cosentino FI, Tedeschi G, Montella P, Marino S, De Salvo S, Rodriguez G, Nobili F, Vernieri F, Ursini F, Mundi C, Richardson JC, Frisoni GB, Rossini PM. Cortical sources of resting state EEG rhythms are sensitive to the progression of early-stage Alzheimer's disease. J Alzheimers Dis. 2013;34(4):1015-35. doi: 10.3233/JAD-121750. PMID: 23340039.

Babiloni C, Lizio R, Vecchio F, Frisoni GB, Pievani M, Geroldi C, Claudia F, Ferri R, Lanuzza B, Rossini PM. Reactivity of cortical alpha rhythms to eye opening in mild cognitive impairment and Alzheimer's disease: an EEG study. J Alzheimers Dis. 2010;22(4):1047-64. doi: 10.3233/JAD-2010-100798. PMID: 20930306.

Ballard C, Waite J. The effectiveness of atypical antipsychotics for the treatment of aggression and psychosis in Alzheimer's disease. Cochrane Database Syst Rev. 2006 Jan 25;(1):CD003476. doi: 10.1002/14651858.CD003476.pub2. PMID: 16437455.

Bekris LM, Yu CE, Bird TD, Tsuang DW. Genetics of Alzheimer disease. J Geriatr Psychiatry Neurol. 2010 Dec;23(4):213-27. doi: 10.1177/0891988710383571. PMID: 21045163; PMCID: PMC3044597.

Bentley, P, Driver, J, Dolan, RJ, 2008. Cholinesterase inhibition modulates visual and attentional brain responses in Alzheimer's disease and health. Brain 131 (Pt 2), 409–424.

Benton AL, A.B. Sivan AB, Hamsher KS, Varney NR, O. Spreen Contribution to Neuropsychological Assessment Oxford University Press, New York. 1983.

Benton AL, Varney NR, Hamsher KS. Visuospatial judgment Archives of Neurology. 1978; pp. 364-367.

Bereczki E, Francis PT, Howlett D, Pereira JB, Höglund K, Bogstedt A, Cedazo-Minguez A, Baek JH, Hortobágyi T, Attems J, Ballard C, Aarsland D. Synaptic proteins predict cognitive decline in Alzheimer's disease and Lewy body dementia. Alzheimers Dement. 2016 Nov;12(11):1149-1158. doi: 10.1016/j.jalz.2016.04.005. Epub 2016 May 22. PMID: 27224930.

Barrett MJ, Cloud LJ, Shah H, Holloway KL. Therapeutic approaches to cholinergic deficiency in Lewy body diseases. Expert Rev Neurother. 2020 Jan;20(1):41-53.

Berridge CW, Schmeichel BE, España RA. Noradrenergic modulation of wakefulness/arousal. Sleep Med Rev. 2012 Apr;16(2):187-97. doi: 10.1016/j.smrv.2011.12.003. Epub 2012 Jan 31. PMID: 22296742; PMCID: PMC3278579.

Berridge CW, Waterhouse BD. The locus coeruleus-noradrenergic system: modulation of behavioral state and state dependent cognitive processes. Brain Res Brain Res Rev. 2003 Apr;42(1):33-84. Rev.

Bertrand E, Lechowicz W, Szpak GM, Dymecki J. Qualitative and quantitative analysis of locus coeruleus neurons in Parkinson's disease. Folia Neuropathol 1997; 35: 80–86.

Beydoun MA, Beydoun HA, Gamaldo AA, Teel A, Zonderman AB,Wang Y. Epidemiologic Studies of Modifiable Factors Associated with 89 Cognition and Dementia: Systematic Review and MetaAnalysis. BMC Public Health 2014; 14:643.

Beyer MK, Larsen JP, Aarsland D. Gray matter atrophy in Parkinson disease with dementia and dementia with Lewy bodies. Neurology. 2007;69:747–54.

Bhat S, Acharya UR, Dadmehr N, Adeli H. Clinical Neurophysiological and Automated EEG-Based Diagnosis of the Alzheimer's Disease. Eur Neurol. 2015; 74: 202-10.

Bickford ME, Günlük AE, Guido W, Sherman SM. Evidence that cholinergic axons from the parabrachial region of the brainstem are the exclusive source of nitric oxide in the lateral geniculate nucleus of the cat. J Comp Neurol. 1993 Aug 15;334(3):410-30. doi: 10.1002/cne.903340307. PMID: 7690785.

Blennow K, de Lean MS, Zettenberg H. Alzheimer's Disease. Lancet 2006; 368(9533):387-403.

Bočková M, Chládek J, Jurák P, Halámek J, Baláž M, Rektor I. Involvement of the subthalamic nucleus and globus pallidus internus in attention. J Neural Transm (Vienna). 2011 Aug;118(8):1235-45.

Boeve BF, Dickson DW, Duda JE, Ferman TJ, Galasko DR, Galvin JE, Adlimoghaddam JG, Growdon JH, Hurtig HI, Kaufer DI, Kantarci K, Leverenz JB, Lippa CF, Lopez OL, McKeith IG, Singleton AB, Taylor A, Tsuang D, Weintraub D, Zabetian CP. Arguing against the proposed definition changes of PD. Mov Disord. 2016 Nov;31(11):1619-1622. doi: 10.1002/mds.26721. Epub 2016 Aug 5. PMID: 27492190; PMCID: PMC5168716.

Bohnen NI, Albin RL. The cholinergic system and Parkinson disease. Behav Brain Res 2011; 221: 564–573.

Bonanni, L, Franciotti, R, Nobili, F, Kramberger, MG, Taylor, JP, Garcia-Ptacek, S, Falasca, NW, Famá, F, Cromarty, R, Onofrj, M, Aarsland, DE-DLB study group, 2016. EEG markers of dementia with Lewy Bodies: a multicenter cohort study. J Alzheimers Dis 54 (4), 1649–1657.

Bonanni, L, Perfetti, B, Bifolchetti, S, Taylor, JP, Franciotti, R, Parnetti, L, 2015. Quantitative electroencephalogram utility in predicting conversion of mild cognitive impairment to dementia with Lewy bodies. Neurobiol Aging 36 (1), 434–445.

Bonanni, L, Thomas, A, Tiraboschi, P, Perfetti, B, Varanese, S, Onofrj, M., 2008. EEG comparisons in early Alzheimer's disease, dementia with Lewy bodies and Parkinson's disease with dementia patients with a 2-year follow-up. Brain 131 (Pt 3), 690–705.

Boot BP. Comprehensive treatment of dementia with Lewy bodies. Alzheimers Res Ther. 2015 May 29;7(1):45. doi: 10.1186/s13195-015-0128-z. PMID: 26029267; PMCID: PMC4448151.

Bosboom, JL, Stoffers, D, Stam, CJ, van Dijk, BW, Verbunt, J, Berendse, HW, ECh, Wolters, 2006. Resting state oscillatory brain dynamics in Parkinson's disease: an MEG study. Clin Neurophysiol 117 (11), 2521–2531.

Bosboom, JL, Stoffers, D, Wolters, ECh, Stam, CJ, Berendse, HW., 2009. MEG resting state functional connectivity in Parkinson's disease related dementia. J Neural Transm 116, 193–202.

Bostrom F, Jonsson L, Minthon L, Londos E. Patients with dementia with Lewy bodies have more impaired quality of life than patients with Alzheimer disease. Alzheimer Dis Assoc Disord 2007a;21: 150–54.

Bostrom F, Jonsson L, Minthon L, Londos E. Patients with Lewy body dementia use more resources than those with Alzheimer's disease. Int J Geriatr Psychiatry 2007b;22: 713–19.

Braak H, Del Tredici K, Rüb U, de Vos RA, Jansen Steur EN, Braak E. Staging of brain pathology related to sporadic Parkinson's disease. Neurobiol Aging. 2003 Mar-Apr;24(2):197-211.

Brassen S, Adler G. Short-term effects of acetylcholinesterase inhibitor treatment on EEG and memory performance in Alzheimer patients: an open, controlled trial. Pharmacopsychiatry. 2003;36:304-8

Breslau J, Starr A, Sicotte N, Higa J, Buchsbaum MS. Topographic EEG changes with normal aging and SDAT. Electroencephalogr Clin Neurophysiol. 1989;72:281-9.

Brett M. Johnsrude IS. Owen AM. The problem of functional localization in the human brain. Nature Reviews Neuroscience. 2002 Mar;3(3):243-249.

Briel RC, McKeith IG, Barker WA, Hewitt Y, Perry RH, Ince PG, Fairbairn AF. EEG findings in dementia with Lewy bodies and Alzheimer's disease. J Neurol Neurosurg Psychiatry. 1999;66:401-3.

Broncel A, Bocian R, Kłos-Wojtczak P, Konopacki J. Effects of locus coeruleus activation and inactivation on hippocampal formation theta rhythm in anesthetized rats. Brain Res Bull. 2020 Sep;162:180-190.

Brown LM, Schinka JA. Development and initial validation of a 15-item informant version of the Geriatric Depression Scale. Int J Geriatr Psychiatry. 2005 Oct;20(10):911-8. DOI: 10.1002/gps.1375. PMID: 16163741.

Brundin P, Dave KD, Kordower JH. Therapeutic approaches to target alpha-synuclein pathology. Exp Neurol. 2017 Dec;298(Pt B):225-235. doi: 10.1016/j.expneurol.2017.10.003. Epub 2017 Oct 4. PMID: 28987463; PMCID: PMC6541231.

Bruscoli M, Lovestone S. Is MCI really just early dementia? A systematic review of conversion studies. Int Psychogeriatr 2004;16(2):129-40

Buchhave P, Minthon L, Zetterberg H, Wallin ÅK, Blennow K, Hansson O. Cerebrospinal fluid levels ofβ-amyloid 1-42, but not of tau, are fully changed already 5 to 10 years before the onset of Alzheimer dementia. Archives of general psychiatry 2012;69(1):98-106.

Burton EJ, Barber R, Mukaetova-Ladinska EB, Robson J, Perry RH, Jaros E, Kalaria RN, O'Brien JT. Medial temporal lobe atrophy on MRI differentiates Alzheimer's disease from dementia with Lewy bodies and vascular cognitive impairment: a prospective study with pathological verification of diagnosis. Brain. 2009 Jan;132(Pt 1):195-203.

Busatto GF, Diniz BS, Zanetti MV. Voxel-based morphometry in Alzheimer's disease. Expert review of neurotherapeutics 2008; 8(11)1691-702.

Buter TC, van den Hout A, Matthews FE, Larsen JP, Brayne C, Aarsland D. Dementia and survival in Parkinson disease: a 12-year population study. Neurology. 2008; 70: 1017-22.

Buzsaki G, Bickford RG, Ponomareff G, Thal LJ, Mandel R, Gage FH. Nucleus basalis and thalamic control of neocortical activity in the freely moving rat. J Neurosci. 1988 Nov;8(11):4007-26

Buzsàki G, Gage FH. The cholinergic nucleus basalis: a key structure in neocortical arousal. EXS. 1989;57:159-71. Rev. Caravias G, Garn H, Sorpresi F, Pievani M, Frisoni GB, D'Antonio F, De Lena C, Güntekin B, Hanoğlu L, Başar E, Yener G, Emek-Savaş DD, Triggiani AI, Franciotti R, De Pandis MF, Bonanni L. Abnormalities of cortical neural synchronization mechanisms in patients with dementia due to Alzheimer's and Lewy body diseases: an EEG study. Neurobiol Aging. 2017a Jul;55:143-158. DOI: 10.1016/j.neurobiolaging.2017.03.030. Epub 2017 Apr 5. PMID: 28454845.

Carter SM, Ritchie JE, Sainsbury P. Doing good qualitative research in public health: not as easy as it looks. N S W Public Health Bull. 2009 Jul-Aug;20(7-8):105-11. doi: 10.1071/NB09018. PMID: 19735621.

Casamenti F, Deffenu G, Abbamondi AL, Pepeu G. Changes in cortical acetylcholine output induced by modulation of the nucleus basalis. Brain Res Bull. 1986 May;16(5):689-95. doi: 10.1016/0361-9230(86)90140-1. PMID: 3742251.

Caviness, JN, Lue, LF, Hentz, JG, Schmitz, CT, Adler, CH, Shill, HA, Sabbagh, MN, Beach, TG, Walker, DG., 2016. Cortical phosphorylated α-Synuclein levels correlate with brain wave spectra in Parkinson's disease. Mov Disord 31 (7), 1012–1019.

Coben LA, Danziger W, Storandt M. A longitudinal EEG study of mild senile dementia of Alzheimer type: changes at 1 year and at 2.5 years. Electroencephalogr Clin Neurophysiol. 1985 Aug;61(2):101-12. doi: 10.1016/0013-4694(85)91048-x. PMID: 2410219.

Colloby SJ, Cromarty RA, Peraza LR, Johnsen K, Jóhannesson G, Bonanni L, Onofrj M, Barber R, O'Brien JT, Taylor JP. Multimodal EEG-MRI in the differential diagnosis of Alzheimer's disease and dementia with Lewy bodies. J Psychiatr Res. 2016;78:48-55.

Colloby SJ, McParland S, O'Brien JT, Attems J. Neuropathological correlates of dopaminergic imaging in Alzheimer's disease and Lewy body dementias. Brain. 2012;135:2798–808.

Compta Y, Buongiorno M, Bargalló N, Valldeoriola F, Muñoz E, Tolosa E, Ríos J, Cámara A, Fernández M, Martí MJ. White matter hyperintensities, cerebrospinal amyloid-β and dementia in Parkinson's disease. J Neurol Sci. 2016 Aug 15;367:284-90.

Connolly BS, Fox SH. Drug treatments for the neuropsychiatric complications of Parkinson's disease. Expert Rev Neurother. 2012;12:1439–49

Cozac, VV, Gschwandtner, U, Hatz, F, Hardmeier, M, Rüegg, S, Fuhr, P, 2016. Quantitative EEG and cognitive decline in Parkinson's Disease. Parkinsons Dis 2016, 9060649. doi:10.1155/2016/9060649.

Crespo-Garcia M, Atienza M, Cantero JL. Muscle artifact removal from human sleep EEG by using independent component analysis. Ann Biomed Eng. 2008 Mar;36(3):467-75. DOI: 10.1007/s10439-008-9442-y. Epub 2008 Jan 29. PMID: 18228142.

Crunelli V, David F, Lőrincz ML, Hughes SW. The thalamocortical network as a single slow wave-generating unit. Curr Opin Neurobiol. 2015 Apr;31:72-80. DOI: 10.1016/j.conb.2014.09.001. Epub 2014 Sep 16. PMID: 25233254.

Crunelli V, Lorincz ML, Connelly WM, David F, Hughes SW, Lambert RC, Leresche N, Errington AC. Dual function of thalamic low-vigilance state oscillations: rhythm-regulation and plasticity. Nat Rev Neurosci. 2018 Feb;19(2):107–118. doi:10.1038/nrn.2017.151. Epub 2018 Jan 11. PMID: 29321683; PMCID: PMC6364803

Cummings, JL, Mega, M, Gray, K, Rosenberg-Thompson, S, Carusi, DA, Gornbein, J., 1994. The Neuropsychiatric Inventory: comprehensive assessment of psychopathology in dementia. Neurology 44 (12), 2308–2314.

Darweesh SK, Ibrahim MF, El-Tahawy MA. Effect of N-Acetylcysteine on Mortality and Liver Transplantation Rate in Non-Acetaminophen-Induced Acute Liver Failure: A Multicenter Study. Clin Drug Investig. 2017 May;37(5):473-482. doi: 10.1007/s40261-017-0505-4. PMID: 28205121.

Del Percio C, Derambure P, Noce G, Lizio R, Bartrés-Faz D, Blin O, Payoux P, Deplanque D, Méligne D, Chauveau N, Bourriez JL, Casse-Perrot C, Lanteaume L, Thalamas C, Dukart J, Ferri R, Pascarelli MT, Richardson JC, Bordet R, Babiloni C; PharmaCog Consortium. Sleep deprivation and Modafinil affect cortical sources of resting state electroencephalographic rhythms in healthy young adults. Clin Neurophysiol. 2019 Sep;130(9):1488-1498.

Del Percio C, Infarinato F, Marzano N, Iacoboni M, Aschieri P, Lizio R, Soricelli A, Limatola C, Rossini PM, Babiloni C. Reactivity of alpha rhythms to eyes opening is lower in athletes than non-athletes: a high-resolution EEG study. Int J Psychophysiol. 2011 Dec;82(3):240-7. doi: 10.1016/j.ijpsycho.2011.09.005. Epub 2011 Sep 22. PMID: 21945479.

Delaville C, De Deurwaerdère P, Benazzouz A. Noradrenaline and Parkinson's disease. Front Syst Neurosci 2011.
Delbeuck X, Van der Linden M, Collette F. Alzheimer's disease as a disconnection syndrome? Neuropsychol Rev. 2003 Jun;13(2):79-92. doi: 10.1023/a:1023832305702. PMID: 12887040.

DeLong, ER, DeLong, DM, Clarke-Pearson, DL., 1988. Comparing the areas under two or more correlated receiver operating characteristic curves: a nonparametric approach. Biometrics 44 (3), 837–845 PMID: 3203132.

Delorme A, Makeig S. EEGLAB: an open source toolbox for analysis of single-trial EEG dynamics including independent component analysis. J Neurosci Methods. 2004 Mar 15;134(1):9-21. doi: 10.1016/j.jneumeth.2003.10.009. PMID: 15102499.

Dey, AK, Stamenova, V, Turner, G, Black, SE, Levine, B., 2016. Pathoconnectomics of cognitive impairment in small vessel disease: A systematic review. Alzheimer's & Dement 12 (7), 831–845.

Dickson DW, Braak H, Duda JE, Duyckaerts C, Gasser T, Halliday GM, Hardy J, Leverenz JB, Del Tredici K, Wszolek ZK, Litvan I. Neuropathological assessment of Parkinson's disease: refining the diagnostic criteria. Lancet Neurol. 2009 Dec;8(12):1150-7. doi: 10.1016/S1474-4422(09)70238-8. Erratum in: Lancet Neurol. 2010 Feb;9(2):140. Erratum in: Lancet Neurol. 2010 Jan;9(1):29. PMID: 19909913.

Dierks T, Jelic V, Pascual-Marqui RD, Wahlund L, Julin P, Linden DE, Maurer K, Winblad B, Nordberg A. Spatial pattern of cerebral glucose metabolism (PET) correlates with localization of intracerebral EEG-generators in Alzheimer's disease. Clin Neurophysiol. 2000;111: 1817-24.

Dringenberg HC, Vanderwolf CH. Involvement of direct and indirect pathways in electrocorticographic activation. Neurosci Biobehav Rev. 1998 Mar;22(2):243-57. doi: 10.1016/s0149-7634(97)00012-2. PMID: 9579316.

Dubois B, Albert ML. Amnestic MCI or prodromal Alzheimer's disease? Lancet Neurol 2004; 3: 246–48.

Dubois B, Feldman HH, Jacova C, Hampel H, Molinuevo JL, Blennow K, DeKosky ST, Gauthier S, Selkoe D, Bateman R, Cappa S, Crutch S, Engelborghs S, Frisoni GB, Fox NC, Galasko D, Habert MO, Jicha GA, Nordberg A, Pasquier F, Rabinovici G, Robert P, Rowe C, Salloway S, Sarazin M, Epelbaum S, de Souza LC, Vellas B, Visser PJ, Schneider L, Stern Y, Scheltens P, Cummings JL. Advancing research diagnostic criteria for Alzheimer's disease: the IWG-2 criteria. Lancet Neurol. 2014; 13: 614-29.

Dubois B, Villain N, Frisoni GB, Rabinovici GD, Sabbagh M, Cappa S, Bejanin A, Bombois S, Epelbaum S, Teichmann M, Habert MO, Nordberg A, Blennow K, Galasko D, Stern Y, Rowe CC, Salloway S, Schneider LS, Cummings JL, Feldman HH. Clinical diagnosis of Alzheimer's disease: recommendations of the International Working Group. Lancet Neurol. 2021 Jun;20(6):484-496. doi: 10.1016/S1474-4422(21)00066-1. Epub 2021 Apr 29. PMID: 33933186; PMCID: PMC8339877.

Dubois, B, Slachevsky, A, Litvan, I, Pillon, B., 2000. The FAB: a Frontal Assessment Battery at bedside. Neurology 55 (11), 1621–1626.

Duong S, Patel T, Chang F. Dementia: What pharmacists need to know. Can Pharm J (Ott). 2017 Feb 7;150(2):118-129. doi: 10.1177/1715163517690745. PMID: 28405256; PMCID: PMC5384525.

Edwards T, Pilutti LA. The effect of exercise training in adults with multiple sclerosis with severe mobility disability: A systematic review and future research directions. Mult Scler Relat Disord. 2017 Aug;16:31-39. doi: 10.1016/j.msard.2017.06.003. Epub 2017 Jun 12. PMID: 28755682.

Emre M, Aarsland D, Brown R, Burn DJ, Duyckaerts C, Mizuno Y, Broe GA, J, Dickson DW, Gauthier S, Goldman J, Goetz C, Korczyn A, Lees A, Levy R, Litvan I, McKeith I, Olanow W, Poewe W, Quinn N, Sampaio C, Tolosa E, Dubois B. Clinical diagnostic criteria for dementia associated with Parkinson's disease.Mov Disord. 2007 Sep 15;22(12):1689-707

Fagan AM, Mintun MA, Shah AR, Aldea P, Roe CM, Mach RH, Marcus D, Morris JC, Holtzman DM. Cerebrospinal fluid tau and ptau(181) increase with cortical amyloid deposition in cognitively normal individuals: implications for future clinical trials of Alzheimer's disease. EMBO Mol Med. 2009 Nov;1(8-9):371-80.

Fahn S, Elton R. Members of the UPDRS Development Committee. Unified Parkinson's disease rating scale. In: Fahn S, Marsden CD, Calne DB, Goldstein M. (Eds.), Recent Developments in Parkinson's Disease, Vol. 2. MacmillanHealth Care Information, Florham Park, NJ, 1987; pp. 293-304.

Fahn S, Marsden CD, Calne DB, Goldstein M, eds. Recent Developments in Parkinson's Disease, Vol 2. Florham Park, NJ. Macmillan Health Care Information 1987, pp 153-163, 293-304.

Farias ST, Mungas D, Reed BR, Harvey D, DeCarli C. Progression of mild cognitive impairment to dementia in clinic- vs community-based cohorts. Arch Neurol. 2009 Sep;66(9):1151-7. doi: 10.1001/archneurol.2009.106. PMID: 19752306; PMCID: PMC2863139.

Ferman TJ, Boeve BF, Smith GE, Lin SC, Silber MH, Pedraza O, Wszolek Z, Graff-Radford NR, Uitti R, Van Gerpen J, Pao W, Knopman D, Pankratz VS, Kantarci K, Boot B, Parisi JE, Dugger BN, Fujishiro H, Petersen RC, Dickson DW. Inclusion of RBD improves the diagnostic classification of dementia with Lewy bodies. Neurology. 2011 Aug 30;77(9):875-82. doi: 10.1212/WNL.0b013e31822c9148. Epub 2011 Aug 17. PMID: 21849645; PMCID: PMC3162640.

Ferman TJ, Smith GE, Kantarci K, Boeve BF, Pankratz VS, Dickson DW, Graff-Radford NR, Wszolek Z, Gerpen JV, Uitti R, Pedraza O, Murray ME, Aakre J, Parisi J, Knopman DS, Petersen RC. Nonamnestic mild cognitive impairment progresses to dementia with Lewy bodies Neurology Dec 2013;81(23):2032-2038.

Ferreira, D, Przybelski, SA, Lesnick, TG, Lemstra, AW, Londos, E, Blanc, F, Nedelska, Z, Schwarz, CG, Graff-Radford, J, Senjem, ML, Fields, JA, Knopman, DS, Savica, R, Ferman, TJ, Graff-Radford, NR, Lowe, VJ, Jack Jr, CR, Petersen, RC, Mollenhauer, B, Garcia-Ptacek, S, Abdelnour, C, Hort, J, Bonanni, L, Oppedal, K, Kramberger, MG, Boeve, BF, Aarsland, D, Westman, E, Kantarci, K., 2020. beta-Amyloid and tau biomarkers and clinical phenotype in dementia with Lewy bodies. Neurology. 95 (24), e3257–e3268.

Fiorenzato E, Strafella AP, Kim J, Schifano R, Weis L, Antonini A, Biundo R. Dynamic functional connectivity changes associated with dementia in Parkinson's disease. Brain. 2019 Sep 1;142(9):2860-2872.

Folstein MF, Folstein SE, McHugh PR. "Mini-mental state". A practical method for grading the cognitive state of patients for the clinician. J Psychiatr Res. 1975 Nov;12(3):189-98. DOI: 10.1016/0022-3956(75)90026-6. PMID: 1202204.

Formaggio E, Rubega M, Rupil J, Antonini A, Masiero S, Toffolo GM, Del Felice A. Reduced Effective Connectivity in the Motor Cortex in Parkinson's Disease. Brain Sci. 2021 Sep 12;11(9):1200.

Franciotti, R, Iacono, D, Della Penna, S, Pizzella, V, Torquati, K, Onofrj, M, Romani, GL, 2006. Cortical rhythms reactivity in AD, LBD and normal subjects: a quantitative MEG study. Neurobiol Aging 27 (8), 1100–1109.

Franciotti, R, Pilotto, A, Moretti, DV, Falasca, NW, Arnaldi, D, Taylor, JP, Nobili, F, Kramberger, M, Ptacek, SG, Padovani, A, Aarlsand, D, Onofrj, M, Bonanni, LE-DLB consortium, 2020. Anterior EEG slowing in dementia with Lewy bodies: a multicenter European cohort study. Neurobiol Aging 93, 55–60.

Francis PT, Perry EK. Cholinergic and other neurotransmitter mechanisms in Parkinson's disease, Parkinson's disease dementia, and dementia with Lewy bodies. Mov Disord. 2007 Sep;22 Suppl 17:S351-7. doi: 10.1002/mds.21683. PMID: 18175396.

Francis PT. The interplay of neurotransmitters in Alzheimer's disease. CNS Spectr. 2005 Nov;10:6-9.

Freund TF, Meskenaite V. Gamma-Aminobutyric acid-containing basal forebrain neurons innervate inhibitory interneurons in the neocortex. Proc Natl Acad Sci U S A. 1992 Jan 15;89(2):738-42. doi: 10.1073/pnas.89.2.738. PMID: 1731348; PMCID: PMC48314.

Friedman BA, Srinivasan K, Ayalon G, Meilandt WJ, Lin H, Huntley MA, Cao Y, Lee SH, Haddick PCG, Ngu H, Modrusan Z, Larson JL, Kaminker JS, van der Brug MP, Hansen DV. Diverse Brain Myeloid Expression Profiles Reveal Distinct Microglial Activation States and Aspects of Alzheimer's Disease Not Evident in Mouse Models. Cell Rep. 2018 Jan 16;22(3):832-847. doi: 10.1016/j.celrep.2017.12.066. PMID: 29346778.

Fritz NE, Kegelmeyer DA, Kloos AD, Linder S, Park A, Kataki M, Adeli A, Agrawal P, Scharre DW, Kostyk SK. Motor performance differentiates individuals with Lewy body dementia, Parkinson's and Alzheimer's disease. Gait Posture. 2016 Oct;50:1-7.

Fujishiro H, Iseki E, Higashi S, Kasanuki K, Murayama N, Togo T, Katsuse O, Uchikado H, Aoki N, Kosaka K, Arai H, Sato K. Distribution of cerebral amyloid deposition and its relevance to clinical phenotype in Lewy body dementia. Neurosci Lett. 2010 Dec 3;486(1):19-23. doi: 10.1016/j.neulet.2010.09.036. Epub 2010 Sep 17. PMID: 20851165.

Fünfgeld, EW., 1995. Computerised brain electrical activity findings of parkinson patients suffering from hyperkinetic side effects (hypersensitive dopamine syndrome) and a review of possible sources. J Neural Transm Suppl. 46, 351–365.

Fuxe K, Ferré S, Genedani S, Franco R, Agnati LF. Adenosine receptor-dopamine receptor interactions in the basal ganglia and their relevance for brain function. Physiol Behav. 2007 Sep 10;92(1-2):210-7. doi: 10.1016/j.physbeh.2007.05.034. Epub 2007 May 21. PMID: 17572452.

Galasko D. Lewy body disorders. Neurol Clin. 2017;35:325–38.

Garcia-Esparcia P, López-González I, Grau-Rivera O, García-Garrido MF, Konetti A, Llorens F, Zafar S, Carmona M, Del Rio JA, Zerr I, Gelpi E, Ferrer I. Dementia with Lewy Bodies: Molecular Pathology in the Frontal Cortex in Typical

and Rapidly Progressive Forms. Front Neurol. 2017 Mar 13;8:89. doi: 10.3389/fneur.2017.00089. PMID: 28348546; PMCID: PMC5346561.

Gelb DJ, Oliver E, Gilman S. Diagnostic criteria for Parkinson disease. Arch Neurol. 1999; 56: 33-9.

Giaquinto S, Nolfe G. The EEG in the normal elderly: a contribution to the interpretation of aging and dementia. Electroencephalogr Clin Neurophysiol. 1986;63:540-6.

Goetz CG, Tilley BC, Shaftman SR, Stebbins GT, Fahn S, Martinez-Martin P, Poewe W, Sampaio C, Stern MB, Dodel R, Dubois B, Holloway R, Jankovic J, Kulisevsky J, Lang AE, Lees A, Leurgans S, LeWitt PA, Nyenhuis D, Olanow CW, Rascol O, Schrag A, Teresi JA, van Hilten JJ, LaPelle N; Movement Disorder Society UPDRS Revision Task Force. Movement Disorder Society-sponsored revision of the Unified Parkinson's Disease Rating Scale (MDS-UPDRS): scale presentation and clinimetric testing results. Mov Disord. 2008 Nov 15;23(15):2129-70. doi: 10.1002/mds.22340. PMID: 19025984.

Goldman JG, Goetz CG, Brandabur M, Sanfilippo M, Stebbins GT. Effects of dopaminergic medications on psychosis and motor function in dementia with Lewy bodies. Mov Disord. 2008;23:2248–50.

Goldman JS, Hahn SE, Bird T. Genetic counseling and testing for Alzheimer disease: Joint practice guidelines of the American College of Medical Genetics and the National Society of Genetic Counselors. Genet Med 2011; 13:597-605.

Gomperts SN, Marquie M, Locascio JJ, Bayer S, Johnson KA, Growdon JH. PET radioligands reveal the basis of dementia in Parkinson's disease and dementia with Lewy bodies. Neurodegener Dis. 2016;16:118–24.

Gomperts SN. Lewy Body Dementias: Dementia with Lewy Bodies and Parkinson Disease Dementia. Continuum (Minneap Minn). 2016 Apr;22:435-63

Gouw AA, Alsema AM, Tijms BM, Borta A, Scheltens P, Stam CJ, van der Flier WM. EEG spectral analysis as a putative early prognostic biomarker in nondemented, amyloid positive subjects. Neurobiol Aging. 2017 Sep;57:133-142. DOI: 10.1016/j.neurobiolaging.2017.05.017. Epub 2017 Jun 1. PMID: 28646686.

Gratwicke J, Jahanshahi M, Foltynie T. Parkinson's disease dementia: a neural networks perspective. Brain. 2015 Jun;138(Pt 6):1454-76. Rev.

Gudala K, Bansal D, Schifano F, Bhansali A. Diabetes mellitus and risk of dementia: A meta-analysis of prospective observational studies. Diabetes Investig 2013;4(6):640-50.

Haass C, Schlossmacher MG, Hung AY, Vigo-Pelfrey C, Mellon A, Ostaszewski BL, Lieberburg I, Koo EH, Schenk D, Teplow DB, et al. Amyloid beta-peptide is produced by cultured cells during normal metabolism. Nature. 1992 Sep 24;359(6393):322-5.

Halassa MM, Siegle JH, Ritt JT, Ting JT, Feng G, Moore CI. Selective optical drive of thalamic reticular nucleus generates thalamic bursts and cortical spindles. Nat Neurosci. 2011 Jul 24;14(9):1118-20. doi: 10.1038/nn.2880. PMID: 21785436; PMCID: PMC4169194.

Halder, T, Talwar, S, Jaiswal, AK, Banerjee, A., 2019. Quantitative evaluation in estimating sources underlying brain oscillations using current source density methods and beamformer approaches. eNeuro 6 (4) ENEURO.0170-19.201.

Hall H, Reyes S, Landeck N, Bye C, Leanza G, Double K et al. Hippocampal Lewy pathology and cholinergic dysfunction are associated with dementia in Parkinson's disease. Brain 2014; 137: 2493–2508.

Halliday GM, Leverenz JB, Schneider JS, Adler CH. The neurobiological basis of cognitive impairment in Parkinson's disease. Mov Disord. 2014 Apr 15;29(5):634-50. doi: 10.1002/mds.25857. PMID: 24757112; PMCID: PMC4049032.

Hanslmayr, S, Sauseng, P, Doppelmayr, M, Schabus, M, Klimesch, W., 2005. Increasing individual upper alpha power by neurofeedback improves cognitive performance in human subjects. Appl Psychophysiol Biofeedback 30 (1), 1–10. Doi:10.1007/s10484-005-2169-8, PMID: 15889581.

Hepp DH, Ruiter AM, Galis Y, Voorn P, Rozemuller AJ, Berendse HW, Foncke EM, van de Berg WD. Pedunculopontine cholinergic cell loss in hallucinating Parkinson disease patients but not in dementia with Lewy bodies patients. J Neuropathol Exp Neurol. 2013 Dec;72(12):1162-70.

Hepp DH, Vergoossen DL, Huisman E, Lemstra AW; Netherlands Brain Bank, Berendse HW, Rozemuller AJ, Foncke EM, van de Berg WD. Distribution and Load of Amyloid-β Pathology in Parkinson Disease and Dementia with Lewy Bodies. J Neuropathol Exp Neurol. 2016 Oct;75(10):936-94

Herholz K, Salmon E, Perani D, Baron JC, Holthoff V, Frölich L, Schönknecht P, Ito K, Mielke R, Kalbe E, Zündorf G, Delbeuck X, Pelati O, Anchisi D, Fazio F, Kerrouche N, Desgranges B, Eustache F, Beuthien-Baumann B, Menzel C, Schröder J, Kato T, Arahata Y, Henze M, Heiss WD. Discrimination between Alzheimer dementia and controls by automated analysis of multicenter FDG PET. Neuroimage. 2002 Sep;17(1):302-16. doi: 10.1006/nimg.2002.1208. PMID: 12482085.

Hoehn MM, Yahr MD. Parkinsonism: onset, progression, and mortality. 1967. Neurology. 1998;50:318 and 16 pages following.

Huang C, Wahlund L, Dierks T, Julin P, Winblad B, Jelic V. Discrimination of Alzheimer's disease and mild cognitive impairment by equivalent EEG sources: a cross-sectional and longitudinal study. Clin Neurophysiol. 2000 Nov;111(11):1961-7. DOI: 10.1016/s1388-2457(00)00454-5. PMID: 11068230

Hughes SW, Crunelli V. Thalamic mechanisms of EEG alpha rhythms and their pathological implications. Neuroscientist. 2005 Aug;11(4):357-72. DOI: 10.1177/1073858405277450. PMID: 16061522.

Ikonomovic MD, Klunk WE, Abrahamson EE, Mathis CA, Price JC, Tsopelas ND, Lopresti BJ, Ziolko S, Bi W, Paljug WR, Debnath ML, Hope CE, Isanski BA, Hamilton RL, DeKosky ST. Post-mortem correlates of in vivo PiB-PET amyloid imaging in a typical case of Alzheimer's disease. Brain. 2008 Jun;131(Pt 6):1630-45.

Ingvar DH, Sjölund B, Ardö A. Correlation between dominant EEG frequency, cerebral oxygen uptake and blood flow. Electroencephalogr Clin Neurophysiol. 1976;41:268-276.

Inouye, SK, van Dyck, CH, Alessi, CA, Balkin, S, Siegal, AP, Horwitz, RI., 1990. Clarifying confusion: the confusion assessment method. A new method for detection of delirium. Ann Intern Med 113 (12), 941–948. doi:10.7326/ 0003-4819-113-12-941, PMID: 2240918.

Iqbal K, Flory M, Khatoon S, Soininen H, Pirttila T, Lehtovirta M, Alafuzoff I, Blennow K, Andreasen N, Vanmechelen E, Grundke-Iqbal I. Subgroups of Alzheimer's disease based on cerebrospinal fluid molecular markers. Ann Neurol. 2005 Nov;58(5):748-57.

Irwin DJ, Lee VM, Trojanowski JQ. Parkinson's disease dementia: convergence of α-synuclein, tau and amyloid-β pathologies. Nat Rev Neurosci. 2013 Sep;14(9):626-36. doi: 10.1038/nrn3549. Epub 2013 Jul 31. PMID: 23900411; PMCID: PMC4017235.

Jack CR Jr, Bennett DA, Blennow K, Carrillo MC, Dunn B, Haeberlein SB, Holtzman DM, Jagust W, Jessen F, Karlawish J, Liu E, Molinuevo JL, Montine T, Phelps C, Rankin KP, Rowe CC, Scheltens P, Siemers E, Snyder HM, Sperling R; Contributors. NIA-AA Research Framework: Toward a biological definition of Alzheimer's disease. Alzheimer's Dement. 2018 Apr;14(4):535-562. doi: 10.1016/j.jalz.2018.02.018. PMID: 29653606; PMCID: PMC5958625.

Jackson, CE, Snyder, PJ., 2008. Electroencephalography and event-related potentials as biomarkers of mild cognitive impairment and mild Alzheimer's disease. Alzheimers Dement 4 (1), S137–S143 Suppl 1.

Janzen, J, van 't Ent, D, Lemstra, AW, Berendse, HW, Barkhof, F, Foncke, EM., 2012. The pedunculopontine nucleus is related to visual hallucinations in Parkinson's disease: preliminary results of a voxel-based morphometry study. J Neurol 259 (1), 147–154.

Jelic V, Johansson SE, Almkvist O, Shigeta M, Julin P, Nordberg A, Winblad B, Wahlund LO. Quantitative electroencephalography in mild cognitive impairment: longitudinal changes and possible prediction of Alzheimer's disease. Neurobiol Aging. 2000 Jul-Aug;21(4):533-40. DOI: 10.1016/s0197-4580(00)00153-6. PMID: 10924766.

Jellinger KA and Korczyn AD. Are dementia with Lewy bodies and Parkinson's disease dementia the same disease? BMC Medicine 2018;16:34.

Jellinger KA. Pathogenesis and treatment of vascular cognitive impairment. Neurodegener Dis Manag. 2014;4(6):471-90. doi: 10.2217/nmt.14.37. PMID: 25531689.

Jellinger KA. Significance of brain lesions in Parkinson disease dementia and Lewy body dementia. Front Neurol Neurosci. 2009;24:114-25.

Jeong J. EEG dynamics in patients with Alzheimer's disease. Clin Neurophysiol. 2004 ;115(7):1490-505.

Jones BE, Moore RY. Ascending projections of the locus coeruleus in the rat. II. Autoradiographic study. Brain Res. 1977 May 20;127(1):25-53. PMID: 301051.

Jones HM. Do selective serotonin reuptake inhibitors cause suicide? Discrediting old drugs may be useful in marketing new ones. BMJ. 2005 May 14;330(7500):1149

Jovicich J, Babiloni C, Ferrari C, Marizzoni M, Moretti DV, Del Percio C, Lizio R, Lopez S, Galluzzi S, Albani D, Cavaliere L, Minati L, Didic M, Fiedler U, Forloni G, Hensch T, Molinuevo JL, Bartrés Faz D, Nobili F, Orlandi D, Parnetti L, Farotti L, Costa C, Payoux P, Rossini PM, Marra C, Schönknecht P, Soricelli A, Noce G, Salvatore M, Tsolaki M, Visser PJ, Richardson JC, Wiltfang J, Bordet R, Blin O, Frisoniand GB; the PharmaCog Consortium. Two-Year Longitudinal Monitoring of Amnestic Mild Cognitive Impairment Patients with Prodromal Alzheimer's Disease Using Topographical Biomarkers Derived from Functional Magnetic Resonance Imaging and Electroencephalographic Activity. J Alzheimers Dis. 2019;69(1):15-35. DOI: 10.3233/JAD-180158. PMID: 30400088.

Jung TP, Makeig S, Humphries C, Lee TW, McKeown MJ, Iragui V, Sejnowski TJ. Removing electroencephalographic artifacts by blind source separation. Psychophysiology. 2000 Mar;37(2):163-78. PMID: 10731767.

Jurcak V, Tsuzuki D and Dan I. 10/20, 10/10, and 10/5 systems revisited: Their validity as relative head-surface-based positioning systems. NeuroImage 2007;34:1600-1611.

Kai, T, Asai, Y, Sakuma, K, Koeda, T, Nakashima, K., 2005. Quantitative electroencephalogram analysis in dementia with Lewy bodies and Alzheimer’s disease. J Neurol Sci 237 (1-2), 89–95.

Kamei S, Morita A, Serizawa K, Mizutani T, Hirayanagi K. Quantitative EEG analysis of executive dysfunction in Parkinson disease. J Clin Neurophysiol 2010;27:193–7.

Kapur S, Meyer J, Wilson AA, Houle S, Brown GM. Activation of specific cortical regions by apomorphine: an [15O] H2O PET study in humans. Neurosci Lett. 1994 Jul 18;176(1):21-4.

Klein JC, Eggers C, Kalbe E, Weisenbach S, Hohmann C, Vollmar S, et al. Neurotransmitter changes in dementia with Lewy bodies and Parkinson disease dementia in vivo. Neurology. 2010;74:885–92.

Klimesch W, Doppelmayr M, Russegger H, Pachinger T, Schwaiger J. Induced alpha band power changes in the human EEG and attention. Neurosci Lett. 1998; 244: 73-6.

Klimesch W, Doppelmayr M, Schimke H, Pachinger T. Alpha frequency, reaction time, and the speed of processing information. J Clin Neurophysiol. 1996; 13: 511-8.

Klimesch W. EEG alpha and theta oscillations reflect cognitive and memory performance: a review and analysis. Brain Res Brain Res Rev. 1999 Apr;29(2-3):169-95. DOI: 10.1016/s0165-0173(98)00056-3. PMID: 10209231.

Klimesch, W, Russegger, H, Doppelmayr, M, Pachinger, T, 1998. Induced and evoked band power changes in an oddball task Electroencephalogr. Clin. Neurophysiol 108, 123–130.

Knox MG, Adler CH, Shill HA, Driver-Dunckley E, Mehta SA, Belden C, Zamrini E, Serrano G, Sabbagh MN, Caviness JN, Sue LI, Davis KJ, Dugger BN, Beach TG. Neuropathological Findings in Parkinson's Disease With Mild Cognitive Impairment. Mov Disord. 2020 May;35(5):845-850.

Knyazeva, MG, Jalili, M, Brioschi, A, Bourquin, I, Fornari, E, Hasler, M, Meuli, R, Maeder, P, Ghika, J., 2010. Topography of EEG multivariate phase synchronization in early Alzheimer’s disease. Neurobiol Aging 31 (7), 1132–1144. doi:10. 1016/j.neurobiolaging.2008.07.019.

Koch W, Teipel S, Mueller S, Benninghoff J, Wagner M, Bokde AL, Hampel H, Coates U, Reiser M, Meindl T. Diagnostic power of default mode network resting state fMRI in the detection of Alzheimer's disease. Neurobiol Aging. 2012 Mar;33(3):466-78. DOI: 10.1016/j.neurobiolaging.2010.04.013. Epub 2010 Jun 11. PMID: 20541837.

Kochunov P, Mangin JF, Coyle T, Lancaster J, Thompson P, Rivière D, Cointepas Y, Régis J, Schlosser A, Royall DR, Zilles K, Mazziotta J, Toga A, Fox PT. Age-related morphology trends of cortical sulci. Hum Brain Mapp. 2005 Nov;26(3):210-20.

Kogan EA, Korczyn AD, Virchovsky RG, Klimovizky SSh, Treves TA, Neufeld MY. EEG changes during long-term treatment with donepezil in Alzheimer's disease patients. J Neural Transm (Vienna). 2001;108(10):1167-73.

Korczyn AD, Hassin-Baer S. Can the disease course in Parkinson's disease be slowed? BMC Med. 2015 Dec 10;13:295. doi: 10.1186/s12916-015-0534-x. PMID: 26653056; PMCID: PMC4675014.
Korotkova TM, Sergeeva OA, Eriksson KS, Haas HL, Brown RE. Excitation of ventral tegmental area dopaminergic and nondopaminergic neurons by orexins/hypocretins. J Neurosci. 2003 Jan 1;23(1):7-11. doi: 10.1523/JNEUROSCI.23-01-00007.2003. PMID: 12514194; PMCID: PMC6742159.

Leblhuber F, Steiner K, Schuetz B, Fuchs D, Gostner JM. Probiotic Supplementation in Patients with Alzheimer's Dementia - An Explorative Intervention Study. Curr Alzheimer Res. 2018;15(12):1106-1113. doi: 10.2174/1389200219666180813144834. PMID: 30101706; PMCID: PMC6340155.

Lehmann, C, Koenig, T, Jelic, V, Prichep, L, John, RE, Wahlund, LO, Dodge, Y, Dierks, T., 2007. Application and comparison of classification algorithms for recognition of Alzheimer's disease in electrical brain activity (EEG). J Neurosci Methods 161 (2), 342–350. doi:10.1016/j.jneumeth.2006.10.023, Epub 2006 Dec 6. PMID: 17156848.

Lemstra AW, de Beer MH, Teunissen CE, Schreuder C, Scheltens P, van der Flier WM, Sikkes SA. Concomitant AD pathology affects clinical manifestation and survival in dementia with Lewy bodies. J Neurol Neurosurg Psychiatry. 2017 Feb;88(2):113-118. doi: 10.1136/jnnp-2016-313775. Epub 2016 Oct 28. PMID: 27794030.

Leodori G, De Bartolo MI, Guerra A, Fabbrini A, Rocchi L, Latorre A, Paparella G, Belvisi D, Conte A, Bhatia KP, Rothwell JC, Berardelli A. Motor Cortical Network Excitability in Parkinson's Disease. Mov Disord. 2022 Apr;37(4):734-744.

Levy G, Tang MX, Cote LJ, Louis ED, Alfaro B, Mejia H, Stern Y, Marder K. Motor impairment in PD: relationship to incident dementia and age. Neurology. 2000;55: 539-44.

Li, S, Franken, P, Vassalli, A., 2018. Bidirectional and context-dependent changes in theta and gamma oscillatory brain activity in noradrenergic cell-specific Hypocretin/Orexin receptor 1-KO mice. Sci Rep 8 (1), 15474.

Lin FR, Ferrucci L, Metter EJ, An Y, Zonderman AB, Resnick SM. Hearing loss and cognition in the Baltimore Longitudinal Study of Aging. Neuropsychology. 2011 Nov;25(6):763-70.

Lin JS, Anaclet C, Sergeeva OA, Haas HL. The waking brain: an update. Cell Mol Life Sci. 2011 Aug;68(15):2499-512.
Liu, Q, Ganzetti, M, Wenderoth, N, Mantini, D., 2018. Detecting large-scale brain networks using EEG: impact of electrode density, head modeling and source localization. Front. Neuroinform. 12, 4.

Lizio, R, Del Percio, C, Marzano, N, Soricelli, A, Yener, GG, Bas¸ ar, E, Mundi, C, De Rosa, S, Triggiani, AI, Ferri, R, Arnaldi, D, Nobili, FM, Cordone, S, Lopez, S, Carducci, F, Santi, G, Gesualdo, L, Rossini, PM, Cavedo, E, Mauri, M, Frisoni, GB, Babiloni, C., 2016. Neurophysiological assessment of Alzheimer's disease individuals by a single electroencephalographic marker. J Alzheimers Dis 49 (1), 159–177. doi:10.3233/JAD-143042, PMID: 26444753.

Lörincz ML, Crunelli V, Hughes SW. Cellular dynamics of cholinergically induced alpha (8-13 Hz) rhythms in sensory thalamic nuclei in vitro. J Neurosci. 2008 Jan 16;28(3):660-71.

Lu J, Sherman D, Devor M, Saper CB. A putative flip-flop switch for control of REM sleep. Nature. 2006 Jun 1;441(7093):589-94. doi: 10.1038/nature04767. Epub 2006 May 10. PMID: 16688184.

Luckhaus C, Grass-Kapanke B, Blaeser I, Ihl R, Supprian T, Winterer G, Zielasek J, Brinkmeyer J. Quantitative EEG in progressing vs stable mild cognitive impairment (MCI): results of a 1-year follow-up study. Int J Geriatr Psychiatry. 2008 Nov;23(11):1148-55. DOI: 10.1002/gps.2042. PMID: 18537220.

Maidan I, Zifman N, Hausdorff JM, Giladi N, Levy-Lamdan O, Mirelman A. A multimodal approach using TMS, and EEG reveals neurophysiological changes in Parkinson's disease. Parkinsonism Relat Disord. 2021 Aug;89:28-33.

Marino, M, Liu, Q, Brem, S, Wenderoth, N, Mantini, D., 2016. Automated detection and labeling of high-density EEG electrodes from structural MR images. J Neural Eng 13 (5), 056003.

Marizzoni M, Ferrari C, Babiloni C, Albani D, Barkhof F, Cavaliere L, Didic M, Forloni G, Fusco F, Galluzzi S, Hensch T, Jovicich J, Marra C, Molinuevo JL, Nobili F, Parnetti L, Payoux P, Ranjeva JP, Ribaldi F, Rolandi E, Rossini PM, Salvatore M, Soricelli A, Tsolaki M, Visser PJ, Wiltfang J, Richardson JC, Bordet R, Blin O, Frisoni GB. CSF cutoffs for MCI due to AD depend on APOEε4 carrier status. Neurobiol Aging. 2020 May;89:55-62. doi: 10.1016/j.neurobiolaging.2019.12.019. Epub 2019 Dec 30. PMID: 32029236.

Masters CL, Simms G, Weinman NA, Multhaup G, McDonald BL, Beyreuther K. Amyloid plaque core protein in Alzheimer disease and Down syndrome. Proc Natl Acad Sci U S A. 1985 Jun;82(12):4245-9.

McBride, JC, Zhao, X, Munro, NB, et al., 2014. Sugihara causality analysis of scalp EEG for detection of early Alzheimer's disease. Neuroimage Clin 7, 258– 265.

McKeith I, O'Brien J, Walker Z, Tatsch K, Booij J, Darcourt J, Padovani A, Giubbini R, Bonuccelli U, Volterrani D, Holmes C, Kemp P, Tabet N, Meyer I, Reininger C; DLB Study Group. Sensitivity and specificity of dopamine transporter imaging with 123I-FP-CIT SPECT in dementia with Lewy bodies: a phase III, multicentre study. Lancet Neurol. 2007 Apr;6(4):305-13. doi: 10.1016/S1474-4422(07)70057-1. PMID: 17362834.

McKeith IG, Dickson DW, Lowe J, Emre M, O'Brien JT, Feldman H, Cummings J, Duda JE, Lippa C, Perry EK, Aarsland D, Arai H, Ballard CG, Boeve B, Burn DJ, Costa D, Del Ser T, Dubois B, Galasko D, Gauthier S, Goetz CG, Gomez-Tortosa E, Halliday G, Hansen LA, Hardy J, Iwatsubo T, Kalaria RN, Kaufer D, Kenny RA, Korczyn A, Kosaka K, Lee VM, Lees A, Litvan I, Londos E, Lopez OL, Minoshima S, Mizuno Y, Molina JA, Mukaetova-Ladinska EB, Pasquier F, Perry RH, Schulz JB, Trojanowski JQ, Yamada M: Consortium on DLB. Diagnosis and management of dementia with Lewy bodies: third report of the DLB Consortium. Neurology 2005;65:1863-72.

McKeith, IG, Boeve, BF, Dickson, DW, Halliday, G, Taylor, JP, Weintraub, D, et al., 2017. Diagnosis and management of dementia with Lewy bodies: Fourth consensus report of the DLB Consortium. Neurology 89 (1), 88–100.

McKhann G, Drachman D, Folstein M, Katzman R, Price D, Stadlan EM. Clinical diagnosis of Alzheimer's disease: report of the NINCDS-ADRDA Work Group under the auspices of Department of Health and Human Services Task Force on Alzheimer's Disease. Neurology 1984;34:939-44.

McKhann, GM, Knopman, DS, Chertkow, H, Hyman, BT, Jack Jr, CR, Kawas, CH, Klunk, WE, Koroshetz, WJ, Manly, JJ, Mayeux, R, Mohs, RC, Morris, JC, Rossor, MN, Scheltens, P, Carrillo, MC, Thies, B, Weintraub, S, Phelps, CH., 2011. The diagnosis of dementia due to Alzheimer's disease: recommendations from the National Institute on Aging-Alzheimer's Association workgroups on diagnostic guidelines for Alzheimer's disease. Alzheimers Dement 7 (3), 263–269.

Megari K. Quality of Life in Chronic Disease Patients. Health Psychol Res. 2013 Sep 23;1(3):e27. doi: 10.4081/hpr.2013.e27. PMID: 26973912; PMCID: PMC4768563.

Melgari JM, Curcio G, Mastrolilli F, Salomone G, Trotta L, Tombini M, di Biase L, Scrascia F, Fini R, Fabrizio E, Rossini PM, Vernieri F. Alpha and beta EEG power reflects L-dopa acute administration in parkinsonian patients. Front Aging Neurosci. 2014;6:302.

Michel, CM, Koenig, T., 2018. EEG microstates as a tool for studying the temporal dynamics of whole-brain neuronal networks: a review. Neuroimage 180 (Pt B), 577–593.

Middleton FA, Strick PL. Basal ganglia and cerebellar loops: motor and cognitive circuits. Brain Res. Brain Res Rev 2000; 31: 236–50

Missonnier, P, Deiber, MP, Gold, G, Millet, P, Gex-Fabry Pun, M, Fazio-Costa, L, Giannakopoulos, P, Ibáñez, V., 2006. Frontal theta event-related synchronization: comparison of directed attention and working memory load effects. J Neural Transm (Vienna) 113 (10), 1477–1486. doi:10.1007/s00702-005-0443-9.

Moënne-Loccoz C, Astudillo-Valenzuela C, Skovgård K, Salazar-Reyes CA, Barrientos SA, García-Núñez XP, Cenci MA, Petersson P, Fuentes-Flores RA. Cortico-Striatal Oscillations Are Correlated to Motor Activity Levels in Both Physiological and Parkinsonian Conditions. Front Syst Neurosci. 2020 Aug 13;14:56.

Molloy GJ, Johnston DW, Witham MD. Family caregiving and congestive heart failure. Review and analysis. Eur J Heart Fail. 2005 Jun;7(4):592-603. doi: 10.1016/j.ejheart.2004.07.008. PMID: 15921800.

Moretti DV. Conversion of mild cognitive impairment patients in Alzheimer's disease: prognostic value of Alpha3/Alpha2 electroencephalographic rhythms power ratio. Alzheimer's Res Ther. 2015 Dec 29;7:80. doi: 10.1186/s13195-015-0162-x. PMID: 26715588; PMCID: PMC4696332.

Moretti, DV, Babiloni, C, Binetti, G, Cassetta, E, Dal Forno, G, Ferreric, F, Ferri, R, Lanuzza, B, Miniussi, C, Nobili, F, Rodriguez, G, Salinari, S, Rossini, PM, 2004. Individual analysis of EEG frequency and band power in mild Alzheimer's disease. Clin Neurophysiol 115 (2), 299–308. doi:10.1016/s1388-2457(03)00345-6, PMID: 14744569.

Morris JC. The Clinical Dementia Rating (CDR): current version and scoring rules. Neurology. 1993 Nov;43(11):2412-4. DOI: 10.1212/wnl.43.11.2412-a. PMID: 8232972.

Moruzzi G, Magoun HW. Brain stem reticular formation and activation of the EEG. Electroencephalogr Clin Neurophysiol. 1949 Nov;1(4):455-73.

Mucke L. Neuroscience: Alzheimer's Disease. Nature 2009; 461(7266):895-897.

Muzur A, Pace-Schott EF, Hobson JA. The prefrontal cortex in sleep. Trends Cogn Sci. 2002 Nov 1;6(11):475-481. doi: 10.1016/s1364-6613(02)01992-7. PMID: 12457899.

Nagano-Saito A, Liu J, Doyon J, Dagher A. Dopamine modulates default mode network deactivation in elderly individuals during the Tower of London task. Neurosci Lett. 2009 Jul 10;458(1):1-5.

Nicolas G, Acuña-Hidalgo R, Keogh MJ, Quenez O, Steehouwer M, Lelieveld S, Rousseau S, Richard AC, Oud MS, Marguet F, Laquerrière A, Morris CM, Attems J, Smith C, Ansorge O, Al Sarraj S, Frebourg T, Campion D, Hannequin D, Wallon D, Gilissen C, Chinnery PF, Veltman JA, Hoischen A. Somatic variants in autosomal dominant genes are a rare cause of sporadic Alzheimer's disease. Alzheimers Dement. 2018 Dec;14(12):1632-1639. doi: 10.1016/j.jalz.2018.06.3056. Epub 2018 Aug 13. PMID: 30114415; PMCID: PMC6544509.

Nobili F, Copello F, Vitali P, Prastaro T, Carozzo S, Perego G, Rodriguez G. Timing of disease progression by quantitative EEG in Alzheimer's patients. J Clin Neurophysiol. 1999 Nov;16(6):566-73. DOI: 10.1097/00004691-199911000-00008. PMID: 10600024.

Noei S, Zouridis IS, Logothetis NK, Panzeri S, Totah NK. Distinct ensembles in the noradrenergic locus coeruleus are associated with diverse cortical states. Proc Natl Acad Sci U S A. 2022 May 3;119(18):e2116507119.

Novelli G, Papagno C, Capitani E, Laiacona M, Vallar G, Cappa SF. Tre test clinici di ricerca e produzione lessicale. Taratura su soggetti normali. Archivio di Psicologia Neurologia e Psichiatria 1986, 4 (47), pp. 477-506

Nunez PL. Spatial analysis of EEG. Electroencephalogr Clin Neurophysiol Suppl. 1996;45:37–8.PMID: 8930514.

Oktem, O., 1992. A verbal test of memory processes: a preliminary study. Arch Neuropsychatry 29, 196–206.

Onofrj M, Thomas A, Iacono D, Luciano AL, Di Iorio A. The effects of a cholinesterase inhibitor are prominent in patients with fluctuating cognition: a part 3 study of the main mechanism of cholinesterase inhibitors in dementia. Clin. Neuropharmacol. 2003;26:239–51.

Oostenveld R and Praamstra P. The five percent electrode system for high-resolution EEG and ERP measurements. Clin Neurophysiol 2001;112:713-719.

Paleologou KE, Kragh CL, Mann DM, Salem SA, Al-Shami R, Allsop D, Hassan AH, Jensen PH, El-Agnaf OM. Detection of elevated levels of soluble alpha-synuclein oligomers in post-mortem brain extracts from patients with dementia with Lewy bodies. Brain. 2009 Apr;132(Pt 4):1093-101. doi: 10.1093/brain/awn349. Epub 2009 Jan 20. PMID: 19155272.

Pascarelli, MT, Del Percio, C, De Pandis, MF, Ferri, R, Lizio, R, Noce, G, Lopez, S, Rizzo, M, Soricelli, A, Nobili, F, Arnaldi, D, Famà, F, Orzi, F, Buttinelli, C, Giubilei, F, Salvetti, M, Cipollini, V, Franciotti, R, Onofri, M, Fuhr, P, Gschwandtner, U, Ransmayr, G, Aarsland, D, Parnetti, L, Farotti, L, Marizzoni, M, D'Antonio, F, De Lena, C, Güntekin, B, Hanoglu, ˇ L, Yener, G, Emek-Savas¸ , DD, Triggiani, AI, Paul Taylor, J, McKeith, I, Stocchi, F, Vacca, L, Hampel, H, Frisoni, GB, Bonanni, L, Babiloni, C, 2020. Abnormalities of resting-state EEG in patients with prodromal and overt dementia with Lewy bodies: Relation to clinical symptoms. Clin Neurophysiol 131 (11), 2716–2731.

Pascual-Marqui RD. Discrete, 3D distributed linear imaging methods of electric neuronal activity. Part 1: exact, zero error localization. arXiv:0710.3341 [math-ph], 2007-October-17, http://arxiv.org/pdf/0710.3341

Passani MB, Giannoni P, Bucherelli C, Baldi E, Blandina P. Histamine in the brain: beyond sleep and memory. Biochem Pharmacol. 2007 Apr 15;73(8):1113-22. doi: 10.1016/j.bcp.2006.12.002. Epub 2006 Dec 15. PMID: 17241615.

Petersen RC, Doody R, Kurz A, Mohs RC, Morris JC, Rabins PV, Ritchie K, Rossor M, Thal L, Winblad B. Current concepts in mild cognitive impairment. Arch Neurol. 2001 Dec;58(12):1985-92.

Pfurtscheller G, Lopes da Silva FH. Event-related EEG/MEG synchronization and desynchronization: basic principles. Clin. Neurophysiol. 1999; 110: 1842–1857.

Plassman BL, Havlik RJ, Steffens DC, Helms MJ, Newman TN, Drosdick D, Phillips C, Gau BA, Welsh-Bohmer KA, Burke JR, Guralnik JM, Breitner JC. Documented head injury in early adulthood and risk of Alzheimer's disease and other dementias. Neurology. 2000 Oct 24;55(8):1158-66

Ponomareva NV, Selesneva ND, Jarikov GA. EEG alterations in subjects at high familial risk for Alzheimer's disease. Neuropsychobiology. 2003;48: 152-9.

Prichep LS, Ghosh Dastidar S, Jacquin A, Koppes W, Miller J, Radman T, O'Neil B, Naunheim R, Huff JS. Classification algorithms for the identification of structural injury in TBI using brain electrical activity. Comput Biol Med. 2014 Oct;53:125-33. DOI: 10.1016/j.compbiomed.2014.07.011. Epub 2014 Aug 1. PMID: 25137412.

Prichep LS, John ER, Ferris SH, Rausch L, Fang Z, Cancro R, Torossian C, Reisberg B. Prediction of longitudinal cognitive decline in normal elderly with subjective complaints using electrophysiological imaging. Neurobiol Aging. 2006 Mar;27(3):471-81. DOI: 10.1016/j.neurobiolaging.2005.07.021. Epub 2005 Oct 6. PMID: 16213630.

Prichep LS, John ER, Ferris SH, Reisberg B, Almas M, Alper K, Cancro R. Quantitative EEG correlates of cognitive deterioration in the elderly. Neurobiol Aging. 1994 Jan-Feb;15(1):85-90. DOI: 10.1016/0197-4580(94)90147-3. Erratum in: Neurobiol Aging 1994 May-Jun;15(3):391. PMID: 8159266.

Pugnetti, L, Baglio, F, Farina, E, Alberoni, M, Calabrese, E, Gambini, A, Di Bella, E, Garegnani, M, Deleonardis, L, Nemni, R., 2010. EEG evidence of posterior cortical disconnection in PD and related dementias. Int J Neurosci 120 (2), 88–98.

Ramanathan KR, Jin J, Giustino TF, Payne MR, Maren S. Prefrontal projections to the thalamic nucleus reuniens mediate fear extinction. Nat Commun. 2018 Oct 30;9(1):4527. doi: 10.1038/s41467-018-06970-z. PMID: 30375397; PMCID: PMC6207683.

Reeves RR, Struve FA, Patrick G. The effects of donepezil on quantitative EEG in patients with Alzheimer’s disease. Clin. Electroencephalogr. 2002; 33:93–96.
Reitan RM. Validity of the Trail Making Test as an Indicator of Organic Brain Damage. Perceptual and Motor Skills 1958, 8, 271-276. https://doi.org/10.2466/pms.1958.8.3.271

Ricci M, Guidoni SV, Sepe-Monti M, Bomboi G, Antonini G, Blundo C, Giubilei F. Clinical findings, functional abilities and caregiver distress in the early stage of dementia with Lewy bodies (DLB) and Alzheimer's disease (AD). Arch Gerontol Geriatr. 2009 Sep-Oct;49(2):e101-4.

Riekkinen M., Kejonen K., Jakala P., Soininen H., Riekkinen P., Jr. (1998). Reduction of noradrenaline impairs attention and dopamine depletion slows responses in Parkinson's disease. Eur. J. Neurosci. 10, 1429–1435.

Ringman JM, Coppola G, Elashoff D, Rodriguez-Agudelo Y, Medina LD, Gylys K, Cummings JL, Cole GM. Cerebrospinal fluid biomarkers and proximity to diagnosis in preclinical familial Alzheimer's disease. Dement Geriatr Cogn Disord. 2012;33(1):1-5.

Rodriguez G, Vitali P, De Leo C, De Carli F, Girtler N, Nobili F. Quantitative EEG changes in Alzheimer patients during long-term donepezil therapy. Neuropsychobiology. 2002;46: 49-56.

Rolinski M, Fox C, Maidment I, McShane R. Cholinesterase inhibitors for dementia with Lewy bodies, Parkinson's disease dementia and cognitive impairment in Parkinson's disease. Cochrane Database Syst Rev. 2012 Mar 14;2012(3):CD006504. doi: 10.1002/14651858.CD006504.pub2. PMID: 22419314; PMCID: PMC8985413.

Rongve A, Boeve B, Aarsland D. P01-370-Impact on caregivers from sleep disturbances is higher in dementia with Lewy bodies as compared to Alzheimer's dementia. Eur Psychiatry 2010a;25:583.

Rongve A, Boeve BF, Aarsland D. Frequency and correlates of caregiver- reported sleep disturbances in a sample of persons with early dementia. J Am Geriatr Soc 2010a;58: 480-86.

Rongve A, Bronnick K, Ballard C, Aarsland D. Core and suggestive symptoms of dementia with Lewy bodies cluster in persons with mild dementia. Dement Geriatr Cogn Disord 2010c;29: 317–324.

Rongve, A, Soennesyn, H, Skogseth, R, Oesterhus, R, Hortobágyi, T, Ballard, C, Auestad, BH, Aarsland, D., 2016. Cognitive decline in dementia with Lewy bodies: a 5-year prospective cohort study. BMJ Open 6 (2), e010357.

Rönnemaa E, Zethelius B, Lannfelt L, Kilander L. Vascular risk factors and dementia: 40-year follow-up of a populationbased cohort. Dement Geriatr Cogn Disord 2011;31(6):460-6.

Rosen WG, Mohs RC, Davis KL. A new rating scale for Alzheimer's disease. Am J Psychiatry. 1984 Nov;141(11):1356-64. DOI: 10.1176/ajp.141.11.1356. PMID: 6496779.

Rosen WG, Terry RD, Fuld PA, Katzman R, Peck A. Pathological verification of ischemic score in differentiation of dementias. Ann Neurol. 1980 May;7(5):486-8. doi: 10.1002/ana.410070516. PMID: 7396427.

Rossini PM, Del Percio C, Pasqualetti P, Cassetta E, Binetti G, Dal Forno G, Ferreri F, Frisoni G, Chiovenda P, Miniussi C, Parisi L, Tombini M, Vecchio F, Babiloni C. Conversion from mild cognitive impairment to Alzheimer's disease is predicted by sources and coherence of brain electroencephalography rhythms. Neuroscience. 2006 Dec;143(3):793-803. doi: 10.1016/j.neuroscience.2006.08.049. Epub 2006 Oct 13. PMID: 17049178.

Rossini PM, Di Iorio R, Vecchio F, Anfossi M, Babiloni C, Bozzali M, Bruni AC, Cappa SF, Escudero J, Fraga FJ, Giannakopoulos P, Guntekin B, Logroscino G, Marra C, Miraglia F, Panza F, Tecchio F, Pascual-Leone A, Dubois B. Early diagnosis of Alzheimer's disease: the role of biomarkers including advanced EEG signal analysis. Report from the IFCN-sponsored panel of experts. Clin Neurophysiol. 2020 Jun;131(6):1287-1310. DOI: 10.1016/j.clinph.2020.03.003. Epub 2020 Mar 12. PMID: 32302946.

Rossor M, Iversen LL. Non-cholinergic neurotransmitter abnormalities in Alzheimer's disease. British Medical Bulletin, 1986;42(1):70-4.

Ruffmann C, Calboli FC, Bravi I, Gveric D, Curry LK, de Smith A, Pavlou S, Buxton JL, Blakemore AI, Takousis P, Molloy S, Piccini P, Dexter DT, Roncaroli F, Gentleman SM, Middleton LT. Cortical Lewy bodies and Aβ burden are associated with prevalence and timing of dementia in Lewy body diseases. Neuropathol Appl Neurobiol. 2016 Aug;42(5):436-50. doi: 10.1111/nan.12294. Epub 2015 Dec 2. PMID: 26527105.

Saeed U, Compagnone J, Aviv RI, Strafella AP, Black SE, Lang AE, et al. Imaging biomarkers in Parkinson's disease and Parkinsonian syndromes: current and emerging concepts. Transl Neurodegener. 2017;6:8.

Sanders TH, Jaeger D. Optogenetic stimulation of cortico-subthalamic projections is sufficient to ameliorate bradykinesia in 6-ohda lesioned mice. Neurobiol Dis. 2016 Nov;95:225-37.

Sarro L, Tosakulwong N, Schwarz CG, Graff-Radford J, Przybelski SA, Lesnick TG, Zuk SM, Reid RI, Raman MR, Boeve BF, Ferman TJ, Knopman DS, Comi G, Filippi M, Murray ME, Parisi JE, Dickson DW, Petersen RC, Jack CR Jr, Kantarci K. An investigation of cerebrovascular lesions in dementia with Lewy bodies compared to Alzheimer's disease. Alzheimers Dement. 2017 Mar;13(3):257-66.

Saunders MG, Westmoreland BF. The EEG in evaluation of disorders affecting the brain diffusely. In: Klass DW, Daly DD, eds. Current Practice of Clinical Electroencephalography. New York: Raven Press; 1979:343-79.

Scatton B, Javoy-Agid F, Rouquier L, Dubois B, Agid Y. Reduction of cortical dopamine, noradrenaline, serotonin and their metabolites in Parkinson's disease. Brain Res 1983;275: 321–8.

Schneider RB, Iourinets J, Richard IH. Parkinson's disease psychosis: presentation, diagnosis and management. Neurodegener Dis Manag. 2017 Dec;7(6):365-76.

Schroeter ML, Stein T, Maslowski N, Neumann, J. Neural correlates of Alzheimer's disease and mild cognitive impairment: a systematic and quantitative meta-analysis involving 1351 patients. Neuroimage 2009 47(4):1196-206

Schumacher J, Taylor JP, Hamilton CA, Firbank M, Cromarty RA, Donaghy PC, Roberts G, Allan L, Lloyd J, Durcan R, Barnett N, O'Brien JT, Thomas AJ. In vivo nucleus basalis of Meynert degeneration in mild cognitive impairment with Lewy bodies. Neuroimage Clin. 2021; 30:102604.

Schumacher J., Thomas A.J., Peraza L.R., Firbank M., Cromarty R., Hamilton C.A., Donaghy P.C., O'Brien J.T., Taylor J.-P. EEG alpha reactivity and cholinergic system integrity in Lewy body dementia and Alzheimer's disease. Alzheimers. Res. Ther. 2020a; 12:46.

Schumacher, J., Taylor, J.-P., Hamilton, C.A., Firbank, M., Cromarty, R.A., Donaghy, P.C., Roberts, G., Allan, L., Lloyd, J., Durcan, R., Barnett, N., O'Brien, J.T., Thomas, A.J., 2020b. Quantitative EEG as a biomarker in mild cognitive impairment with Lewy bodies. Alzheimers. Res. Ther. 12 (1), 82.

Selikhova M, Williams DR, Kempster PA, Holton JL, Revesz T, Lees AJ. A clinico-pathological study of subtypes in Parkinson's disease. Brain. 2009 Nov;132(Pt 11):2947-57. doi: 10.1093/brain/awp234. Epub 2009 Sep 16. PMID: 19759203.
Selkoe DJ. The molecular pathology of Alzheimer's disease. Neuron 1991;6(4):487-98.

Seppala TT, Nerg O, Koivisto AM, Rummukainen J, Puli L, Zetterberg H, Pyykkö OT, Helisalmi S, Alafuzoff I, Hiltunen M, Jääskeläinen JE, Rinne J, Soininen H, Leinonen V, Herukka SK. CSF biomarkers for Alzheimer disease correlate with cortical brain biopsy findings. Neurology. 2012 May 15;78(20):1568-75.

Serizawa, K, Kamei, S, Morita, A, Hara, M, Mizutani, T, Yoshihashi, H, Yamaguchi, M, Takeshita, J, Hirayanagi, K., 2008. Comparison of quantitative EEGs between Parkinson disease and age-adjusted normal controls. J Clin Neurophysiol 25 (6), 361–366.

Shadli SM, Ando LC, McIntosh J, Lodhia V, Russell BR, Kirk IJ, Glue P, McNaughton N. Right frontal anxiolytic-sensitive EEG 'theta' rhythm in the stop-signal task is a theory-based anxiety disorder biomarker. Sci Rep. 2021 Oct 5;11(1):19746. doi: 10.1038/s41598-021-99374-x. PMID: 34611294; PMCID: PMC8492763.

Shimada H, Hirano S, Shinotoh H, Aotsuka A, Sato K, Tanaka N, Ota T, Asahina M, Fukushi K, Kuwabara S, Hattori T, Suhara T, Irie T. Mapping of brain acetylcholinesterase alterations in Lewy body disease by PET. Neurology. 2009 Jul 28;73(4):273-8.

Sloan EP, Fenton GW. EEG power spectra and cognitive change in geriatric psychiatry: a longitudinal study. Electroencephalogr Clin Neurophysiol. 1993 Jun;86(6):361-7. DOI: 10.1016/0013-4694(93)90131-e. PMID: 7686470.

Small GW, Ercoli LM, Silverman DH, Huang SC, Komo S, Bookheimer SY, Lavretsky H, Miller K, Siddarth P, Rasgon NL, Mazziotta JC, Saxena S, Wu HM, Mega MS, Cummings JL, Saunders AM, Pericak-Vance MA, Roses AD, Barrio JR, Phelps ME. Cerebral metabolic and cognitive decline in persons at genetic risk for Alzheimer's disease. Proc Natl Acad Sci U S A. 2000 May 23;97(11):6037-42.

Snaedal J, Johannesson GH, Gudmundsson TE, Blin NP, Emilsdottir AL, Einarsson B, Johnsen K. Diagnostic accuracy of statistical pattern recognition of electroencephalogram registration in evaluation of cognitive impairment and dementia. Dement Geriatr Cogn Disord. 2012;34:51-60.

Sobow T. Parkinson's disease-related visual hallucinations unresponsive to atypical antipsychotics treated with cholinesterase inhibitors: a case series. Neurol Neurochir Pol. 2007;41:276-9.

Soininen H, Partanen J, Laulumaa V, Helkala EL, Laakso M, Riekkinen PJ. Longitudinal EEG spectral analysis in early stage of Alzheimer's disease. Electroencephalogr Clin Neurophysiol. 1989 Apr;72(4):290-7. DOI: 10.1016/0013-4694(89)90064-3. PMID: 2467794.

Sperling RA, Aisen PS, Beckett LA, Bennett DA, Craft S, Fagan AM, Iwatsubo T, Jack CR Jr, Kaye J, Montine TJ, Park DC, Reiman EM, Rowe CC, Siemers E, Stern Y, Yaffe K, Carrillo MC, Thies B, Morrison-Bogorad M, Wagster MV, Phelps CH.Toward defining the preclinical stages of Alzheimer's disease: recommendations from the National Institute on Aging-Alzheimer's Association workgroups on diagnostic guidelines for Alzheimer's disease. Alzheimers Dement. 2011 May;7(3):280-92.

Stam CJ, Jones BF, Manshanden I, van Cappellen van Walsum AM, Montez T, Verbunt JP, de Munck JC, van Dijk BW, Berendse HW, Scheltens P. Magnetoencephalographic evaluation of resting-state functional connectivity in Alzheimer's disease. Neuroimage 2006;32:1335-44.

Steriade M, Datta S, Paré D, Oakson G, Curró Dossi RC. Neuronal activities in brain-stem cholinergic nuclei related to tonic activation processes in thalamocortical systems. J Neurosci. 1990 Aug;10(8):2541-59. doi: 10.1523/JNEUROSCI.10-08-02541.1990. PMID: 2388079; PMCID: PMC6570275.

Stern Y. Cognitive reserve in ageing and Alzheimer's disease. Lancet Neurol 2012;11(11):1006-12.

Stipacek, A, Grabner, RH, Neuper, C, Fink, A, Neubauer, AC., 2003. Sensitivity of human EEG alpha band desynchronization to different working memory components and increasing levels of memory load. Neurosci Lett 353 (3), 193–196.

Stomrud E, Hansson O, Blennow K, Minthon L, Londos E. Cerebrospinal fluid biomarkers predict decline in subjective cognitive function over 3 years in healthy elderly. Dementia and geriatric cognitive disorders 2007;24(2):118-124.
Stroop, J.R., 1935. Studies of interference in serial verbal reactions. J. Exp. Psychol. 18, 643–662. doi:10.1037/h0054651.

Swirski M, Miners JS, de Silva R, Lashley T, Ling H, Holton J, Revesz T, Love S. Evaluating the relationship between amyloid-β and α-synuclein phosphorylated at Ser129 in dementia with Lewy bodies and Parkinson's disease. Alzheimers Res Ther. 2014;6:77

Tiraboschi P, Hansen LA, Alford M, Sabbagh MN, Schoos B, Masliah E, Thal LJ, Corey-Bloom J. Cholinergic dysfunction in diseases with Lewy bodies. Neurology. 2000 Jan 25;54(2):407-11
Tolosa E, Garrido A, Scholz SW, Poewe W. Challenges in the diagnosis of Parkinson's disease. Lancet Neurol. 2021 May;20(5):385-397.

Tsuboi Y, Uchikado H, Dickson DW. Neuropathology of Parkinson's disease dementia and dementia with Lewy bodies with reference to striatal pathology. Parkinsonism Relat Disord. 2007;13 Suppl 3: S221-4.

Tsuno N. The potential role of donepezil for the treatment of dementia with Lewy bodies. J Alzheimers Dis Parkinsonism. 2016;6:214.

Turco F, Canessa A, Olivieri C, Pozzi NG, Palmisano C, Arnulfo G, Marotta G, Volkmann J, Pezzoli G, Isaias IU. Cortical response to levodopa in Parkinson's disease patients with dyskinesias. Eur J Neurosci. 2018 Sep;48(6):2362-2373.

van der Hiele K, Vein AA, Reijntjes RH, Westendorp RG, Bollen EL, van Buchem MA, van Dijk JG, Middelkoop HA. EEG correlates in the spectrum of cognitive decline. Clin Neurophysiol. 2007 Sep;118(9):1931-9. DOI: 10.1016/j.clinph.2007.05.070. Epub 2007 Jun 28. PMID: 17604688.

Varma AR, Snowden JS, Lloyd JJ, Talbot PR, Mann DM, Neary D. Evaluation of the NINCDS-ADRDA criteria in the differentiation of Alzheimer's disease and frontotemporal dementia. J Neurol Neurosurg Psychiatry 1999; 66: 184–88.

Vorobyov, V, Bakharev, B, Medvinskaya, N, Nesterova, I, Samokhin, A, Deev, A, Tatarnikova, O, Ustyugov, AA, Sengpiel, F, Bobkova, N., 2019. Loss of midbrain dopamine neurons and altered apomorphine EEG effects in the 5xFAD mouse model of Alzheimer's Disease. J Alzheimer's Dis 70 (1), 241–256.

Walker MP, Stickgold R. Sleep-dependent learning and memory consolidation. Neuron. 2004 Sep 30;44(1):121-33. doi: 10.1016/j.neuron.2004.08.031. PMID: 15450165.

Walker Z, Possin KL, Boeve BF, Aarsland D. Lewy body dementias. Lancet. 2015;386:1683-97. Rev

Walker, MP, Ayre, GA, Cummings, JL, Wesnes, K, McKeith, IG, O'Brien, JT, Ballard, CG., 2000a. The clinician assessment of fluctuation and the one day fluctuation assessment scale. Two methods to assess fluctuating confusion in dementia. Br J Psychiatry 177, 252–256.

Walker, MP, Ayre, GA, Perry, EK, Wesnes, K, McKeith, IG, Tovee, M, Edwardson, JA, Ballard, CG., 2000b. Quantification and characterization of fluctuating cognition in dementia with Lewy bodies and Alzheimer's disease. Dement Geriatr Cogn Disord 11 (6), 327–335.

Wan L, Huang, H, Schwab, N, Tanner, J, Rajan, A, Lam, NB, Zaborszky, L, Li, CR, Price, CC, Ding, M., 2019. From eyes-closed to eyes-open: Role of cholinergic projections in EC-to-EO alpha reactivity revealed by combining EEG and MRI. Hum Brain Mapp 40 (2), 566–577.

Wang HF, Yu JT, Tang SW, Jiang T, Tan CC, Meng XF, Wang C, Tan MS, Tan L. Efficacy and safety of cholinesterase inhibitors and memantine in cognitive impairment in Parkinson's disease, Parkinson's disease dementia, and dementia with Lewy bodies: systematic review with meta-analysis and trial sequential analysis. J Neurol Neurosurg Psychiatry. 2015 Feb;86(2):135-43.

Wechsler D. WMS-R: Wechsler Memory Scale-Revised: Manual. San Antonio, TX: Psychological Corporation. 1987

Weiss D, Klotz R, Govindan RB, Scholten M, Naros G, Ramos-Murguialday A, Bunjes F, Meisner C, Plewnia C, Krüger R, Gharabaghi A. Subthalamic stimulation modulates cortical motor network activity and synchronization in Parkinson's disease. Brain. 2015 Mar;138(Pt 3):679-93.

Winblad B, Palmer K, Kivipelto M, Jelic V, Fratiglioni L, Wahlund LO, Nordberg A, Bäckman L, Albert M, Almkvist O, Arai H, Basun H, Blennow K, de Leon M, DeCarli C, Erkinjuntti T, Giacobini E, Graff C, Hardy J, Jack C, Jorm A, Ritchie K, van Duijn C, Visser P, Petersen RC. Mild cognitive impairment--beyond controversies, towards a consensus: report of the International Working Group on Mild Cognitive Impairment. J Intern Med. 2004 Sep;256(3):240-6. doi: 10.1111/j.1365-2796.2004.01380.x. PMID: 15324367.

Winslow BT, Onysko MK, Stob CM, Hazlewood KA. Treatment of Alzheimer disease. Am Fam Physician. 2011 Jun 15;83(12):1403-12. Erratum in: Am Fam Physician. 2014 Aug 15;90(4):209. PMID: 21671540.

Yeomans, JS., 2012. Muscarinic receptors in brain stem and mesopontine cholinergic arousal functions. Handb Exp Pharmacol 208, 243–259

Zager A, Brandão WN, Margatho RO, Peron JP, Tufik S, Andersen ML, Kornum BR, Palermo-Neto J. The wake-promoting drug Modafinil prevents motor impairment in sickness behavior induced by LPS in mice: Role for dopaminergic D1 receptor. Prog Neuropsychopharmacol Biol Psychiatry. 2018 Feb 2;81:468-476. doi: 10.1016/j.pnpbp.2017.05.003. Epub 2017 May 9. PMID: 28499899.

Zhang Q, Kim YC, Narayanan NS. Disease-modifying therapeutic directions for Lewy body dementias. Front Neurosci. 2015;9:293.

Zhang, Yw., Thompson, R., Zhang, H. et al. APP processing in Alzheimer's disease. Mol Brain 4, 3 (2011). https://doi.org/10.1186/1756-6606-4-3

Acknowledgements

These have been years full of changes, not all of them positive, and carrying on such a journey has not been easy at all. Although this time I certainly have to give myself a good deal of credit for this achievement, I don't think it would have been possible without the support of many people close to me.

The first person I would like to thank is my fiancée Marilina. In order not to write thanks that are longer than the thesis itself, I will only say that one thing I love very much about her is the fact that she has always been there for me and has always helped me, often putting her own interests second. She has always understood how passionate I am and how important research is to me. She has always helped me to find direction and for that I cannot say thank you enough. I love you.

At this point I can only thank Professor Claudio Babiloni for the important opportunity he gave me three years ago.

Now I should say that I thank my colleagues, but that would not be the truth. I thank people who I consider friends, who have helped me so much both in the work environment and in different personal experiences. From the first day I joined, it was a pleasure for me to discover that they are very good people with a big heart. Thank you Claudio, Roberta, Giuseppe, Susanna and Dudù for everything.

I would like to thank my family who have seen me navigate the academic world for years, offering me constant support. In particular, I thank my mother for encouraging me when I lose heart and I thank my father for reminding me whenever I need reminding that 'Nun putimm perdere'. I love you all. As I did for my first thesis ever, I would like to thank my grandmother Bianca, as long as she was there, for all her care. I miss you very much.

Finally, it might seem that friends count for little in an academic research path, but this is not the case. Their contribution is more than they can imagine and unfortunately cannot be summarised in these few lines. However, I hope that each of them knows how much I appreciate and love them.